**UNIVERSIDAD COMPLUTENSE DE MADRID**
FACULTAD DE MEDICINA


# TESIS DOCTORAL

## Respuestas de las células ganglionares de la retina a la lesión y su prevención

## Retinal ganglion cell responses to lesion and their prevention

MEMORIA PARA OPTAR AL GRADO DE DOCTOR

PRESENTADA POR

**Beatriz Vidal Villegas**

Directores

**Julián García Feijoo**
**José María Martínez de la Casa**
**Manuel Vidal**

Madrid

# UNIVERSIDAD COMPLUTENSE DE MADRID

FACULTAD DE MEDICINA

PROGRAMA DE DOCTORADO EN CIENCIAS DE LA VISIÓN

DEPARTAMENTO DE INMUNOLOGÍA, OFTALMOLOGÍA Y OTORRINOLARINGOLOGÍA



## TESIS DOCTORAL

# RESPUESTAS DE LAS CÉLULAS GANGLIONARES DE LA RETINA A LA LESIÓN Y SU PREVENCIÓN
# RETINAL GANGLION CELL RESPONSES TO LESION AND ITS PREVENTION

MEMORIA PARA OPTAR AL GRADO DE DOCTORA
CON MENCIÓN INTERNACIONAL
PRESENTADA POR


Beatriz Vidal Villegas

DIRECTORES:

**Julián García Feijoo**
**José María Martínez de la Casa**
**Manuel Vidal Sanz**


**Madrid 2021**

UNIVERSIDAD COMPLUTENSE DE MADRID
FACULTAD DE MEDICINA
PROGRAMA DE DOCTORADO EN CIENCIAS DE LA VISIÓN
DEPARTAMENTO DE INMUNOLOGÍA, OFTALMOLOGÍA Y OTORRINOLARINGOLOGÍA

# RESPUESTAS DE LAS CÉLULAS GANGLIONARES DE LA RETINA A LA LESIÓN Y SU PREVENCIÓN

**Tesis Doctoral**

**BEATRIZ VIDAL VILLEGAS**

**Madrid 2021**

**Directores:**

**Prof. Julián García Feijoo**

**Prof. José María Martínez de la Casa**

**Prof. Manuel Vidal Sanz**

# UNIVERSIDAD COMPLUTENSE DE MADRID

FACULTAD DE MEDICINA

PROGRAMA DE DOCTORADO EN CIENCIAS DE LA VISIÓN

DEPARTAMENTO DE INMUNOLOGÍA, OFTALMOLOGÍA Y OTORRINOLARINGOLOGÍA



## TESIS DOCTORAL

# RESPUESTAS DE LAS CÉLULAS GANGLIONARES DE LA RETINA A LA LESIÓN Y SU PREVENCIÓN
# RETINAL GANGLION CELL RESPONSES TO LESION AND THEIR PREVENTION

MEMORIA PARA OPTAR AL GRADO DE DOCTORA
CON MENCIÓN INTERNACIONAL
PRESENTADA POR


Beatriz Vidal Villegas

DIRECTORES:

**Julián García Feijoo**
**José María Martínez de la Casa**
**Manuel Vidal Sanz**

# INDICE

# I. AGRADECIMIENTOS

Quisiera agradecer a todos los que me han ayudado en la realización de esta Tesis Doctoral, pues sin ellos no habría sido posible.

En primer lugar, quisiera agradecer a los Directores de esta Tesis, los profesores García Feijoo, Martínez de la Casa, y Vidal Sanz su disponibilidad para dirigirme.

A los Profesores García Feijoo y Martínez de la Casa debo agradecerles todo lo que me han enseñado durante la residencia y su apoyo constante desde que comencé a realizar mi primer trabajo de investigación clínica para el Trabajo de Fin de Máster.

Al Profesor García Feijoo quiero agradecerle su dedicación y su apoyo incondicional tanto en este como en otros proyectos.

Al Profesor Martínez de la Casa le agradezco su amabilidad y generosidad en todos los momentos que hemos compartido.

Al Profesor Vidal Sanz, mi padre, por su empuje, por su estímulo constante y su apoyo durante todo el proceso. Además, debo agradecerle también el inculcarme la importancia del trabajo constante.

También quisiera agradecer a todos los componentes del Laboratorio de Oftalmología Experimental de la Universidad de Murcia sus enseñanzas y ayuda desde hace muchos años que comencé allí mi Trabajo de Fin de Grado. Sus enseñanzas continuas, su paciencia, disponibilidad y amabilidad han hecho de mi iniciación a la investigación una tarea agradable. Son para mí un ejemplo de "cómo se hacen las cosas bien".

Quisiera también dar las gracias a todo el conjunto de profesionales que componen el Servicio de Oftalmología del Hospital Clínico San Carlos de Madrid, por recibirme con los brazos abiertos y por permitirme aprender las tareas de la especialidad a su lado. Este ha sido un periodo importante de mi vida del que me llevo los mejores recuerdos. Quisiera agradecer especialmente a mis compañeros residentes la ayuda de todo tipo que me han prestado durante este periodo y en particular, a mis dos compañeras de batallas, Bárbara y Pili, sin las que estos 4 años no habrían sido iguales.

Quisiera agradecer también a la Sociedad Española de Glaucoma su "Beca para formación de jóvenes investigadores" que me ha permitido financiar mi estancia internacional en el Imperial College Ophthalmology Research Group, en el Western Eye Hospital de Londres. Y a la directora del grupo, la Profesora Maria Francesca Cordeiro su dirección amable e inteligente durante los tres meses que he pasado allí.

También quisiera agradecerles la ayuda prestada a todo el personal del Servicio de Oftalmología del Hospital General Universitario Reina Sofía de Murcia, que me han acogido, enseñado y tratado inmejorablemente durante los dos meses de la especialidad que he rotado en el Servicio.

Pero sin duda el mayor agradecimiento sería para mi familia. A mis padres que son mi ejemplo a seguir y la razón de todo lo que soy a día de hoy. A mi madre que me da

siempre todo sin esperar nada a cambio. A mi hermana por tener siempre palabras de ánimo y aliento conmigo. Y a mis tíos y primos, en especial a Gabi, por allanarme el camino.

Sin la aportación de todas estas personas el trabajo que viene a continuación no habría sido posible. Espero que todos os sintáis partícipes de esta Tesis, porque para mi sois parte imprescindible.

## III. ORGANIZACIÓN GENERAL DE LA TESIS

Esta Tesis sigue la modalidad de Tesis en formato publicaciones, según artículo 10.3 del Real Decreto 99/2011, de 28 de enero (BOE 10/02/2011) que regula los estudios de doctorado en la Universidad Complutense de Madrid.

Con esta Tesis, la doctoranda opta a la Mención de Doctor Internacional. Para ello, ha realizado una estancia de tres meses en el Grupo de Investigación Oftalmológica del Imperial College en el Western Eye Hospital de Londres. Al optar a la Mención de Doctorado Internacional, la actual regulación de la Universidad Complutense de Madrid exige que al menos el resumen y las conclusiones estén redactados y sean defendidos en una lengua de comunicación científica diferente a las lenguas oficiales en España, que esta Tesis sea informada por dos doctores de instituciones pertenecientes a una institución de educación superior o instituto de investigación no español y que un miembro del Tribunal que debe juzgarla pertenezca a una institución de educación superior o instituto de investigación no español. Para facilitar la tarea de los doctores extranjeros, se han redactado todos los apartados de esta Tesis en inglés y además varios apartados, incluyendo el resumen y las conclusiones, se han redactado también en castellano.

El índice de la Tesis incluye una primera parte administrativa (números romanos) y una segunda parte que es la Tesis en sí (números arábigos).

La parte administrativa contiene los agradecimientos, los anexos administrativos, la organización general de la tesis y los hallazgos originales del trabajo presentado en la Tesis, tanto en español como en inglés, la estancia de investigación, las publicaciones, comunicaciones a congresos o reuniones y los premios o becas de la doctoranda durante su periodo de formación postgraduada y la lista de abreviaturas.

El índice de la Tesis contiene el Resumen y los apartados preceptivos de la Tesis según la regulación actual del Doctorado de la Universidad Complutense de Madrid: Introducción, Hipótesis y Objetivos, el Compendio de los tres artículos publicados que constituyen el trabajo, Discusión, Conclusiones y Bibliografía que están todos redactados en inglés. Esta Tesis por lo tanto no contiene los apartados Material y

Métodos y Resultados porque han sido sustituidos por los tres artículos publicados de acuerdo con la regulación actual de las Tesis en formato de publicaciones.

## III. GENERAL ORGANIZATION OF THE THESIS

This Ph.D. Thesis follows the modality of publication format as stated in the article 10.3 of the "Real Decreto 99/2011, de 28 de enero (BOE 10/02/2011)" that regulates the graduate studies of the Complutense University of Madrid.

The Ph.D. student opts with this Thesis to a Mention of International Doctorate. For this purpose, she has completed a three month stay at the Imperial College Ophthalmic Research Group, located at the Western Eye Hospital of London. The Complutense University of Madrid regulates that in order for a Thesis to opt to the Mention of International Doctorate, at least the summary and the conclusions of the Thesis should be written and defended in a scientific language different from the official languages of Spain, the Thesis has to be informed by two doctors belonging to institutions of higher education or research institutes not Spanish and a member of the Tribunal has to belong to one institution of higher education or research institute not Spanish. To facilitate the work of the foreign doctors, all the parts of this Thesis have been written in English and various parts, including the summary and the conclusions, have been written also in Spanish.

The list of contents includes a first administrative part (in roman numbers) and a second one, the Thesis itself (in arabic numbers).

The administrative part comprises the acknowledgement, the administrative annexes, the general organization of the Thesis, and the original findings of the study, both in Spanish and in English, the research stay, the publications, the presentations to congresses or meetings and the scholarships and awards of the student during her postgraduate training, both in Spanish and in English and the list of abbreviations.

The list of contents of the Thesis includes the Abstracts and the following sections which are mandatory according to the actual regulations of the Complutense University of Madrid: Introduction, Hypotheses and Objectives, the Compendium of the three published articles that make up the work presented, Discussion, Conclusions

and References. Thus, this Thesis does not contain a Methods nor a Results section, because these sections have been substituted by the three published articles, in accordance with the actual regulations for Thesis in the publication format.

## IV. HALLAZGOS ORIGINALES

Este trabajo ha permitido documentar los siguientes hallazgos originales:

1. **En el estudio sobre lesión excitotóxica** de las células ganglionares de la retina (CGR) de la rata adulta mediante la inyección intravítrea de N-metil-D-aspartato (NMDA) se ha documentado:

- La puesta a punto de un modelo de lesión excitotóxica de las CGR.
- La dosis de NMDA que produce una muerte moderada de CGR similar a la producida por sección intraorbitaria del nervio óptico, que es de 5µL de una solución 100mM.
- El patrón espacio-temporal de muerte de las CGR que se marcan con anticuerpos contra el factor de transcripción Brn3a (CGRBrn3a$^{+}$) tras la lesión excitotóxica, que es diferente de la que se observa después de la sección del nervio óptico pues ocurre en los primeros 7 días solamente.
- La disminución transitoria de la expresión de melanopsina durante los primeros días en las CGR que se marcan con anticuerpos contra la melanopsina (CGRm+), pero que no se produce muerte de CGRm+, por lo que estas células son resistentes a la lesión excitotóxica.
- La capacidad de la Tomografía Óptica de Coherencia de dominio espectral (SD-OCT) para observar *in vivo* la degeneración de la retina y documentar una disminución del espesor de la retina y sobre todo de las capas internas a largo plazo.

2. **En la revisión bibliográfica** sobre CGR intrínsecamente fotosensibles (CGRif) se han puesto al día los conocimientos actuales sobre este tema:

- En la actualidad se conocen seis tipos (M1-M6) diferentes de CGRif. Se ha actualizado el conocimiento de los tipos celulares descritos hasta la fecha en roedores (ratón y rata) y en humanos.
- Se han resumido sus características anatómicas, funcionales, moleculares, proyecciones centrales y sus diferentes responsabilidades en comportamientos visuales.
- Se han resumido sus principales funciones no formadoras de imágenes y formadoras de imágenes.

- Se han revisado las características principales de estas células en su periodo postnatal, pues son las primeras CGR que nacen en la retina.
- Se destaca que se trata de uno de los campos de investigación en visión más activo de los últimos 20 años, y por lo tanto la progresión del conocimiento en este campo es muy dinámica.

3. **En el estudio** sobre la lesión de las CGR de la rata adulta mediante la **sección del nervio óptico y la neuroprotección con 7,8-dihidroxiflavona** (DHF) se ha documentado:

- El patrón espacio-temporal de la muerte de CGRBrn3a$^+$ y de CGRm$^+$ tras la sección intraorbitaria del nervio óptico, que es diferente del observado en la lesión excitotóxica.
- La disminución transitoria de expresión de melanopsina en las CGRm$^+$
- La neuroprotección por vez primera *in vivo* de las CGR con DHF.
- La neuroprotección parcial de las CGRBrn3a$^+$ y de las CGRm$^+$ y que ésta es temporal (21 días) para las CGRBrn3a$^+$ pero permanente (15 meses) para las CGRm$^+$.
- La curva dosis-respuesta de los efectos neuroprotectores de la DHF administrada i.p. diariamente sobre las CGRBrn3a$^+$.
- La dosis óptima de DHF para realizar una neuroprotección de las CGRBrn3a$^+$ que es de 5 mg/kg.
- La activación (fosforilación) del receptor TrkB por el DHF en la retina.
-

## IV. ORIGINAL FINDINGS

This work has made it possible to document the following original findings:

1. **In the study on excitotoxic damage** to the retinal ganglion cells (RGCs) of adult rats by intravitreal injection of N-methyl-D-aspartate (NMDA), it has been documented:

- The development of a model of excitotoxic lesion for the RGC population.

- The dose of NMDA that produces a moderate death of RGCs similar to that produced by intraorbital section of the optic nerve is 5µL of a 100mM solution.

- The spatio-temporal pattern of death of RGCs labelled with antibodies against the transcription factor $Brn3a^+$ ($Brn3a^+$RGCs) after excitotoxic injury, which is different from that observed after optic nerve section, since it occurs in the first 7 days only.
- A transient decrease of the expression of melanopsin in the RGCs labelled with antibodies against melanopsin ($m^+$RGCs) during the first days, but no death of $m^+$RGCs and thus, these cells are resistant to excitotoxic injury.
- The capability of the Spectral Domain Optic Coherence Tomography (SD-OCT) to observe *in vivo* the retinal degeneration and to document a long-term reduction of the retinal thickness and especially of the inner layers.

2. **In the bibliographic review**, the current knowledge on intrinsically photosensitive melanopsin ganglion cells (ipRGCs) has been updated:
-At present, six different types (M1-M6) are known. The knowledge of the cell types described to date in rodents (mouse and rat) and in humans has been updated.
-Their anatomical, functional, molecular characteristics, central projections and their different responsibilities in visual behaviors have been summarized.
-Their main non-image forming and image forming functions have been summarized.
- Since they are the first RGCs to be born in the retina, the main characteristics of these cells in the postnatal period have been summarized.
-Finally, it should be noted that this is one of the most active fields of vision research in the last 20 years, and therefore the progression of knowledge in this field is very dynamic.

3. **In the study** on the lesion of the RGCs of the adult rat by the **section of the optic nerve and neuroprotection with 7,8-dihydroxyflavone** (DHF), it has been documented:

- The spatio-temporal pattern of death of Brn3a$^+$RGCs and m$^+$RGCs after intraorbital section of the optic nerve, which is different from that observed in the excitotoxic lesion.
- The transient decrease in melanopsin expression in m$^+$RGCs.
- The neuroprotection for the first time *in vivo* of RGCs with DHF.
- The partial neuroprotection of Brn3a$^+$RGCs and m$^+$RGCs and that this is temporary (21 days) for Brn3a$^+$RGCs but permanent (15 months) for m$^+$RGCs.
- The dose-response curve of the neuroprotective effects of DHF administered i.p. daily on the Brn3a$^+$RGCs.
- The optimal dose of DHF to carry out neuroprotection of Brn3a$^+$RGCs which is 5 mg/kg.
- The activation (phosphorylation) in the retina of the TrkB receptor by DHF

.

## V. ESTANCIA DE INVESTIGACIÓN, PUBLICACIONES Y COMUNICACIONES A CONGRESOS, PREMIOS Y BECAS DURANTE EL PERIODO DE DOCTORADO

## V. RESEARCH STAY, PUBLICATIONS, PRESENTATIONS AT MEETINGS AND SCHOLARSHIPS AND AWARDS DURING THE DOCTORATE PERIOD

### ESTANCIA DE INVESTIGACION/RESEARCH STAY

Estancia de investigación durante los meses de junio, julio y agosto 2021 en el *Imperial College Ophthalmic Research Group (ICORG) del Western Eye Hospital de Londres*. Bajo la dirección de la **Profa. Dra. Maria Francesca Cordeiro**, aprendiendo nuevas técnicas de investigación.

### ARTICULOS EN REVISTAS CIENTIFICAS/ARTICLES IN SCIENTIFIC JOURNALS

Gallego-Ortega A, **Vidal-Villegas B**, Norte-Muñoz M, Salinas-Navarro M, Avilés-Trigueros M, Villegas-Pérez MP, Vidal-Sanz M. 7,8-Dihydroxiflavone maintains retinal functionality and protects various types of RGCs in adult rats with optic nerve transection. *International Journal of Molecular Sciences*. IJMS-1429179 **Submitted.**

**Vidal-Villegas B**, Miralles de Imperial-Ollero JA, Santos Bueso E, García Feijoo J, Villegas-Pérez MP. Multimodal imaging, OCT en face and OCT angiography of an anomalous retinal artery; case report and review of the literature. *Case Rep Ophthalmol* 2021. **In Press**.

**Vidal-Villegas B**, Burgos-Blasco B, Santiago JL, Espino-Paisán L, Fernández-Vigo JI, Andrés-Guerrero V, García-Feijoo J, Martínez-de-la-Casa JM. Proinflammatory cytokine profile differences between primary open angle and pseudoexfoliative glaucoma. *Ophthalmic Research* 2021. **In Press**

Galindo-Romero C, **Vidal-Villegas B**, Asís-Martínez J, Lucas-Ruiz F, Gallego-Ortega A, Vidal-Sanz M. 7,8-Dihydroxiflavone protects adult rat axotomized retinal ganglion cells through MAPK/ERK and PI3K/AKT activation. *International Journal of Molecular Sciences*. 2021, 22, 10896. https://doi.org/10.3390/ijms221910896.

**Vidal-Villegas B**, Llorente La-Orden C, Calvo González C, Villegas-Pérez MP, Santos Bueso. Congenital retinal macrovessels: Case presentation. *Arch Soc Esp Oftalmol* 2021 Sep;96(9):492-495. doi: 10.1016/j.oftal.2020.07.026. PMID: 32962920.

Guemes-Villahoz N, Burgos-Blasco B, **Vidal-Villegas B**, Donate-López J, Herrera de la Muela M, Lopez-Guajardo L, Martín-Sánchez F, García-Feijoo J. (2021). Reduced macular vessel density in COVID-19 patients with and without associated thrombotic events using optical coherence tomography angiography. *Graefe's Arch Clin Exp Ophthalmol* 2021 Aug;259(8):2243-2249. doi: 10.1007/s00417-021-05186-0. Epub 2021 May 7. PMID: 33961108.

Burgos-Blasco B, Güemes-Villahoz N, **Vidal-Villegas B**, Garcia-Feijoo J, Donate-Lopez J, Martin-Sanchez F, Gonzalez-Armengol J, Mendez-Hernandez C, Carmen. (2021). Optic Nerve Head Vessel Density Assessment in Recovered COVID-19 Patients: A Prospective Study Using Optical Coherence Tomography Angiography. *J Glaucoma* 2021 Aug 1;30(8):711-717. doi: 10.1097/IJG.0000000000001858. PMID: 33927148.

Arriola-Villalobos P, Burgos-Blasco B, **Vidal-Villegas B**, Oribio-Quinto C, Ariño-Gutiérrez M, Díaz-Valle D, Benitez-del-Castillo JM (2021). Effect of face mask on tear film stability in eyes with moderate-to-severe dry eye disease. *Cornea* 2021. Publish Ahead of Print. 10.1097/ICO.0000000000002734. PMID: 34481410

Moreno-Morillo F, Fernández-Vigo JI, Burgos-Blasco B, Llorente La Orden C, **Vidal-Villegas B**, Santos-Bueso E (2021). Optical coherence tomography angiography of choroidal nodules in neurofibromatosis type-1: A case series. *Eur J Ophthalmol* 2021 Jul 7:11206721211030781. doi: 10.1177/11206721211030781. Online ahead of print. PMID: 34231401.

**Vidal-Villegas B**, Di Pierdomenico J, Gallego-Ortega A, Galindo-Romero C, Martínez-de-la-Casa JM, García-Feijoo J, Villegas-Pérez MP, Vidal-Sanz M. Systemic treatment with 7,8-Dihydroxiflavone activates TrkB and affords protection of two different retinal ganglion cell populations against axotomy in adult rats. *Exp Eye Res* 2021 Jul 8;210:108694. doi: 10.1016/j.exer.2021.108694. Online ahead of print. PMID: 34245756.

**Vidal-Villegas B**, Gallego-Ortega A, Miralles de Imperial-Ollero JA, Martínez-de-la-Casa JM, Garcia-Feijoo J, Vidal-Sanz M (2020). Células ganglionares fotosensibles: una población diminuta pero esencial. *Arch Soc Esp Oftalmol* 2021 Jun;96(6):299-315. doi: 10.1016/j.oftal.2020.06.032. Epub 2020 Oct 31. PMID: 33139132.

Guemes-Villahoz N, Burgos-Blasco B, **Vidal-Villegas B**, Donate-López J, Martín-Sánchez FJ, Porta-Etessam J, López-Guajardo L, Martín JLR, González-Armengol JJ, Julián García-Feijoo. Reduced retinal vessel density in COVID-19 patients and elevated D-dimer levels during the acute phase of the infection. *Medicina Clínica* (Barc). 2021 Jun 11;156(11):541-546. doi: 10.1016/j.medcli.2020.12.006. Epub 2021 Jan 28. PMID: 33593634.

Burgos-Blasco B, Güemes-Villahoz N, **Vidal-Villegas B**, Martinez-de-la-Casa JM, Donate-Lopez J, Martín-Sánchez FJ, González-Armengol JJ, Porta-Etessam J, Martin JLR, Garcia-Feijoo J. Optic nerve and macular optical coherence tomography in recovered COVID-19 patients. *Eur J Ophthalmol* 2021 Mar 15:11206721211001019. doi: 10.1177/11206721211001019. Online ahead of print. PMID: 33719624.

**Vidal-Villegas B**, Benitez-Del-Castillo JM. Current Knowledge in Allergic Conjunctivitis. *Turk J Ophthalmol*. 2021 Feb 25;51(1):45-54. PMID: 33631915. PMCID: PMC7931656 DOI: 10.4274/tjo.galenos.2020.11456

Burgos-Blasco B, Güemes-Villahoz N, **Vidal-Villegas B**, Donate-Lopez J, Garcia-Feijoo J. Evaluation of retinotoxicity of COVID-19 treatment: Hydroxychloroquine and lopinavir/ritonavir. *J Med Virol*. 2021 Feb;93(2):644-646. doi: 10.1002/jmv.26420. Epub 2020 Sep 28. PMID: 32786041

Burgos-Blasco B, Güemes-Villahoz N, Donate-Lopez J, **Vidal-Villegas B**, García-Feijóo J. Optic nerve analysis in COVID-19 patients. *J Med Virol*. 2021 Jan;93(1):190-191. doi: 10.1002/jmv.26290. Epub 2020 Jul 19. PMID: 32648939. LETTER TO THE EDITOR:

Güemes-Villahoz, N., Burgos-Blasco, B., **Vidal-Villegas, B**. et al. Novel Insights into the Transmission of SARS-CoV-2 Through the Ocular Surface and its Detection in Tears and Conjunctival Secretions: A Review. *Adv Ther* 2020 Oct;37(10):4086-4095. doi: 10.1007/s12325-020-01442-7. Epub 2020 Aug 18. PMID: 32809211.

Burgos-Blasco B, **Vidal-Villegas B**, Saenz-Frances F, Morales-Fernandez L, Perucho-Gonzalez L, Garcia-Feijoo J, Martinez-de-la-Casa JM. Tear and aqueous humour cytokine profile in primary open-angle glaucoma. *Acta Ophthalmol* 2020 Sep;98(6):e768-e772. doi: 10.1111/aos.14374. Epub 2020 Feb 11. PMID: 32043817.

Güemes-Villahoz N *, Burgos-Blasco B*, Arribi-Vilela A, Arriola-Villalobos P, **Vidal-Villegas B**, Mendez-Fernandez R, Delgado-Iribarren A, Garcia-Feijoo J. SARS-CoV-2 RNA detection in tears and conjunctival secretions of COVID-19 patients with conjunctivitis. *J Infect* 2020 Sep;81(3):452-482. doi: 10.1016/j.jinf.2020.05.070. Epub 2020 Jun 3. PMID: 32504746. LETTER TO THE EDITOR:

**Vidal-Villegas B**, Arcos-Villegas G, Fernández-Vigo JI, Díaz-Valle D Atypical Syphilitic Outer Retinitis and Severe Retinal Vasculitis as Onset Manifestations in a Patient with Concurrent HIV and Syphilis Infection. *Ocul Immunol Inflamm* 2020 Jul 23:1-5. doi: 10.1080/09273948.2020.1787464. Online ahead of print. PMID: 32701010

**Vidal-Villegas B**, Di Pierdomenico J, Miralles de Imperial-Ollero JA, Ortín-Martínez A, Nadal-Nicolás FM, Bernal-Garro JM, Cuenca Navarro N, Villegas-Pérez MP, Vidal-Sanz M. Melanopsin+RGCs Are fully Resistant to NMDA-Induced Excitotoxicity. *International Journal of Molecular Sciences*. 2019 Jun 20;20(12):3012. doi: 10.3390/ijms20123012. PMID: 31226772.

Agudo-Barriuso M, Nadal-Nicolás FM, Madeira MH, Rovere G, **Vidal-Villegas B**, Vidal-Sanz M. Melanopsin expression is an indicator of the well-being of melanopsin-expressing retinal ganglion cells but not of their viability. *Neural Regen Res*. 2016 Aug;11(8):1243-4. doi: 10.4103/1673-5374.189182. PMID: 27651769

## CAPITULOS DE LIBRO/BOOK CHAPTERS:

Manuel Vidal-Sanz, **Beatriz Vidal-Villegas**, Juan Antonio Miralles de Imperial-Ollero, María Paz Villegas-Pérez. Neuroprotección. En: *Glaucoma* (Lerner SF, García-Feijóo J, Júlvez L. eds). 1ª edición (2021). Ediciones Journal, Buenos Aires, Argentina. ISBN 9789874922724. Capítulo 47, Pp: 338-344.

## COMUNICACIONES EN CONGRESOS Y REUNIONES DURANTE PERIODO DOCTORADO/ CONGRESS OR MEETINGS PRESENTATIONS:

**AUTORES: Beatriz Vidal-Villegas***, Johnny Di Pierdomenico*, Juan A Miralles de Imperial-Ollero, Arturo Ortín-Martínez, Francisco M Nadal-Nicolás, Jose M Bernal-Garro, Nicolás Cuenca Navarro, Maria P Villegas-Pérez, Manuel Vidal-Sanz.
**TITULO:** Melanopsin+RGCs are fully resistant to NMDA induced excitotoxicity.
**TIPO DE PARTICIPACIÓN:** Comunicación oral.
**PUBLICACIÓN**: Acta Opththalmologica 2019 Dec 19; 97(S263):.
**CONGRESO:** 22nd European Vision and Eye Research (EVER) Congress
**LUGAR, FECHA**: Palais des Congres Akropolis, 1 John Fitzgerald kennedy, 06000, Nice, France. 17-19 Octubre 2019.
**Premio "Young Investigator Awards" del 22 EVER Congress**

**AUTORES**: **Beatriz Vidal-Villegas**, Johnny Di Pierdomenico, Manuel Salinas-Navarro, Jose Manuel Bernal-Garro, Marta Agudo-Barriuso, María Paz Villegas-Pérez, Jose M. Martínez de la Casa, Julián García-Feijoo, Manuel Vidal-Sanz.
**TITULO**: 7,8-Dihydroxyflavone protects axotomy-induced retinal ganglion cell loss in adult albino rats
**TIPO DE PARTICIPACIÓN**: Poster.
**PUBLICACIÓN:** Acta Opththalmologica 2019 Dec 19; 97(S263).
**CONGRESO:** European Association for Vision and Eye Research (EVER) Congress
**LUGAR DE CELEBRACIÓN**: Nice Akropolis Convention Centre, 1 esplanade Kennedy, 06302 Nice cedex 4, France.
**AÑO**: Niza, 17 al 19 de octubre de 2019.

**AUTORES: Vidal Villegas B**, Burgos Blasco B, Moreno Morillo FJ, Sáenz-Francés-San Baldomero F., Martinez de la Casa, JM..
**TITULO:** Biomarcadores de glaucoma primario de ángulo abierto y pseudoexfoliativo en lágrima y humor acuoso
**TIPO DE PARTICIPACIÓN:** Poster.
**LUGAR, FECHA**: Reunión anual de la Sociedad Oftalmológica de Madrid, 13 de Diciembre 2019. Círculo de Bellas Artes, Calle de Alcalá, 42, 28014 Madrid.
**Premio a la mejor comunicación en panel.**

**AUTORES: Vidal Villegas B**, Burgos Blasco B, Moreno Morillo FJ, Sáenz-Francés-San Baldomero F., Martinez de la Casa, JM..
**TITULO:** Niveles de citoquinas en lágrima y humor acuoso en pacientes con glaucoma primario de ángulo abierto y glaucoma pseudoexfoliativo.
**TIPO DE PARTICIPACIÓN:** Poster.

**LUGAR, FECHA:** XV Congreso de la Sociedad Española de Glaucoma (Congreso Virtual por pandemia COVID-19, programado en Palma de Mallorca, del 5 al 7 de marzo de 2020)

**AUTORES: Vidal Villegas B**.
**TITULO:** ¿Qué cirugía de glaucoma será la primera línea en un futuro?
**TIPO DE PARTICIPACIÓN:** Comunicación oral. Ponente en la Mesa Redonda "El Futuro del Glaucoma desde la perspectiva del Residente de Oftalmología" programada en el XV Congreso de la Sociedad Española de Glaucoma con el tema "¿Qué cirugía de glaucoma será la primera línea? Presentado de forma telemática el día 14 de mayo de 2020 en formato webinar.
**LUGAR, FECHA:** 15 Congreso de la Sociedad Española de Glaucoma (Palma de Mallorca, del 5 al 7 de marzo de 2020). Presentado de manera telemática el día 14 de mayo de 2020 en formato webinar por suspensión del Congreso por pandemia COVID-19.

**AUTORES**: Vidal-Sanz, Manuel A.; **Vidal-Villegas, Beatriz**; Di Pierdomenico, Johnny; Gallego-Ortega, Alejandro; Galindo-Romero, Caridad; Bernal-Garro, Jose M.; Agudo-Barriuso, Marta; Martinez de la Casa, Jose Maria; Maria Garcia-Feijo, Jose; Paz Villegas-Perez, Maria
**TITULO:** 7,8-Dihydroxyflavone protects axotomy-induced retinal ganglion cell loss in adult albino rats
**PUBLICACIÓN**: Investigative Ophthalmology & Visual Science Jun 2020;61:7.
**CONGRESO**: Annual Meeting of the Association-for-Research-in-Vision-and-Ophthalmology (ARVO) 2020.
**LUGAR, FECHA**: Congreso On line.

**AUTORES:** Burgos Blasco B, **Vidal Villegas B**, Oribio-Quinto Carlos Alberto, Arriola Villalobos Pedro.
**TITULO:** El efecto del uso de mascarilla en la estabilidad de la película lagrimal en pacientes con ojo seco moderado a grave.
**TIPO DE PARTICIPACIÓN:** Poster. Presentado de forma telemática
**LUGAR, FECHA:** 2º Congreso Virtual (por pandemia COVID-19) Nacional Multidisciplinar COVID19 de las Sociedades Científicas de España (12 de Junio al 16 Abril 2021).

**AUTORES: Vidal-Villegas B**, Di Pierdomenico J, Gallego-Ortega A, Galindo-Romero C, Martínez de la Casa JM, García-Feijoo J, Villegas-Pérez MP, Vidal-Sanz M.
**TITULO:** Systemic Administration of 7,8-Dihydroxyflavone Protects Adult Rat Retinal Ganglion Cells from Axotomy-induced Loss.
**TIPO DE PARTICIPACIÓN:** Comunicación oral. Presentado de manera telemática
**PUBLICACIÓN**: Ophthalmic Res 2021;64 (suppl 1):1-120. doi: 10.1159/000517823
**CONGRESO:** VII International Congress SIREV (Sociedad de Investigación en Retina y Ciencias de la Visión) Congress.
**LUGAR, FECHA**: Universidad de Murcia, Murcia. 24-26 de junio de 2021.

## PREMIOS Y BECAS/SCHOLARSHIPS AND AWARDS

**Premio Young Investigator Award del Congreso Anual (2019) de la European Association for Vision and Eye Research (EVER) a la Comunicación Oral**: «Short and long term effects of NMDA-induced retinal excitotoxicity on melanopsin and nonmelanopsin containing retinal ganglion cells». Autores: **Beatriz Vidal-Villegas**, Johnny Di Pierdomenico, Juan Antonio Miralles de Imperial-Ollero, Jose Manuel Bernal-Garro, María Paz Villegas-Pérez, Manuel Vidal-Sanz. XXII EVER Congress, Nice Acropolis Convention Centre, 1 esplanade Kennedy, 06302 Nice cedex 4, France. Niza, 17 al 19 de octubre de 2019.

**Premio a la mejor comunicación en panel de la Reunión Anual (2019) de la Sociedad Oftalmológica de Madrid** a la comunicación "Biomarcadores de glaucoma primario de ángulo abierto y pseudoexfoliativo en lágrima y humor acuoso" de los autores**: Vidal Villegas B**, Burgos Blasco B, Moreno Morillo FJ, Sáenz-Francés-San Baldomero F y Martinez de la Casa JM. Reunión anual de la Sociedad Oftalmológica de Madrid, 13 de Diciembre 2019, Círculo de Bellas Artes, Calle de Alcalá, 42, 28014 Madrid.

**Segundo premio THEA-SEG a las mejores publicaciones en glaucoma del XV Congreso (2020) de la Sociedad Española de Glaucoma por el artículo** titulado: "Melanopsin$^{+}$RGCs are fully Resistant to NMDA-Induced Excitotoxicity" publicado por los autores: **Vidal-Villegas B**, Di Pierdomenico J, Miralles de Imperial-Ollero JA, Ortín-Martínez A, Nadal-Nicolás FM, Bernal-Garro JM, Cuenca Navarro N, Villegas-Pérez MP y Vidal-Sanz M en el International Journal of Molecular Sciences. 2019 Jun 20;20(12):3012. doi: 10.3390/ijms20123012. PMID: 31226772. XV Congreso (Virtual por pandemia COVID) de la Sociedad Española de Glaucoma, 5-7 de marzo de 2020.

**Beca de la Sociedad Española de Glaucoma para Jóvenes investigadores del año 2020** para realizar una estancia de investigación en el extranjero. XV Congreso (Virtual por pandemia COVID) de la Sociedad Española de Glaucoma, 5-7 de marzo de 2020. Estancia realizada durante los meses de junio, julio y agosto 2021 en el Imperial College Ophthalmic Research Group (ICORG) del Western Eye Hospital de Londres.

## VI. List of Abbreviations/ Abreviaturas

| | | | |
|---|---|---|---|
| BDNF | Brain Derived Neurotrophic Factor | µ | Microns |
| Brn3a | Brain specific homeobox 3 a | mM | miliMolar |
| Brn3b | Brain specific homeobox 3 b | mRNA | Messenger RNA |
| Brn3a$^{+}$RGC(s) | Brn3a positive Retinal Ganglion Cell(s) by immunohistochemistry | m$^{+}$RGC(s) | Melanopsin positive Retinal Ganglion Cell(s) by immunohistochemistry |
| Brn3a$^{-}$RGC(s) | Brn3a negative Retinal Ganglion Cells by immunohistochemistry | MW | Molecular Weight |
| CGR | Células Ganglionares de la Retina | M1-6 | Subtypes of ipRGCs |
| CGRif | Células Ganglionares de la Retina intrínsecamente fotosensibles | NT4/5 | Neurotrophin 4/5 |
| CGRBrn3a$^{+}$ | Células Ganglionares de la Retina Brn3a positivas por inmunocitoquímica | NFI | No formadoras de imagen |
| CGRm$^{+}$ | Células Ganglionares de la Retina melanopsina positivas por inmunocitoquímica | NIF | Non image forming |
| CNS | Central Nervous System | ONL | Outer Nuclear Layer |
| CNTF | Ciliary Neurotrophic Factor | Opn4 | Melanopsin gene |
| dGM1 | Displaced Giant M1 ipRGC | Opn4L | Melanopsin gene isoform L |
| DHF | 7,8-Dihydroxyflavone | Opn4S | Melanopsin gene isoform S |
| dM1 | Displaced M1 ipRGC | OPN | Olivary Pretectal Nucleus |
| dLGN | dorsal Lateral Geniculate Nucleus | OSL | Outer Segment Layer |
| ELM | External Limiting Membrane | PACAP | Pituitary adenylate cyclase-activating polypeptide |

LIST OF ABBREVIATIONS

| | | | |
|---|---|---|---|
| ERG | Electroretinogram | PHbN | Perihabenular nucleus |
| FI | Formadoras de Imagen | PNS | Peripheral Nervous System |
| GCL | Ganglion Cell Layer | RGC(s) | Retinal Ganglion Cell(s) |
| IF | Image-Forming | RNA | Ribonucleic Acid |
| IGL | Intergeniculate Leaflet | RNFL | Retinal Nerve Fibre Layer |
| ILM | Internal Limiting Membrane | RPE | Retinal Pigment Epithelium |
| INL | Inner Nuclear Layer | S | Short wavelength absorbing (cones/opsin) |
| IPL | Inner Plexiform Layer | SD-OCT | Spectral Domain-Optic Coherence Tomography |
| i.p. | Intraperitoneal | SC | Superior Colliculus |
| ipRGCs | Intrinsically photosensitive Retinal Ganglion Cells | SCN | Suprachiasmatic Nucleus |
| L | Long wavelength absorbing (cones/opsin) | TrkB | Tropomyosin Related Kinase B |
| LGN | Lateral Geniculate Nucleus | VF | Visual Functions |
| M | Medium wavelength absorbing (cones/opsin) | VLPO | Ventrolateral Preoptic Nucleus |

## RESUMEN

**Introducción:**

Las células ganglionares de la retina (CGR) son las únicas células de la retina que envían la información de la retina al cerebro y por ello son indispensables para la visión. Se trata de una población heterogénea ya que se ha documentado que comprende hasta 46 tipos celulares diferentes en el ratón. Los diferentes tipos de CGR codifican un aspecto particular de la información visual y la transmiten al cerebro para realizar funciones formadoras de imagen (FI) o no formadoras de imagen (NFI). Un tipo de CGR contiene el pigmento visual melanopsina, lo que le permite realizar fototransducción y por ello se denomina CGR intrínsecamente fotosensible (CGRif). Se han descrito hasta 6 tipos de CGRif en el ratón que realizan las funciones NFI de nuestro sistema visual. Los diferentes tipos de CGR responden de un modo diferente a diferentes tipos de lesión y también a la neuroprotección.

**Objetivos:**

El objetivo principal de esta Tesis ha sido la caracterización en la rata Sprague-Dawley de la respuesta de dos poblaciones de CGR: las que expresan el factor de transcripción Brn3a (CGRBrn3a$^+$), que representan la mayoría de las CGR y las que expresan melanopsina (CGRm$^+$), que representan solamente un 2.5% de las CGR y que en su mayoría no expresan Brn3a, a dos tipos de lesión, la excitotoxicidad y la sección del nervio óptico, así como a la neuroprotección con 7,8 dihidroxiflavona (DHF).

**Métodos y Resultados:**

En esta Tesis presentamos tres artículos de investigación:

En el primer artículo, hemos investigado la respuesta a corto y largo plazo (hasta 15 meses) de las CGRBrn3a$^+$ y de las CGRm$^+$ a la lesión excitotóxica inducida por una inyección intravítrea de 5 µl de una solución 100mM de N-Metil-D-Aspartato (NMDA). Además, hemos estudiado mediante tomografía óptica de coherencia de dominio espectral (SD-OCT) el efecto a largo plazo de la excitotoxicidad en la estructura de la retina. Documentamos que mientras que un 80% de las CGRBrn3a$^+$ mueren en los primeros 7 días tras la lesión, las CGRm$^+$ muestran una disminución transitoria de la expresión de melanopsina durante 10 días pero no mueren tras la lesión. Además, mostramos la capacidad de la SD-OCT para documentar una disminución del espesor de la retina y en especial de las capas internas a largo plazo tras la lesión excitotóxica.

En el segundo artículo realizamos una revisión de las CGRif, células descubiertas recientemente y cuyas características y funciones no son del todo conocidas por lo que se prevé que continúen siendo un objetivo preferente de investigación en el futuro. Hacemos notar que las técnicas inmunohistoquímicas habituales permiten identificar principalmente los tipos M1-M3, pero no los tipos M4-M6 pues expresan cantidades de melanopsina muy pequeñas.

En el tercer artículo hemos investigado la respuesta de las CGRBrn3a$^+$ y CGRm$^+$ a la sección del nervio óptico y su posible neuroprotección con el agonista selectivo del receptor TrkB de las neurotrofinas, la DHF, durante 60 días. Documentamos que tras la sección del nervio óptico un 90% de CGRBrn3a$^+$ mueren y además presentan un curso de degeneración temporal similar al descrito en estudios previos, pero que sólo el 60% de las CGRm$^+$ mueren y además presentan una disminución transitoria en la expresión de melanopsina en los primeros 10 días. Además, documentamos que el DHF muestra un potente efecto neuroprotector sobre las CGRBrn3a$^+$ y las CGRm$^+$ y que, aunque este efecto neuroprotector se observa solo durante 21 días para las CGRBrn3a$^+$, es permanente para las CGRm$^+$. Por último, documentamos que la DHF produce una estimulación (fosforilación) del receptor TrkB, por lo que es posible que su efecto neuroprotector se deba a su efecto agonista sobre estos receptores.

**Discusión y conclusiones:**

Las CGRBrn3a$^+$ y las CGRm$^+$ tienen diferentes respuestas a dos lesiones: la excitotoxicidad producida por la inyección intravítrea de NMDA y la sección del nervio óptico. La lesión excitotóxica produce una muerte de la mayoría de las CGRBrn3a$^+$ pero no produce muerte de las CGRm$^+$ y esta degeneración retiniana puede ser documentada mediante SD-OCT. La sección del nervio óptico produce una muerte de la mayoría de las CGRBrn3a$^+$ y de solo un 60% de las CGRm$^+$. La DHF tiene un efecto neuroprotector después de la sección del nervio óptico sobre las dos poblaciones de CGR, pero su duración es de solo 21 días para las CGRBrn3a$^+$ y sin embargo es permanente para las CGRm$^+$. Las CGRBrn3a$^+$ y CGRm$^+$ responden pues de forma diferente a la lesión excitotóxica y a la sección del nervio óptico y también a la neuroprotección con DHF después de la sección del nervio óptico

## ABSTRACT

**Introduction:**

The Retinal Ganglion Cells (RGCs) are the only retinal cells that send information to the brain and thus are essential for vision. It is a heterogeneous population since up to 46 different RGC types have been documented in mice. The different RGC types encode a particular aspect of visual information and send it to the brain, where they contribute to image forming (IF) and non-image forming (NIF) visual functions. A type of RGC contains the visual pigment melanopsin and performs phototransduction and thus has been named intrinsically photosensitive RGC (ipRGC). Six types of ipRGCs have been described in mice that perform the NIF functions of the visual system. Recent studies have documented that the different RGC types respond differently to different types of injury and to neuroprotection.

**Objectives:**

The main objective of this Thesis has been to characterize in Sprague-Dawley rats the response of two different RGC populations: the RGCs that express the transcription factor Brn3a (Brn3a$^+$RGCs) that represent the great majority of RGCs, and those that express melanopsin (m$^+$RGCs), that represent only 2.5% of the RGC population and that in general do not express Brn3a, to two different types of lesions, excitotocicity and optic nerve section, and to their neuroprotection with 7,8 dihidroxyflavone (DHF).

**Methods and results:**

In this Thesis we present three research articles:

In the first article we have investigated the short and long-term (up to 15 months) response of the Brn3a$^+$RGCs and the m$^+$RGCs to an excitotoxic injury induced by intravitreal injection of 5 µl of a 100mM solution of N-Methyl-D-Aspartate (NMDA). Also, we have studied using spectral domain optic coherence tomography (SD-OCT) the long term excitotoxic effects on retinal structure. We document that while 80% of the Brn3a$^+$RGC population die in the first 7 days after the lesion, the m$^+$RGC population shows a transient melanopsin downregulation for 10 days but do not die. We also show the capability of the SD-OCT to document decreased retinal thickness and specially the thinning of the inner retinal layers long term after the excitotoxic lesion.

In the second article, we have conducted a comprehensive review of the ipRGCs, which were discovered two decades ago, and whose characteristics and functions are

not well known yet and thus it is foreseeable that they continue to be a preferential research objective in the near future. We point out that the classic immunocytochemical techniques used at present for ipRGC labelling allow the identification of the M1-M3 types, but not of the M4-M6 types, since they express very small amounts of melanopsin.

In the third article, we have investigated the response of the Brn3a$^+$RGCs and m$^+$RGCs to optic nerve section and their neuroprotection with the TrkB selective agonist DHF for 60 days. We document that after optic nerve section 90% of the Brn3a$^+$RGC population dies exhibiting the typical course of degeneration described in previous studies, but that only 60% of the m$^+$RGC die and also show a transient downregulation of melanopsin expression in the first 10 days. Furthermore, we show that DHF has a potent neuroprotective effect on Brn3a$^+$RGCs and m$^+$RGCs and that, although this effect is observed only in the first 21 days for the Brn3a$^+$RGCs, it is permanent for the m$^+$RGCs. Finally, we document that DHF causes the stimulation (phosphorylation) of the TrkB receptor and thus it is possible that DHF neuroprotective effects are due to activation of this receptor.

**Discussion and Conclusions:**

The Brn3a$^+$RGC and m$^+$RGC show different responses to two different lesions: excitotoxicity induced by intravitreal NMDA injection and optic nerve section. The excitotoxic lesion causes death of the majority of the Brn3a$^+$RGC but not of the m$^+$RGC and this degeneration can be documented with SD-OCT. Optic nerve section causes death of the majority of the Brn3a$^+$RGCs but of only 60% of the m$^+$RGCs. The administration of DHF has neuroprotective effects on both populations, but the duration of its effect is of only 21 days for the Brn3a$^+$RGC population and permanent for the m$^+$RGC population. Therefore, the Brn3a$^+$RGCs and the m$^+$RGCs respond differently to excitotoxicity and optic nerve section and also to neuroprotection with DHF after optic nerve section.

# 1. INTRODUCTION

In this Thesis we study primarily the retinal ganglion cells (RGCs), their response to different insults and also their neuroprotection. In this introduction we review some information relevant to the subject. We start assessing the central nervous system and its components, the visual system with its different visual pathways and the retina. Later, we survey the different types of RGCs and specifically the intrinsically photosensitive RGCs (ipRGCs). We continue with special characteristics of the rat visual system, the model employed in these studies. Finally, we review the two types of RGC lesions and the neuroprotective strategy that we use.

## 1.1. The Central Nervous System

The central nervous system (CNS) is the part of the nervous system that includes the brain, the spinal cord, the cerebellum and the olfactory and optic nerves. The rest, situated outside skull and spine, is the peripheral nervous system (PNS)[1]. Both CNS and PNS contain neurons and supporting cells that are known as glial cells (Figure 1). Neurons are located in the CNS grey matter, while axons are contained within the white matter.

The neurons can be divided into soma, dendrites and axon. The soma contains the nucleus, most of the mitochondria and organelles. The dendrites are ramified extensions of the soma. The axons are polarized nervous fibres that transmit information or nerve impulses to other neurons via synapsis (Figure 1).

There are three glial cell types in the CNS: astrocytes, oligodendrocytes and microglial cells, whilst the PNS contains only one type of glial cell: the Schwann cell. The glial cells that are in charge of the production of myelin to envelop the axons, are different

in the CNS and the PNS: oligodendrocytes and Schwann cells respectively (Figure 1)[1–4].

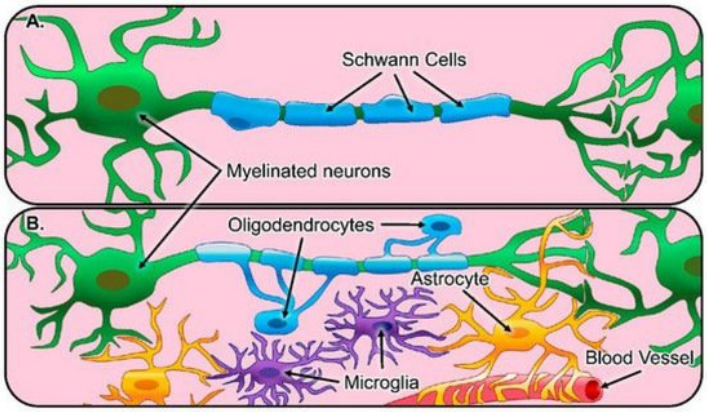


Figure 1. From: Gradišnik L et al (2021)[4] Neuronal and glial cell relationships A. Peripheral Nervous System B. Central Nervous System.

Neuronal cells are highly specialized nerve cells that cannot divide and thus, when a neuron dies, the function performed or carried out by that neuron is lost. Neurons can be injured in their cell body, dendrites or axonal projection, which may cause degeneration and death. There are two types of axon degeneration: anterior (or Wallerian) and retrograde degeneration[1,5–7]. The lesion of the axonal projection causes anterograde degeneration in the axon distal to site of injury, and retrograde degeneration of the axon proximal to the lesion and attached to the cell body (Figure 2). This retrograde degeneration concludes sometimes with the death of the parent neuron, while both cause the disconnection of the neuronal circuit formed by that neuron[8].

The visual system is contained within the CNS and the long-projecting neurons of the retina are the RGCs whose cell bodies are in the retina; their axons travel through the optic nerve, chiasm and tract (see section 2). Lesions to the RGC axons cause the anterograde and retrograde degeneration of the parent RGCs and subsequently

blindness. However, the RGCs that survive the injury could in theory regenerate and restore vision, but the regenerative capacities of RGCs are very variable depending on the animal species considered. Lower vertebrates like fish and amphibians have important regenerative capacities: the RGCs that survive the injury regenerate extensively with the return of vision[6,9,10]. Higher vertebrates: mammals, rodents and humans show massive RGC death and have very limited regenerative capacities[6,10–12]. This difference between lower vertebrates and mammals is believed to be due both to genetic and environmental differences between these species[10].

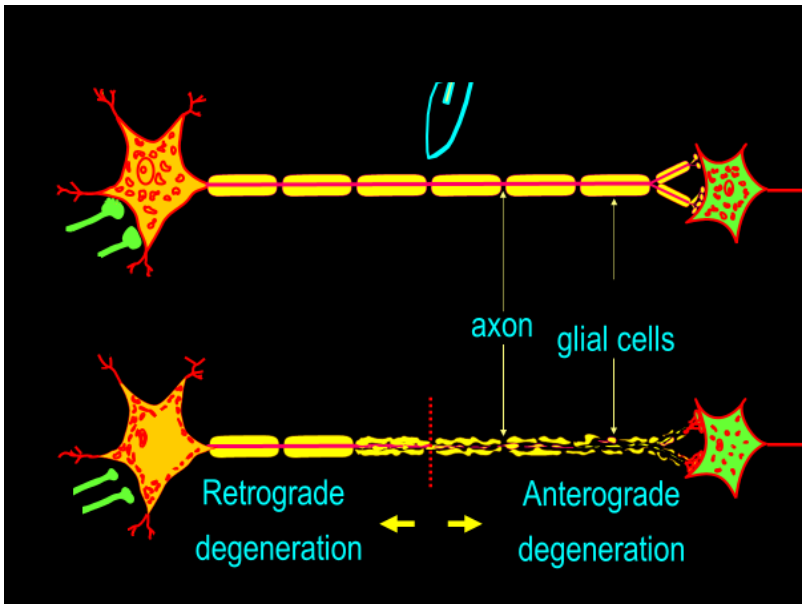


Figure 2. Retrograde and anterograde neuronal degeneration (Scheme from Albert J Aguayo's Laboratory)

In adult mammals, the neuronal regenerative response differs between the CNS and the PNS. The axons of the PNS regenerate extensively and this is followed by the return of function, but CNS axons show very limited regenerative capacities. This is believed to be in part the result of the different glial environments of CNS and PNS that stimulates regrowth in the PNS but not in the CNS, where a glial scar is formed [5,6,10,12–17] (Figure 3). However, mammalian central neurons have regenerative

capacities as demonstrated in rats, if a peripheral nerve segment is grafted to the ocular stump of sectioned optic nerve there is extensive RGC axonal regeneration, and the regenerated axons can innervate their target territories in the brain and establish functional synapses that are permanent [12,16,18,19].

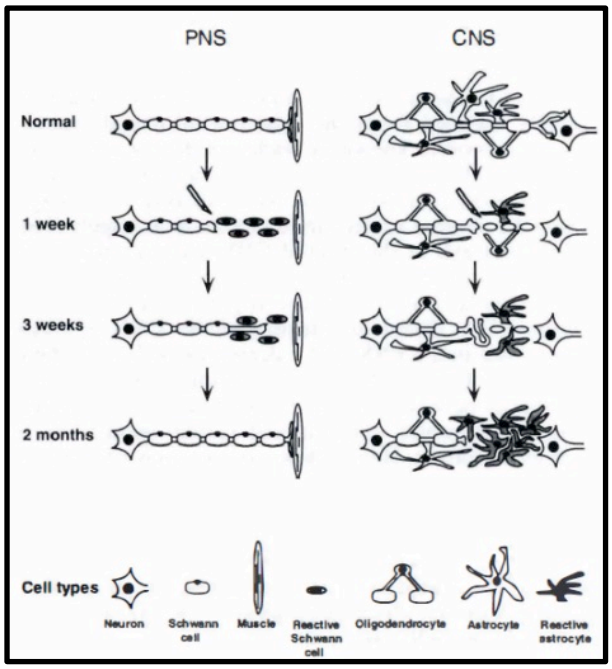


Figure 3 From: Frisen J. et al., 1997. Neuronal degeneration in the Peripheral Nervous System (PNS) and the Central Nervous System (CNS)

### 1.2. The Visual System

The visual system belongs to the CNS, it is made up of central neurons and their axons are myelinated by oligodendrocytes. It is composed of, from periphery to the brain, the retina, optic nerve, optic chiasm, optic tract, optic radiations and the different projection zones in cortical and subcortical areas of the brain. These structures allow us to perceive and integrate the visual information from our surroundings. The visual system converts light into electrical stimuli that are processed in the form of image and non-image forming functions (see section 2.1.). The retina converts light into electrical stimuli through a process named phototransduction and begins the light

information processing. The electrical information in the retina is conveyed to the RGCs whose axons leave the eye through the optic disk[20–22]. The optic nerve is thus composed of the axons of the RGC that carry the visual information to different centres in the brain. In humans, the axonal projection of the nasal retina (60% of the axons in the optic nerve) decussates at the chiasm and forms the optic tract along with the ipsilateral projection of the temporal retina. Therefore, each optic tract carries the information of the contralateral visual field. From the optic tract, the RGC axons are directed to different structures in the diencephalon and midbrain that have different functional roles and form different image forming and non-image forming pathways[1,23].

### 1.2.1. Image-forming and Non image-forming Visual Pathways

The information sent by the retina to the brain is necessary for the formation of images (image-forming, IF) of our conscious visual perception of the world around us, but it serves also for visual functions that do not form images (non-image-forming, NIF), that however have important implications in our physiology and everyday behaviour[1,24,25].

In humans, the vast majority of our RGCs (about 90%) work towards the IF of our visual environment, this is our conscious visual perception, the location and perception of shapes, their texture, colour, movement and perspective. These RGCs receive visual information from the bipolar cells and project to the dorsolateral geniculate nucleus (dLGN) of the thalamus, where they synapse (Figure 4)[1,26]. The axons of the dLGN neurons travel through a portion of the internal capsule named the optic radiation and terminate in the primary visual cortex (striate cortex, Brodmann's area 17 or V1) situated in the interhemispheric portion of the occipital lobe, at both sides of the

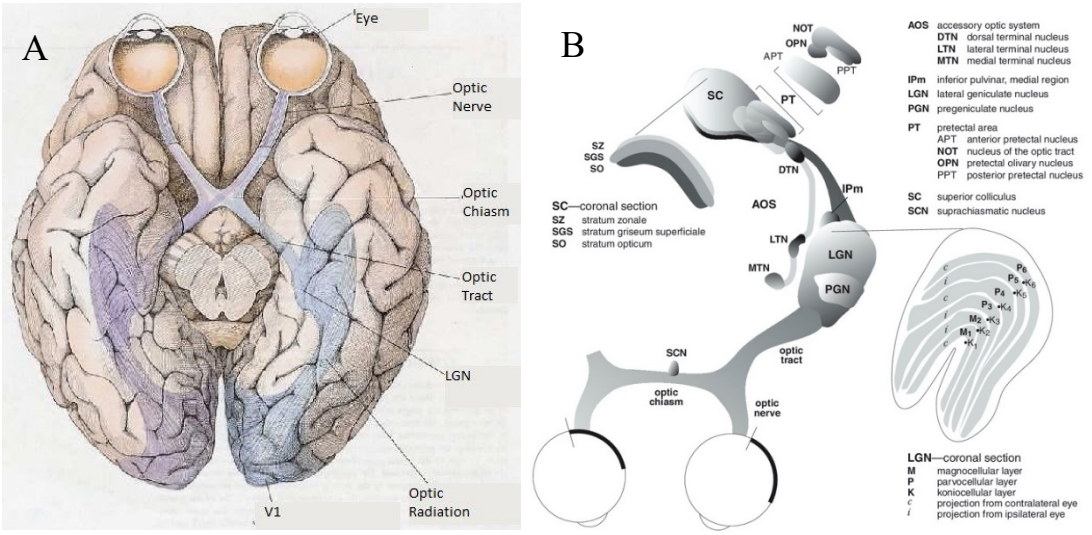


Figure 4. A: Human Visual System[28]. From: Hubel DH 2000. B: Retinal Ganglion Cell Projections in the Human Visual System[29]. From: Dacey D 2011. Abbreviations embedded.

calcarine fissure. From there, the visual information passes on to secondary visual cortex areas (extrastriate cortex: V2-V6). There is some degree of visual information processing at every level of the visual system, with further complexity from the retina to the cortex[1,27].

Around ten per cent of RGC axons also carry IF visual information; they do not terminate in the dLGN but in other brain nuclei such as the superior colliculus (SC; quadrigeminal tubercle in humans) (Figure 4) where they mediate reflex maintenance tasks, of which we are not aware, but which also contribute to IF visual functions, as they are fundamental for our vision, such as our eye movements in front of a new visual scene or to stabilize a moving object, or to accommodate and converge for objects in proximity, or the opposite, to focus on distant objects [1,30]. All nuclei that participate in IF visual functions generally have a topographic representation of the retinal surface, also called retinotopic map[31].

Finally, a small proportion of the RGC axons in the optic nerve (between 0.5 and 1.5%[32]) belong to the intrinsically photosensitive class of RGCs (ipRGCs, see section 2.2.4.) and carry NIF visual information to other brain nuclei[32] (see section 2.2.4.4.). The most important NIF nuclei that receive projections are: i) the olivary pretectal nucleus (OPN) that controls the pupillary reflex and projects to the Edinger-Westphal nucleus; ii) the suprachiasmatic nucleus (SCN) of the diencephalon that regulates most, if not all, circadian rhythms of our body and also sleep; iii) the ventrolateral preoptic nucleus (VLPO), which is important for sleep regulation[33,34](Figure 4). There are other NIF nuclei, but they are less well characterized. In this way the ipRGCs use the intensity of environmental light (irradiance) to regulate behaviours and physiological functions. These NIF circuits do not form images and are not related to the conscious perception of vision, but they mediate important functions, such as: setting of the central circadian clock, behavioural responses to changes in the environment, and regulation of the pupillary photomotor reflex[35]. Out circadian rhythm is an endogenous biological cycle that synchronizes our body to solar light and its 24-hour cycle, and it is of great importance because it regulates many physiological mechanisms[36].

Many other behaviours also depend on our perception of the level of ambient light such as: our mood and cognitive abilities[37], body temperature [38], induction of sleep and alertness[39], inhibition of motor activity (masking) and aversion to light [40], or exacerbation of migraines and photophobia [41].

### 1.2.2. The Retina

The retina is the most peripheral structure of the visual system. It is situated in the innermost part of the eye and is surrounded externally by the choroid and sclera. The

choroid is a vascular structure that provides nutrition to the external retinal layers, while the sclera is mainly a fibrous protecting structure.

#### 1.2.2.1. Retinal Anatomy and Vascularization

The retina is part of the visual system and of the CNS, but it is isolated within the eye, which makes it a unique model for studying neurodegeneration and neuroprotection for its relatively easy access. It is a diaphanous structure, except for the blood cells that are contained in the blood vessels and can be observed in vivo through the pupil using an ophthalmoscope (Figure 5). The orange reflex observed corresponds to the outer most retinal layer, the retinal pigment epithelium which is normally pigmented, and the underlying choroidal vasculature[21].

Each vertebrate has some variant of topographic specialization of its retina making it unique, but the basic layering is constant throughout [20–22,42–44]. In human and primates there is a four-lobed retino-vascular organization and a specialized non-vascularized central area named macula (Fig 5A), whereas rodents show a radial retinovascular organization[45] (Fig 5B).

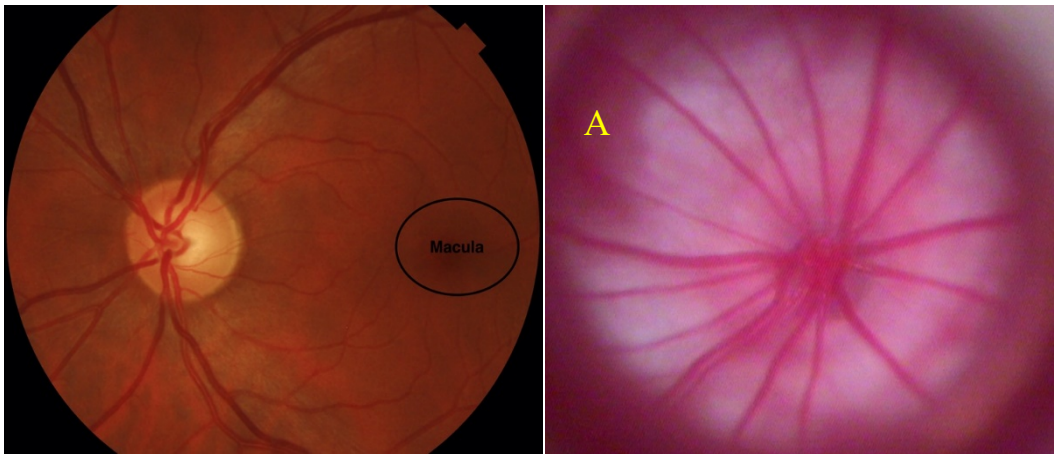


Figure 5. Eye fundus of a normal patient (A) and of a normal albino Sprague-Dawley rat (B).

The retina can be divided into 10 layers [20–22,42] (Figure 6) that from the inner to the outer surface are: internal limiting membrane (ILM), retinal nerve fibre layer (RNFL),

ganglion cell layer (GCL), inner plexiform layer (IPL), inner nuclear layer (INL), outer plexiform layer (OPL), outer nuclear layer (ONL), external limiting membrane (ELM), photoreceptor outer segments layer (OSL), and retinal pigment epithelium (RPE). The RNFL contains the axons of the RGCs; and the GCL contains the cell bodies of the RGCs and displaced amacrine cells, while their dendrites are in the IPL. The INL contains the cell bodies of displaced RGCs, amacrine cells, bipolar cells, horizontal cells and Müller cells. Displaced RGCs and amacrine cells extend their dendritic processes in the IPL and the bipolar cells send their axons to this layer to make synapsis with amacrine and RGCs. Müller cells are macroglial cells characteristic of the retina with long processes that extend through all the retinal layers. The OPL contains the dendritic trees of the bipolar and horizontal cells that make synapsis there with the axonal projections of the photorreceptors. The ONL contains the nuclei of the photoreceptor cells while the OSL is formed by their outer segments. The RPE is formed by a monolayer of neuroepithelial cells with tight junctions between them, and although it is always included in the description of retinal layers, it is not retinal tissue because it has a different embryologic origin. The ELM is formed by tight junctions formed between Müller cells and photoreceptors. The ILM is formed by the end feet of Müller cells.

The retina contains five types of neurons: RGCs, amacrine cells, bipolar cells, horizontal cells and photoreceptors; and three types of glial cells. The macroglial cells are astrocytes, whose cell bodies and dendrites are located in the RNFL and GCL; and the Müller cells with their cell bodies in the inner nuclear layer ang prolongations that span throughout all the retinal layers. The microglial cells are normally observed in the OPL, IPL, GCL and RNFL46–48.

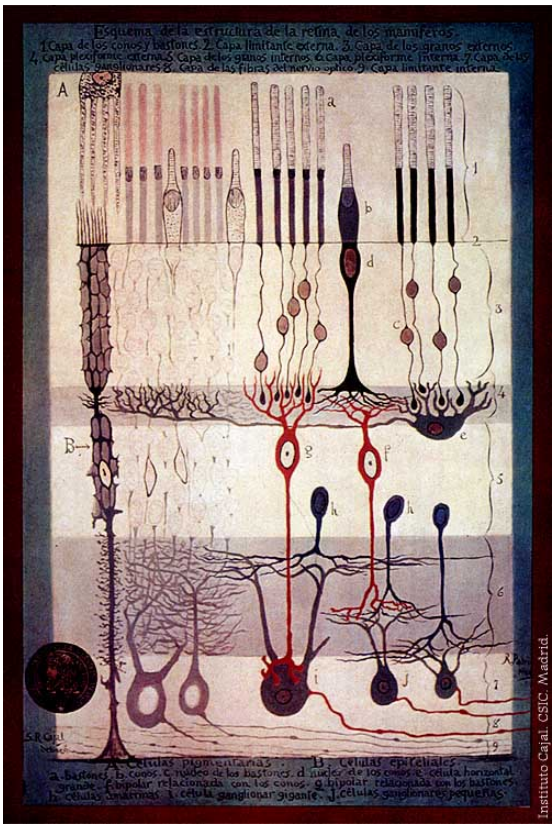


Figure 6. The Retinal Cells and Layers. From: Ramon y Cajal S (1900)[43].

The retina is supplied by two vascular systems that do not connect: the retinal vessels and the choriocapillaris[49] (Figure 7). The retinal vessels supply the two inner thirds of the retina. The outer third of the retina that contains the photoreceptors depends on the choroid vascular supply and hence, the external retina is nourished by the choriocapillaris [21,50]. The retinal vessels originate from the central retinal artery that enters the eye through the optic nerve. However, some individuals may also have small cilio-retinal arteries that enter the eye around the optic nerve to supply the papillo-macular area and that come from the posterior ciliary arteries[51]. The retinal vessels form three plexuses in the retina: superficial, intermediate and deep that show communications between them. The deep plexus is situated at the level of the ganglion cell and nerve fibre layers; and the intermediate and deep are located on either side of

the inner nuclear layer[21,49,50] (Figure 7). There are two blood retinal barriers: an external barrier formed by the RPE and the ELM, and the inner barrier formed by the retinal junctions of the vascular endothelial cells of the retinal vessels and the surrounding cells: perycites and astrocytes[52].

### 1.2.2.2. Light processing in the retina

Two retinal neurons are capable of capturing electromagnetic energy (wavelengths within the visible spectrum) and transform it into electrical energy in a process called phototransduction: photoreceptors and intrinsically photosensitive RGCs (ipRGCs, see section 2.2.4.)[34,35,53]. Photoreceptors are to a great extent implicated in IF functions, while ipRGCs are mostly dedicated to NIF functions.

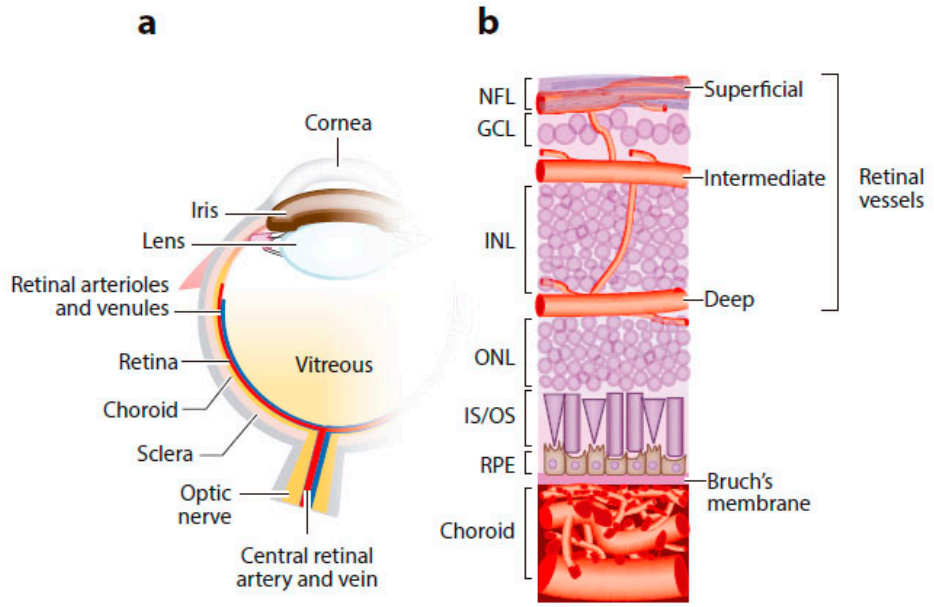


Figure 7. Modified from: Sun and Smith, 2018[49]. a): Cross-section of a Human Eye. B): The retinal layers and vascular plexuses.

For image-forming functions (see also section 2.1.) the incoming rays of light have to travel through all the retinal layers to reach the outermost layer of the photoreceptors, (cones and rods; Figures 6, 7) the OSL. There, rods and cones convert this light into electric information (see next paragraph) and pass it on to bipolar cells which in turn

transmit these impulses to the ganglion cells. This is the vertical retinal circuit, formed by photoreceptors, bipolar and ganglion cells, which is modulated by the rest of cells in the retina [54]. In particular by two retinal cells: the horizontal and the amacrine cells form transversal retinal circuits in the OPL and the IPL, respectively, and contribute to the processing of the visual information in the retina[20–22,54].

Photoreceptors are specialized neurons full of visual pigments, named opsins in the case of cones and rhodopsin in the case of rods. These pigments absorb light of different wavelengths showing an absorption peak each (Figure 8). In humans there are three types of cones that contain three different opsins that maximally absorb light with short (S; ~420 nm), medium (M; ~534 nm) or long (L; ~564 nm) wavelengths, thus affording us vision in colour. Rods contain only one type of visual pigment: rhodopsin that absorbs maximally light with 498 nm, a spectrum between those of the short and medium wavelength opsins [20–22,53](Figure 8).

In rods and cones, the uptake of a photon by visual pigments induces a conformational change in the molecule that results in the activation of a G protein. This, in turn, sets off an intracellular cascade that ends in a transient change in the photoreceptor membrane potential (hyperpolarization), a signal that serves as interneuron communication and is transmitted to bipolar cells and from them to retinal ganglion cells and the brain[20–22].

For non-image forming functions (see also section 2.1.), the light that enters the eye does not have to go through the retina, because it is captured by one type of RGC, the named ipRGC, which is situated in the innermost retinal layers, the GCL and in the INL. These neurons contain a visual pigment named melanopsin that absorbs light maximally at ~480 nm, a spectrum between those of the short wavelength opsin

and of rods[53] (Figure 8). When melanopsin is stimulated by photons it activates a G protein like the opsins in rods and cones. However, this phototransduction culminates in ipRGC depolarization, similarly to invertebrates and contrary to what happens in rods and cones where light induces hyperpolarization. This depolarization is transmitted by the RGCs axons to different parts of the brain[53,55–57] (see section 2.1.).

It was thought that the IF and the NIF constituted independent circuits in the retina, but this is not the case[33]. The ipRGCs receive input also through bipolar cells from the photoreceptors (see section 2.2.4.) and there is also evidence that the information of the ipRGCs reaches the primary visual cortex (V1) where they could modulate the IF visual information [53,57].

#### 1.2.2.3. The Retinal Ganglion Cells

The retina and the visual system belong to the CNS. The RGCs are thus frequently used as a model in which to study aetiology and pathology of different types of CNS lesions, and the efficacy of prevention strategies and experimental treatments for neuroprotection.

The information processed in the retina is transmitted to the brain encoded in a train of nerve impulses or action potentials by the axons of the RGCs. Axons from the RGCs have a small intraretinal unmyelinated portion which constitutes the RNFL and coalesce at the papilla where they form the optic nerve. The axons of the RGCs are the only axons that leave the retina. As they enter the laminar part of the optic nerve head, they are myelin coated by oligodendrocytes and remain that way through the optic nerve and optic tract[58]. The number of axons in the optic disk varies in humans between 770,000 and 1,700,000 axons[59]. Since RGC axons are the only axons coursing through

the optic nerve and in this part of the visual system there are no axonal exits, optic nerve injury affects the whole population of RGCs and may cause RGC retrograde degeneration (see section 1)[16,46,59–66].

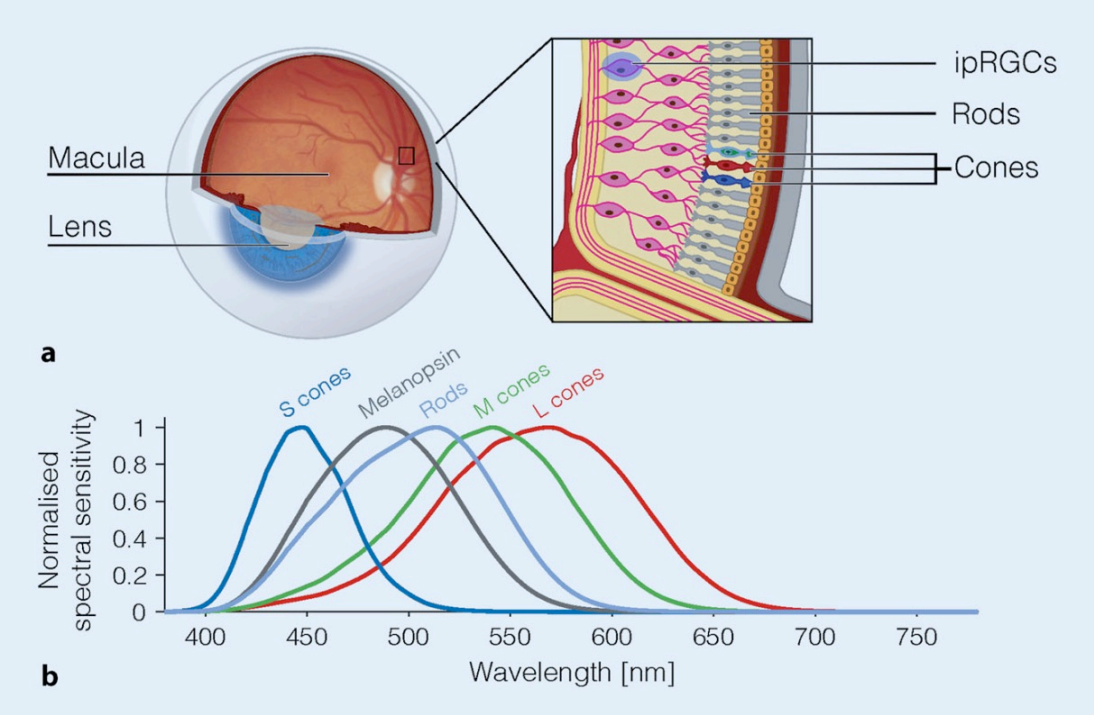


Figure 8. Spectral Sensitivities of Human Opsins. From: Blume C et al., 2019[53]

The RGCs are situated in the GCL of the retina, which has a different thickness depending on the region and species considered. In humans, in the macula it has up to eight layers, while in the periphery there is only one layer that shows cellular gaps [67]. A small percentage of RGCs have their cell bodies within the INL and are thus called displaced ganglion cells[67,68].

At present, according to morphological, physiological, topographic, molecular and innervation territory criteria, up to 46 different types of RGCs have been distinguished in mice[67,69,70]. Each of these types has different morphologic features and collects different aspects of the visual scene that are transmitted in parallel forming different distinctive pathways to different subcortical regions that perform specific tasks [67,70,71].

The RGCs extract in parallel different attributes of the image like spatial contrast, colour, motion, textures, absolute light level, and deliver this information to different sites within the visual system [29,67,72].

The morphological classification distinguishes RGCs by their soma size and the characteristics of their dendritic tree [67]. Using this classification, the RGCs of the human retina have been distinguished into up to 10 different types, but only three of these (midget, parasol and small bistratified) are recognized by all authors[67]. The midget cells are small sized RGCs which are also known as P cells because they project to the parvocellular layers of the dLGN. There are two types: ON- or OFF-centre, they represent up to 80% of the RGCs in humans and subserve colour discrimination, detailed vision and depth perception. The parasol cells are large cells that are also known as M-cells because they project to the magnocellular layers of the dLGN. They account for 10% of the RGC population and specialize in motion perception and depth processing. The parasol (M-cells) and the midget cells (P-cells) resemble the α-cells and β-cells respectively described in cats [67,72,73](see next section). The small bistratified cells project to the koniocellular layers of the dLGN. These cells represent 5-10% of the RGC population and assist blue yellow colour opponency. The ipRGCs constitute 0.4-1.5% of the RGC population in humans[32], their number decreases with age[32] and have been classically described as performing NIF functions[33] (see next section). Three subtypes of these cells: M1, M2 and M4 have been described in humans[32,67,74]. These cells can be explored using chromatic pupillometry and have been reported to be resistant to some mitochondrial optic neuropathies, such as Leber hereditary optic neuropathy and autosomal dominant optic atrophy. However, these cells may die in other optic neuropathies like glaucoma and late-onset neurodegenerative disorders (Alzheimer and Parkinson diseases)[32,67,75].

#### 1.2.2.3.1 The Retinal Ganglion Cells in Rats and Mice

The RGCs form a monolayer in the retinal GCL in mice and rats, and in both there are some displaced RGCs (Dogiel's cells) in the INL[76]. These cells have been thoroughly investigated in rats, where approximately 0.5 to 2.5% of the total RGC population are displaced RGCs [65,77]. Rodents do not have a macula but they show high RGC densities, that increase from the peripheral to the central retina and thus there is a region of maximal RGC density in a semicircular region 1 mm above the optic disk, creating a visual streak [76–82]. This area expands from the nasal to the temporal retina and shows the highest RGC densities in the temporal retina, along with cone bipolar cells, and thus it is considered the "area centralis" or highly specialized area of the rodeMnt retina[76–83].

There are approximately 80,000 RGCs in the rat retina and 45,000 RGCs in the mouse retina [77–83]. These animals have many types of RGCs, and classic morpho functional techniques had allowed the differentiation of between 15 and 20 RGC types in the mammalian retina[72,84]. However, newer transcriptional labelling techniques have allowed the differentiation of up to 46 different types in mice and it is thought that there are still a few left to discover[70]. Extensive studies in the cat retina have distinguished three main morphological types: the α, β and γ cells that physiologically correspond to the X, Y and W cells [85]. In humans, the α-cells and the β-cells resemble the parasol (M-cells) and the midget cels (P-cells) respectively[67,72,73]. Most mammals contain at least these three types of RGCs and more additional cell types, such as the ipRGCs, of which there are 4 described in humans, 5 in rats and 6 in mice[32,70,75] (see next section).

Functionally, the mammalian RGCs were classified as having a centre-surround response with centre ON- or OFF-response as early as 1953 by Stephen Kuffler[86]. A typical ON-centre RGC responds to a spot of light in the centre of its receptive field with increasing numbers of action potentials, whereas in an OFF-centre RGC the response to illumination of the centre consists in the silencing of the neuron with an increase in the number of action potentials when the spot of light is turned OFF. Such an OFF-response was elicited from the surround portion of the receptive field of an ON-centre, and an ON-response could be elicited from the surround portion of the receptive field of an OFF-center RGC (Kuffler, 1953). Later it was found that the dendrites of the OFF-RGCs stratified within the outer half of the inner plexiform layer (IPL) (sublamina a) whereas the dendrites of the ON-RGCs stratified within the inner half of the IPL (sublamina b)[87], and these finding were the basis for the subdivision of the IPL in ON and OFF sublayers.

More recently, using various morphofunctional criteria, many types of RGCs have been distinguished that include: 4 types of α-RGCs (sustained ON, sustained-OFF, transient-ON and transient-OFF), 2 types of β-RGCs, 4 types of ON-OFF directionally selective (DS-RGCs), 3 types of ON DS-RGCs, 3 types of JamB-expressing RGCs (J-RGCs), orientation-sensitive RGCs, chromatically sensitive RGCs, suppressed by contrast RGCs and others[72,88].

#### 1.2.2.4. The intrinsically photosensitive RGCs

The pigment melanopsin takes its name from the melanophores of frog skin where it was discovered[89]. Shortly after this discovery, the presence of ipRGCs containing melanopsin was described in the retinas of monkeys and mice[90,91], and later in the human retina [92,93]. Melanopsin is expressed mainly in the soma and dendrites of ipRGCs[94].

The RGCs dedicated mainly to NIF visual functions or ipRGCs constitute a very small proportion of the RGCs, around 1% in humans and ≈3-6% in rodents[32,70,92,95–98] (see below). These cells are distinguished by the expression of the pigment melanopsin, encoded by the Opn4 gene. In mammals, the Opn4 gene is expressed only in the ipRGCs, differing from the frog where it was originally discovered in the skin. As reviewed before, this pigment has its light absorption peak at around 480 nm and allows the transduction of light into electrical signals (see section 2.2.2.). The ipRGCs' sensitivity to light is much lower than that of the classical photoreceptors: rods and cones[95,99]; their signal is slower, and they also have a low spatial resolution[100,101]. The ipRGCs generate depolarization in response to light stimulation of melanopsin, even in the absence of information from rods and cones, and also i*n vitro*[91]. As mentioned above, this information is conveyed to different parts of the brain (see section 2.1. and next sections).

The ipRGCs cells are also called melanopsinic RGCs ($m^+$RGC) or third photoreceptor of the retina[91,94]. However, the terms ipRGC and $m^+$RGC are not interchangeable at present. The expression of melanopsin in ipRGCs is variable: the subtypes M4, M5 and M6 show lower expression[32,57], which is beneath detection threshold by usual antibody staining methods without amplification[102]. Thus, not all the techniques used for ipRGC identification based in melanopsin content or expression can detect all the ipRGCs and the $m^+$RGCs detected in most studies represent only a proportion of the ipRGCs (M1, M2 and M3 in most studies), where M1 and M2 ipRGCs account for the majority (74 to 90%) of ipRGCs (Kim et al., 2021). Indeed, the originally described cells are now known to correspond only to the M1 subtype[95,102,103].

As mentioned before, ipRGCs project mainly to NIF nuclei (see section 2.1. and next sections). However, it has been documented that ipRGCs also project to brain regions

responsible for IF functions, such as the SC and the dLGN both in mice[104,105] and in humans[93]. In genetically modified mice (rd/rd cl), which do not have cones or rods, but do have ipRGCs, it was possible to observe a gross visual behaviour that was able to resolve visual patterns and detect contrast[104,106]. In humans they seem to contribute to the perception of brightness, spatial vision and increment the appearance of images[107].

#### 1.2.2.4.1. Functions of ipRGCs in Rats and Mice

Most of the knowledge we have on ipRGCs and their NIF and visual functions (VF) comes from studies carried out in rodents[99], mainly in mice, because of the development of genetic mouse models to selectively label or ablate these cells[33,103,108–110]. Using transgenic mice, it has been documented that ipRGCs intervene in[111]: the pupillary light reflex, neuroendocrine regulation, entrainment of circadian rhythms to light/dark cycles, and aspects of conscious visual perception[112–118]. The elimination of melanopsin expression in transgenic mice results in an attenuation of the circadian pacing and the photomotor reflex[119]; and the elimination of functional photoreception in the three photoreceptors (rods, cones and ipRGC) results in animals that fail to show any significant pupil reflex, to entrain to light/dark cycles, and to show any masking response to light[35]. Genetic ablation of the ipRGCs in mice results in a loss of NIF visual functions, demonstrating that the origin of this pathway is in the ipRGCs[120,121]. Although all ipRGCs respond to 480nM wavelengths, their response to light differs between subtypes[102,122]. Their functions also differ[111]; M1 has been described to intervene in photoentrainment and pupillary reflex[123] while M4 enhances contrast sensitivity[117] (see next section).

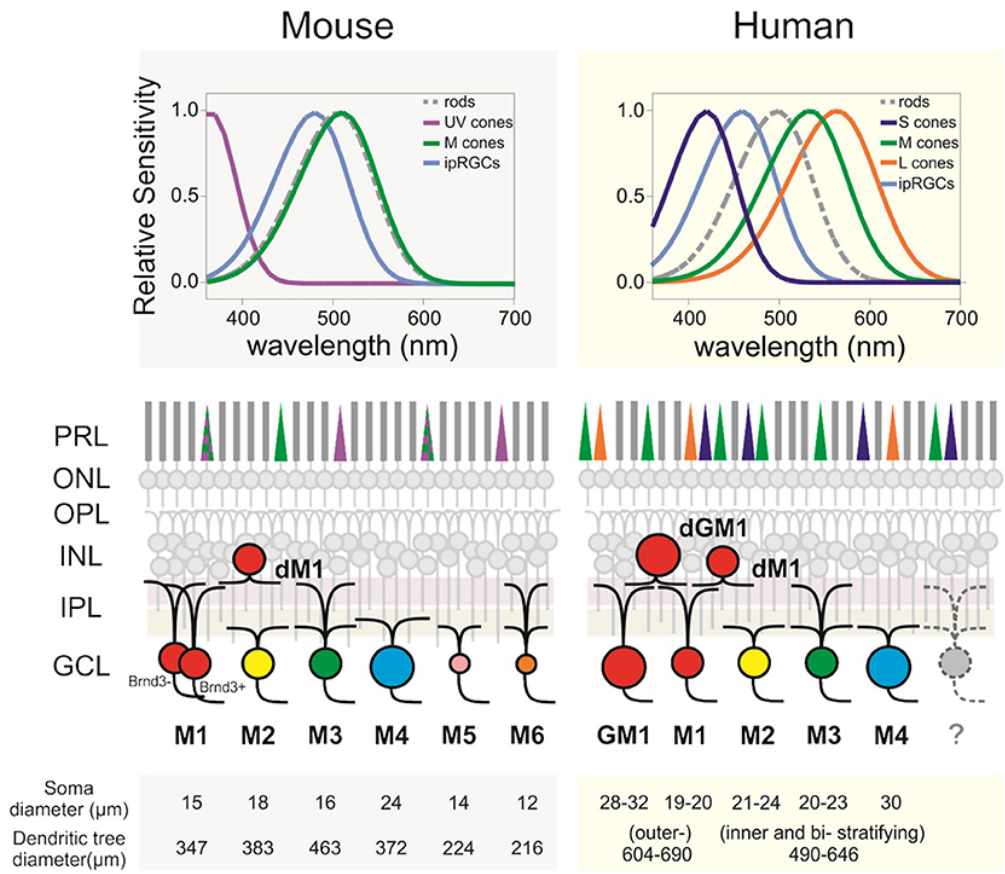


Figure 9. From: Mure LS[32]. The intrinsically photosensitive retinal ganglion cells (ipRGCs) of mouse and human retinas (M1-6). Upper row: Absorption peaks of the different opsins. Medium row: Different subtypes of ipRGCs in mouse and human retinas. Lower row: Soma and dendritic tree measurements for ipRGCs. GM1: gigantic M1; dM1, displaced M1; dGM1, displaced gigantic M1; PRL, photoreceptors layer; ONL, outer nuclear layer; OPL, outer plexiform layer; INL, inner plexiform layer; IPL, inner plexiform layer; GCL, ganglion cells layer.

#### 1.2.2.4.2. Types of ipRGCs in Rats and Mice

The first ipRGCs described in mice were the M1 type [90,91,124]. Subsequent studies in mice revealed the existence of more subtypes and were named M2 through M6[99,102] (Figure 9). Five subtypes M1 to M5 have been described in rats up to present-day that correspond to the same subtypes observed in mice[102] (see next section). These subtypes are distinguished based on their morphological characteristics, size of their soma, extension and stratification of their dendritic arborization, level of expression of melanopsin, intrinsic and extrinsic responses, characteristics of their peripheral

receptor fields, brain regions to which they project, and specific markers[94,99,104,108,125–130].

The M1 ipRGCs were the first to be described[90,91,99,124]. They have a relatively small soma (14-16μm) and are mostly found in the GCL, with only about 980 per mouse retina[91,105,127]. Their dendritic arborizations stratify in the OFF sublamina of the IPL[99,108] (Figure 9) and they project to approximately 15 NIF brain nuclei[94]. One of their principal targets is the SCN to mediate the synchronization of the circadian rhythm[99,102,123]; this nucleus receives information mostly from M1 (around 80%[131]) and, less importantly, from M2[132]. They also participate in mood regulation by light, via an SCN-independent pathway linking ipRGCs to a thalamic region, named perihabenular nucleus (PHbN)[37].

The OPN also receives afferences from M1, as part of the circuit mediating the pupillary light reflex[123,131,133]. Of the ipRGCs that project to the OPN, approximately 55% are M1, which project to the "shell" of the OPN; and 45% are M2, which project to the "core" region of the OPN[131]. This outer "shell" is where neurons that project to the Edinger-Westphal nucleus are situated[95], suggesting a major role in pupillary light reflex[99].

Various studies have documented that the M1 subtype consists of two distinct subpopulations that are molecularly defined by the expression of the Brn3b transcription factor[108,123]. Thus, there would exist M1 cells that would become labelled with antibodies against the transcription factor Brn3b (Brn3b$^+$RGCs) and M1 cells that would not be labelled with these antibodies (Brn3b$^-$RGCs)[123]. Even when M1 Brn3b$^+$ are genetically ablated, M1 Brn3b$^-$RGCs (around 200 cells per retina) have been proven to be sufficient for circadian rhythm synchronization[123], whereas the pupillary light response is severely affected[123].

The M2 ipRGCs have a slightly bigger soma size (16-19 μm) than M1, and there are around 830 per mouse retina[91,105,127,134]. They stratify in the ON sublamina of the IPL along with M4 and M5[99] (Figure 9). The M2, M4 and M5 are sometimes grouped together since their dendrite stratification is similar and no specific marker has been found for each subtype[108]. They project to image forming areas like the SC, dLGN and OPN[99]. In particular, M2 ipRGCs project strongly to the OPN "core", as stated previously and minimally to the SCN[123,131].

The M3 ipRGCs are bistratified, as they stratify in the ON and OFF sublaminas of the IPL and the proportion of stratification varies considerably between cells[99,108]. Their soma is 17-19 μm in size (Figure 9), they are scarce, accounting for around 10% of all ipRGCs and are not distributed regularly throughout the whole retina[125]. Their projection targets are not well known[99,108], but it has been suggested that they might be the SC[122] and the PHbN[37].

The M4 ipRGCs have the biggest soma size out of all ipRGCs, around 19-24 μm[117,135]. In mice, they are distributed throughout the retina with a naso-temporal gradient (maximum cell density in the superotemporal quadrant)[135]. They stratify in the ON sublamina of the IPL, like the M2 and M5[99,108] (Figure 9). They are normally not detected by classic immunohistochemical techniques, but if the signal is amplified, cell labelling becomes apparent[57].

In mice it has been shown that the M4 ipRGCs correspond to the alfa ON sustained RGCs and thus are named M4/α-ON sustained RGCs. These cells are involved in contrast sensitivity[117], visual acuity and object tracking[104,105,117,127,136]. Most of their projections reach the dLGN[99], but there is also evidence that they project to the SC and scarcely (lower density of innervation) to the IGL[99].

The M5 ipRGCs stratify in the ON sublamina, their soma size is smaller than M4, but they have not been completely characterized[108] and are difficult to distinguish from M4 cells[135]. Their distinctive characteristic lies in their colour opponency, where ultraviolet is excitatory and green is inhibitory[128]. They project to the dLGN, which may infer that they provide chromatic signals to the visual cortex[128]. They also project to the intergeniculate leaflet and from there to the SCN, likewise, suggesting a pathway for chromatic information to the SCN[137].

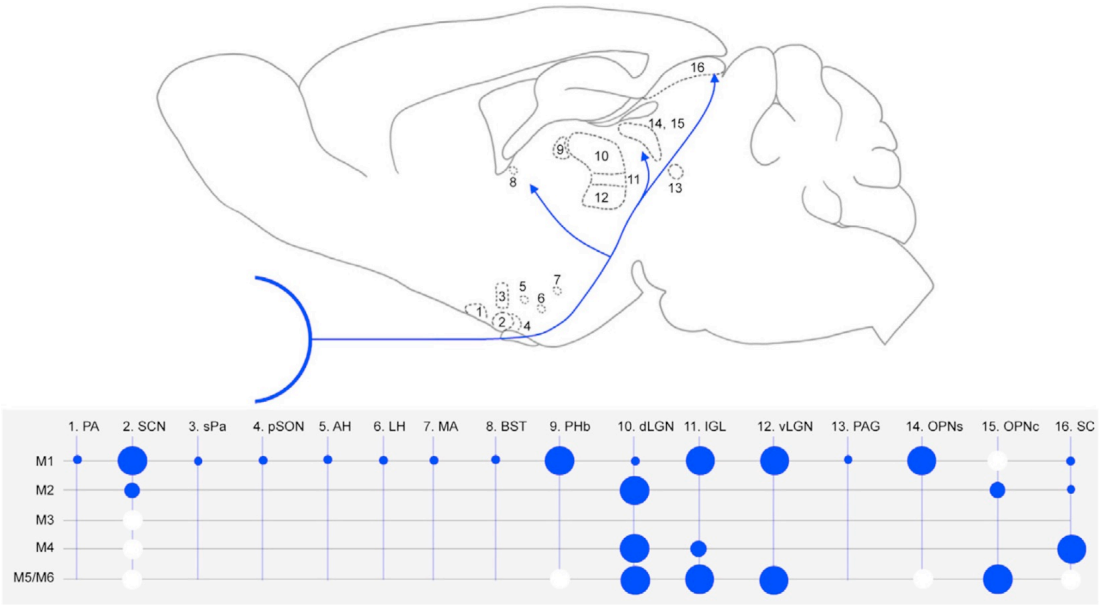


Figure 10. From: La Morgia C et al., 2021[99]. Quasisagittal section of the mouse brain showing in the upper diagram the main brain targets of ipRGCs and in the lower diagram the density of innervation (blue dots) or undetected innervation (white dots). AH: anterior hypothalamus; BST: bed nucleus of the stria terminalis; dLGN: dorsal lateral geniculate nucleus; IGL: intergeniculate leaflet; LH: lateral hypothalamus; MA: medial amygdala; OPN: olivary pretectal nucleus (with shell, s, and core, c, regions); PA: preoptic area, including the VLPO (ventrolateral preoptic area); PAG: periaqueductal gray matter; PHb: perihabenular zone; pSON: perisupraoptic nucleus; SC: superior colliculus; SCN: suprachiasmatic nucleus; sPa: subparaventricular zone; and vLGN: ventral lateral geniculate nucleus.

The M6 ipRGCs have only been identified in the mouse. They have the smallest soma size (11-15 µm) and dendritic arborization out of all ipRGCs[129]. They are bistratified, with dendrites distributed in the OFF but mostly in the ON sublamina of the IPL (Figure 9)[129]. They project to typical target areas for NIF functions like the OPN, the

intergeniculate leaflet and the dorsal and ventral areas of the lateral geniculate nucleus[129]. It has been suggested that they may contribute to pattern vision[138].

#### 1.2.2.4.3. Number and Distribution of ipRGCs in Rats and Mice

In rats, melanopsin expressing ipRGCs constitute approximately 2.5 to 2.7% of the total RGC population in albino and pigmented rat retinas[77,81,94,124,139–142]. In pigmented mice, the total number of ipRGC shown in studies has ranged from 1,021[143], 2,058[105] to 2,570[125] and represent ≈3% of the mouse RGC population[108,144]. These variations in numbers are due to the methodology and procedures used to identify the ipRGCs; differences in the type of antibody against melanopsin, immunohistochemical technique, the use (or not) of signal amplifiers or of transgenic animals that express a marker at the melanopsin locus[33].

In rodents, the expression of melanopsin is regulated both by light and by retinal circadian rhythms[145–147]. In mice, two isoforms of melanopsin, Opn4L and Opn4S, whose expression is forty times higher, have been described[74,148]. M1 and M3 both express them (Opn4S and Opn4L) while M2 and M4 only express Opn4L, Opn4S is abundant in M1 and Opn4L in non-M1s[149]. Experiments resulting in loss of function of these isoforms[149] suggest Opn4S is important for the pupillary light reflex, while Opn4L works towards negative masking and both types for circadian and sleep regulation[149,150]. Of the different subtypes, M1-M3 constitute the majority of the ipRGC population and are the easiest to identify since they express more melanopsin, while M4[127,151], M5[152] and M6[138] express melanopsin in very small amounts and are more difficult to identify with standard immunohistochemical techniques without amplification[98]. This led to the use of techniques that increase the visibility of melanopsin or that use markers inserted at the locus corresponding to melanopsin. For

example, replacing the melanopsin gene with the sequence encoding tau-LacZ, a protein composed of the enzyme β galactosidase linked to a signal sequence of tau (an actin-associated protein that facilitates antegrade transport through the axon to the axonal terminal) $Opn4^{tauLacZ94}$. Immunohistochemical signal amplification techniques have also been used, such as Cre recombinase[105], or the expression of green fluorescent protein. Axonal projections can be identified with intravitreal injection of an adeno-associated virus (AAV) that transfects the human placental alkaline phosphatase gene (AAV-fles-plap) into transgenic mice expressing Cre under the melanopsin promoter ($Opn4^{Cre}$)[105,153].

Using enhanced immunohistochemistry in transgenic mice it has been possible to quantify the different subtypes of ipRGCs. Different studies have reported: 890 M1 and M1d; 830 M2[125], 570 M4[117], and 69 ipRGC M6[138] but this figure may underestimate the real magnitude of this subtype since in the transgenic mouse used to label them, they appeared only in the ventral retina[138]. It is unknown at present the number of M3 and M5.

The distribution of the ipRGCs on the retina differs between the different subtypes; almost all cell subtypes (except M3, see previous section) tile the retina, M1 and M2 are more abundant in the upper hemiretina, M5 are abundant in the lower hemiretina, and M4 present a naso-temporal gradient with maximum densities in the superotemporal region[154,155] and for rats within the inferior-temporal retina[156].

#### 1.2.2.4.4. Projections of ipRGCs in Rats and Mice

The ipRGC projections have been studied in detail in rodents with techniques that increase the visibility of melanopsin or that use markers inserted at the locus corresponding to melanopsin, as stated earlier (see section 2.2.4.3.)

In general, ipRGC project to different nuclei than the rest of IF RGCs (Figure 10). As reviewed before, the majority project to the SCN which regulates the circadian rhythm influencing melatonin secretion by the pineal gland[124,157]. A smaller proportion projects to the intergeniculate leaflet, also involved in the circadian time-keeping system[158], and the OPN, in charge of pupillary reflex[98].

In mice and rats the ipRGCs project to the basal forebrain and hypothalamus, the thalamus and habenula region, and the midbrain[153]. In the basal forebrain, they innervate the preoptic areas (lateral, medial, and ventrolateral), the subparaventricular area, the SCN, the lateral regions of the hypothalamus, and regions of the amygdala (anterior, medial, and central). In the thalamus and the habenula region, they innervate the lateral habenula, the dorsal lateral geniculate (dLGN), ventral (vLGN), intergeniculate leaflet (IGL), and the uncertain zone[133,153]. In the midbrain they innervate the nucleus of the OPN the anterior, medial and posterior pretectal nuclei, and the nucleus of the optic tract. In addition, they innervate the nuclei of the accessory optic system (dorsal, medial and terminal lateral nuclei), and the visual layers of the SC[153,157].

As a broad summary for rodents, it could be said that most of the M1 and the rest of the ipRGCs (M2-M6) are Brn3b$^{+}$, project to the dLGN and SC, are capable of mediating a gross spatial vision in the absence of rod and cone function, and mediate contrast sensitivity (M4) or colour vision (M4, M5); while M1Brn3b$^{-}$ project exclusively to NIF nuclei[99,133].

#### 1.2.2.4.5. ipRGCs in Humans

In humans, the total number of ipRGCs varies between 0.2%[93], 0.4%[159], 0.8%[25,74,92] of the RGC population[75]. These variations may be due to technical differences to detect melanopsin, as well as the lower expression of melanopsin in some ipRGC subtypes[99]. The somas and dendritic trees of the ipRGCs are among the largest of all RGCs[99,159]. Hannibal et al.,[74], based on the location and size of the soma, and on the stratification of their dendritic trees, classified the ipRGCs according to the nomenclature previously used in rats and mice. Of the 6 subtypes described in mice and 5 in rats, only M1, M2 and M4 were clearly identified[74]. A fourth subtype, the M3 has been described but not all authors agree that it constitutes a distinct subtype, since it doesn't tile the whole retina[74]. In humans no M5 or M6 ipRGCs have been described up to present[33,74].

The predominant subtype in humans is M1, with the highest expression of melanopsin, and with a high proportion of displaced cells (dM1) in the INL. A type of giant M1 (GM1), which projects to the dLGN, presents an opponent response to the yellow-ON blue-OFF colour, mediated by the S-OFF cones, wich are antagonized by an (L+M)-ON cone response[93]. The GM1d displaced giants have also been identified. Some of the M1 have axonal collaterals that extend into the retina[74]. Humans and primates have very high densities of M1 ipRGCs in the central perifoveal region, with lower densities in the periphery[74,75]. Different densities of ipRGC in the perifoveal and peripheral region may be related to different functions in the perception of colour opposition[33,99]. The M2 are less abundant and express less melanopsin in humans than in mice or rats[74]. They are distributed in a similar way to M4 ipRGCs[74,75]. The M4 are distributed

in the naso-temporal axis, with a higher density in the temporal hemiretina[25]. However, other studies have reported a higher density of M4 ipRGCs in the nasal hemiretina[74]. In humans there are also ipRGCs similar to M3 that stratify in the ON and OFF sections of the IPL, but they are few, do not tile the retina and their characterization is still very poor[25,74].

Differences found between humans and mice ipRGCs include: mouse M1 cells do not project to the dLGN[102] whilst the human's do[93] and that M2 cells in humans do not possess center/surround antagonism in their receptive fields[93] whilst mouse M2 do[102,122].

### 1.3. The Visual System of rats and mice

This Thesis has used rats as the experimental animal model. Rat and mice are very frequently used for medical research because they resemble humans in terms of genetics, anatomy, and physiology but also for other reasons such as the easiness to produce genetics models of disease, especially in mice. Also, animal models are often preferable for experimental disease research because of their unlimited supply and ease of manipulation.

The rat and mice visual system contain the same parts as the human visual system[160], but both differ in some aspects that we will review here. The rat eyeball is spherical with a diameter of 6.4 mm and the lens is almost spherical with an axial diameter of 3.9 and an equatorial diameter of 4.5[161]. The rat eye is myopic[161]. The retinas of rats and mice have ten layers similar to humans, but their vascularization is radial from the optic nerve and do not contain a fovea (Figure 5). However, recent investigations in rats and mice have found increased RGC and photoreceptor densities in a naso-

temporal band of the retina just above the optic disk and this has been interpreted as the visual streak or area centralis[76–83].

The cells contained within the layers differ from those of humans in many aspects. For example, rats and mice are nocturnal species and their retinas are rod dominated. Although most mammals contain more rods than cones; in rats and mice this ratio is exaggerated, around 97.2% of the photoreceptors are rods and only 1%[162] and 2.8% are cones respectively[163,164]. These species have only two types of cones with S and L/M absorption peak sensitivities and are thus dichromats[79,82,165] and the S-cones are much less numerous than the L/M cones in both species[79,82].

The rat and mice RGCs are situated in the GCL along with the displaced amacrine cells. The total number of RGCs per retina vary between 85,000 and 90,000 in albino and pigmented rats, respectively[77,78,80,81] and between 30,000 and 90, 000 in different mice strains[76,78,166]. Of these, 400 and 2,400 are displaced RGCs in albino and pigmented rats, respectively and 2,400 are ipRGCs[66,77,167,168]. The displaced amacrine cells represent 50 to 60% of the cells in the GCL in rats and mice, respectively[164,169]. In rats and mice, RGCs and displaced amacrine cells form a monolayer at the GCL and thus it is possible to quantify them, even automatically, in retinal wholemounts[65].

The axons of the RGCs converge in the optic nerve and become myelinated by oligodendrocytes, like in humans. In primates' retinas and contrary to rodents, RGC are divided by the horizontal raphe into superior and inferior hemiretina, with their axons reaching the optic disk head via its superior and inferior pole. In rodents all axons converge radially towards the optic disk. RGC axons are grouped into differentiated fibre bundles with a retinotopical distribution according to the corresponding retina quadrant and centripetal position[170–176]. In mice and rats, the central retinal arteries and veins do not have a trajectory in the centre of the optic

nerve, and quickly leave the optic nerve head to course in its inferonasal portion. Thus, it is possible in mice and rats to crush or section the optic nerve at its exit from the eye and even to replace it by a peripheral nerve graft without injuring the retinal vascularization[16].

In mammals other than primates and humans, a large proportion of the RGC axons decussate at the chiasm and the axons that decussate represent RGCs from almost the entire retina, while the axons that do not decussate come from RGCs situated only in the peripheral temporal retina[76,177,178]. This is believed to be due to the lateral position of the eyes in the head that determines a small binocular visual field, and to a less specialized retina[172]. In the rat, more than 95% of the optic nerve axons cross the optic chiasm[76,169,179,180], in contrast to humans, where only 60% decussate. In mice, between 1.8 and 2.8% project ipsilaterally in albino and pigmented strains respectively[181]. Albino animals usually show reduced ipsilateral projection[76,81,177,182].

From the optic tract, RGCs project to many different brain areas. In mice and rats, the majority of RGC project to the SC [76,78,83,156,177,179,180,183], while only 37% project to the dLGN[156,184] and most axons that project to the dLGN come from bifurcating axons that project also to the superior colliculus[156,184–186]. Thus, in mice and rats, as well as in most mammals, the main retinorecipient nuclei are two IF nuclei: the dLGN and the SC. However, mice and rats have projections to more than 40 additional brain nuclei that include the NIF nuclei to which the ipRGC project[99,125,187–191] (see section X).

### 1.3.1. Identification and quantification of RGCs in the rat

The rat GCL is composed not only by these cells, but also by displaced amacrine cells which may take up over 50% of neurons in the GCL[65,192]. Although displaced amacrine cells have smaller cell size than RGCs, there is some overlap, and thus it is not possible

to distinguish RGCs from displaced amacrine cells only by their morphological characteristics. Consequently, different retrogradely transported markers and molecular markers have been used to identify these cell populations (reviewed by Saleeba et al., 2019[193]).

The first markers used for RGC identification were markers that when applied in the different parts of the visual system were taken up by the RGCs that transported them anterogradely or retrogradely. These techniques were named tract-tracing or neuroanatomical tracing techniques. Among the first tracers used as anterograde tracer was horseradish peroxidase[156,194]. This marker was applied first in chick[195] and later in rats and mice[16,196–198]. Byocitin was also used as anterograde and retrograde cell marker[199]. Many tracers were used, but not all were anterogradely and retrogradely transported. Some, like wheat germ agglutinin-horseradish peroxidase[200] were anterogradely transported only and others like Fluorogold[61,201] or the carbocyanine dye diI[11,12,202] or fast blue[197,202,203] were retrogradely transported. Some dyes were also administered by intracellular injection, such as lucifer yellow[203] or neurobiotin[204].

Later, immunocytochemical techniques were used for RGC identification. These rely on the principle of specificity antibody-antigen and must be directed against a protein expressed only in RGCs. Also, if these cells can be identified after a lesion, the protein expression should not be stopped after the insult. The advantages of these techniques over the tract-tracing methods is that they do not need to be applied *in vivo*. Also, because they are applied *ex vivo*, no other cells can become labelled through phagocytosis of the injured cells, as it sometimes occurred with the tract-tracing methods[205]. Some of the most common antigens used for RGC immunodetection are proteins. However, there are proteins synthetized only in a subset of RGCs, while others are produced in most RGCs. Research has focused in this later type in an attempt

to find markers for the whole RGC population. The most frequently used markers for that purpose have been antibodies against: Thy-1[206], Brain-expressed X-linked protein-1 and 2 (Bex1 and 2)[207], the Neuronal Nuclear protein NeuN[208], the Ribonucleic acid (RNA) binding protein RBPMs[209,210], BM-88[211], and the Brain specific homeobox 3 (Brn3) which has 3 different subtypes: Brn3a, Brn3b, Brn3c[81,191]. The antibodies against melanopsin allow the identification of a small subset of RGCs: the ipRGC, and in particular the M1, M2 and M3 populations since these subtypes express melanopsin in higher amounts than the other cell types[57,144,152]. Some of these antibodies can be combined to immunodetect different populations of RGCs. For example, since Brn3a and melanopsin are very rarely expressed by the same RGC, using these two markers has allowed us in this Thesis to study in parallel but independently both populations in the same retina with the same insult and/or neuroprotection[57,140,212]. Brn3a and melanopsin are both expressed after retinal injury, as demonstrated by previous studies [63–65,168,213]. This is of utmost importance since changes in morphology, gene expression and physiology of RGCs after an insult may impair the ability to correctly identify them[214–218].

The identification of RGCs using molecular techniques was introduced more recently. These techniques provide a precise microscopic localization of nucleic acids such as deoxyribonucleic acid (DNA), messenger RNA (mRNA) and microRNA using “in situ” hybridization. The detection may use chromogenic or fluorescent techniques that have been named chromogenic in situ hybridization (ISH) or fluorescence in situ hybridization (FISH). Although these techniques are more specific, they are also more difficult and thus, they have been less used than immunohistochemistry. A number of transcriptional factors have been localized in RGCs using these techniques, such as γ-synuclein, POU domain factors and between them the Brn3, sect[70,191,219], etc. Although

some molecular markers such as those analysing γ-Synuclein and Brn3a expression may identify nearly the whole population of RGCs, they have been used to label the RGCs to analyse posteriorly other genes and thus to define RGC subtypes[70,191].

*In vivo* labelling and observation of RGCs is also possible using different cell markers. For example, there are transgenic mice models that express different types of proteins and, it is possible using a specific RGC gene such as Thy-1 as promoter to induce fluorescent protein labelling of RGCs[220,221]. The previously reported RGC tracers could also be administered and observed *in vivo*[222]. Also, other fluorescent markers could be delivered to RGCs through intravitreal injection, such as Cholera toxin subunit B conjugated to a fluorescent marker[223] or adeno-associated viral (AAV) vectors expressing fluorescent proteins[224]. Finally, it is possible to detect RGC apoptosis *in vivo* after intravenous injection of fluorescently labelled annexin-5[225] or intravitreal injection of CapQ, a cell-penetrating, caspase-activated apoptotic probe[226]. These *in vivo* techniques of RGC identification have the advantage over the *ex vivo* techniques that they permit not only the observation of cells but also their follow-up in diseases coursing with RGC degeneration such as glaucoma or other optic neuropathies.

#### 1.3.1.1. Identification and quantification of rat RGCs with antibodies against Brn3a and melanopsin

In the studies included in Thesis we have identified RGCs by immunocytochemistry. We have used two different antibodies: goat anti-Brn3a (C-20 Santa Cruz Biothechology, Heidelberg, Germany) and rabbit anti-melanopsin (1:500 dilution, PAI-780, Invitrogen, Thermo Fisher Scientific, Alcobendas, Madrid, Spain).

The Brn3 family (a, b and c) is a group of related transcription factors that belong to the POU family. They are expressed in the nucleus of some sensory neurons and play an important role in their differentiation and survival during development[65,77,80,81,188,227–230]. They continue to be expressed in adulthood and in the retina they are expressed only by RGCs[81,231]. In the adult rat it has been calculated that Brn3a is expressed by the vast majority of rat RGCs[80,81] even after optic nerve transection[63,81] and thus, antibodies against this marker have been used widely to selectively identify this population[80,81]. In rats[81] and in mice[188,231] it has been documented that most Brn3a$^+$RGCs project contralaterally to both the superior colliculi and the lateral geniculate nucleus. Thus, Brn3a$^+$RGCs contribute only to the IF nuclei, but not to the NIF nuclei[231]. In accordance, most Brn3a$^+$RGCs (99.8%) do not express melanopsin[78,81,83,232,233].

As described earlier, melanopsin is expressed in the cytoplasmic membrane of ipRGCs. By immunodetection of this protein we label the M1, M2 and M3 since these subtypes express melanopsin in higher amounts than the other subtypes of ipRGCs[57,103,144,152], and therefore we refer to them as m$^+$RGCs. In rats, the m$^+$RGCs do not express Brn3a and most Brn3a$^+$RGCs do not express melanopsin[81]. Thus, in the studies included in this Thesis, using immunodetection of Brn3a and melanopsin[140,212] we are studying in parallel two different populations of RGCs.

### 1.3.2. Identification and quantification of RGC loss in rats with Spectral Domain Optic Coherence Tomography

Optic coherence tomography (OCT) is a non-invasive imaging technique that uses low-coherence interferometry to obtain high-resolution cross-sectional images of biologic tissues[234,235]. Although it was developed in 1991[234], the first ophthalmic OCT

instruments became available in 1996[235] and since then has become a fundamental technique for imaging in Ophthalmology because it allows to obtain accurate information on the structure of different parts of the eye. The first ophthalmic OCTs used Time Domain detection (TD-OCT) and had slow speed acquisition. Later, Fourier Domain detection was introduced and the Spectral Domain OCT (SD-OCT) and Swept Source OCT (SS-OCT) were developed with faster image acquisition and increased detection sensitivity that results in improved image quality[235]. The ultra-high-resolution OCT (UHR-OCT) uses a longer light wavelength for deeper tissue penetration[236]. Recently, OCT angiography (OCT-A) has been developed. This technique uses OCT emitted through a SD-OCT or SS-OCT and detects its reflectance on the moving red blood cells to depict vessels *in vivo*[237]. Since it is a non-invasive technique that does not require a dye injection, it has replaced in part previous techniques such as fluorescein angiography or indocyanine green angiography.

SD-OCT (with or without angiography) is currently the standard for ophthalmic clinical examination in the world because, although SS-OCT may have superior detection capabilities, its acceptance has been lower due to various factors, such as its high cost and lack of normative database[235]. There are various commercial SD-OCT apparatus on the market at present that have A-scans rates of 20,000 to 52,000 per second and a resolution of 5–7 μm[236]. In this Thesis we use the SD-OCT Spectralis (Heidelberg Engineering).

SD-OCT is a fast non-invasive and essential technique for standard ophthalmic care because it allows the in vivo examination of various ocular structures reached by light such as the cornea, the anterior segment of the eye, the iridocorneal angle and the retina and optic nerve (Figure 11). The SD-OCT does not only acquire images, but also permits segmentation of the whole retina or different retinal layers to obtain their

thickness and compare it with existent patient databases[237]. These comparisons let you know if the values obtained are normal or abnormal as it occurs in various eye diseases and well as the degree and progression of damage[236]. In the next paragraphs we will focus on the capabilities of the SD-OCT to explore the retina and the optic nerve, because in one article of this Thesis we use SD-OCT to measure retinal thickness[140].

At present SD-OCT apparatus use four main scan protocols to explore the retina: lineal, radial, cube or circular. The lineal protocol acquires only one line while the cube protocol contains many equally spaced lineal horizontal B-scans of a determined length; the radial protocol acquires various equally spaced radial lines custom centred; the peripapillary circular scan has a 500 μm diameter that is usually centred in the optic disk, it is thus named optic disk circle (Figure 11). The lineal or cube B scans are usually used to assess the macula whilst the circular scan is used to explore the peripapillary RNFL (pRNFL), and the radial scan may be used for macula or optic disk. Some commercial apparatus show the cross sectioned retina in colour, such as the Cirrus (Zeiss) but in the SD-OCT Spectralis the section in shown in a black and white; white regions are the most hyperreflective and black are hyporeflective.

The SD-OCT Spectralis (Heidelberg Engineering) provides multimodal imaging because it includes SD-OCT and various techniques of confocal scanning laser ophthalmoscopy (multicolour imaging, red free infrared, blue and blue peak autofluorescence), which provides various fundus imaging modalities. The Spectralis SD-OCT also contains a software named Heyex™EyeExplorer that allows image analysis such as automatic segmentation of different retinal layers, measurement and comparison with a normative human database. Thus, the different scan protocols analyse different retinal thicknesses and express them in numbers (microns) and in

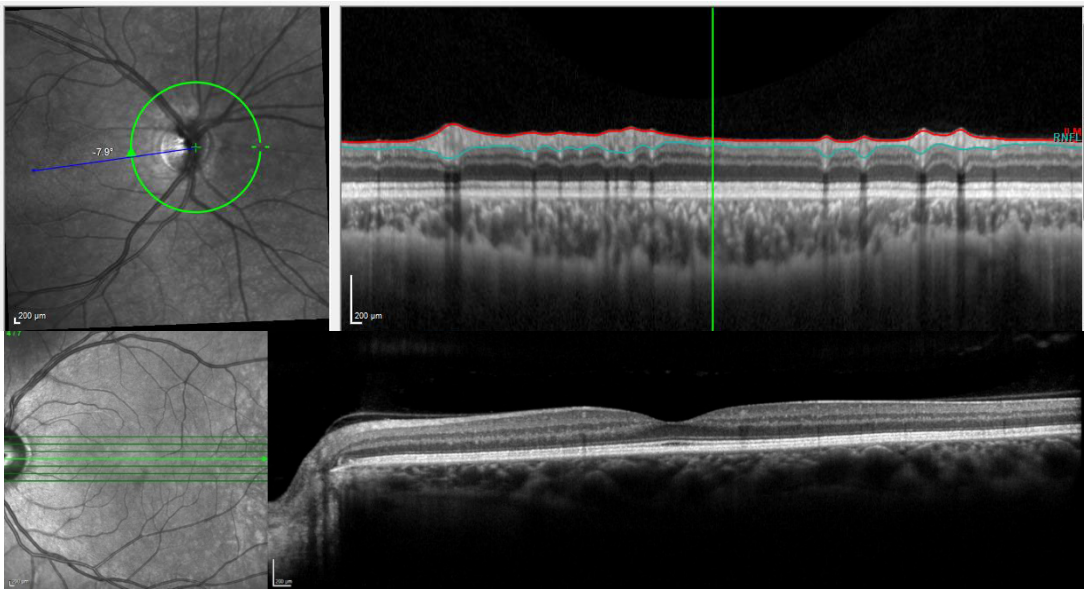

*Figure 11. Optic Disk Circle and Cube Protocols of Spectralis SD-OCT.*

colours depending on whether they have normal values (green), reduced values (yellow) or significantly reduced values (red).

Soon after the appearance of the first commercial OCT apparatus, these were used in different animal species from mice to monkeys[79,238–241]. Animals need to be anesthetized and sometimes even fixation of the globe is required. To avoid corneal desiccation, frequent irrigation, artificial tears or specially designed contact plano rigid permeable contact lenses are used[79,140,241]. The apparatus should be adapted for each animal species and for rats a 78-D double aspheric fundus lens is usually placed in front of the lens[79,140,242]. Automatic segmentation may not be possible specially in small animals because it shows frequent errors, but the software usually permits manual segmentation. Finally, measurement units may be corrected for different animals[79].

Examination of the rat retina and nerve fibre layer using OCT has been carried out by different authors[79,239,240,242] and progressive retinal thickness decrease has been documented with this technique after different insults such as optic nerve transection[242,243], optic neuritis [244] or ocular hypertension[245,246].

In one study included in this Thesis[140] we have used SD-OCT (Spectralis, Heidelberg) to investigate total retinal thickness (TR) and inner retina (IR) thickness in rats after intravitreal NMDA injection. For the OCT examination, a customized permeable contact lens (3.5-mm posterior radius of curvature, 5.0-mm optical zone diameter, 5.0-diopter back vertex power) was placed over the cornea to compensate for the rat corneal curvature. In the mentioned study, we used a cube raster scan (3000 microns wide x 3600 microns high) centred in the optic nerve head containing 31 equally spaced horizontal B-scans. The follow up tool of the program was used for the two consecutive scans taken per animal in order to acquire and compare posteriorly the exact same regions in each animal. In three of these scans, the most central and the two most peripheral (superior and inferior, situated at a distance of 1800 microns from the centre of the optic disc[140]), we measured total retinal (TR) thickness (from the inner limiting membrane to the outer limit of the pigmented epithelial layer) and inner retinal (IR) thickness (from the inner limiting membrane to the outer limit of the inner nuclear layer) thickness. Thickness measurement was done manually using the calliper provided by the software in 5 areas in the superior and inferior scans and in 4 areas in the central scan (two on each side of the optic disk). Thus, fourteen measures were taken per animal[140]. We have used this technique to analyse retinal thickness longitudinally at short (3 months) and long (15 months) survival intervals.

### 1.4. RGC Response to Different Insults

RGCs and their axons are contained within the CNS. The neurons of the CNS have different responses to a lesion depending on the animal considered. Lower vertebrates like fish and amphibians have important regenerative capacities: most RGCs survive the injury and regenerate extensively with the return of vision[9,10]. However, in higher vertebrates such as rodents and humans, RGCs suffer retrograde degeneration, most of them die and do not regenerate[10–12]. In mammals, the RGCs do not regenerate spontaneously, but suffer an anterograde and retrograde degeneration that culminates many times in cell death. This is believed to be due both to genetic and environmental differences between these species[10].

RGCs are indispensable for vision because they are the only neurons that connect the eye with the brain, and therefore, RGC lesion results in blindness. The RGCs and their axons can be damaged, as it occurs in many human diseases such as glaucoma, hereditary, traumatic and optic nerve neuropathies or neurodegenerative diseases like Alzheimer's or Parkinson[10].

As reviewed before, after a lesion, CNS neurons such as RGCs in mammals show very limited regenerative capacities and massive cell death. When RGCs are lesioned, a death signal pathway is initiated, and the majority of the RGCs are destined to die. At present there are no treatments available to prevent or halt the process of neuronal death. There are, however, experimental evidences that this process may be slowed or reduced, and these are the rescue or neuroprotective strategies. Although different cell death pathways are differentially activated by different types of injury[10], it is believed that most RGC injuries cause death by apoptosis[64,225,247–250]. However, the various cell death pathways may be initiated or activated by different pathogenic mechanisms such

as calcium accumulation, oxidative stress, autoimmune responses, trophic factor deprivation endoplasmic reticulum stress and excitotoxicity[251].

To study and emulate the different human diseases that cause RGC death, various experimental models have been used in animals such as optic nerve crush or transection, ocular hypertension, administration of excitatory aminoacids or autoimmune activation[10]. In this Thesis we have used two of these strategies in rats: optic nerve transection[212] and excitotoxicity[140]. Thus, we will review these injuries in the next sections.

### 1.4.1. Intraorbital Optic Nerve Section

Optic nerve injury is observed in various human diseases such as glaucoma, traumatic or other optic neuropathies. Numerous studies in mammals have shown that injury to the optic nerve, which is made up of RGC axons causes the death of parent neurons[11,12,249] and the severity of this loss of RGCs depends on various factors, such as: the quantity of axons affected[12,252]; the distance from the cell body at which the lesion is undertaken, with a larger distance being accountable for a slower rate of loss[11,247]; the type of injury, where optic nerve transection induces quicker and more severe RGC degeneration[11,61,62,80,253] than optic nerve crush[62,80,247,254].

One of the experimental models used in this Thesis is optic nerve section in rats, causing axotomy of the entire RGC population. This model has been characterized in detail both in rats and mice, including RGC loss in time and severity[11,12,61,62,65,242,247,254–256] molecular changes [215–217,257], morphology [258], electrophysiological responses [259,260], retinal topography [65] and their response to neuroprotectants[142,254,261–266].

It is now known that, in mice, various RGC subtypes respond differently both to injury and regenerative therapies[267,268]. Two weeks following optic nerve crush, some subtypes survive in high proportions, while others are decimated[70,267].

### 1.4.2. NMDA-induced Excitotoxicity

One of the mechanisms of RGC death after a lesion may be initiated by increased levels of the excitatory amino acid glutamate. This neurotransmitter is used by many neurons in the retina, among them the photoreceptors, bipolar and ganglion cells[269] but is toxic for the neurons of the inner retina at increased concentrations[270,271]. There are two types of neuronal receptors for glutamate: ionotropic and metabotropic. The ionotropic receptors form the ion channel pores and can be divided into three pharmacologic types depending on their main agonist: N-methyl-D-Aspartate (NMDA), α-amino-3-hydroxy-5-methyl-4-isoxazolepropionic acid (AMPA) and kainate. The NMDA receptors are permeable to calcium and the intracellular calcium concentration is increased in neuronal lesions[251].

Glutamate excitotoxicity has even been thought to play a role in neuronal death in CNS diseases[271,272]. Several studies have previously documented that glutamate excitotoxicity plays an important role in various retinal injuries in which there is a significant RGC loss[270,273] including glaucoma[274–278], transient ischemia[279] and optic nerve injury[280,281].

It has been suggested that glutamate excitotoxicity may be the result of NMDA receptor stimulation resulting in variations in $Na^+/K^+$ and $Cl^-$ homeostasis, osmotic imbalance[282] and in the intracellular influx of $Ca^{2+}$ [283], which activates apoptosis via c-AMP[284] and also enzymes which cause DNA and cell membrane damage[285].

Glutamate excitotoxicity can be simulated experimentally producing an excessive stimulation of NMDA receptors, by administration of intravitreal injections of NMDA.

Previous work[286–294] has used NMDA induced excitotoxicity on animal models in order to study RGC neuroprotection and cell death mechanisms.

RGC's susceptibility to NMDA-induced excitotoxicity has already been studied in rats[287,288] and in mice[289,295]. The responses of the $m^+$RGCs to intravitreal injections of NMDA have also been studied but only up to 58 days after the injection[289,295] and, thus, long term effects on the population of $m^+$RGCs have not been investigated up to date. In one of the articles included in this Thesis[140] we investigate short- (3, 7, 14 days) and long-term (15 months) effects of the intravitreal injection of NMDA on the rat $Brn3a^+$ and $m^+$RGC populations.

### 1.5.- Neuroprotection

When mammalian RGCs are lesioned, a death signal pathway is initiated, and the RGCs are destined to die. However, pioneer work by Ramón y Cajal and his disciples at the beginning of the last century showed some signs of axonal regeneration if the cut optic nerve was placed in contact with a peripheral nerve graft[13–15]. Since then, there were no advances in the field and therefore until the late 1980s it was accepted that the axonal lesions within the adult mammalian central nervous system resulted in both neuronal degeneration and death, and irreversible disconnection of the injured neurons from their target territories. However, in the late eighties of the last century, in a series of experimental studies carried out in Albert J Aguayo´s Laboratory in Montreal[5,17,296] (Canada), it was documented that the section of the rat optic nerve resulted in retrograde degeneration and death of the vast majority of the RGCs within a few days[12,16] but that the RGC response could be modulated. Thus, if after the section of the optic nerve, an autologous segment of peripheral nerve was grafted onto the ocular stump, the death of a proportion of RGCs could be prevented[12] and, in addition,

there was axonal regeneration of the surviving RGCs that could grow over long distances and reinnervate their target territories in the brain and form synaptic connections[16]. These works were the basis for neuroprotection and neuroregeneration, that is, the therapeutic processes to prevent neuronal death and/or regrow and repair the nervous tissues after a lesion. Since then, many rescue or neuroprotective experimental strategies have been shown to slow or prevent mammalian neuronal death after a lesion[10,88,271]. We will review only the strategies that involve the neurotrophic factors and specially brain-derived neurotrophic factor (BDNF), as in this Thesis we have used for neuroprotection an agonist of the BDNF receptor.

### 1.5.1. Neuroprotection with neurotrophic factors and DHF

When it was shown that peripheral nerve grafting to the optic nerve neuroprotected a proportion of RGCs after optic nerve section[12], it was suggested that among the multiple substances that could be responsible for this neuroprotective effect, there were the trophic factors secreted by denervated Schwann cells, including neurotrophic factors and neurotrophins.

Neurotrophic factors are endogenous substances that during development contribute to the survival, growth and differentiation of neuronal populations, and in adulthood they contribute to the maintenance and homeostasis of multiple neuronal populations, including the RGCs. Among the neurotrophic factors most studied for their protective effects on RGCs, the most notable are BDNF, ciliary neurotrophic factor (CNTF), and glial-derived neurotrophic factor (GDNF). All of them have clear neuroprotective effects in RGC injury models[10,88,266,271].

BDNF is a powerful neuroprotectant, of the family of the neurotrophins, that include three structurally related factors: Nerve Growth Factor (NGF), Neurotrophin 3 (NT3) and Neurotrophin 4/5 (NT4/5). Neurotrophins are produced by neurons and glial cells

and exert their neuroprotective actions by binding to cell receptors[297,298]. Neurotrophins bind to two receptors: low affinity or p75 and high affinity or tropomyosin related kinase receptors (Trk), but their effects are mediated through the latter. There are three Trk receptors: TrkA, TrkB and TrkC and they are specific for the different neurotrophins: TrkA is for NGF, TrkB for BDNF and NT 4/5; and TrkC for NT3, although there is some overlap between them[297–299]. The effects of BDNF are thus mediated by the activation of its high affinity receptor TrkB [300–302], which can also be activated by NT 4/5.

In neurons, TrkB binding activates various intracellular pathways involved in neuronal differentiation and survival, such as mitogen-activated protein kinase/extracellular signal regulated kinase (MAPK/ERK), the phospholipase C-γ (PLC-γ), the phosphoinositol-3 kinase/protein kinase B (PI3K/AKT), the Janus kinase/signal transducers and activators of transcription (JAK/STATS) and the nuclear factor kappa-light-chain enhancer of activated B-cells[298] (NF-κB). These pathways result in different functional and complex effects in different cells. For example, the GRB2-Ras-MAPK-Erk signalling regulates neuronal differentiation including neurite development[303–305] and the phospholipase Cγ pathway regulates neuronal synaptic plasticity[297]. Thus, TrkB activation intervenes in various neuronal physiological functions whose importance becomes evident when considering that TrkB homozygous knockout (TrkB−/−) mice experience neonatal death and serious abnormalities in their nervous system[306–308].

In the retina, it has been shown that RGCs express BDNF[309] and the TrkB receptor[309–311]. It has been documented that BDNF influences the development of RGCs, as it improves the stability of developing synapses[312], controls the development of their dendritic trees and enhances arborization of their axons[313–315] and their maturation[312].

It has been shown also using genetically modified mice that BDNF-TrkB signalling regulate the lamination of dendrites in ON but not in ON-OFF RGCs[316].

Changes in retinal expression of BDNF and/or TrkB may be involved in the pathogenesis and/or RGC death progression in different retinal diseases[298]. It has been documented that RGCs may show downregulation of TrkB receptors after an injury[298]. However, expression of BNDF in RGCs has also been documented in the first hours after NMDA exposure[317] and this has been interpreted as an endogenous neuroprotective strategy[88].

A large number of retinal injury models[79,253,318,319] including optic nerve lesions[61,63,64,253,261,266,272,320] have studied the neuroprotective effects of BDNF and have concluded that it is one of the most efficacious neuroprotectants, especially for RGCs. However, several disadvantages are linked to its use as a neuroprotectant and thus partially impair its use, such as its very short plasma half-life and its inability to cross the blood-brain barrier[321]. Thus, TrkB receptor agonists have been essayed.

The flavonoid 7,8-Dihydroxyflavone (DHF), a powerful mimetic of BDNF[322] displays its same neuroprotective effects through TrkB receptor activation and initiation of survival pathways [323,324] . DHF can cross the blood-brain barrier [323,325–327] thanks to its small size (MW 254gr/mol) and lipophilic qualities. Furthermore, DHF has a longer half-life [327–329] than BDNF. The response induced by DHF TrkB receptor coupling is stronger, faster and lasts longer when compared to BDNF[326,330]. It has also been proven that DHF is safe for systemic administration both in short/acute or chronical regimens[330–332]. For all the above-mentioned reasons, DHF has been proposed to possess many advantages over BDNF as a neuroprotectant agent.

Previous *in vivo* studies in new-born rats[331,333] have shown that DHF may be able to prevent injury induced by oxidative stress, apoptosis and excitotoxicity. However,

there are still no *in vivo* adult animal studies examining its mechanism of action and ability to prevent RGC death. In our article included in this Thesis[212] we have analysed the responses of Brn3a$^+$RGCs and m$^+$RGCs to optic nerve section and their neuroprotection with systemically administered DHF, at short and long term survival intervals (7, 10, 14, 21, 30 or 60 days after optic nerve section). We have also investigated if DHF produced retinal TrkB phosphorylation, to try to elucidate if DHF treatment confers neuroprotection via TrkB activation.

## 2. HYPOTHESES

1) Does NMDA-mediated retinal excitotoxicity cause differential neuronal death in two different RGC populations: Brn3a$^+$RGCs and m$^+$RGCs, and can it be assessed *in vivo* using SD-OCT?

2) Does systemically administered DHF afford Brn3a$^+$RGC and/or m$^+$RGC neuroprotection after optic nerve transection, and is this effect mediated through the TrkB receptor?

In order to test these hypotheses in adult rats, we pursued the following research objectives:

### 2.1. OBJECTIVES

1) To characterize short- and long-term Brn3a$^+$RGC and m$^+$RGC neuronal loss after intravitreal administration of a single dose of 5 µl of a solution of 100mM NMDA.

2) To evaluate using SD-OCT if NMDA-mediated retinal excitotoxicity causes changes in total retinal thickness or inner retinal thickness.

3) To characterize short- and long-term Brn3a$^+$RGC and m$^+$RGC neuronal loss after optic nerve transection.

4) To determine if systemically administered DHF can neuroprotect Brn3a$^+$RGCs and/or m$^+$RGCs after optic nerve transection.

5) To determine what dose of systemically administered DHF is optimal for neuroprotection of Brn3a$^+$RGCs after optic nerve section.

6) To determine how long this DHF-afforded neuroprotection lasts for after optic nerve section in Brn3a$^+$RGCs and m$^+$RGCs.

7) To determine if DHF neuroprotection after optic nerve section is mediated by activation of the TrkB receptor.

## 3. PUBLICATIONS COMPENDIUM/ COMPENDIO DE PUBLICACIONES.

Los tres artículos que presentamos en esta Tesis pueden consultarse en:

https://pubmed.ncbi.nlm.nih.gov/?term=vidal-villegas

- **Vidal-Villegas Beatriz** et al. Melanopsin$^{+}$RGCs Are fully Resistant to NMDA-Induced Excitotoxicity. *Int J Mol Sci*. 2019 Jun 20;20(12):3012. doi: 10.3390/ijms20123012.
- **Vidal-Villegas Beatriz** et al. Photosensitive ganglion cells: A diminutive, yet essential population. *Arch Soc Esp Oftalmol*. 2021 Jun; 96(6): 299-315. doi: 10.1016/j.oftal.2020.06.032.
- **Vidal-Villegas Beatriz** et al. Systemic treatment with 7,8-Dihydroxiflavone activates TrkB and affords protection of two different retinal ganglion cell populations against axotomy in adult rats. *Exp Eye Res*. 2021 Jul 8;210:108694. doi: 10.1016/j.exer.2021.108694.

International Journal of
*Molecular Sciences*

MDPI

*Article*

# Melanopsin$^+$RGCs Are fully Resistant to NMDA-Induced Excitotoxicity

**Beatriz Vidal-Villegas [1,†], Johnny Di Pierdomenico [1,†], Juan A Miralles de Imperial-Ollero [1], Arturo Ortín-Martínez [1,‡], Francisco M Nadal-Nicolás [1,§], Jose M Bernal-Garro [1], Nicolás Cuenca Navarro [2], María P Villegas-Pérez [1] and Manuel Vidal-Sanz [1,*]**

1 Department of Ophthalmology, University of Murcia and Instituto Murciano de Investigación Biosanitaria (IMIB)-Virgen de la Arrixaca, 30120 Murcia, Spain; beatrizvidalvillegas@gmail.com (B.V.-V.); johnnydp@um.es (J.D.P.); juanantonio.miralles@um.es (J.A.M.d.I.-O.); Arturo.OrtinMartinez@uhnresearch.ca (A.O.-M.); fm.nadalnicolas@um.es (F.M.N.-N.); jmbg@um.es (J.M.B.-G.); mpville@um.es (M.P.V.-P.)

2 Department of Physiology, Genetics and Microbiology and Multidisciplinary Institute for Environmental Studies "Ramón Margalef", University of Alicante, 03690 Alicante, Spain; cuenca@ua.es

* Correspondence: manuel.vidal@um.es

† These authors contributed equally to this work.

‡ Present address: Donald K Johnson Eye Institute, Krembil Research Institute, University Health Network, Toronto, ON M5G 2C4, Canada.

§ Present address: Retinal Neurophysiology Section, John Edward Porter Neuroscience Research Center, National Eye Institute, National Institutes of Health, Bethesda, MD 20892, USA.

Received: 19 May 2019; Accepted: 18 June 2019; Published: 20 June 2019

check for updates

**Abstract:** We studied short- and long-term effects of intravitreal injection of *N*-methyl-D-aspartate (NMDA) on melanopsin-containing (m$^+$) and non-melanopsin-containing (Brn3a$^+$) retinal ganglion cells (RGCs). In adult SD-rats, the left eye received a single intravitreal injection of 5µL of 100nM NMDA. At 3 and 15 months, retinal thickness was measured in vivo using Spectral Domain-Optical Coherence Tomography (SD-OCT). Ex vivo analyses were done at 3, 7, or 14 days or 15 months after damage. Whole-mounted retinas were immunolabelled for brain-specific homeobox/POU domain protein 3A (Brn3a) and melanopsin (m), the total number of Brn3a$^+$RGCs and m$^+$RGCs were quantified, and their topography represented. In control retinas, the mean total numbers of Brn3a$^+$RGCs and m$^+$RGCs were 78,903 ± 3572 and 2358 ± 144 (mean ± SD; $n$ = 10), respectively. In the NMDA injected retinas, Brn3a$^+$RGCs numbers diminished to 49%, 28%, 24%, and 19%, at 3, 7, 14 days, and 15 months, respectively. There was no further loss between 7 days and 15 months. The number of immunoidentified m$^+$RGCs decreased significantly at 3 days, recovered between 3 and 7 days, and were back to normal thereafter. OCT measurements revealed a significant thinning of the left retinas at 3 and 15 months. Intravitreal injections of NMDA induced within a week a rapid loss of 72% of Brn3a$^+$RGCs, a transient downregulation of melanopsin expression (but not m$^+$RGC death), and a thinning of the inner retinal layers.

**Keywords:** NMDA; excitotoxicity; glaucoma; melanopsin-RGCs; intrinsically photosensitive-RGCs; Brn3a$^+$RGCs; adult albino rat; retina; SD-OCT

## 1. Introduction

Light is converted by photoreceptors (rods and cones) into electrical signals, which are initially processed at the outer synaptic layer of the retina where photoreceptor information is modulated by horizontal cells and conveyed onto bipolar cells. Signals are further processed at the inner synaptic layer, where the bipolar information is modulated by amacrine cells and finally passed on to retinal

ganglion cells (RGCs) in the innermost retinal layer. RGCs, the only ones whose axon leaves the retina, convey the information processed in the retina to the retinorecipient nuclei of the brain. This projection obtains relevant information from our visual world from the retina and provides it to the brain to produce image-forming as well as nonimage-forming visual functions. Retinal information that produces image-forming visual functions is carried out by the general population of RGCs that have the expression of brain-specific homeobox/POU domain protein 3A (Brn3a) in common, while the information necessary to produce nonimage-forming visual functions is carried out by a small subpopulation of RGCs that express the photopigment melanopsin ($m^+$RGCs), rendering them intrinsically photosensitive (ipRGCs)—the so-called third photoreceptor cell-type of the retina [1].

In adult rodents, RGCs constitute less than 1% of all retinal cells [2–4]. Based on their morphology (soma size and dendritic arborization), extension of their dentritic arborization into the inner synaptic layer, electrophysiological responses to light stimulus within their receptive field, target region of the brain, and genetic background, it has been proposed that the rodent retina may have up to 40 different types of RGCs [5–8]. In rats it has been estimated that excluding endothelial cells, the ganglion cell layer is composed of approximately 50% displaced amacrine cells (ACs), 10% glial cells, and 40% RGCs [9]. Displaced ACs not only share their location in the retina with RGCs but overlap in size, thus making it difficult to distinguish RGCs from ACs, and this has obliged the use of retrogradely transported neuronal tracers [10,11] or neuronal markers to identify RGCs. There are several markers that identify large proportions of RGCS (pan-markers) or many RGC types, including Thy-1 [12], Brn3a [13,14], RBPMS [15], class III beta-tubulin [16], Neuronal Nuclei (NeuN) [17], and Microtubule-associated protein 1A (MAP 1A) [7,18]. In addition, there are several markers that allow identification of specific types of RGCs, such as melanopsin [19] and others [7,8,20]. However, after retinal injury, many of the physiological and morphological attributes of RGCs, including their dendritic arborization, may change [8,21,22], and the molecular markers may be downregulated, rendering the identification of RGCs difficult [23–28].

The characterization of the expression of Brn3a by rodent RGCs has allowed identification of the main population of RGCs that convey image-forming visual information to the brain, which represents approximately 96% of the RGC population [14]. Nonimage-forming visual behaviours depend on intrinsically photosensitive RGCs (ipRGCs), one type of RGC with a large dendritic arbor that contains the photopigment melanopsin ($m^+$RGCs), which is responsible for the circadian photoentrainment, pupillary reflexes, and the regulation of pineal melatonin secretion [1,29,30]. Six subtypes of ipRGCs have been described to express at least small amounts of melanopsin (also known as Opn4), and are named M1-M6 [31,32]. Antibodies against melanopsin allow the identification of the large majority of ipRGCs, preferentially M1–M3, because M4 (which corresponds to the ON αRGC subtype [33,34]), M5 [35], and M6 [32] express less Opn4 than M1–M3 and are difficult to identify with standard immunohistochemistry [31,32,36–40]. In rats, the population of $m^+$RGCs constitute approximately 2.5 and 2.7% of the pigmented and albino RGC populations, respectively [13,14,19,41,42]. Moreover, because Brn3a and melanopsin are rarely expressed in the same RGC, immunohistofluorescent studies using these two markers together allows the study, in parallel but independently, of the responses of these two types of RGCs to different retinal injuries [28,43].

Glutamate excitotoxicity may be induced by the intravitreal injection of *N*-methyl D-Aspartate (NMDA), which results in the excessive stimulation of NMDA receptors, one of the three ionotropic glutamate receptor subtypes widely expressed by inner retinal neurons. Glutamate excitotoxicity is thought to play an important role in the loss of RGCs in various retinal injuries [44,45], including glaucoma [46–50], transient ischemia [51], and optic nerve injury [52,53], and may also play a key role in many CNS diseases involving neuronal death [54]. Excessive NMDA receptor stimulation may result in alterations of the $Na^+/K^+$ homeostasis, excessive influx of large amounts of $Ca^{2+}$ into the cell [55], which may result in direct damage by activation of enzymes that damage DNA and cell membranes [56] and by the induction of apoptosis through activation of c-AMP [57]. Animal models

of NMDA-induced retinal excitotoxicity are often used to explore molecular mechanisms of RGC apoptosis and its protection [58–66].

The susceptibility of RGCs to NMDA-mediated excitotoxicity has been studied previously in adult rats [58,62] and mice [59,67], as well as the effects of intravitreal NMDA on the specific type population of $m^+$RGCs [59,67]. However, these were short term studies spanning up to 58 days after NMDA injection, and thus the short- and long-term effects of NMDA excitotoxicity on the population of RGCs expressing Brn3a have not been investigated so far. Moreover, to what extent NMDA-induced neurotoxicity may result in long term effects on the retinal architecture and on the population of ipRGCs itself have not been previously investigated.

In the present study we take advantage of recent techniques developed in the laboratory to identify, count, and map in the same retinal wholemounts the populations of RGCs expressing Brn3a or melanopsin. Moreover, we use modern non-invasive techniques, such as the Spectral Domain Optical Coherence Tomography (SD-OCT), to image and analyze retinal thickness longitudinally at short (3 months) and long (15 months) survival intervals. We investigate the responses of the general population of RGCs ($Brn3a^+$) and the population of ipRGCs ($m^+$RGCs) to excitotoxicity induced by the intravitreal injection of NMDA. Overall, our studies indicate that the general population of $Brn3a^+$RGCs is quite sensitive to NMDA-mediated excitotoxicity, which in one week induces the loss of approximately 72% of the population. In contrast, $m^+$RGCs, after a transient downregulation of melanopsin, show a remarkable capacity for survival of the entire $m^+$RGC population for periods of up to 15 months. Examination of these retinas with SD-OCT reveals that NMDA-injected retinas showed a marked reduction in the thickness of the total and inner retina that was present at 3 months and progressed up to 15 months. Short accounts of this work have been published in abstract format [68].

## 2. Results

We have included in this study a total of 51 rats whose left eye received an intraocular injection of 5 µL NMDA (100 nM). The first 28 were analyzed within the first 14 days after the injection while the remaining 23 were analyzed at 15 months to investigate the long-term effects of the excitotoxic insult on the survival of two RGC populations—the $Brn3a^+$RGCs and the $m^+$RGCs. Five additional naïve rats were used as controls. In addition, SD-OCT was used to measure retinal thickness in both retinas of 18 animals at 3 and 15 months after NMDA injection.

### *2.1. Rapid and Massive Loss of $Brn3a^+$RGCs Shortly after NMDA Injection*

When the right or naïve retinas were examined under a fluorescence microscope, $Brn3a^+$RGCs showed typical distribution throughout the entire retina with higher densities on the superior retina, just above the optic nerve along the visual streak, as described in detail previously [69–71]. Changing the fluorescent filter allowed us to see $m^+$RGCs distributed in a complementary fashion to $Brn3a^+$RGCs, and as previously shown by this laboratory [14,19], we were not able to see any doubly immunolabelled RGC, thus confirming that these markers are exclusive to one population (Figure 1).

Total numbers of $Brn3a^+$RGCs (78,903 ± 3573 mean ± SD, $n$ = 10) in the naïve retinas were comparable to those in the right fellow retinas of our experimental groups analyzed at 3, 7, and 14 days (76,472 ± 5815 $Brn3a^+$RGCs mean ± SD, $n$ = 29), or 15 months (81,480 ± 5602 mean ± SD, $n$ = 20) after NMDA injection, as well as to those obtained in previous studies from this laboratory [13,14,19,72] (Figures 1 and 2, Table 1).

The left NMDA-injected retinas showed significant decreases in the total numbers of $Brn3a^+$RGCs. By 3 days after NMDA injection, the total number of $Brn3a^+$RGCs was 38,940 ± 22,443 ($n$ = 9), which is significantly smaller than naïve controls and contralateral retinas (Mann Whitney test, $p \leq 0.001$). There were further reductions at 7 (21,811 ± 9750 mean ± SD, $n$ = 6) and 14 days (19,348 ± 8502 mean ± SD, $n$ = 10) but these were not statistically significant when compared to 3 days, indicating that in this injury model RGC loss occurs early after NMDA injection, but there is no further progression between 3 and 14 days (Figure 2, Table 1). Moreover, at 15 months, the left NMDA-injected retinas

showed significantly lower numbers than their fellow retinas (15,099 ± 8595 mean ± SD, $n = 23$) that corresponded to a survival of approximately 19%, and these values were significantly smaller than those observed at 3 days (Mann Whitney test, $p = 0.019$), but not from those obtained at 7 days (Mann Whitney test, $p = 0.187$), indicating that there is no further loss of Brn3a$^+$RGCs between 7 days and 15 months (Figures 1–3, Table 1).

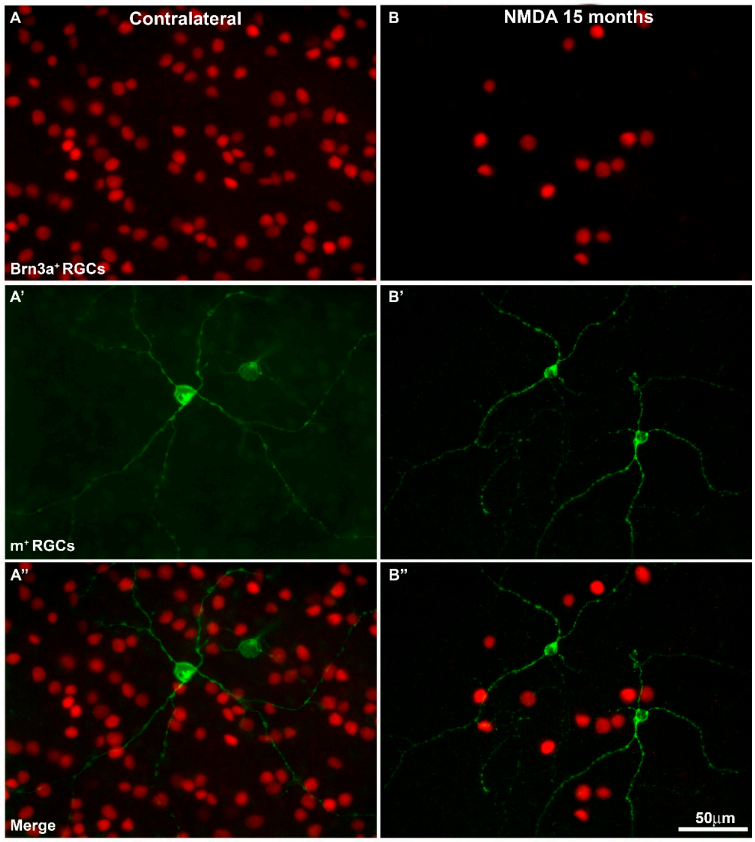


**Figure 1.** Magnifications from flat mounted retinas showing brain-specific homeobox/POU domain protein 3A positive retinal ganglion cells Brn3a$^+$RGCs (**A**,**B**) and melanopsin positive retinal ganglion cells m$^+$RGCs (**A′**,**B′**), and both signals (merge) (**A″**,**B″**) in contralateral (**A**,**A″**) and *N*-methyl-D-aspartate (NMDA)-treated retinas (**B**,**B″**) analyzed at 15 months after the injection. Brn3a labels cell nuclei, while melanopsin allows one to see cell somata as well as primary dendrites on the plane of focus. When both images are overlapped (**A″**,**B″**), one can appreciate the smaller density of m$^+$RGCs compared to Brn3a$^+$RGCs, as well as the fact that there are no doubly labelled RGCs. Note that 15 months after NMDA injection there are fewer Brn3a$^+$RGCs. Scale bar = 50 μm.

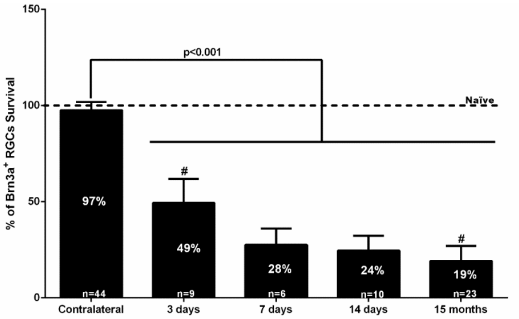


**Figure 2.** Bar graph showing the percent vs. intact retinas of the total numbers of Brn3a$^+$RGCs ± standard deviation quantified in the contralateral uninjured and experimental retinas analyzed 3, 7, 14 days, or 15 months after the intraocular injection of 100 nM NMDA. The number of Brn3a$^+$RGCs in the intact naïve retinas was considered 100%. The number of analyzed retinas is shown at the bottom of each bar. Statistically significant differences were observed (Kruskal-Wallis test, $p < 0.001$) between values obtained in intact retinas (naïve) or right eye retinas (contralateral) and experimental retinas examined at 3, 7, 14 days, or 15 months. When compared with the previous time study interval (at 7 days, 14 days, or 15 months), there were no significant differences (Kruskal-Wallis test, $p > 0.05$). However, there were significant differences between 3 days and 15 months ($^{\#}$ Mann Whitney test, $p = 0.019$), but not from those obtained at 7 days (Mann Whitney test, $p = 0.187$), which suggests that NMDA-induced Brn3a$^+$RGC loss does not progress between 7 days and 15 months.

**Table 1.** Total numbers of Brn3a$^+$RGCs in right (RE) or left (LE) eye retinas.

| Retinas | Naïve | | 3 Days | | 7 Days | | 14 Days | | 15 Months | |
|---|---|---|---|---|---|---|---|---|---|---|
| | **RE** | **LE** | **RE** | **LE** | **RE** | **LE** | **RE** | **LE** | **RE** | **LE** |
| 1 | 80,293 | 82,587 | 72,071 | 46,569 | 74,963 | 24,880 | 71,159 | 16,434 | 89,717 | 14,852 |
| 2 | 80,399 | 79,044 | 79,209 | 52,957 | 77,604 | 12,227 | 80,940 | 13,785 | 93,939 | 9538 |
| 3 | 78,344 | 71,826 | 78,178 | | 72,411 | 33,105 | 78,786 | 10,593 | 88,081 | 24,936 |
| 4 | 74,865 | 77,395 | 79,256 | 19,910 | 66,564 | | 73,895 | 39,166 | 81,353 | 21,955 |
| 5 | 84,031 | 80,247 | 82,406 | 15,648 | 66,086 | 31,097 | 77,579 | 16,132 | 78,436 | 22,369 |
| 6 | | | 74,244 | 15,721 | 63,952 | 9238 | 82,321 | | 68,961 | 1951 |
| 7 | | | | 62,993 | 71,202 | 20,321 | 87,289 | 15,318 | 83,471 | 5796 |
| 8 | | | | 62,344 | | | 80,773 | 22,261 | 80,699 | 21,478 |
| 9 | | | | 61,640 | | | 84,397 | 20,945 | | 16,245 |
| 10 | | | | 12,681 | | | 80,789 | 12,209 | | 24,937 |
| 11 | | | | | | | 76,135 | 26,641 | 74,808 | 16,594 |
| 12 | | | | | | | | | 88,721 | 8588 |
| 13 | | | | | | | | | 75,941 | 1990 |
| 14 | | | | | | | | | | 2754 |
| 15 | | | | | | | | | 80,213 | 10,950 |
| 16 | | | | | | | | | 81,595 | 5404 |
| 17 | | | | | | | | | 80,424 | 5584 |
| 18 | | | | | | | | | 79,487 | 25,879 |
| 19 | | | | | | | | | 79,093 | 25,486 |
| 20 | | | | | | | | | 77,667 | 21,966 |
| 21 | | | | | | | | | 81,417 | 11,286 |
| 22 | | | | | | | | | 83,543 | 25,152 |
| 23 | | | | | | | | | 82,032 | 21,587 |
| Mean | 78,903 | | 77,561 | 38,940 | 70,397 | 21,811 | 79,460 | 19,348 | 81,480 | 15,099 |
| ± SD | 3572 | | 3757 | 22,443 | 5038 | 9751 | 4631 | 8502 | 5602 | 8595 |
| **Total RE** | | | | | **Mean** 78,677 | | **SD** 6260 | | | |

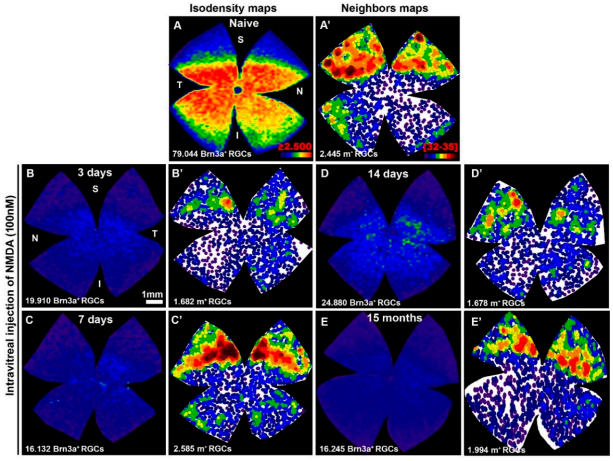


**Figure 3.** (**A**–**E**) Isodensity maps showing the retinal topography of Brn3a$^+$RGCs in intact retinas (**A**) or in representative retinas analyzed at 3 (**B**), 7 (**C**), 14 (**D**) days, or 15 (**E**) months after intravitreal injection of 100 nM NMDA. (**A'**–**E'**) Neighbor maps illustrating the distribution of m$^+$RGCs in the same retinas shown in (**A**–**E**). Isodensity maps color scale ranges from 0 (purple) to ≥ 2500 (red) cells/mm$^2$. Neighbor map color scale, where each color represents an increase of 4 neighbors in a radius of 0.22 mm from purple (0–4 neighbors) to dark red (32–35 neighbors). Below each map is shown the total number of Brn3a$^+$RGCs or m$^+$RGCs counted. Note: S = superior; I = inferior; N = nasal; T = temporal. Scale bar = 1 mm.

Retinal distribution of Brn3a$^+$RGCs in the NMDA-injected retinas did not adopt any particular spatial pattern; their loss was diffuse and distributed over the entire amount of retinas (Figure 3), although occasionally there was a smaller density in the superior temporal quadrant that could be explained by the proximity to the intraocular puncture, and thus, a region exposed to a greater concentration of the injected NMDA.

### *2.2. After A Transient Downregulation of Melanopsin, m$^+$RGCs Appear Fully Resistant to NMDA Injection*

Total numbers of m$^+$RGCs (2358 ± 143 mean ± SD, $n$ = 10) in the naïve retinas were comparable to those obtained in the right fellow retinas of our experimental groups analyzed at 3, 7, and 14 days (2257 ± 228 m$^+$RGCs mean ± SD, $n$ = 29), or at 15 months (2166 ± 96 mean ± SD, $n$ = 9) after NMDA injection, as well as to those obtained in previous studies from this laboratory [13,19,69] (Figures 1, 3 and 4, Table 2).

By 3 days after intravitreal injection of NMDA, the total number of m$^+$RGCs was 1516 ± 312 ($n$ = 10), a significant reduction when compared to naïve or contralateral retinas (Kruskal Wallis test, $p \leq 0.001$) (Figure 2). Surprisingly, the total number of m$^+$RGCs at 7 or 14 days after NMDA injection was 2105 ± 445 ($n$ = 7) or 2419 ± 257 ($n$ = 11), showing a significant increase when compared to the values observed at 3 days, and reached comparable values to those of control retinas by 14 days (Kruskal Wallis test, $p > 0.05$). By 15 months after NMDA injection, the left retinas showed a total number of m$^+$RGCs (2027 ± 134 mean ± SD, $n$ = 11) comparable with the data obtained in their right fellow retinas (2166 ± 96 mean ± SD, $n$ = 9) (Mann Whitney test, $p$ = 0.518).

We interpret this abrupt decrease and subsequent recovery of the total number of m$^+$RGCs as a transient downregulation of melanopsin, shortly after intravitreal injection of NMDA, which recovers

up to normal levels of expression and total number of $m^+$RGCs by 7 days, 14 days, and 15 months. In addition, these results also indicate that $m^+$RGCs are resistant to NMDA-induced excitotoxicity. In contrast with the $Brn3a^+$RGC population, whose total numbers were reduced to approximately one quarter to one fifth of their normal values, the $m^+$RGCs show a complete population that is comparable to that found in their fellow contralateral and in naïve retinas (Figures 1, 3 and 4, Table 2).

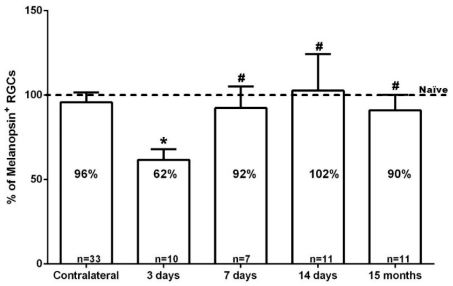


**Figure 4.** Bar graph showing the percent vs. intact retinas of the total number of $m^+$RGCs ± standard deviation quantified in the contralateral uninjured and experimental retinas analyzed 3, 7, 14 days, or 15 months after the intraocular injection of 100 nM NMDA. The number of analyzed retinas is shown at the bottom of each bar. Note: * Significant differences compared to naïve, contralateral retinas, and other time points (Kruskal-Wallis test, $p < 0.001$); # the percent of $m^+$RGCs in the experimental groups analyzed at 7 days, 14 days, or 15 months did not differ significantly from their contralateral fellow retinas (Mann-Whitney Test, $p > 0.05$).

**Table 2.** Total numbers of $m^+$RGCs in right (RE) or left (LE) eye retinas.

| Retinas | Naive | | 3 Days | | 7 Days | | 14 Days | | 15 Months | |
|---|---|---|---|---|---|---|---|---|---|---|
| | **RE** | **LE** | **RE** | **LE** | **RE** | **LE** | **RE** | **LE** | **RE** | **LE** |
| 1 | 2434 | 2201 | 2135 | 2062 | 2163 | 1678 | 2034 | 2409 | | 1994 |
| 2 | 2373 | 2445 | 1972 | 1293 | 2496 | 1650 | 2026 | 2276 | | 2018 |
| 3 | 2366 | 2103 | 2294 | 1187 | 1962 | 1860 | 2055 | 2149 | 2154 | 1997 |
| 4 | 2362 | 2249 | 2547 | 1682 | 2262 | 1971 | 2242 | 2425 | 2297 | 1987 |
| 5 | 2612 | 2433 | 1966 | 1043 | 2040 | 2174 | 2566 | 2585 | 2207 | 1904 |
| 6 | | | 2183 | 1448 | 2471 | 2662 | 2363 | 2145 | 2016 | 1857 |
| 7 | | | | 1719 | 2612 | 2746 | 1950 | 2661 | 2267 | 2019 |
| 8 | | | | 1473 | | | 2537 | 2701 | 2022 | 2284 |
| 9 | | | | 1850 | | | 2267 | 1955 | 2156 | 1961 |
| 10 | | | | 1411 | | | 2559 | 2660 | 2196 | 2004 |
| 11 | | | | | | | 2467 | 2652 | 2181 | 2273 |
| Mean | 2358 | | 2183 | 1453 | 2287 | 2106 | 2279 | 2420 | 2166 | 2027 |
| ± SD | 144 | | 219 | 371 | 247 | 446 | 235 | 257 | 95 | 133 |
| **Total RE** | | | | | **Mean** 2257 | | **SD** 229 | | | |

### *2.3. In Vivo SD-OCT Measurements*

We wanted to examine the effects of the NMDA-induced retinal degeneration on the retinal layers, and thus retinas were analyzed at 3 and 15 months with SD-OCT to determine the total and inner retinal thickness. Figure 5 shows representative SD-OCT images from both eyes in two representative experimental rats analyzed longitudinally in vivo 3- and 15-months after NMDA-injection. The SD-OCT provided measurements of the 31 sections acquired, and we selected three sections located superior, central, or inferior for analysis. Because the measurements of these three sections were comparable within each individual retina and time interval examined, the values from these 3 sections were pooled and used as a value for each retina and time point.

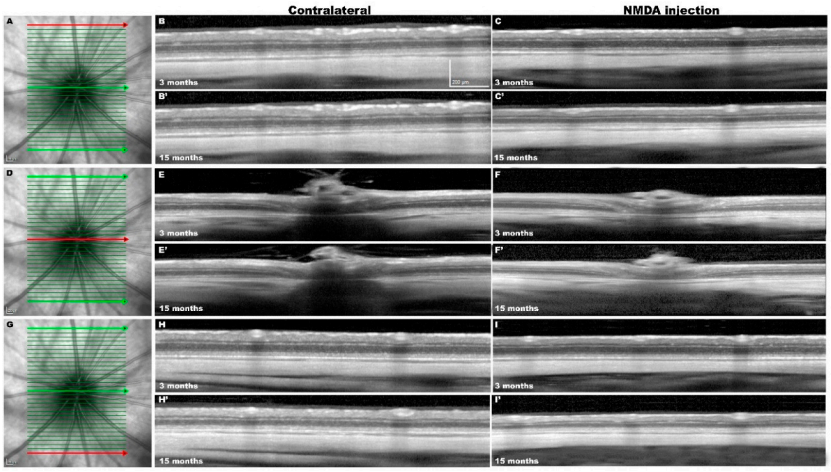


**Figure 5.** In vivo Spectral Domain-Optical Coherence Tomography (SD-OCT) images from the same contralateral and experimental retinas analyzed 3 and 15 months after NMDA injection. (**A**,**D**,**G**) Representative images of the ocular fundus of the contralateral retina and position of the 31 sections acquired. The superior (**A**), central (**D**), or inferior (**G**) retinal sections are marked in red. (**B**,**C**,**E**,**F**,**H**,**I**) Representative sections acquired (in red) from SD-OCT volume raster scan in contralateral (**B**,**E**,**H**) and NMDA-injected (**C**,**F**,**I**) retinas examined longitudinally at 3-months (**B**–**I**) and at 15-months (**B'**–**I'**) after NMDA injection.

Total retinal (TR) thickness (as measured in μm from the inner side of the nerve fiber layer to the outer limit of the outer segment layer) was significantly smaller in the NMDA-injected retinas as compared to their contralateral fellow retinas at 3 months (185 ± 4 versus 211 ± 3.9; $n$ = 18) and 15 (162 ± 6.1 versus 195 ± 6.1; $n$ = 18) months. In fact, the thinning of the TR was mainly due to the thinning of the inner retina (IR) (as measured in μm from the inner side of the nerve fiber layer to the outer limit of the inner nuclear layer). The IR thickness in the left NMDA-injected eyes was significantly smaller than in their fellow retinas at 3 months (83 ± 3.7 versus 96 ± 2.6; $n$ = 18) and 15 (71 ± 2.8 versus 91 ± 3.4; $n$ = 18) months (Figures 5 and 6).

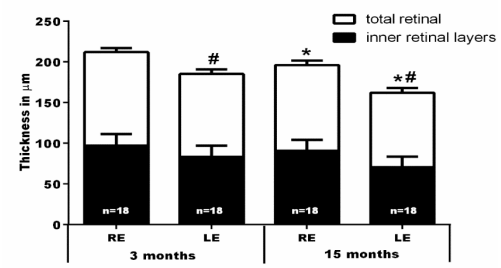


**Figure 6.** Graph bars showing the reduction of the mean ± SD thickness (μm) of the total (from inner side of the nerve fiber layer to outer segment layer) and inner (from the inner side of the nerve fiber layer to outer margin of inner nuclear layer) retina after NMDA intravireal injection into the left eye, measured in the volume scan analyses shown in Figure 5. Note: * Significant differences compared to the same eyes analyzed at 3 months (Kruskal-Wallis test, $p < 0.001$); # significant differences when compared to their contralateral eyes at the same time interval (Mann-Whitney Test, $p < 0.001$); RE = right fellow eye; LE = left eye (NMDA-injected).

The TR thickness of the fellow retinas diminished significantly between 3 (211 ± 3.2; $n$ = 18) and 15 (195 ± 6.1; $n$ = 18) months, a finding that is in agreement with recent studies in adult albino rats showing a physiological thinning of the TR and IR of approximately 16 and 6 μm, respectively, with age [69]. However, superimposed to the physiological age-related thinning of the retina, in the experimental NMDA-injected retinas there was further significant thinning of the TR (23 μm) and IR (12 μm) between 3 and 15 months (Figures 5 and 6).

**3. Discussion**

Here we have investigated the short- and long-term responses of the populations of Brn3a$^+$ and melanopsin expressing (m$^+$) RGCs after an excitotoxic insult to the retina. Our studies show that following an intraocular injection of 100 nM NMDA, there is a rapid and massive loss of the general population of Brn3a$^+$RGCs; by 3 days, 14 days, or 15 months, the surviving population represents approximately 49%, 24%, or 19%, respectively, of the original population. When examined with SD-OCT there was an important reduction in the thickness of the total and the inner retina at 3 months that further progressed up to 15 months.

Compared to the population of Brn3a$^+$RGCs, m$^+$RGCs show by 3 days a transient downregulation of melanopsin that recovers over the next weeks, and by 14 days or 15 months the numbers of m$^+$RGCs are comparable to their contralateral fellow eyes.

When studying the responses of RGCs to retinal injuries it is important to be able to identify different types of RGCs to understand how these respond to injury [43,73]. Here, we use modern techniques developed in the laboratory to count, image, and represent the retinal topography of two RGC populations that can be readily identified with Brn3a and melanopsin [43,74]. Recent studies from this laboratory have demonstrated that in the adult rat, retinal injuries induce a transient downregulation

of melanopsin [28], followed by the expression of melanopsin in injured neurons surviving long periods of time [9,19,75,76]. Of the six main subtypes of ipRGCs M1–M6, immunocytochemistry against melanopsin identifies mainly M1–M3 because they show higher levels of melanopsin expression [32–35, 37,38], and thus when interpreting our data, we should take into account that our immunohistochemical methods primarily identify the M1–M3 ipRGC subtypes. In fact, although not analyzed in this work, it is conceivable that most of our results refer to the M1 and M2 subtypes, which are the most abundant and readily identified with melanopsin antibodies [37,38,40,77].

### *3.1. Intravitreal Injection of NMDA Induces Brn3a$^+$RGC Death*

The loss of RGCs observed after the injection of NMDA in our studies is comparable to that found by others in mice [59,67] or rats [53,58,78] analyzed at survival intervals ranging 3–58 days. We noticed certain inter-animal variability in the total number of surviving Brn3a$^+$RGCs at 3 days after NMDA injection, which was also reported by others [58,67] and could be due to an individual animal susceptibility, or to the fact that RGC loss has not concluded by that time interval. Inter-animal variability following other types of retinal injuries, such as intraorbital optic nerve cut or crush, an insult that results in axotomy of the entire RGC population, have been shown [9,79]. Another possible explanation for the inter-animal variability could be the fact that intravitreal injections may suffer a small reflux of the injected volume rendering the concentration of NMDA unequal for all eyes. We have not investigated shorter survival intervals than 3-days after NMDA injection, but other studies have suggested that following NMDA injection RGC loss appears as early as 6-h after injection [80]. It is currently thought that NMDA-induced excitotoxicity results in activation of the NMDA receptor and this leads to a massive influx of $Ca^{++}$ that acts as a second messenger to activate pathways that lead to apoptotic neuronal death [81], although the exact signalling pathways involved in NMDA-induced RGC death are not completely understood [61].

By 14 days, approximately 75% of the original Brn3a$^+$RGC population has degenerated. Their topography does not reveal any particular distribution, such as the patchy or sectorial patterns observed after acute or chronic ocular hypertension, respectively [82–84], but rather a diffuse pattern of RGC loss much like the pattern observed after crushing or cutting of the intraorbital optic nerve [70,74]. In some instances, over the general diffuse pattern of RGC loss, there was a marked decrease in the superior temporal quadrant, the region where NMDA was injected, and thus where NMDA may have reached a higher concentration.

Our results indicate that RGC loss is not progressive, since between 7-days and 15-months after NMDA injection there are no significant changes in total numbers of Brn3a$^+$RGCs. Our results appear in disagreement with those of Huang and colleagues [78] that reported a progressive RGC loss between 12 h and 58 days, but these authors employed Neu-N antibodies as a marker to identify RGCs, which identify displaced amacrine cells in addition to RGCs [17], and RGC densities were obtained by averaging 16 samples obtained throughout the retina, whereas our numbers were obtained after counting the entire amount of retinas. Nevertheless, Huang and colleagues [78] reported the loss of approximately 67% of the RGC population at 58 days, which is analogous to the 75% loss observed in our studies.

### *3.2. Intravitreal Injection of NMDA Induces A Progressive Retinal Thinning*

RGC degeneration results in the loss of neural processes that extend into the inner synaptic layer, where they contact cone-bipolar and amacrine cells of different types forming an extensive neuropil that makes up a substantial proportion of the inner synaptic layer's volume. Our results indicate that NMDA-induced retinal excitotoxicity results in a significant decrease of the total (TR) and inner (IR) retinal thickness. This thinning was already apparent in the left NMDA-injected experimental retinas at 3 months when compared to their fellow retinas. The retinal thinning may be explained because over 75% of the Brn3a$^+$RGC population is missing and their dendrites have degenerated, thus prompting a thinning of the IPL [78], but also because NMDA-excitotoxiticy results in loss of

amacrine cells, as shown with Terminal deoxynucleotidyl transferase dUTP nick end labeling (TUNEL) and morphometric techniques in adult pigmented mice [85–87] and albino rats [78,88]. The thinning of the TR and IR observed in the fellow retinas between 3 and 15 months is consistent with the physiological thinning of the adult SD rat retina with age [72]. However, superimposed on this physiological thinning, in the experimental retinas there was a progressive thinning of the TR and IR between 3 and 15 months, indicating a continuing retinal degeneration prolonged beyond the time of NMDA injection and the period of Brn3a$^+$RGC loss, which concluded at 7 days after the injection. A possible explanation for the progressive thinning of the IR could be the secondary amacrine cell loss that follows RGC death observed after NMDA-induced neurotoxicity. Indeed, approximately 72% of the RGC types in the mice retina are coupled to ACs [89], which may possibly facilitate secondary cell loss of calretinin, calbindin, and choline acetyltransferase immunopositive ACs via gap junctions [87].

### *3.3. The m$^+$RGCs Resilience to Retinal Disease and Injury*

In the adult rat, m$^+$RGCs only represent approximately 2.7% or 2.5% of the total population of RGCS in albino or pigmented populations, respectively [14,19,72]. Yet, the availability of specific molecular markers for this type of RGCs has made it possible to learn in a very short period of time a great deal about the morphological and functional properties of these neurons, including their idiosyncratic response to different types of inherited or acquired retinal lesions [43]. A number of different laboratories have shown that ipRGCs demonstrate a much better survival against a variety of retinal injuries than the general population of RGCs [90], and this particular resilience has been shown against ocular hypertension in rats [39,91] or mice [92], crushing or cutting of the optic nerve in rats [93,94] or mice [35,76,95,96], and transient ischemia of the retina in rats [84]. However, ipRGCs do not appear to be particularly resilient in inherited models of retinal degeneration [95–99], mitochondrial optic neuropathies [100], or degenerative diseases [77], such as Alzheimer's [101], Parkinson's [102], or Huntington's [103] disease. A detailed characterization of the RGC responses to NMDA-induced excitotoxicity may shed light into the paradigm of the different responses of different populations of RGCs to injury; why some populations die while others survive.

### *3.4. The m$^+$RGCs Are Resistant to NMDA-Induced Retinal Excitotoxicity*

Our results demonstrate that following a transient downregulation of melanopsin expression, the total number of m$^+$RGCs at 14 days or 15 months is comparable to their contralateral fellow eyes, thus indicating an outstanding endurance to NMDA-induced excitotoxicity.

Survival of the entire m$^+$RGC population at 15-months after NMDA injection is underscored in view of the important inner retinal degeneration and loss of approximately 81% of the Brn3a$^+$RGC population. The degeneration of RGCs following NMDA-induced excitotoxicity has been explored in adult pigmented mice analyzed at 6 [67] or from 1 to 21 [59] days, respectively. However, these studies showed slight differences in terms of the survival of the m$^+$RGC population. DeParis and colleagues [67] found that 6 days after NMDA injection there was a full component of m$^+$RGC population surviving in the retina with no downregulation of the expression of melanopsin, while Wang and colleagues [59] reported the loss of approximately one half of the m$^+$RGC population at 21-days after NMDA injection. These differences may be explained by the diverse amount of NMDA injected (3 µL of 10 mM NMDA versus 1 µL of 40 mM NMDA).

The downregulation of melanopsin expression that occurs after retinal injury requires further consideration. Our studies reveal that following NMDA injection there is a transient downregulation of melanopsin that recovers fully by 14 days. A similar transient downregulation of melanopsin has been described in previous studies from this laboratory in adult rats following optic nerve injury [94], transient elevation of the intraocular pressure [84], the use of retrogradely transported neuronal tracers [104], or acute light-induced retinal degeneration [75]. The differences between our results and those observed by DeParis and colleagues [67] may be a species-specific response of m$^+$RGCs, because

in parallel studies of m$^+$RGC survival in adult mice following intraorbital optic nerve injury, we did not find a transient downregulation of melanopsin [28,76].

Of all the retinal injuries examined so far, m$^+$RGCs best tolerate NMDA-induced excitotoxicity. The reasons for the remarkable resilience of ipRGCs to survive different types of injury-induced retinal degeneration remains an open issue for future studies, but several hypotheses have been forwarded to explain m$^+$RGC resilience. One hypothesis proposes that these ipRGCs have large dendrites within the inner synaptic layer, and thus their intra-retinal connections may be enough to provide trophic support for survival in the absence of brain-target-derived trophic support [29,90,93,105]. Although it has been postulated that the absence of NMDA receptors in m$^+$RGCs could explain their particular resistance to NMDA-mediated excitotoxicity, it has been shown that all RGCs express NMDA receptors [106], including m$^+$RGCs [66,107], and that the particular resilience of m$^+$RGCs is not related to pigmentation, genetic background, the presence of photoreceptors, or the activation of the endogenous survival JAK/STAT pathway [67]. Other possible explanations include the activation of the PI3K/AKT pathway after cutting of the optic nerve or ocular hypertension [108], but this was not apparent in NMDA-induced excitotoxicity [67]. Melanopsin itself could be thought to have an effect on cell survival, but the fact that many ipRGCs survive with a transient, but lower, expression of melanopsin makes this unlikely. Another hypothesis explains the resilience on the basis of their neurotransmitter (PACAP) and it is hypothesized that PACAP would act as a neuroprotectant conferring these neurons their particular resistance, since exogenous administration of PACAP protects RGCs against optic nerve transection [109], ocular hypertension [110], or NMDA administration [111]. It could also be possible that different types of RGCs may have different responses to the same insult, thus arguing in favour of a type-specific susceptibility. For example, recent studies using genetic markers to identify different types of RGCs have shown that the type of αRGC is particularly resistant to NMDA induced neurotoxicity [8] or to optic nerve crush [35,39], in contrast to the very low survival of junction adhesion molecules B-expressing RGCs (J-RGCs) [8]. Moreover, recent studies indicate that different subtypes of ipRGCs have different susceptibility to specific insults; for instance, in a mouse model of Huntington's disease (HD), M1 were reduced compared to non-M1 ipRGCs that survived to HD progression [112]. Furthermore, in a mouse model of ocular hypertension, subtypes of αRGCs were found to have different susceptibility, with OFF-transient αRGCs being more vulnerable than ON- or OFF-sustained αRGCs [22,73]. Overall, the particular resilience of m$^+$RGCs makes them a suitable candidate to study changes in protein expression after injury, which furthers our knowledge about what makes a neuron survive better than others, and this could in turn result in the design of new neuroprotective strategies for RGCs against noxious stimuli. Thus, future studies are needed to decipher the molecular correlations that provide these neurons with a self-built neuroprotection against various types of injury, including NMDA-induced RGC death.

## 4. Material and Methods

### *4.1. Animal Handling and Experimental Groups*

Experiments were prepared in 56 adult female SD rats (250 g) obtained from the animal house (Murcia University, Murcia, Spain) and treated according to the European Union guidelines for Animal Care and use of scientific purpose (Directive 2010/63/UE). All procedures were approved by the Ethical and Animal Studies Committee of the University of Murcia, Spain (Comité Ético de Experimentación Animal (CEEA) de la Universidad de Murcia, 11 January 2017, Code: A13170110 and A13170111). Animals had free access to food and water and were kept in a temperature and light controlled room with 12-h/12-h light/dark cycles. Animals were anaesthetized with a mixture of xylazine (10 mg/kg Rompun; Bayer, Kiel, Germany) and ketamine (60 mg/Kg bw, Ketolar; Pfizer, Alcobendas, Madrid, Spain); 0.5% proparacaine hydrochloride eye drops (Alcon Co., Fort Worth, TX, USA) were used to achieve topical anaesthesia. After the surgical procedures, an ocular ointment was placed over the corneas of both eyes to prevent corneal desiccation (Tobrex®; Alcon-Cusí, S.A., Barcelona, Spain).

Animals were divided into experimental and control groups. The experimental group received an intraocular injection of NMDA and was divided into four subgroups that were examined at 3 ($n$ = 10), 7 ($n$ = 7), or 14 ($n$ = 11) days, or 15 months ($n$ = 23). Additional naïve rats ($n$ = 5) were used as controls. For animal sacrifice an overdose of sodium pentobarbital was injected intraperitoneally (Dolethal, Vetoquinol®, Especialidades Veterinarias, S.A., Madrid, Spain).

*4.2. Intraocular Injections of NMDA*

Retinal excitotoxicity was induced in the left eye of the experimental animals by intraocular injection of 5 µL of 100nM NMDA *N*-methyl-D-Aspartate (NMDA) (M3262; Sigma-Aldrich Química S.A., Madrid, Spain) dissolved in 0.1 M phosphate buffer saline (PBS) following standard techniques in our laboratory [113–115]. In brief, a small puncture in the sclera approximately 1 mm from the limbus was made with a 30-gauge needle, and then NMDA was injected slowly with a Hamilton syringe whose needle was introduced through the sclerotomy. After injection, the needle was withdrawn slowly and an ointment (Tobrex pomada; Alcon S.A., Barcelona, Spain) was placed over the eyes to prevent corneal dehydration until anaesthesia recovery. The contralateral non-injected eye was used as control, and 5 naïve rats (10 eyes) were also used as controls. Preliminary experiments allowed us to try increasing doses of NMDA to find one that would result in consistent RGC death. Previous studies from this Laboratory did not find any effect of the intraocular injection of vehicle alone (0.1 M phosphate buffer saline, PBS) on the survival of the Brn3a$^+$ or melanopsin$^+$ RGC populations, and thus, we did not employ additional animals for this purpose.

*4.3. In Vivo Measurements of the Retinal Thickness with SD-OCT*

SD-OCT measurements were obtained to analyze changes in the thickness of the retina following NMDA intraocular injection, and the eyes were imaged at 3 and 15 months, as previously described in detail [72,116]. Rats were anaesthetized systemically, and eye drops were placed on both eyes to induce mydriasis (Tropicamida 1%; Alcon-Cusí, S.A.) and to prevent corneal desiccation (artificial tears). Rats were placed in prone position over a platform with their heads upright and turned to the opposite side of the inspected eye. The head position was kept similar for all animals, and for the following examination the follow up tool of the OCT program was used to compare the same regions. Both retinas were examined with OCT following manufacturer guidelines (Spectralis; Heidelberg Engineering, Heidelberg, Germany). To compensate for the rat's corneal curvature and to maintain its hydration, we placed over the cornea a customized permeable contact lens (3.5-mm posterior radius of curvature, 5.0-mm optical zone diameter, 5.0-diopter back vertex power). To observe the rat's eye fundus we placed in front of the camera a commercially available 78-diopter double aspheric lens (Volk Optical, Inc., Mentor, OH, USA). Photographs were taken with a software package (EyeExplorer, version 3.2.1.0; Heidelberg Engineering). Retinal thickness was determined with a raster scan of 31 equally spaced horizontal B-scans (3000 µm length) centred on the optic nerve head. For each section total retinal (TR) (as measured from the inner limiting membrane to the outer limit of the pigmented epithelial layer) and inner retinal (IR) (as measured from the inner limiting membrane to the outer limit of the inner nuclear layer) thickness were measured at distances of 1800 µm from optic disc. A total of 18 rats were analyzed longitudinally at 3 and 15 months.

*4.4. Retinal Dissection, Immunohistochemistry and Image Acquisition*

At different survival intervals, rats were sacrificed and perfused through the heart, first and briefly with a solution of 0.9% NaCl, and then slowly with a 4% paraformaldehyde solution in PBS. The superior pole of the eye was marked with a small suture, and retinas were then dissected and prepared as flattened wholemounts, as previously described [117]. Retinas were double-immunodetected following previously described methods for Brn3a and melanopsin to identify surviving RGCs expressing these two markers [14]. Primary antibodies were goat anti-Brn3a (1:750 dilution, C-20 Santa Cruz Biothechology, Heidelberg, Germany) and rabbit anti melanopsin (1:500 dilution, PAI-780,

Invitrogen, Thermo Fisher Scientific, Alcobendas, Madrid, Spain). Secondary antibodies were Alexa Fluor conjugated (donkey anti-rabbit Alexa 594, donkey anti-goat Alexa 488) (Molecular Probes Thermo-Fisher, Madrid, Spain). At the end of the immunohistochemical procedure, both retinas were mounted (vitreal side up) on gelatinized slides with an antifading solution [14].

Using epifluorescence microscopy (Axioscop 2 Plus; Zeiss Mikroscopie, Jena, Germany) retinas were photographed according to standard methods in the laboratory [76,118]. A total of 154 frames were obtained in the microscope to reconstruct the whole retina. These reconstructions were obtained under both filters to allow identification of Brna3a$^+$RGCs and m$^+$RGCs, respectively. Following standard procedures in the laboratory [74,119,120], wholemount reconstructions were further processed to automatically obtain the total number of Brn3a$^+$RGCs and their topographical distribution was represented as isodensity maps. For the m$^+$RGCs, these were quantified manually and dotted on the photomontage with the aid of a graphic editing software Adobe Photoshop CS8.01 (Adobe Systems, Inc., San Jose, CA, USA). Dots were automatically identified, and their topographical distribution was represented as neighbour maps following previously described methods [120].

### *4.5. Statistics*

All data is expressed as means ± standard deviation (SD). Statistical analysis employed the program GraphPad Prism® for Windows (Version 5.01; GraphPad Software Inc., La Jolla, CA, EEUU) using non-parametric tests (Kruskal Wallis and Mann Whitney). Differences were considered significant if $p < 0.05$.

## 5. Conclusions

Intravitreally administered NMDA in adult albino rats: (i) induces a massive diffuse loss of Brn3$^+$RGCs, which is evident within the first week and does not progress further; (ii) causes a thinning of the inner retina at 3 months that further progresses up to 15 months; (iii) triggers a transient downregulation of melanopsin expression that is evident at 3 days and recovers fully by 14 days, and; (iv) does not induce m$^+$RGC loss.

**Author Contributions:** B.V.-V., J.D.P., M.V.-S., and N.C.N. conceptualized the study. B.V.-V., J.D.P., F.M.N.-N., J.A.M.d.I.-O., A.O.-M., J.M.B.-G., N.C.N., M.P.V.-P., and M.V.S. planned and performed all experiments and analyzed data. J.A.M.d.I.-O. and A.O.-M. performed preliminary experiments to set up the model. J.M.B.-G. analyzed retinas and performed image analysis for RGC counts. B.V.-V., J.D.P., N.C.N., and M.V.-S. wrote the paper with input from all authors. M.P.V.-P. and M.V.-S. provided research funds for the study.

**Funding:** This study was supported by the Fundación Séneca, Agencia de Ciencia y Tecnología Región de Murcia (19881/GERM/15), and the Spanish Ministry of Economy and Competitiveness, Instituto de Salud Carlos III, Fondo Europeo de Desarrollo Regional "una manera de hacer Europa" (SAF2015-67643-P, PI16/00380, RD16/0008/0026 and RD16/0008/0016).

**Conflicts of Interest:** The authors declare no conflict of interest. The funders had no role in the design of the study; in the collection, analyses, or interpretation of data; in the writing of the manuscript, or in the decision to publish the results.

## References

1. Lucas, R.J.; Peirson, S.N.; Berson, D.M.; Brown, T.M.; Cooper, H.M.; Czeisler, C.A.; Figueiro, M.G.; Gamlin, P.D.; Lockley, S.W.; O'Hagan, J.B.; et al. Measuring and using light in the melanopsin age. *Trends Neurosci.* **2014**, *37*, 1–9. [CrossRef] [PubMed]
2. Smith, C.A.; Chauhan, B.C. Imaging retinal ganglion cells: Enabling experimental technology for clinical application. *Prog. Retin. Eye Res.* **2015**, *44*, 1–14. [CrossRef] [PubMed]
3. Masland, R.H. The neuronal organization of the retina. *Neuron* **2012**, *76*, 266–280. [CrossRef] [PubMed]
4. Macosko, E.Z.; Basu, A.; Satija, R.; Nemesh, J.; Shekhar, K.; Goldman, M.; Tirosh, I.; Bialas, A.R.; Kamitaki, N.; Martersteck, E.M.; et al. Highly Parallel Genome-wide Expression Profiling of Individual Cells Using Nanoliter Droplets. *Cell* **2015**, *161*, 1202–1214. [CrossRef] [PubMed]

5. Baden, T.; Berens, P.; Franke, K.; Roman Roson, M.; Bethge, M.; Euler, T. The functional diversity of retinal ganglion cells in the mouse. *Nature* **2016**, *529*, 345–350. [CrossRef] [PubMed]
6. Sanes, J.R.; Masland, R.H. The types of retinal ganglion cells: Current status and implications for neuronal classification. *Annu. Rev. Neurosci.* **2015**, *38*, 221–246. [CrossRef] [PubMed]
7. Rheaume, B.A.; Jereen, A.; Bolisetty, M.; Sajid, M.S.; Yang, Y.; Renna, K.; Sun, L.; Robson, P.; Trakhtenberg, E.F. Single cell transcriptome profiling of retinal ganglion cells identifies cellular subtypes. *Nat. Commun.* **2018**, *9*, 2759. [CrossRef] [PubMed]
8. Christensen, I.; Lu, B.; Yang, N.; Huang, K.; Wang, P.; Tian, N. The Susceptibility of Retinal Ganglion Cells to Glutamatergic Excitotoxicity Is Type-Specific. *Front. Neurosci.* **2019**, *13*, 219. [CrossRef]
9. Nadal-Nicolas, F.M.; Salinas-Navarro, M.; Vidal-Sanz, M.; Agudo-Barriuso, M. Two methods to trace retinal ganglion cells with fluorogold: From the intact optic nerve or by stereotactic injection into the optic tract. *Exp. Eye Res.* **2015**, *131*, 12–19. [CrossRef] [PubMed]
10. Thanos, S.; Vidal-Sanz, M.; Aguayo, A.J. The use of rhodamine-B-isothiocyanate (RITC) as an anterograde and retrograde tracer in the adult rat visual system. *Brain Res.* **1987**, *406*, 317–321. [CrossRef]
11. Vidal-Sanz, M.; Bray, G.M.; Villegas-Perez, M.P.; Thanos, S.; Aguayo, A.J. Axonal regeneration and synapse formation in the superior colliculus by retinal ganglion cells in the adult rat. *J. Neurosci.* **1987**, *7*, 2894–2909. [CrossRef] [PubMed]
12. Barnstable, C.J.; Dräger, U.C. Thy-1 antigen: A ganglion cell specific marker in rodent retina. *Neuroscience* **1984**, *11*, 847–855. [CrossRef]
13. Nadal-Nicolas, F.M.; Jimenez-Lopez, M.; Salinas-Navarro, M.; Sobrado-Calvo, P.; Alburquerque-Bejar, J.J.; Vidal-Sanz, M.; Agudo-Barriuso, M. Whole number, distribution and co-expression of brn3 transcription factors in retinal ganglion cells of adult albino and pigmented rats. *PLoS ONE* **2012**, *7*, e49830. [CrossRef] [PubMed]
14. Nadal-Nicolas, F.M.; Salinas-Navarro, M.; Jimenez-Lopez, M.; Sobrado-Calvo, P.; Villegas-Perez, M.P.; Vidal-Sanz, M.; Agudo-Barriuso, M. Displaced retinal ganglion cells in albino and pigmented rats. *Front. Neuroanat.* **2014**, *8*, 99. [CrossRef] [PubMed]
15. Rodriguez, A.R.; de Sevilla Müller, L.P.; Brecha, N.C. The RNA binding protein RBPMS is a selective marker of ganglion cells in the mammalian retina. *J. Comp. Neurol.* **2014**, *522*, 1411–1443. [CrossRef] [PubMed]
16. Jiang, S.M.; Zeng, L.P.; Zeng, J.H.; Tang, L.; Chen, X.M.; Wei, X. beta-III-Tubulin: A reliable marker for retinal ganglion cell labeling in experimental models of glaucoma. *Int. J. Ophthalmol.* **2015**, *8*, 643–652. [CrossRef]
17. Dijk, F.; Bergen, A.A.; Kamphuis, W. GAP-43 expression is upregulated in retinal ganglion cells after ischemia/reperfusion-induced damage. *Exp. Eye Res.* **2007**, *84*, 858–867. [CrossRef]
18. McKerracher, L.; Vallee, R.B.; Aguayo, A.J. Microtubule-associated protein 1A (MAP 1A) is a ganglion cell marker in adult rat retina. *Vis. Neurosci.* **1989**, *2*, 349–356. [CrossRef]
19. Galindo-Romero, C.; Jimenez-Lopez, M.; Garcia-Ayuso, D.; Salinas-Navarro, M.; Nadal-Nicolas, F.M.; Agudo-Barriuso, M.; Villegas-Perez, M.P.; Aviles-Trigueros, M.; Vidal-Sanz, M. Number and spatial distribution of intrinsically photosensitive retinal ganglion cells in the adult albino rat. *Exp. Eye Res.* **2013**, *108*, 84–93. [CrossRef]
20. Kim, I.J.; Zhang, Y.; Yamagata, M.; Meister, M.; Sanes, J.R. Molecular identification of a retinal cell type that responds to upward motion. *Nature* **2008**, *452*, 478–482. [CrossRef]
21. Agostinone, J.; Di Polo, A. Retinal ganglion cell dendrite pathology and synapse loss: Implications for glaucoma. *Prog. Brain Res.* **2015**, *220*, 199–216. [CrossRef] [PubMed]
22. Ou, Y.; Jo, R.E.; Ullian, E.M.; Wong, R.O.; Della Santina, L. Selective Vulnerability of Specific Retinal Ganglion Cell Types and Synapses after Transient Ocular Hypertension. *J. Neurosci.* **2016**, *36*, 9240–9252. [CrossRef] [PubMed]
23. Chidlow, G.; Casson, R.; Sobrado-Calvo, P.; Vidal-Sanz, M.; Osborne, N.N. Measurement of retinal injury in the rat after optic nerve transection: An RT-PCR study. *Mol. Vis.* **2005**, *11*, 387–396. [PubMed]
24. Lönngren, U.; Napankangas, U.; Lafuente, M.; Mayor, S.; Lindqvist, N.; Vidal-Sanz, M.; Hallböök, F. The growth factor response in ischemic rat retina and superior colliculus after brimonidine pre-treatment. *Brain Res. Bull.* **2006**, *71*, 208–218. [CrossRef] [PubMed]
25. Agudo, M.; Perez-Marin, M.C.; Lonngren, U.; Sobrado, P.; Conesa, A.; Canovas, I.; Salinas-Navarro, M.; Miralles-Imperial, J.; Hallböök, F.; Vidal-Sanz, M. Time course profiling of the retinal transcriptome after optic nerve transection and optic nerve crush. *Mol. Vis.* **2008**, *14*, 1050–1063. [PubMed]

26. Agudo, M.; Perez-Marin, M.C.; Sobrado-Calvo, P.; Lonngren, U.; Salinas-Navarro, M.; Canovas, I.; Nadal-Nicolas, F.M.; Miralles-Imperial, J.; Hallböök, F.; Vidal-Sanz, M. Immediate upregulation of proteins belonging to different branches of the apoptotic cascade in the retina after optic nerve transection and optic nerve crush. *Investig. Ophthalmol. Vis. Sci.* **2009**, *50*, 424–431. [CrossRef] [PubMed]
27. Agudo-Barriuso, M.; Lahoz, A.; Nadal-Nicolas, F.M.; Sobrado-Calvo, P.; Piquer-Gil, M.; Diaz-Llopis, M.; Vidal-Sanz, M.; Mullor, J.L. Metabolomic changes in the rat retina after optic nerve crush. *Investig. Ophthalmol. Vis. Sci.* **2013**, *54*, 4249–4259. [CrossRef]
28. Agudo-Barriuso, M.; Nadal-Nicolas, F.M.; Madeira, M.H.; Rovere, G.; Vidal-Villegas, B.; Vidal-Sanz, M. Melanopsin expression is an indicator of the well-being of melanopsin-expressing retinal ganglion cells but not of their viability. *Neural Regen. Res.* **2016**, *11*, 1243–1244. [CrossRef]
29. Vugler, A.; Semo, M.; Ortin-Martinez, A.; Rojanasakul, A.; Nommiste, B.; Valiente-Soriano, F.J.; Garcia-Ayuso, D.; Coffey, P.; Vidal-Sanz, M.; Gias, C. A role for the outer retina in development of the intrinsic pupillary light reflex in mice. *Neuroscience* **2015**, *286*, 60–78. [CrossRef]
30. Hannibal, J.; Christiansen, A.T.; Heegaard, S.; Fahrenkrug, J.; Kiilgaard, J.F. Melanopsin expressing human retinal ganglion cells: Subtypes, distribution, and intraretinal connectivity. *J. Comp. Neurol.* **2017**, *525*, 1934–1961. [CrossRef]
31. Berson, D.M.; Castrucci, A.M.; Provencio, I. Morphology and mosaics of melanopsin-expressing retinal ganglion cell types in mice. *J. Comp. Neurol.* **2010**, *518*, 2405–2422. [CrossRef]
32. Quattrochi, L.E.; Stabio, M.E.; Kim, I.; Ilardi, M.C.; Michelle Fogerson, P.; Leyrer, M.L.; Berson, D.M. The M6 cell: A small-field bistratified photosensitive retinal ganglion cell. *J. Comp. Neurol.* **2019**, *527*, 297–311. [CrossRef] [PubMed]
33. Sonoda, T.; Lee, S.K.; Birnbaumer, L.; Schmidt, T.M. Melanopsin Phototransduction Is Repurposed by ipRGC Subtypes to Shape the Function of Distinct Visual Circuits. *Neuron* **2018**, *99*, 754–767 e754. [CrossRef] [PubMed]
34. Estevez, M.E.; Fogerson, P.M.; Ilardi, M.C.; Borghuis, B.G.; Chan, E.; Weng, S.; Auferkorte, O.N.; Demb, J.B.; Berson, D.M. Form and function of the M4 cell, an intrinsically photosensitive retinal ganglion cell type contributing to geniculocortical vision. *J. Neurosci.* **2012**, *32*, 13608–13620. [CrossRef] [PubMed]
35. Duan, X.; Qiao, M.; Bei, F.; Kim, I.J.; He, Z.; Sanes, J.R. Subtype-specific regeneration of retinal ganglion cells following axotomy: Effects of osteopontin and mTOR signaling. *Neuron* **2015**, *85*, 1244–1256. [CrossRef] [PubMed]
36. Berry, M.; Ahmed, Z.; Logan, A. Return of function after CNS axon regeneration: Lessons from injury-responsive intrinsically photosensitive and alpha retinal ganglion cells. *Prog. Retin. Eye Res.* **2018**. [CrossRef] [PubMed]
37. Schmidt, T.M.; Chen, S.K.; Hattar, S. Intrinsically photosensitive retinal ganglion cells: Many subtypes, diverse functions. *Trends Neurosci.* **2011**, *34*, 572–580. [CrossRef] [PubMed]
38. Schmidt, T.M.; Do, M.T.; Dacey, D.; Lucas, R.; Hattar, S.; Matynia, A. Melanopsin-positive intrinsically photosensitive retinal ganglion cells: From form to function. *J. Neurosci.* **2011**, *31*, 16094–16101. [CrossRef] [PubMed]
39. Li, S.; Yang, C.; Zhang, L.; Gao, X.; Wang, X.; Liu, W.; Wang, Y.; Jiang, S.; Wong, Y.H.; Zhang, Y.; et al. Promoting axon regeneration in the adult CNS by modulation of the melanopsin/GPCR signaling. *Proc. Natl. Acad. Sci. USA* **2016**, *113*, 1937–1942. [CrossRef]
40. Reifler, A.N.; Chervenak, A.P.; Dolikian, M.E.; Benenati, B.A.; Meyers, B.S.; Demertzis, Z.D.; Lynch, A.M.; Li, B.Y.; Wachter, R.D.; Abufarha, F.S.; et al. The rat retina has five types of ganglion-cell photoreceptors. *Exp. Eye Res.* **2015**, *130*, 17–28. [CrossRef]
41. Hannibal, J.; Hindersson, P.; Knudsen, S.M.; Georg, B.; Fahrenkrug, J. The photopigment melanopsin is exclusively present in pituitary adenylate cyclase-activating polypeptide-containing retinal ganglion cells of the retinohypothalamic tract. *J. Neurosci.* **2002**, *22*, RC191. [CrossRef] [PubMed]
42. Hattar, S.; Liao, H.W.; Takao, M.; Berson, D.M.; Yau, K.W. Melanopsin-containing retinal ganglion cells: Architecture, projections, and intrinsic photosensitivity. *Science* **2002**, *295*, 1065–1070. [CrossRef] [PubMed]
43. Vidal-Sanz, M.; Nadal-Nicolas, F.M.; Valiente-Soriano, F.J.; Agudo-Barriuso, M.; Villegas-Perez, M.P. Identifying specific RGC types may shed light on their idiosyncratic responses to neuroprotection. *Neural Regen. Res.* **2015**, *10*, 1228–1230. [CrossRef] [PubMed]

44. Lucas, D.R.; Newhouse, J.P. The toxic effect of sodium L-glutamate on the inner layers of the retina. *AMA Arch. Ophthalmol.* **1957**, *58*, 193–201. [CrossRef] [PubMed]
45. Choi, D.W. Glutamate neurotoxicity and diseases of the nervous system. *Neuron* **1988**, *1*, 623–634. [CrossRef]
46. Dreyer, E.B.; Zurakowski, D.; Schumer, R.A.; Podos, S.M.; Lipton, S.A. Elevated glutamate levels in the vitreous body of humans and monkeys with glaucoma. *Arch. Ophthalmol.* **1996**, *114*, 299–305. [CrossRef] [PubMed]
47. Izzotti, A.; Bagnis, A.; Sacca, S.C. The role of oxidative stress in glaucoma. *Mutat. Res.* **2006**, *612*, 105–114. [CrossRef]
48. Tezel, G. Immune regulation toward immunomodulation for neuroprotection in glaucoma. *Curr. Opin. Pharmacol.* **2013**, *13*, 23–31. [CrossRef]
49. Vorwerk, C.K.; Kreutz, M.R.; Bockers, T.M.; Brosz, M.; Dreyer, E.B.; Sabel, B.A. Susceptibility of retinal ganglion cells to excitotoxicity depends on soma size and retinal eccentricity. *Curr. Eye Res.* **1999**, *19*, 59–65. [CrossRef]
50. Vorwerk, C.K.; Zurakowski, D.; McDermott, L.M.; Mawrin, C.; Dreyer, E.B. Effects of axonal injury on ganglion cell survival and glutamate homeostasis. *Brain Res. Bull.* **2004**, *62*, 485–490. [CrossRef]
51. Lam, T.T.; Siew, E.; Chu, R.; Tso, M.O. Ameliorative effect of MK-801 on retinal ischemia. *J. Ocul. Pharmacol. Ther.* **1997**, *13*, 129–137. [CrossRef] [PubMed]
52. Schuettauf, F.; Naskar, R.; Vorwerk, C.K.; Zurakowski, D.; Dreyer, E.B. Ganglion cell loss after optic nerve crush mediated through AMPA-kainate and NMDA receptors. *Investig. Ophthalmol. Vis. Sci.* **2000**, *41*, 4313–4316.
53. Kermer, P.; Klöcker, N.; Bähr, M. Modulation of metabotropic glutamate receptors fails to prevent the loss of adult rat retinal ganglion cells following axotomy or N-methyl-D-aspartate lesion in vivo. *Neurosci. Lett.* **2001**, *315*, 117–120. [CrossRef]
54. Almasieh, M.; Wilson, A.M.; Morquette, B.; Cueva Vargas, J.L.; Di Polo, A. The molecular basis of retinal ganglion cell death in glaucoma. *Prog. Retin. Eye Res.* **2012**, *31*, 152–181. [CrossRef] [PubMed]
55. Manev, H.; Favaron, M.; Guidotti, A.; Costa, E. Delayed increase of Ca2+ influx elicited by glutamate: Role in neuronal death. *Mol. Pharmacol.* **1989**, *36*, 106–112. [PubMed]
56. Stavrovskaya, I.G.; Kristal, B.S. The powerhouse takes control of the cell: Is the mitochondrial permeability transition a viable therapeutic target against neuronal dysfunction and death? *Free Radic. Biol. Med.* **2005**, *38*, 687–697. [CrossRef]
57. Hardingham, G.E.; Fukunaga, Y.; Bading, H. Extrasynaptic NMDARs oppose synaptic NMDARs by triggering CREB shut-off and cell death pathways. *Nat. Neurosci.* **2002**, *5*, 405–414. [CrossRef]
58. Gomez-Vicente, V.; Lax, P.; Fernandez-Sanchez, L.; Rondon, N.; Esquiva, G.; Germain, F.; de la Villa, P.; Cuenca, N. Neuroprotective Effect of Tauroursodeoxycholic Acid on N-Methyl-D-Aspartate-Induced Retinal Ganglion Cell Degeneration. *PLoS ONE* **2015**, *10*, e0137826. [CrossRef]
59. Wang, S.; Gu, D.; Zhang, P.; Chen, J.; Li, Y.; Xiao, H.; Zhou, G. Melanopsin-expressing retinal ganglion cells are relatively resistant to excitotoxicity induced by *N*-methyl-D-aspartate. *Neurosci. Lett.* **2018**, *662*, 368–373. [CrossRef]
60. Pichavaram, P.; Palani, C.D.; Patel, C.; Xu, Z.; Shosha, E.; Fouda, A.Y.; Caldwell, R.B.; Narayanan, S.P. Targeting Polyamine Oxidase to Prevent Excitotoxicity-Induced Retinal Neurodegeneration. *Front. Neurosci.* **2018**, *12*, 956. [CrossRef]
61. Fahrenthold, B.K.; Fernandes, K.A.; Libby, R.T. Assessment of intrinsic and extrinsic signaling pathway in excitotoxic retinal ganglion cell death. *Sci. Rep.* **2018**, *8*, 4641. [CrossRef] [PubMed]
62. Kobayashi, M.; Hirooka, K.; Ono, A.; Nakano, Y.; Nishiyama, A.; Tsujikawa, A. The Relationship between the Renin-Angiotensin-Aldosterone System and NMDA Receptor-Mediated Signal and the Prevention of Retinal Ganglion Cell Death. *Investig. Ophthalmol. Vis. Sci.* **2017**, *58*, 1397–1403. [CrossRef] [PubMed]
63. Manabe, S.; Gu, Z.; Lipton, S.A. Activation of matrix metalloproteinase-9 via neuronal nitric oxide synthase contributes to NMDA-induced retinal ganglion cell death. *Investig. Ophthalmol. Vis. Sci.* **2005**, *46*, 4747–4753. [CrossRef] [PubMed]
64. Lambuk, L.; Iezhitsa, I.; Agarwal, R.; Bakar, N.S.; Agarwal, P.; Ismail, N.M. Antiapoptotic effect of taurine against NMDA-induced retinal excitotoxicity in rats. *Neurotoxicology* **2019**, *70*, 62–71. [CrossRef] [PubMed]
65. Tsoka, P.; Barbisan, P.R.; Kataoka, K.; Chen, X.N.; Tian, B.; Bouzika, P.; Miller, J.W.; Paschalis, E.I.; Vavvas, D.G. NLRP3 inflammasome in NMDA-induced retinal excitotoxicity. *Exp. Eye Res.* **2019**, *181*, 136–144. [CrossRef]

66. Ito, A.; Tsuda, S.; Kunikata, H.; Toshifumi, A.; Sato, K.; Nakazawa, T. Assessing retinal ganglion cell death and neuroprotective agents using real time imaging. *Brain Res.* **2019**, *1714*, 65–72. [CrossRef] [PubMed]
67. DeParis, S.; Caprara, C.; Grimm, C. Intrinsically photosensitive retinal ganglion cells are resistant to *N*-methyl-D-aspartic acid excitotoxicity. *Mol. Vis.* **2012**, *18*, 2814–2827.
68. Vidal-Villegas, B.; Miralles de Imperial-Ollero, J.A.; Nadal-Nicolás, F.M.; Ortín-Martínez, A.; Bernal-Garro, J.M.; Vidal-Sanz, M.; Villegas-Pérez, M.P. Effectss of intravitreal injections of *N*-Methyl-D-Aspartate on melanopsin and non-melanopsin containing retinal ganglion cells in the adult rat. *Ophtalmic Res.* **2017**, *57*, 25.
69. Salinas-Navarro, M.; Mayor-Torroglosa, S.; Jimenez-Lopez, M.; Aviles-Trigueros, M.; Holmes, T.M.; Lund, R.D.; Villegas-Perez, M.P.; Vidal-Sanz, M. A computerized analysis of the entire retinal ganglion cell population and its spatial distribution in adult rats. *Vis. Res.* **2009**, *49*, 115–126. [CrossRef]
70. Nadal-Nicolas, F.M.; Jimenez-Lopez, M.; Sobrado-Calvo, P.; Nieto-Lopez, L.; Canovas-Martinez, I.; Salinas-Navarro, M.; Vidal-Sanz, M.; Agudo, M. Brn3a as a marker of retinal ganglion cells: Qualitative and quantitative time course studies in naive and optic nerve-injured retinas. *Investig. Ophthalmol. Vis. Sci.* **2009**, *50*, 3860–3868. [CrossRef]
71. Ortin-Martinez, A.; Jimenez-Lopez, M.; Nadal-Nicolas, F.M.; Salinas-Navarro, M.; Alarcon-Martinez, L.; Sauve, Y.; Villegas-Perez, M.P.; Vidal-Sanz, M.; Agudo-Barriuso, M. Automated quantification and topographical distribution of the whole population of S- and L-cones in adult albino and pigmented rats. *Investig. Ophthalmol. Vis. Sci.* **2010**, *51*, 3171–3183. [CrossRef] [PubMed]
72. Nadal-Nicolas, F.M.; Vidal-Sanz, M.; Agudo-Barriuso, M. The aging rat retina: From function to anatomy. *Neurobiol. Aging* **2018**, *61*, 146–168. [CrossRef] [PubMed]
73. Della Santina, L.; Ou, Y. Who's lost first? Susceptibility of retinal ganglion cell types in experimental glaucoma. *Exp. Eye Res.* **2017**, *158*, 43–50. [CrossRef] [PubMed]
74. Vidal-Sanz, M.; Galindo-Romero, C.; Valiente-Soriano, F.J.; Nadal-Nicolas, F.M.; Ortin-Martinez, A.; Rovere, G.; Salinas-Navarro, M.; Lucas-Ruiz, F.; Sanchez-Migallon, M.C.; Sobrado-Calvo, P.; et al. Shared and Differential Retinal Responses against Optic Nerve Injury and Ocular Hypertension. *Front. Neurosci.* **2017**, *11*, 235. [CrossRef] [PubMed]
75. Garcia-Ayuso, D.; Galindo-Romero, C.; Di Pierdomenico, J.; Vidal-Sanz, M.; Agudo-Barriuso, M.; Villegas Perez, M.P. Light-induced retinal degeneration causes a transient downregulation of melanopsin in the rat retina. *Exp. Eye Res.* **2017**, *161*, 10–16. [CrossRef]
76. Sanchez-Migallon, M.C.; Valiente-Soriano, F.J.; Nadal-Nicolas, F.M.; Di Pierdomenico, J.; Vidal-Sanz, M.; Agudo-Barriuso, M. Survival of melanopsin expressing retinal ganglion cells long term after optic nerve trauma in mice. *Exp. Eye Res.* **2018**, *174*, 93–97. [CrossRef] [PubMed]
77. Lax, P.; Ortuño-Lizarán, I.; Maneu, V.; Vidal-Sanz, M.; Cuenca, N. Melanopsin-containing ganglion cells in the healthy and disease retina. *Int. J. Mol. Sci.* **2019**. submitted.
78. Huang, W.; Hu, F.; Wang, M.; Gao, F.; Xu, P.; Xing, C.; Sun, X.; Zhang, S.; Wu, J. Comparative analysis of retinal ganglion cell damage in three glaucomatous rat models. *Exp. Eye Res.* **2018**, *172*, 112–122. [CrossRef]
79. Villegas-Perez, M.P.; Vidal-Sanz, M.; Rasminsky, M.; Bray, G.M.; Aguayo, A.J. Rapid and protracted phases of retinal ganglion cell loss follow axotomy in the optic nerve of adult rats. *J. Neurobiol.* **1993**, *24*, 23–36. [CrossRef]
80. Endo, K.; Nakamachi, T.; Seki, T.; Kagami, N.; Wada, Y.; Nakamura, K.; Kishimoto, K.; Hori, M.; Tsuchikawa, D.; Shinntani, N.; et al. Neuroprotective effect of PACAP against NMDA-induced retinal damage in the mouse. *J. Mol. Neurosci.* **2011**, *43*, 22–29. [CrossRef]
81. Lebrun-Julien, F.; Duplan, L.; Pernet, V.; Osswald, I.; Sapieha, P.; Bourgeois, P.; Dickson, K.; Bowie, D.; Barker, P.A.; Di Polo, A. Excitotoxic death of retinal neurons in vivo occurs via a non-cell-autonomous mechanism. *J. Neurosci.* **2009**, *29*, 5536–5545. [CrossRef] [PubMed]
82. Salinas-Navarro, M.; Alarcon-Martinez, L.; Valiente-Soriano, F.J.; Jimenez-Lopez, M.; Mayor-Torroglosa, S.; Aviles-Trigueros, M.; Villegas-Perez, M.P.; Vidal-Sanz, M. Ocular hypertension impairs optic nerve axonal transport leading to progressive retinal ganglion cell degeneration. *Exp. Eye Res.* **2010**, *90*, 168–183. [CrossRef] [PubMed]

83. Cuenca, N.; Pinilla, I.; Fernandez-Sanchez, L.; Salinas-Navarro, M.; Alarcon-Martinez, L.; Aviles-Trigueros, M.; de la Villa, P.; Miralles de Imperial, J.; Villegas-Perez, M.P.; Vidal-Sanz, M. Changes in the inner and outer retinal layers after acute increase of the intraocular pressure in adult albino Swiss mice. *Exp. Eye Res.* **2010**, *91*, 273–285. [CrossRef]
84. Rovere, G.; Nadal-Nicolas, F.M.; Wang, J.; Bernal-Garro, J.M.; Garcia-Carrillo, N.; Villegas-Perez, M.P.; Agudo-Barriuso, M.; Vidal-Sanz, M. Melanopsin-Containing or Non-Melanopsin-Containing Retinal Ganglion Cells Response to Acute Ocular Hypertension With or Without Brain-Derived Neurotrophic Factor Neuroprotection. *Investig. Ophthalmol. Vis. Sci.* **2016**, *57*, 6652–6661. [CrossRef] [PubMed]
85. Lam, T.T.; Abler, A.S.; Kwong, J.M.; Tso, M.O. *N*-methyl-D-aspartate (NMDA)—Induced apoptosis in rat retina. *Investig. Ophthalmol. Vis. Sci.* **1999**, *40*, 2391–2397.
86. Li, Y.; Schlamp, C.L.; Nickells, R.W. Experimental induction of retinal ganglion cell death in adult mice. *Investig. Ophthalmol. Vis. Sci.* **1999**, *40*, 1004–1008.
87. Akopian, A.; Atlasz, T.; Pan, F.; Wong, S.; Zhang, Y.; Völgyi, B.; Paul, D.L.; Bloomfield, S.A. Gap junction-mediated death of retinal neurons is connexin and insult specific: A potential target for neuroprotection. *J. Neurosci.* **2014**, *34*, 10582–10591. [CrossRef]
88. Siliprandi, R.; Canella, R.; Carmignoto, G.; Schiavo, N.; Zanellato, A.; Zanoni, R.; Vantini, G. *N*-methyl-D-aspartate-induced neurotoxicity in the adult rat retina. *Vis. Neurosci.* **1992**, *8*, 567–573. [CrossRef]
89. Völgyi, B.; Chheda, S.; Bloomfield, S.A. Tracer coupling patterns of the ganglion cell subtypes in the mouse retina. *J. Comp. Neurol.* **2009**, *512*, 664–687. [CrossRef]
90. Cui, Q.; Ren, C.; Sollars, P.J.; Pickard, G.E.; So, K.F. The injury resistant ability of melanopsin-expressing intrinsically photosensitive retinal ganglion cells. *Neuroscience* **2015**, *284*, 845–853. [CrossRef]
91. Valiente-Soriano, F.J.; Nadal-Nicolas, F.M.; Salinas-Navarro, M.; Jimenez-Lopez, M.; Bernal-Garro, J.M.; Villegas-Perez, M.P.; Agudo-Barriuso, M.; Vidal-Sanz, M. BDNF Rescues RGCs But Not Intrinsically Photosensitive RGCs in Ocular Hypertensive Albino Rat Retinas. *Investig. Ophthalmol. Vis. Sci.* **2015**, *56*, 1924–1936. [CrossRef] [PubMed]
92. Jakobs, T.C.; Ben, Y.; Masland, R.H. Expression of mRNA for glutamate receptor subunits distinguishes the major classes of retinal neurons, but is less specific for individual cell types. *Mol. Vis.* **2007**, *13*, 933–948. [PubMed]
93. Perez de Sevilla Müller, L.; Sargoy, A.; Rodriguez, A.R.; Brecha, N.C. Melanopsin ganglion cells are the most resistant retinal ganglion cell type to axonal injury in the rat retina. *PLoS ONE* **2014**, *9*, e93274. [CrossRef] [PubMed]
94. Nadal-Nicolas, F.M.; Sobrado-Calvo, P.; Jimenez-Lopez, M.; Vidal-Sanz, M.; Agudo-Barriuso, M. Long-Term Effect of Optic Nerve Axotomy on the Retinal Ganglion Cell Layer. *Investig. Ophthalmol. Vis. Sci.* **2015**, *56*, 6095–6112. [CrossRef] [PubMed]
95. Robinson, G.A.; Madison, R.D. Axotomized mouse retinal ganglion cells containing melanopsin show enhanced survival, but not enhanced axon regrowth into a peripheral nerve graft. *Vis. Res.* **2004**, *44*, 2667–2674. [CrossRef] [PubMed]
96. Daniel, S.; Clark, A.F.; McDowell, C.M. Subtype-specific response of retinal ganglion cells to optic nerve crush. *Cell Death Discov.* **2018**, *4*, 7. [CrossRef] [PubMed]
97. Vugler, A.A.; Semo, M.; Joseph, A.; Jeffery, G. Survival and remodeling of melanopsin cells during retinal dystrophy. *Vis. Neurosci.* **2008**, *25*, 125–138. [CrossRef]
98. Esquiva, G.; Lax, P.; Cuenca, N. Impairment of intrinsically photosensitive retinal ganglion cells associated with late stages of retinal degeneration. *Investig. Ophthalmol. Vis. Sci.* **2013**, *54*, 4605–4618. [CrossRef]
99. Garcia-Ayuso, D.; Di Pierdomenico, J.; Esquiva, G.; Nadal-Nicolas, F.M.; Pinilla, I.; Cuenca, N.; Vidal-Sanz, M.; Agudo-Barriuso, M.; Villegas-Perez, M.P. Inherited Photoreceptor Degeneration Causes the Death of Melanopsin-Positive Retinal Ganglion Cells and Increases Their Coexpression of Brn3a. *Investig. Ophthalmol. Vis. Sci.* **2015**, *56*, 4592–4604. [CrossRef]
100. La Morgia, C.; Ross-Cisneros, F.N.; Sadun, A.A.; Hannibal, J.; Munarini, A.; Mantovani, V.; Barboni, P.; Cantalupo, G.; Tozer, K.R.; Sancisi, E.; et al. Melanopsin retinal ganglion cells are resistant to neurodegeneration in mitochondrial optic neuropathies. *Brain* **2010**, *133*, 2426–2438. [CrossRef]

101. Georg, B.; Ghelli, A.; Giordano, C.; Ross-Cisneros, F.N.; Sadun, A.A.; Carelli, V.; Hannibal, J.; La Morgia, C. Melanopsin-expressing retinal ganglion cells are resistant to cell injury, but not always. *Mitochondrion* **2017**, *36*, 77–84. [CrossRef] [PubMed]
102. Lax, P.; Esquiva, G.; Esteve-Rudd, J.; Otalora, B.B.; Madrid, J.A.; Cuenca, N. Circadian dysfunction in a rotenone-induced parkinsonian rodent model. *Chronobiol. Int.* **2012**, *29*, 147–156. [CrossRef] [PubMed]
103. Wulff, K.; Gatti, S.; Wettstein, J.G.; Foster, R.G. Sleep and circadian rhythm disruption in psychiatric and neurodegenerative disease. *Nat. Rev. Neurosci.* **2010**, *11*, 589–599. [CrossRef] [PubMed]
104. Nadal-Nicolas, F.M.; Madeira, M.H.; Salinas-Navarro, M.; Jimenez-Lopez, M.; Galindo-Romero, C.; Ortin-Martinez, A.; Santiago, A.R.; Vidal-Sanz, M.; Agudo-Barriuso, M. Transient Downregulation of Melanopsin Expression After Retrograde Tracing or Optic Nerve Injury in Adult Rats. *Investig. Ophthalmol. Vis. Sci.* **2015**, *56*, 4309–4323. [CrossRef] [PubMed]
105. Semo, M.; Gias, C.; Ahmado, A.; Vugler, A. A role for the ciliary marginal zone in the melanopsin-dependent intrinsic pupillary light reflex. *Exp. Eye Res.* **2014**, *119*, 8–18. [CrossRef] [PubMed]
106. Zhang, J.; Diamond, J.S. Subunit- and pathway-specific localization of NMDA receptors and scaffolding proteins at ganglion cell synapses in rat retina. *J. Neurosci.* **2009**, *29*, 4274–4286. [CrossRef] [PubMed]
107. Jakobs, T.C.; Libby, R.T.; Ben, Y.; John, S.W.; Masland, R.H. Retinal ganglion cell degeneration is topological but not cell type specific in DBA/2J mice. *J. Cell Biol.* **2005**, *171*, 313–325. [CrossRef]
108. Li, S.Y.; Yau, S.Y.; Chen, B.Y.; Tay, D.K.; Lee, V.W.; Pu, M.L.; Chan, H.H.; So, K.F. Enhanced survival of melanopsin-expressing retinal ganglion cells after injury is associated with the PI3 K/Akt pathway. *Cell. Mol. Neurobiol.* **2008**, *28*, 1095–1107. [CrossRef]
109. Seki, T.; Nakatani, M.; Taki, C.; Shinohara, Y.; Ozawa, M.; Nishimura, S.; Ito, H.; Shioda, S. Neuroprotective effect of PACAP against kainic acid-induced neurotoxicity in rat retina. *Ann. N. Y. Acad. Sci.* **2006**, *1070*, 531–534. [CrossRef]
110. Nakatani, M.; Seki, T.; Shinohara, Y.; Taki, C.; Nishimura, S.; Takaki, A.; Shioda, S. Pituitary adenylate cyclase-activating peptide (PACAP) stimulates production of interleukin-6 in rat Muller cells. *Peptides* **2006**, *27*, 1871–1876. [CrossRef]
111. Belenky, M.A.; Smeraski, C.A.; Provencio, I.; Sollars, P.J.; Pickard, G.E. Melanopsin retinal ganglion cells receive bipolar and amacrine cell synapses. *J. Comp. Neurol.* **2003**, *460*, 380–393. [CrossRef] [PubMed]
112. Lin, M.S.; Liao, P.Y.; Chen, H.M.; Chang, C.P.; Chen, S.K.; Chern, Y. Degeneration of ipRGCs in Mouse Models of Huntington's Disease Disrupts Non-Image-Forming Behaviors Before Motor Impairment. *J. Neurosci.* **2019**, *39*, 1505–1524. [CrossRef] [PubMed]
113. Aviles-Trigueros, M.; Sauve, Y.; Lund, R.D.; Vidal-Sanz, M. Selective innervation of retinorecipient brainstem nuclei by retinal ganglion cell axons regenerating through peripheral nerve grafts in adult rats. *J. Neurosci.* **2000**, *20*, 361–374. [CrossRef] [PubMed]
114. Lindqvist, N.; Peinado-Ramonn, P.; Vidal-Sanz, M.; Hallböök, F. GDNF, Ret, GFRalpha1 and 2 in the adult rat retino-tectal system after optic nerve transection. *Exp. Neurol.* **2004**, *187*, 487–499. [CrossRef] [PubMed]
115. Di Pierdomenico, J.; Garcia-Ayuso, D.; Jimenez-Lopez, M.; Agudo-Barriuso, M.; Vidal-Sanz, M.; Villegas-Perez, M.P. Different Ipsi-and Contralateral Glial Responses to Anti-VEGF and Triamcinolone Intravitreal Injections in Rats. *Investig. Ophthalmol. Vis. Sci.* **2016**, *57*, 3533–3544. [CrossRef] [PubMed]
116. Rovere, G.; Nadal-Nicolas, F.M.; Agudo-Barriuso, M.; Sobrado-Calvo, P.; Nieto-Lopez, L.; Nucci, C.; Villegas-Perez, M.P.; Vidal-Sanz, M. Comparison of Retinal Nerve Fiber Layer Thinning and Retinal Ganglion Cell Loss After Optic Nerve Transection in Adult Albino Rats. *Investig. Ophthalmol. Vis. Sci.* **2015**, *56*, 4487–4498. [CrossRef] [PubMed]
117. Ortin-Martinez, A.; Salinas-Navarro, M.; Nadal-Nicolas, F.M.; Jimenez-Lopez, M.; Valiente-Soriano, F.J.; Garcia-Ayuso, D.; Bernal-Garro, J.M.; Aviles-Trigueros, M.; Agudo-Barriuso, M.; Villegas-Perez, M.P.; et al. Laser-induced ocular hypertension in adult rats does not affect non-RGC neurons in the ganglion cell layer but results in protracted severe loss of cone-photoreceptors. *Exp. Eye Res.* **2015**, *132*, 17–33. [CrossRef]
118. Sanchez-Migallon, M.C.; Valiente-Soriano, F.J.; Nadal-Nicolas, F.M.; Vidal-Sanz, M.; Agudo-Barriuso, M. Apoptotic Retinal Ganglion Cell Death after Optic Nerve Transection or Crush in Mice: Delayed RGC Loss with BDNF or a Caspase 3 Inhibitor. *Investig. Ophthalmol. Vis. Sci.* **2016**, *57*, 81–93. [CrossRef]

119. Vidal-Sanz, M.; Salinas-Navarro, M.; Nadal-Nicolas, F.M.; Alarcon-Martinez, L.; Valiente-Soriano, F.J.; de Imperial, J.M.; Aviles-Trigueros, M.; Agudo-Barriuso, M.; Villegas-Perez, M.P. Understanding glaucomatous damage: Anatomical and functional data from ocular hypertensive rodent retinas. *Prog. Retin. Eye Res.* **2012**, *31*, 1–27. [CrossRef]
120. Vidal-Sanz, M.; Valiente-Soriano, F.J.; Ortin-Martinez, A.; Nadal-Nicolas, F.M.; Jimenez-Lopez, M.; Salinas-Navarro, M.; Alarcon-Martinez, L.; Garcia-Ayuso, D.; Aviles-Trigueros, M.; Agudo-Barriuso, M.; et al. Retinal neurodegeneration in experimental glaucoma. *Prog. Brain Res.* **2015**, *220*, 1–35. [CrossRef]

ARCH SOC ESP OFTALMOL. 2021;96(6):299–315

ARCHIVOS DE LA SOCIEDAD ESPAÑOLA DE OFTALMOLOGÍA

www.elsevier.es/oftalmologia

Revisión

# Células ganglionares fotosensibles: una población diminuta pero esencial

*B. Vidal-Villegas*[a,*], *A. Gallego-Ortega*[b], *J.A. Miralles de Imperial-Ollero*[b], *J.M. Martínez de la Casa*[a], *J. García Feijoo*[a] y *M. Vidal-Sanz*[b]

[a] *Servicio de Oftalmología, Hospital Clínico San Carlos, Instituto de Investigación Sanitaria del Hospital Clínico San Carlos (IdISSC), Madrid, España*

[b] *Departamento de Oftalmología, Universidad de Murcia e Instituto Murciano de Investigación Biosanitaria (IMIB) Virgen de la Arrixaca, El Palmar, Murcia, España*

INFORMACIÓN DEL ARTÍCULO

*Historia del artículo:*
Recibido el 21 de mayo de 2020
Aceptado el 15 de junio de 2020
*On-line* el 31 de octubre de 2020

*Palabras clave:*
Células ganglionares intrínsecamente fotosensibles
Células ganglionares melanosínicas
Retina
Células M1-M6
Sistema visual no formador de imágenes

RESUMEN

Nuestro sistema visual ha evolucionado para proveernos una imagen de la escena que nos rodea informándonos de su textura, color, movimiento y profundidad con una enorme capacidad de resolución tanto espacial como temporal, y a esta finalidad la formación de imágenes (FI) dedica la inmensa mayoría de nuestras células ganglionares de la retina (CGR) y gran parte de nuestra corteza cerebral. Por otra parte, una proporción minúscula de las CGR, además de recibir información de fotorreceptores clásicos conos y bastones, expresan melanopsina y son intrínsecamente fotosensibles (CGRif). Estas CGRif se dedican a funciones visuales no formadoras de imágenes (NFI), de las que somos inconscientes, pero que resultan imprescindibles para aspectos relacionados con nuestra fisiología cotidiana como la puesta en hora de nuestros ritmos circadianos y nuestro reflejo fotomotor, entre otras muchas. Desde el descubrimiento de las CGRif se pensó que las funciones FI y NFI eran compartimentos distintos regulados por diferentes CGR, pero este concepto ha evolucionado en los últimos años con el descubrimiento de nuevos tipos de CGRif que inervan regiones subcorticales FI y, por tanto, presentan funciones FI. Hoy se conocen 6 tipos diferentes de CGRif que se denominan M1-M6 y difieren en sus propiedades morfológicas, funcionales, moleculares, proyecciones centrales y responsabilidades en comportamientos visuales. En este trabajo revisamos el sistema visual melanopsínico, el campo de investigación más activo en visión y cuyo conocimiento ha crecido exponencialmente durante las últimas 2 décadas, desde que se descubrieron por primera vez las CGR que dan origen a esta vía.



* *Autor para correspondencia.*
Correo electrónico: beatrizvidalvillegas@gmail.com (B. Vidal-Villegas).

https://doi.org/10.1016/j.oftal.2020.06.032

## Photosensitive ganglion cells: A diminutive, yet essential population

*Keywords:*
Intrinsically photosensitive retinal ganglion cells
Melanopsin retinal ganglion cells
Retina
M1-M6 melanopsin cells
Non-image forming visual system

A B S T R A C T

Our visual system has evolved to provide us with an image of the scene that surrounds us, informing us of its texture, colour, movement, and depth with an enormous spatial and temporal resolution, and for this purpose, the image formation (IF) dedicates the vast majority of our retinal ganglion cell (RGC) population and much of our cerebral cortex. On the other hand, a minuscule proportion of RGCs, in addition to receiving information from classic cone and rod photoreceptors, express melanopsin and are intrinsically photosensitive (ipRGC). These ipRGC are dedicated to non-image-forming (NIF) visual functions, of which we are unaware, but which are essential for aspects related to our daily physiology, such as the timing of our circadian rhythms and our pupillary light reflex, among many others. Before the discovery of ipRGCs, it was thought that the IF and NIF functions were distinct compartments regulated by different RGCs, but this concept has evolved in recent years with the discovery of new types of ipRGCs that innervate subcortical IF regions, and therefore have IF visual functions. Six different types of ipRGCs are currently known. These are termed M1-M6, and differ in their morphological, functional, molecular properties, central projections, and visual behaviour responsibilities. A review is presented on the melanopsin visual system, the most active field of research in vision, for which knowledge has grown exponentially during the last 2 decades, when RGCs giving rise to this pathway were first discovered.



### La retina

Una de las principales funciones de la retina, la obtención de información lumínica de nuestro entorno, la desarrollan los fotorreceptores, unas neuronas llenas de pigmentos visuales y especializadas para la fototransducción, esto es, captar energía electromagnética (longitudes de onda dentro del espectro visible) y transformarla en energía eléctrica. La captación de un fotón por los pigmentos visuales induce un cambio conformacional de la molécula que se traduce en la activación de una proteína G que, a su vez, pone en marcha una cascada intracelular que termina en un cambio transitorio del potencial de membrana del fotorreceptor, una hiperpolarización, señal que sirve de comunicación interneuronal y se transmite a otras neuronas de la retina para su elaboración posterior. Además, la retina tiene como función adicional comparar la señal luminosa que detectan los fotorreceptores y producir patrones de respuesta que pueden oscilar desde la información básica del nivel de iluminación medioambiental al patrón de imagen puntual detectada por un solo fotorreceptor en la región foveal; una región de la retina especializada para nuestra visión fina que determina nuestra agudeza visual espacial y temporal, así como nuestra capacidad para ver colores[1]. La retina es capaz de realizar estas funciones adaptándose a intensidades de iluminación en un rango de 10 unidades logarítmicas y mantiene, a pesar del cambio de intensidad de luz ambiental, la misma apariencia de los objetos que vemos.

### Vías formadoras y no formadoras de imágenes

La información que envía la retina es responsable por una parte de la formación de imágenes (FI) para nuestra percepción visual consciente del mundo que nos rodea y, por otra, de funciones visuales no formadoras de imágenes (NFI), pero que tienen importantes implicaciones en nuestra fisiología y comportamiento cotidiano.

La inmensa mayoría de nuestras células ganglionares de la retina (CGR) trabaja para la FI de nuestro entorno visual, esto es, nuestra percepción visual consciente, la localización y la percepción de formas, su textura, colorido, movimiento y perspectiva. En humanos y primates, aproximadamente el 90% de las CGR se dirigen al núcleo geniculado del tálamo, la estación central de relevo más importante de la información visual antes de dirigirse a la corteza visual estriada, primera estación de trabajo en la ardua elaboración de nuestra percepción visual consciente.

Otro grupo de un poco menos del 10% de las CGR se dedica a labores de mantenimiento reflejas, de las que no somos conscientes, pero que contribuyen también a la FI pues resultan fundamentales para nuestra visión, como, por ejemplo, nuestros movimientos oculares ante una escena visual nueva o para estabilizar una escena visual en movimiento, o para acomodar y converger frente a objetos cercanos, o lo contrario, para enfocar en objetos lejanos. Todos los núcleos que participan en la FI tienen en general una representación topográfica de la superficie de la retina o mapa retinotópico.

Por último, en humanos y primates hay un muy pequeño porcentaje de CGR que expresan el fotopigmento melanopsina y utilizan la intensidad de la luz medioambiental (irradian-

cia) para regular comportamientos y funciones fisiológicas, cuyos circuitos no forman imágenes y no tienen relación con la percepción consciente de la visión. Estas funciones se denominan colectivamente funciones visuales NFI, permiten al organismo poner en hora nuestro reloj circadiano central y anticiparse a los cambios del entorno modificando su comportamiento, y regular el reflejo fotomotor[2]. Otros muchos comportamientos adicionales dependen también del nivel de iluminación ambiental, como son la regulación de la homeostasis metabólica[3], la síntesis de melatonina[2], nuestro estado de ánimo y capacidades cognitivas[4], la temperatura corporal[5], la inducción del sueño y del estado de alerta[6], el enmascaramiento de la actividad motora *(masking)* y la aversión a la luz[7], o el exacerbamiento de las migrañas y fotofobia[8].

Si bien el conocimiento que se tiene hoy en día sobre nuestras funciones FI procede en su mayoría de estudios realizados en el sistema visual de primates y humanos[1], la mayoría del conocimiento que tenemos en la actualidad sobre las funciones visuales NFI procede de estudios realizados en roedores, principalmente en ratones, por las herramientas de que se ha dispuesto para su identificación y distinción de las otras CGR[2,9–11]. La utilización de técnicas de ingeniería genética y molecular ha permitido el avance de nuestro conocimiento sobre el sistema visual del ratón hasta el punto de que es en la actualidad el sistema sensorial que mejor se conoce y sorprendentemente es mucho más parecido al del primate de lo que se pensaba. En este trabajo repasaremos conceptos actuales sobre la vía melanopsínica y sus funciones, obtenidos de estudios recientes realizados principalmente en ratones. Haremos también una breve mención a las alteraciones de la vía melanopsínica en algunas enfermedades.

## Las células ganglionares de la retina

La información procesada en la retina se transmite al cerebro codificada en un tren de impulsos nerviosos por los axones de las CGR, las únicas cuyos axones abandonan la retina y que suponen una diminuta proporción de las neuronas retinianas. Por ejemplo, en el roedor adulto, las CGR no llegan al 1% de la población de neuronas retinianas[12]. En la actualidad, atendiendo a criterios morfológicos, fisiológicos, topográficos, moleculares y de territorios de inervación, se piensa que hay hasta 40 tipos diferentes de CGR[13]. Cada uno de estos recoge aspectos particulares de la escena visual que se transmiten en paralelo a regiones subcorticales que ejecutan labores específicas[14]. En el ratón, se han descrito hasta 46 dianas subcorticales diferentes[15].

## Células ganglionares de la retina intrínsecamente fotosensibles

### *Características generales de las células ganglionares de la retina intrínsecamente fotosensibles*

Las CGR que se dedican a funciones visuales NFI constituyen una muy pequeña proporción (en humanos ≈1% y en roedores ≈3%, véase más adelante). Estas células se singularizan por la expresión del pigmento melanopsina (codificado por el gen Opn4), que transduce la luz en señales eléctricas, de ahí que se denominen melanopsínicas (CGRm+), intrínsecamente fotosensibles (CGRif), fotosensibles o tercer fotorreceptor de la retina[16,17]. La melanopsina toma su nombre de los melanóforos de la piel de la rana donde se descubrió[18], poco después se observaron CGRif en mono y ratón[16,19] y en la retina humana[20,21]. Las CGRif en roedores y humanos expresan 2 neurotransmisores, el glutamato y el polipéptido activador de la adenilato ciclasa pituitaria (PACAP)[22]. Las CGRif se despolarizan en respuesta a la estimulación luminosa de la melanopsina, incluso en ausencia de información de conos y bastones, y también *in vitro*[16]. La eliminación de la expresión de melanopsina resulta en una atenuación de la sincronización circadiana y del reflejo fotomotor[23], y la eliminación de fotorrecepción funcional de los 3 fotorreceptores (bastones, conos y CGRif)[24] o la ablación genética de las CGRif[25,26] resultan en una pérdida de las funciones visuales NFI, demostrando que el origen de esta vía melanopsínica está en las CGRif.

Las primeras CGRif descritas fueron las M1[16,19,27]. Pocos años después, se documentó que las CGRif también proyectaban a regiones cerebrales responsables de la FI, como el colículo superior (CS) (tubérculo cuadrigémino en humanos) y el núcleo dorsal del geniculado lateral (núcleo geniculado dorsal en humanos), tanto en humanos[21] como en ratones[28,29]. En ratones (rd/rd cl), que no tienen conos ni bastones, pero sí CGRif, se pudo observar un comportamiento visual burdo que resolvía patrones visuales y detectaba contrastes[28]. Posteriormente, se documentó que la mayoría de las aferencias de las CGRif a la división dorsal del núcleo geniculado lateral (NGLd) procedía de las M4[30], que pronto se identificaron como CGR α-ON sostenidas con una gran sensibilidad al contraste[31]. Más recientemente, se han identificado 2 CGRif adicionales con proyección al NGLd y posible contribución a la visión espacial, la M5, que presenta respuestas color oponentes[32], y la M6[33]. La contribución de las CGRif a la visión espacial se ha caracterizado en ratones[34] y humanos, en los que parecen contribuir a la percepción del brillo, de la visión espacial y a incrementar la apariencia de las imágenes[35]. En la actualidad, se han descrito en roedores 6 tipos diferentes de CGRif que se denominan M1-M6 y se distinguen con base en sus características morfológicas, tamaño de su soma, extensión y estratificación de su árbol dendrítico, nivel de expresión de melanopsina, respuestas intrínsecas y extrínsecas, características de sus campos receptores periféricos, regiones del cerebro a las que proyectan y marcadores específicos[17,28,30,32,33,36–40].

### *Número y distribución de las células ganglionares de la retina intrínsecamente fotosensibles*

En roedores adultos, se puede utilizar el marcador Brn3a, un factor de transcripción Pou4f1, para identificar la inmensa mayoría de las CGR convencionales que representan ≈96% de las CGR[41]. Como la inmensa mayoría de las CGR Brn3a+ no expresan melanopsina y viceversa, la utilización conjunta de ambos marcadores permite estudiar de forma paralela pero independiente estas 2 poblaciones de CGR en condiciones normales y frente a diferentes tipos de lesiones[42–52]. En ratas la población de CGRif constituye aproximadamente el 2,5-2,7% de la población total de CGR en retinas albinas y pigmentadas[17,27,41–43,49,53,54] (fig. 1).

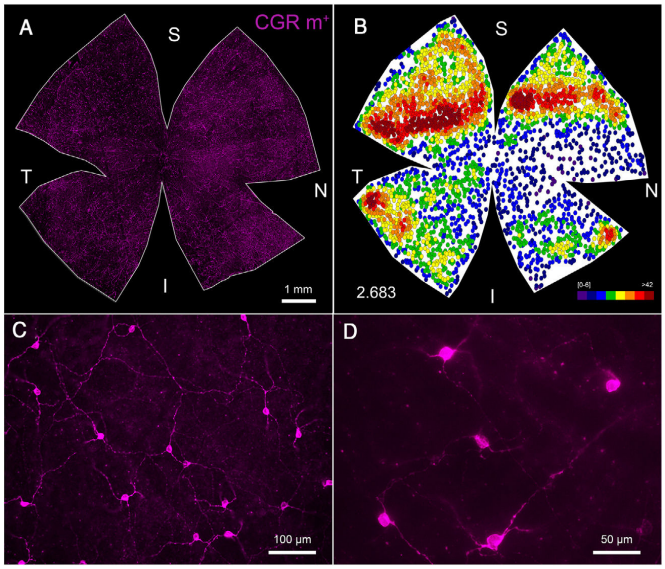


**Figura 1 – A) Fotomontaje de una retina de rata adulta en la que se aprecian células ganglionares de la retina intrínsecamente fotosensibles (CGRif) marcadas con melanopsina (CGRm+), distribuidas por toda la retina. B) Mapa de vecinos de la misma retina (A) que muestra la distribución topográfica de las CGRm+, que se contabilizaron manualmente, un total de 2.683. Escala de color del mapa de vecinos en la que cada color representa un incremento de 4 vecinos en un radio de 0,22 mm y oscila desde púrpura (0-6 vecinos) a rojo oscuro (42-48 vecinos). C y D) Detalles a mayor aumento en los que se aprecia el marcaje de las CGRif, tanto en sus somas celulares como en sus extensas dendritas en el plano de foco. Barra: A: = 1 mm, C: = 50 µm, D = 25 µm; I: inferior; N: nasal; S: superior; T: temporal.**

De modo análogo la utilización de Brn3b, otro factor de transcripción Pou4f2, y la melanopsina como marcadores celulares permite identificar una pequeña subpoblación de CGRif M1 Brn3b$^{-}$ y distinguirlas de la gran mayoría de las M1 y todas las demás M2-M6 que son Brn3b$^{+}$[55,56]. En el ratón pigmentado el número total de CGRif ha oscilado de 1.021[57], 2.058[29] a 2.570[36]. Estas variaciones se deben a la metodología empleada para identificar las CGRif, diferencias en el tipo de anticuerpo antimelanopsina, técnica inmunohistoquímica, utilización o no de amplificadores de la señal o de animales transgénicos que expresan un marcador en el *locus* de la melanopsina[11]. En roedores, la expresión de melanopsina se regula tanto por la luz como por ritmos circadianos retinianos[58–60] y en ratón se han descrito 2 isoformas de melanopsina, una larga (Opn4L) y otra corta (Opn4S), que se expresa 40 veces más que la larga[61,62]. M1 y M3 expresan ambas (Opn4S y Opn4L), mientras que M2 y M4 solo expresan Opn4L. De los diferentes subtipos, las M1-M3 constituyen la mayoría de las CGRif y son las más fáciles de identificar pues expresan más melanopsina, mientras que las M4[30,63], las M5[64] y las M6[33] expresan melanopsina en cantidades muy pequeñas y son muy difíciles de identificar con técnicas inmunohistoquímicas estándar, sin amplificación. En la actualidad, se acepta que las CGRif constituyen ≈3% de las CGR del ratón[40,65].

La distribución de las CGRif difiere; casi todos los subtipos celulares (excepto las M3) embaldosan la retina, las M1 y M2 son más abundantes en la hemirretina superior, las M5 abundan en la hemirretina inferior y las M4 presentan un gradiente naso-temporal con máximas densidades en la región superotemporal[11].

### *Proyecciones generales de las células ganglionares de la retina intrínsecamente fotosensibles*

Las proyecciones de las CGRif se han estudiado en detalle con técnicas que incrementan la visibilidad de la melanopsina o que utilizan marcadores insertados en el *locus* que corresponde a la melanopsina. Por ejemplo, reemplazando el gen de la melanopsina por la secuencia que codifica tau-LacZ, una proteína compuesta por el enzima β galactosidasa, unido a una secuencia de señal de tau (una proteína asociada a la actina lo que facilita el transporte anterógrado por el axón hasta el terminal axonal) Opn4$^{tauLacZ}$ (Hattar[17], 2002). También se han utilizado técnicas inmunohistoquímicas de amplificación de la señal, como la recombinasa Cre[29], o la expresión de la proteína fluorescente verde. Las proyecciones axonales se pueden identificar con la inyección intravítrea de un virus adeno asociado (AAV) que transfecta el gen humano de la fosfatasa alcalina placentaria (AAV-fles-plap) en ratones transgénicos que expresan Cre bajo el promotor de la melanopsina (Opn4$^{Cre}$[29,66]).

**Tabla 1 – Principales territorios de inervación de las células ganglionares de la retina intrínsecamente fotosensibles (CGRif) en el ratón**

| Principales territorios de inervación de las CGRif | |
|---|---|
| Prosencéfalo e hipotálamo | Área preóptica (ventrolateral, lateral, medial), zona subparaventricular, **núcleo supraquiasmático**, núcleo perisupraóptico, regiones anterior y laterales del hipotálamo, amígdala (anterior, medial y central), núcleo del lecho de la estría terminal |
| Tálamo y habénula | Núcleo perihabenular, *geniculado lateral dorsal*, geniculado lateral ventral, lengüeta intergeniculada, zona incerta |
| Mesencéfalo | Sustancia gris periacueductal, **núcleo olivar pretectal**, núcleos pretectales (anterior, medial y posterior), núcleo del tracto óptico, *capas visuales del colículo superior* |
| Sistema óptico accesorio | Núcleos terminales dorsal, lateral y medial |

Destacamos los núcleos retinorrecipientes más importantes de las funciones visuales no formadoras de imágenes NFI (negrita) y formadoras de imágenes FI (cursiva).
Fuente: Fernández et al.[4], Duda et al.[10], Sondereker et al.[11], Delwig et al.[66], Gooley et al.[67], Li y Schmidt[68], Do[69] y Lucas et al.[70].

De los 46 territorios subcorticales que inervan las CGR, el 30% carece de inervación de las CGRif[15]. En general, las CGRif proyectan al prosencéfalo basal e hipotálamo, la región del tálamo y habénula, al mesencéfalo y al sistema óptico accesorio (tabla 1). En el prosencéfalo basal inervan las áreas preópticas (lateral, medial y ventrolateral), el núcleo perisupraóptico, la zona subparaventricular (sPVZ), el núcleo supraquiasmático (NSQ), las regiones anterior y laterales del hipotálamo y las regiones de la amígdala (anterior, medial y central), así como el núcleo del lecho de la estría terminal. En el tálamo y la región de la habénula inervan el núcleo perihabenular (PHb), el NGLd y el núcleo geniculado lateral ventral (NGLv), la lengüeta intergeniculada y la zona incerta. En el mesencéfalo inervan el núcleo olivar pretectal (NOP), los núcleos pretectales anterior, medial y posterior, y el núcleo del tracto óptico. Además, inervan las capas visuales del CS, la sustancia gris periacueductal y los núcleos del sistema óptico accesorio (núcleos terminales dorsal, lateral y medial)[4,10,11,66–70].

Como resumen, se podría decir que la mayoría de las M1 y el resto de las CGRif (M2-M6) son Brn3b$^+$, proyectan al núcleo dorsal del geniculado y CS, son capaces de mediar una visión burda espacial en ausencia de función de bastones y conos y de mediar la sensibilidad al contraste (M4) o la visión del color (M5), mientras que las M1Brn3b$^-$ proyectan exclusivamente a centros circadianos[68].

## Características morfológicas y proyecciones de las células ganglionares de la retina intrínsecamente fotosensibles

### *Las M1*

Fueron las primeras en identificarse, asientan en la capa de CGR pero pueden aparecer desplazadas en la nuclear interna (NI) (M1d); su número oscila alrededor de 980 por retina y el tamaño del soma celular es de los más pequeños (14-16 μm)[16,29,30,36,40]. Se ha descrito una M1d, denominada interneurona melanopsínica, pues carece de axón en el nervio óptico[57]. El árbol dendrítico de M1 está poco ramificado, se extiende en la parte más externa de la sublámina OFF de la PI (S1) con un diámetro de ≈300-350 μm[29,30] y efectúa sinapsis *en passant* con axones de bipolares ON tipo 6 y con amacrinas dopaminérgicas. Durante el desarrollo, una pequeña proporción de M1 y M1d extienden sus dendritas también a la PE (dendritas retinianas externas) y allí se asocian con terminales axonales de los conos, se denominan CGRif biplexiformes y contribuyen a la estratificación de la retina y laminación de los conos[71,72]. En ratones y monos se ha descrito un pequeño subgrupo de M1 con colaterales axonales que terminan en la PI[73,74] y contribuyen a la regulación de la adaptación de la retina a la luz a través de sus conexiones con amacrinas dopaminérgicas[74]. Las M1 apenas presentan actividad espontánea en la oscuridad y su respuesta intrínseca es muy sensible a la luz, presentando respuestas rápidas y de gran amplitud. Las M1 presentan respuestas extrínsecas ON a la luz que son pequeñas y mantenidas.

Las M1 proyectan aproximadamente a unas 15 dianas cerebrales involucradas en funciones visuales NFI clásicas[17]. Una de sus principales dianas es el NSQ, un núcleo par de ≈1 mm de diámetro sito por encima del quiasma con una zona nuclear que recibe aferencia retiniana directa del tracto retino-hipotalámico y una cortical con neuronas que actúan como osciladores circadianos. La aferencia retiniana principal al NSQ procede de las M1 y en menor medida de las M2[75].

Las GCRif se pueden diferenciar según expresen brn3b en CGR M1Brn3b$^-$ y CGRBrn3b$^+$. La población de CGRif M1Brn3b$^-$ (unas 200) inerva el NSQ y es suficiente para sincronizar el ritmo circadiano, pues cuando se eliminan genéticamente las CGRifM1Brn3b$^+$, se produce la abolición de la mayoría de las funciones NFI, pero persiste la sincronización circadiana[55]. El NSQ inerva, a su vez, áreas involucradas en el estado de ánimo (área ventral tegmental y rafe) y cognitivas (el hipocampo). Estas áreas se pueden ver influidas a través del NSQ o directamente a través una vía directa de axones de CGRif a estos núcleos, la amígdala medial y el núcleo núcleo perihabenular (PHb), respectivamente[4]. Tanto las M1Brn3b$^-$ como las M1Brn3b$^+$ proyectan ambas a la lengüeta interniculada y la región ventral NGLv, que son núcleos encargados de alargar el período de los ritmos circadianos[68]. Las CGRif M1Brn3b$^+$ inervan profusamente núcleos del mesencéfalo no relacionados con los ritmos circadianos, núcleos del tálamo y del hipotálamo. La corteza del NOP, implicado en el control del reflejo pupilar a la luz[55], está inervada por CGRif M1Brn3b$^+$[68], mientras que la región nuclear está inervada fundamentalmente por CGRif no-M1Brn3b$^+$. Las CGRifM1Brn3b$^+$ proyectan al núcleo PHb a través de la vía retino-perihabenular, una vía recientemente descrita formada por unas 76 CGRif M1 Brn3b$^+$

que media directamente los efectos de la luz en el estado de ánimo[4].

*Las M2*

Tienen sus somas en la capa de las CGR, son discretamente mayores que las M1 (16-19 μm) y su número oscila alrededor de 830 por retina[29,30,40]. El árbol dendrítico estratifica en la subcapa interna (ON) de la PI con un diámetro de ≈316-324 μm y con más ramificaciones regulares que las M1[29,30]. Reciben aferencias de las células bipolares de cono ON tipo 8, contienen significativamente menos melanopsina que las M1 y presentan una sensibilidad a la luz de un orden de magnitud inferior a las M1. Su respuesta extrínseca es del tipo ON amplia y sostenida, y su campo receptor presenta la clásica estructura de centro periferia antagonista.

Las M2 proyectan a regiones subcorticales típicas NFI, inervan el NSQ e inervan profusamente la región central del NOP. También inervan regiones FI, como el NGLd[10,29].

*Las M3*

Se caracterizan por ser biestratificadas, su árbol dendrítico es de los más grandes (457-497 μm) y se extiende en ambas subcapas de la PI; sus somas (17-19 μm) asientan en la capa de las CGR y representan menos del 10% de las CGRif. Las propiedades de membrana y las respuestas intrínsecas a la estimulación luminosa de las M3 son similares a las de las M2. Las repuestas extrínsecas de las M3, similares a las M2, presentan una respuesta robusta de la vía ON que induce despolarización celular[40]. Este tipo celular es escaso y no forma un mosaico que embaldose la retina[36], criterio necesario para considerar un subtipo diferente de CGR[14].

El destino de las proyecciones de las M3 se desconoce con exactitud, aunque se ha sugerido que proyectan al CS[76] y al núcleo PHb[4].

*Las M4*

Son muy sensibles al contraste, asientan en la capa de CGR y sus somas son los más grandes de todas las CGRif (19-24 μm). Sus árboles dendríticos, radiales y muy ramificados, crecen en el eje temporonasal (210-420 μm)[31,77] y se distribuyen siguiendo un gradiente naso-temporal, con un máximo en la región superotemporal. El árbol dendrítico monoestratifica en la sublámina ON de la PI, discretamente más externo que las M2, y probablemente recibe aferencias de terminales de bipolares de cono tipo 7[30,31]. Las M4 carecen de inmunofluorescencia contra melanopsina detectable con técnicas estándar, pero cuando la señal se amplifica aparece un claro marcaje celular.

Las M4 tienen respuestas intrínsecas débiles que varían en función de la adaptación a la luz; respuesta débil en retina adaptada a la luz, pero mayor en adaptación a la oscuridad[78]. Esta respuesta intrínseca de la melanopsina contribuye a aumentar la excitabilidad de la célula y haría que la M4 disparase a intensidades luminosas muy bajas[63]. En ratones knockout ($Opn4^{-}$) que no expresan melanopsina, se aprecian déficits en la sensibilidad al contraste debidos a la carencia de melanopsina en las M4[31].

Las M4 presentan respuestas extrínsecas conducidas por conos, con campos receptores grandes organizados en centro-ON periferia antagónica-OFF, que recuerdan los campos convencionales de las CGR, con sensibilidad al movimiento, pero sin selectividad direccional. Recientemente, se ha documentado que cuando se registran adaptadas a la luz presentan oponencia al color, como las M5[77].

Las M4 corresponden a las clásicas CGR α-ON sostenidas y expresan neurofilamentos de alto peso molecular no fosforilados, osteopontina y calbindina, además de bajos niveles de melanopsina[77,79]. Se pueden identificar por la colocalización de neurofilamentos de alto peso molecular no fosforilados y calbindina, con anticuerpos SMI32 y anticalbindina (fig. 2). En ratones transgénicos que expresan el chivato de la melanopsina con una proteína fluorescente verde, se contabilizaron una media de 570 $SMI32^{+}$/retina que se clasificaron como CGRif M4 (Schmidt et al.[31], 2014).

Las M4 inervan en su inmensa mayoría el sector ventromedial del NGLd y median la sensibilidad al contraste en ausencia de conos y bastones. En presencia de conos y bastones, también contribuyen a la agudeza visual y al seguimiento de objetos[28–31,78].

*Las M5*

Son células con oponencia cromática que tienen su soma (12-16 μm) en la capa de las CGR, con árboles dendríticos (149-274 μm) muy ramificados y compactos que estratifican en la sublámina ON de la PI[30,32,77]. Presentan respuestas intrínsecas muy débiles, menores que las M4. Su inmunorreactividad contra la melanopsina apenas se detecta con técnicas estándar y cuando se amplifica la señal se aprecia marcaje en el soma, pero no en las dendritas. Las M5 presentan respuestas extrínsecas de tipo ON sostenidas, al menos un orden de magnitud superior a las intrínsecas. Su característica particular es su oponencia cromática ultravioleta-verde; el campo receptor está construido de modo que tienen un centro con aferencia selectiva de conos UV (a través de bipolares de cono tipo 9) y mezcla de conos UV y M (a través de bipolares de cono tipos 6, 7 y 8), y una fuerte periferia supresora dominada por aferencias de conos M a través de amacrinas gabaérgicas[32]. Al igual que otras CGRif, las respuestas escotópicas probablemente estén mediadas por bipolares de bastón, amacrinas AII (vía primaria) y por el acoplamiento del bastón-cono (vía secundaria de los bastones).

Las M5 proyectan al NGLd y de este modo pueden proveer señales cromáticas a la corteza visual[32], pero se piensa que también pueden inervar el NOP y los otros núcleos inervados por M6. Además, proyectan a la lengüeta intergeniculada que a su vez proyecta al NSQ, sugiriendo una vía para que las M5 provean información cromática a las neuronas de oponencia espectral del NSQ[80].

*Las M6*

Son células biestratificadas espinosas que asientan en la capa de CGR. Tanto el soma (11-15 μm) como su árbol dendrítico (190-250 μm) altamente ramificado son los más pequeños de todas las CGRif. En retinas de ratones pigmentados transgénicos Cdh3-GFP se contabilizaron unas pocas docenas de

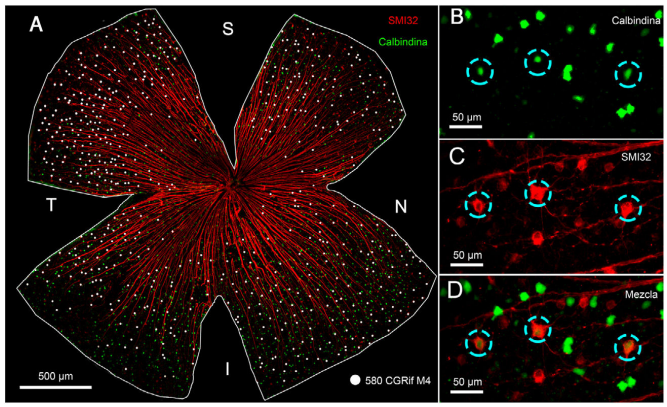


**Figura 2 – A) Fotomontaje de una retina de ratón pigmentado en la que se aprecian células ganglionares de la retina marcadas con anticuerpos que reconocen neurofilamentos de alto peso molecular no fosforilados (SMI32) y calbindina. Las células marcadas con SMI32 corresponden a las CGR tipo α, mientras que las doblemente marcadas aparecen señaladas con puntos blancos y corresponden a las CGR intrínsecamente fotosensibles tipo M4. En esta retina se contabilizaron 580 CGRif M4. Nótese la distribución de estas células en el eje naso-temporal con una densidad mayor en el cuadrante superotemporal. B-D) Detalles a mayor aumento en los que se aprecia el marcaje de las CGR α con SMI32 (B), calbindina (C) y doble marcaje de las CGRif M4 (D).**
**Barra: A = 500 µm, B-D = 50 µm; I: inferior; N: nasal; S: superior; T: temporal.**

CGRif M6, una cifra que puede subestimar la magnitud real de este subtipo pues en este ratón solo se marcan en la retina ventral[33]. La ramificación dendrítica externa se extiende en el margen distal de la PI, próxima a la NI, donde estratifican la M1 y el árbol externo de la M3. La ramificación dentrítica interna supone aproximadamente el 85% del volumen dendrítico y se extiende en el margen interno de la PI[33]. Las M6 expresan niveles muy bajos de melanopsina detectables con técnicas amplificadoras de tiramida y cuando la tinción aparece lo hace a modo de parches en la región del soma, pero no en dendritas. Las M6 presentan respuestas intrínsecas muy débiles, menores que las M4 y M5. Las M6 presentan respuestas del tipo ON sostenidas cuando se ilumina la totalidad de su campo receptor, relativamente pequeño y organizado en centro-periferia fuertemente antagonista. Aunque tienen parte de su árbol dendrítico en la región OFF de la PI, sus respuestas son, como las de todas las CGRif, del tipo ON sostenido. Se piensa que el árbol dendrítico externo recibe en la sublámina OFF de la PI aferencias ectópicas *en passant* de axones de bipolares ON. Estas células carecen de respuesta al color y de selectividad direccional[33].

Las M6 proyectan, por una parte, a territorios típicos NFI como el centro del NOP, el núcleo posterior pretectal, la lengüeta intergeniculada y NGLv y, por otra, proyectan débilmente al NGLd[33].

### *Células ganglionares de la retina intrínsecamente fotosensibles en primates y humanos*

En humanos, el número total de CGRif varía entre el 0,2[21], el 0,4[81], el 0,8[20,62,82] y el 1,5%[83] de la población de CGR[84]. Estas variaciones se deben a diferencias técnicas para detectar la melanopsina, así como a la menor expresión de melanopsina en M2 y M4, comparadas con las M1. Al igual que en roedores, la melanopsina se expresa en una isoforma corta más abundante, presente en las M1 y M3, y una isoforma larga presente en todas las melanopsínicas.

Los somas y los árboles dendríticos de las CGRm$^+$ de las retinas de humanos y macacos son de los más grandes. En un principio, estas CGRif se clasificaron según su estratificación en las subláminas OFF y ON de la PI en CGRif externas e internas, respectivamente[21,59,81,82]. Más recientemente, utilizando anticuerpos contra los terminales N y C de la melanopsina humana, Hannibal et al.[62] (2017), basándose en la localización y el tamaño del soma, y en la estratificación de sus árboles dendríticos, clasificaron las CGRif según la nomenclatura utilizada en roedores. El tipo predominante en humanos es el M1, con una elevada proporción de células desplazadas (dM1) y con mayor expresión de melanopsina. Un tipo de M1 gigante (GM1), que proyecta al nGDL, presenta respuesta oponente al color amarillo-ON azul-OFF, mediada por conos S-OFF antagonizada por una respuesta de conos (L + M)-ON[21], en la que participan células amacrinas descritas recientemente que reciben de bipolares de cono S-ON[85]. Se identificaron también gigantes desplazadas GM1d. Algunas de las M1 presentaban colaterales axonales que se extendían en la retina. Las M2 (denominadas internas) son menos abundantes y expresan menos melanopsina. En humanos también hay CGRif similares a las M3 que estratifican en S1 y S5, pero su frecuencia es muy pequeña y su caracterización, muy pobre[62,82]. También se han descrito en humanos M4, distribuidas en el eje naso-temporal y con mayor densidad en la hemirretina temporal[82]. Hasta la fecha se desconoce si la retina humana y de primate posee M5 y M6[11]. La distribución de las M1 en humanos

contrasta con la de las M1 en roedores, pues en humanos y primates presentan densidades muy altas en la región central perifoveal y menores en la periferia, mientras que las M2 son menos abundantes y se distribuyen de modo similar a las M4[62,84]. Esta densidad diferente de CGRif en la región perifoveal y periférica puede significar una función diferente en la percepción de la oponencia al color[11].

En el primate, las proyecciones de las CGRif se han estudiado combinando un trazador anterógrado muy sensible, la subunidad B de la toxina colérica, e inmunohistoquímica para revelar la presencia de PACAP[86]. Se documentó la presencia de terminales PACAP$^{+}$ en regiones que sustentan funciones visuales NFI. Así, las CGRif del primate proyectan densamente al NSQ, al NOP y al complejo pregeniculado (que corresponde a la lengüeta intergeniculada del roedor). En la región pretectal, también mostraron inervación densa en el núcleo del tracto óptico pero escasa en el núcleo pretectal medial posterior. También se han observado fibras doblemente marcadas en regiones que sustentan funciones visuales FI, el *brachium* del SC y las capas visuales del CS, así como en núcleo geniculado lateral en las capas correspondientes contralaterales (1, 4 y 6) o ipsilaterales (2, 3 y 5), en las regiones principales (parvo o magno) pero no en las koniocelulares[62].

## Contribución de las células ganglionares de la retina intrínsecamente fotosensibles a funciones visuales no formadoras de imágenes

En ratones, la ablación de las CGRif[25,26,87] resulta en pérdida de las funciones visuales NFI con mantenimiento de la visión clásica y de las CGR convencionales, indicando que las CGRif constituyen la unidad funcional del sistema NFI, que transmite al cerebro la información obtenida tanto de los fotorreceptores clásicos como de la activación de la melanopsina[88]. Las funciones NFI consisten principalmente en: 1) la sincronización diaria de nuestros ritmos circadianos; 2) regulación del reflejo fotomotor; 3) regulación de nuestros ritmos sueño-vigilia; 4) regulación de la temperatura corporal; 5) regulación de la actividad metabólica; 6) regulación de nuestras capacidades cognitivas y estado de ánimo; 7) la aversión a la luz, y 8) la adaptación de la retina a la luz.

### *Sincronización de los ritmos circadianos*

La sincronización de nuestros ritmos circadianos consiste en la puesta en hora de nuestro marcapasos circadiano central, sito en el NSQ, que recibe información directa de la retina a través del tracto retino-hipotalámico, inervado principalmente por CGRif M1. Todas las especies estudiadas tienen ritmos circadianos (que oscilan en un período de 24 h; circa = aproximado; día = 24 h) gobernados por un marcapasos principal, que impone un ritmo propio incluso en condiciones de luz constantes, pero que se retrasa todos los días un poco. Estos marcapasos se sincronizan con claves temporales y en nuestro caso la luz solar actúa de temporizador para poner en hora nuestro marcapasos circadiano. La sincronización del ritmo circadiano depende de una subpoblación de 200 M1Brn3b$^{-4}$, y desaparece en animales que carecen del tracto retino-hipotalámico[89].

La sincronización circadiana modula directamente los ritmos de muchas funciones fisiológicas, como el apetito, los ciclos de temperatura y el nivel de hormonas circulantes, que a su vez sincroniza relojes presentes en muchos tejidos del organismo[90]. El NSQ, además de regular los ritmos circadianos, actúa también como estación de relevo para conducir información luminosa a otros territorios que reciben aferencia directa de las CGRif, proporcionando así una vía indirecta para funciones relacionadas con el sueño/vigilia, nuestras capacidades cognitivas y nuestro estado de ánimo. La secreción de melatonina, que modifica nuestros ritmos cardíacos, y la supresión de la actividad motora, son ejemplos de este concepto; aunque se regulan de modo circadiano, también se suprimen de forma aguda por la exposición a la luz (lo que se conoce como enmascaramiento; «*masking*»)[38], un efecto mediado por aferencias directas al núcleo ventral de la zona subparaventricular[67], y se piensa que las mismas CGRif que inervan el NSQ son responsables de ambos comportamientos[5].

### *Reflejo pupilar a la luz*

Una de las funciones clásicas NFI es la regulación del reflejo pupilar a la luz por el NOP inervado en su corteza por las M2 y otras CGRif no-M1Brn3b$^{+}$ y en su centro por CGRif M1Brn3b$^{+}$. En el reflejo fotomotor participan los 3 tipos de fotorreceptores. Las típicas respuestas rápidas y amplias al comienzo del estímulo dependen de conos y bastones, mientras que las respuestas mantenidas que siguen a las respuestas agudas dependen de la melanopsina. Esto se ha documentado en ratones que carecen de conos y bastones (rd/rd cl), que presentaban respuestas lentas pero duraderas, que proceden de las CGRif, y en ratones knock out (Opn4$^{-/-}$) carentes de respuestas intrínsecas mediadas por la melanopsina[23] que presentaban respuestas rápidas transitorias, sin respuesta a irradiancias altas[28]. En ratones triples knock out, que no expresan melanopsina y tienen alterada la fototransducción de bastones y conos (Gnat1$^{-/-}$; Cnga3$^{-/-}$; Opn4$^{-/-}$), se aprecia una retina normal, pero ausencia total de respuesta pupilar a la luz, acompasamiento circadiano, supresión de actividad motora o cualquier otra de las típicas funciones NFI desencadenadas por la luz[24], resultados similares se obtuvieron de ratones en los que se habían ablacionado genéticamente las CGRif[25]. En humanos, se ha examinado la contribución de los distintos fotorreceptores utilizando la pupilometría cromática que cuantifica el reflejo fotomotor con base en la sensibilidad espectral de cada fotorreceptor y se han descrito los distintos componentes de este reflejo[91]. Tras la presentación de la luz se produce una respuesta fásica, de aparición rápida y duración corta, con una contracción robusta de la pupila mediada por bastones y conos. Posteriormente, la pupila se relaja gradualmente a un estado más dilatado y si la intensidad de la luz supera el dintel de activación de la melanopsina, la pupila se mantiene contraída con un tamaño constante, esta respuesta se denomina respuesta posfásica. Si la luz se ha mantenido durante más de 3 min, al apagarla la constricción pupilar persiste durante unos segundos antes de relajarse a valores normales, y esta se denomina respuesta pupilar postiluminación (PIPR), que es dependiente de la melanopsina[67,91,92]. Las PIPR se suman binocularmente cuando el estímulo se presenta

binocularmente[93] y no parecen estar influidas directamente por el color[94].

*Ritmos sueño/vigilia*

Se pensaba que los ciclos sueño/vigilia se regulaban indirectamente a través de nuestros ritmos circadianos, pero se ha documentado que las CGRif Brn3b$^+$ envían información directa intrínseca y extrínseca a la región del hipotálamo lateral y área preóptica ventrolateral para regular tanto el comienzo como la duración del ciclo de sueño[5,6,67,95]. Todavía se desconoce con exactitud cuál de los 6 tipos de CGRif Brn3b$^+$ es responsable de la regulación de estos ritmos, pero se ha sugerido que serían las M1 o M2 que expresan mayores niveles de melanopsina[5].

*Ritmos de temperatura corporal*

La termorregulación corporal sigue ritmos circadianos y su control se ha atribuido a la función del marcapasos central del NSQ. Hoy sabemos que el NSQ realiza el control circadiano de la temperatura corporal con la información aferente que le llega a través de las CGRif M1Brn3b$^-$, pero que las CGRif Brn3b$^+$ son necesarias para el control agudo directo de la temperatura corporal; por ejemplo, tras la presentación de un pulso luminoso nocturno. Se piensa que las CGRif Brn3b$^+$ ejercen su efecto a través de proyecciones directas a los núcleos preópticos mediano y ventrolateral del hipotálamo[5].

*Regulación de la actividad metabólica*

La actividad metabólica diaria se adapta a los ritmos circadianos impuestos por los ciclos de luz oscuridad. Esta actividad está controlada por núcleos hipotalámicos que contienen marcapasos regulados a su vez por el marcapasos central del NSQ. En ratones con expresión hipomórfica selectiva de Pitx3, en los que el tracto retino-hipotalámico está ausente, se produce un desacompasamiento de los marcapasos del NSQ (responsable de los ritmos circadianos) y del hipotálamo ventromedial (responsable de ritmos de la ingesta y balance energético) que resulta en alteraciones del comportamiento y del metabolismo que afectan a la actividad locomotora, los ritmos de alimentación y de gasto energético, así como de secreción de corticosterona[89]. Se piensa que estas alteraciones se deben a la ausencia de maduración del marcapasos del NSQ durante el desarrollo por la carencia de aferencias retinianas[56,89,96].

*Estado de ánimo y capacidades cognitivas*

Es conocido el efecto de la luz para modular nuestros estados de ánimo y capacidad intelectual. Por ejemplo, un vuelo que cruza varias zonas horarias desacopla nuestro ritmo circadiano con la hora solar *(jet lag)* y se tarda unos días en regularizarse. Durante estos días, sufrimos alteraciones de nuestro ritmo sueño/vigilia, deterioro cognitivo, malestar e irritabilidad que desaparecen cuando nuestro ritmo circadiano se acompasa de nuevo con la hora solar local. Este tipo de alteraciones también se experimentan por trabajadores corre-turnos (alternan turnos de trabajo día/noche), nocturnos, o en aquellas personas que sufren desorden afectivo estacional que aparece a finales del otoño y durante el invierno como consecuencia del acortamiento rápido de los días[65]. Clásicamente, se pensó que tanto la regulación de las funciones cognitivas como del estado de ánimo dependían del NSQ. Hoy se sabe que el NSQ influencia indirectamente estas funciones[65], pero que hay 2 proyecciones diferentes de CGRif responsables directas de estas funciones. Por una parte, una subpoblación de aproximadamente 71 CGRif M1Brn3b$^+$ que inerva el núcleo talámico PHb (vía retino-habenular) es responsable directa de la modulación del estado de ánimo[4]. Además, estas CGRif que inervan el núcleo PHb emiten colaterales que proyectan al estriado dorsal y ventral y a la corteza prefrontal, núcleos todos ellos involucrados en el control de procesos afectivo-emocionales, estado de ánimo y depresión, y regulación del estado de ánimo y trastornos depresivos, respectivamente[4].

Por otra parte, las CGRif M1Brn3b$^-$ (aproximadamente unas 200) que inervan el NSQ son responsables de la modulación de capacidades cognitivas, independientemente de la sincronización del ritmo circadiano[4], aunque se desconocen los núcleos inervados responsables de estas capacidades. Por ejemplo, ratones carentes de CGRif M1Brn3b$^+$ presentaban funciones cognitivas y de aprendizaje normales en pruebas de reconocimiento de objetos nuevos y del laberinto acuático de Morris, documentando de este modo que la ausencia de esta subpoblación no afecta a las funciones cognitivas de estos animales pues están mediadas por CGRif M1Brn3b$^-$[4].

*Aversión a la luz*

La aversión a la luz, esto es el desplazamiento a distancia de la luz[97], es una respuesta sensorial refleja que se observa en ratones neonatales tan pronto como P6, un período en el que la única sensibilidad a la luz se produce por la activación de las CGRif, mucho antes de que las señales procedentes de conos y bastones comiencen a producirse y enviarse a las CGR. En ratones Opn4$^{-/-}$ neonatales no se aprecia aversión a la luz, indicando que la melanopsina es necesaria para la aversión a la luz[98]. Este comportamiento está mediado por el CS[99], por lo que es probable que se deba a las aferencias de las CGRif no M1, pues son las únicas que inervan el CS a esas edades posnatales[100].

*Adaptación de la retina a la luz*

Una pequeña población de CGRif M1 Brn3b$^-$ tiene colaterales axonales intrarretinianas que proyectan a la retina externa[73,74], transmiten señales de luminancia a través del sistema dopaminérgico y de este modo influencian la adaptación de la retina a la luz, facilitando que pueda operar en niveles de iluminación que abarcan 10 unidades logarítmicas. La señal excitadora de las M1 provoca la secreción de dopamina por las amacrinas dopaminérgicas[74,101] que forman una vía de retroalimentación intrarretiniana transmitiendo señales de conos, bastones y CGRif en sentido centrífugo de la retina interna a la externa. La dopamina liberada ejerce su acción a través de receptores dopaminérgicos D1-D5 y la activación de estos modifica los circuitos retinianos en función de la iluminación prevalente; esto es, el desacoplamiento eléctrico a través de

la retina, modulando los receptores excitadores de glutamato en las horizontales y regulando la actividad de los canales de sodio de las CGR y bipolares. La depleción de dopamina en la retina resulta en una alteración de la adaptación a la luz de nuestra visión[102].

## Contribución de las células ganglionares de la retina intrínsecamente fotosensibles a funciones visuales formadoras de imágenes

El descubrimiento de nuevos subtipos de CGRif en ratones y primates que proyectaban al NGLd y CS, núcleos involucrados directamente en la FI y en la percepción visual consciente, sugería la participación de CGRif en funciones visuales FI. Ratones Gnat1$^{-/-}$; Cnga3$^{-/-}$, que carecen de bastones y conos funcionales y dependen de la melanopsina para la detección de la luz, presentaban comportamientos visuales burdos, que necesitaban aproximadamente el doble de tiempo que los ratones control para superar las pruebas visuales[28]. Estas capacidades visuales desaparecían en ratones knock out triples (Gnat1$^{-/-}$; Cnga3$^{-/-}$; Opn4$^{-/-}$), carentes de todo tipo de fotorrecepción funcional[29]. Estudios posteriores han documentado que ratones carentes de melanopsina (Opn4$^{-/-}$)[28] o carentes de CFRif M4 (ratones Opn4$^{Cre/+}$; Bnr3b$^{zDTA/+}$)[55] presentan déficits en la sensibilidad al contraste tanto en tareas visuales comportamentales subcorticales (seguimiento optocinético) como corticales (laberinto acuático visual)[103], demostrando que la melanopsina de estas células influencia sus propiedades fisiológicas[31].

Hoy se acepta que las CGRif contribuyen a la detección del contraste[31], la discriminación de la intensidad luminosa[28], la adaptación de la actividad del NGLd en función de la irradiancia[28,104] y la codificación de patrones espaciales[10,34]. Utilizando técnicas para presentar imágenes en las que se modula independientemente la visibilidad de la melanopsina vs. conos y bastones, se registraron respuestas evocadas del NGLd en animales control de las que un 20% respondían a patrones visibles únicamente por la melanopsina. Las señales melanopsínicas tienen resolución espacio-temporal suficiente para codificar patrones espaciales, una resolución espacial modesta con campos receptores de ≈13° y una frecuencia temporal modesta ≈1 Hz[34].

### *El color de la luz en la sincronización circadiana*

La sincronización de los ritmos circadianos a los ciclos luz/oscuridad no solo tiene en cuenta la información sobre oscilaciones en intensidad de la luz, sino también sus variaciones cromáticas. A medida que avanza el crepúsculo se produce un enriquecimiento progresivo de luz de onda corta. Esto es debido al filtrado de la luz de longitud de onda larga por la banda Chappuis de la capa de ozono (efecto de filtro Chappuis) cuando el sol se encuentra por debajo del horizonte, en una hora del día en la que el cielo aparece particularmente azul (la hora azul) y que se observa tanto al final del crepúsculo como al comienzo del alba[105]. En el NSQ, ≈25% de las neuronas registradas intracelularmente son sensibles a cambios espectrales con respuestas color oponente dependiente de los conos, la mayoría con respuestas azul-ON/amarillo-OFF y una minoría con respuestas amarillo-ON/azul-OFF[80]. La información del color de la luz permite al NSQ obtener información precisa del momento en que se produce la transición, el crepúsculo o el amanecer, y así se logra una puesta en hora más fidedigna del marcapasos circadiano, y le permite además al NSQ distinguir una disminución de la irradiancia, porque se ha nublado el cielo, de la que ocurre durante el anochecer o el amanecer[106]. Se ha postulado que el uso del color para determinar con exactitud el inicio del cambio de fase de nuestros ritmos circadianos podría ser una estrategia conservada evolutivamente y quizás uno de los propósitos originales de la visión del color[80]. En roedores, se ha sugerido que las M5, caracterizadas por su oponencia cromática, podrían informar al NSQ de las variaciones espectrales a través de sus aferencias a la lengüeta intergeniculada[32]. En primates, se han descrito CGRif GM1 cromáticas (azul-OFF/amarillo-ON)[21] y recientemente se ha documentado que esta información podría estar mediada por las aferencias de las bipolares de cono S-ON a una célula amacrina nueva que recibe aferencias excitadoras de las bipolares de cono S-ON y, a su vez, efectúa contactos inhibidores en CGRif M1 que resultan en una respuesta azul-OFF[85]. Estas CGRif M1 con respuestas S-OFF de los primates podrían ser la aferencia al NSQ para el afinamiento de la puesta en hora del reloj circadiano en el alba y el ocaso, cuando se producen los mayores contrastes cromáticos de la luz[85].

## Funciones visuales no formadoras de imágenes en la enfermedad

Estudios clínicos realizados en enfermedades neurodegenerativas han documentado alteraciones de la vía melanopsínica asociadas a anomalías de las funciones visuales NFI[82,84]. Así, pacientes con enfermedad de Parkinson presentan una disminución significativa de la población de CGRif que podría ser responsable de las alteraciones del estado de ánimo y de los ciclos de sueño/vigilia reportados en estos pacientes[107]. Del mismo modo, en retinas de donantes de edad avanzada (> 70 años) se observó una disminución de la densidad de CGRif y atrofia de sus árboles dendríticos que también podrían estar relacionadas con las alteraciones de los ritmos circadianos que se observan en ancianos[108]. En un estudio realizado en retinas de pacientes con enfermedad de Alzheimer se documentó la degeneración de CGRif y alteraciones de sus árboles dendríticos, y estos hallazgos se correlacionaron con alteraciones de funciones circadianas[109]. En un estudio realizado en pacientes completamente ciegos, con ausencia completa de percepción de luz, por diversas causas (retinosis pigmentaria, retinopatía del prematuro, retinopatías por retinitis o por síndrome de la rubéola, glaucoma congénito, neuropatía o neuritis óptica, o de causa desconocida) se documentó que una pequeña fracción de estos (≈33%) presentaban supresión de la secreción de melatonina cuando se exponían a la luz, lo que sugería la preservación de ritmos circadianos y la persistencia del tracto retinohipotalámico. Esta observación estaba ausente, sin embargo, en los 3 enfermos del estudio que presentaban enucleaciones bilaterales[110]. En otro estudio se examinó la prevalencia de las alteraciones circadianas en 123 mujeres ciegas sin percepción alguna de luz o con percepción de luz, estudiando alteraciones de los ritmos sueño/vigilia y

del ritmo de la secreción de melatonina para lo que se examinó el diario de sueño/vigilia de estas enfermas, así como la excreción urinaria cada 4-8 h de la 6-sulfatoximelatonina, principal metabolito urinario de la melatonina. De las participantes sin percepción alguna de luz, la mayoría (≈63%) presentaban anomalías de sus ritmos circadianos o no estaban acompasados y se trataba de enfermas con enucleaciones bilaterales o retinopatía del prematuro. De las participantes con percepción de luz, una mayoría (≈69%) presentaba ritmos circadianos normales y se trataba de enfermas con retinosis pigmentaria o degeneración macular asociada a la edad[111].

## Funciones visuales de las células ganglionares de la retina intrínsecamente fotosensibles en el período posnatal

En ratas y ratones, las CGRif están presentes en la retina desde el nacimiento (P0) y muestran respuestas fotosensibles mucho antes de que los conos y bastones comiencen a funcionar y enviar sus señales a la retina, lo que coincide aproximadamente con la apertura ocular (P10). Las CGRif se identificaron y clasificaron en registros efectuados en la retina posnatal (P10-12) según su latencia, sensibilidad e intensidad de respuesta a la luz en 3 tipos: I, las más frecuentes 78%; II (15%) y III (13%)[112]. Los registros electrofisiológicos y el uso combinado de anticuerpos antimelanopsina y SMI32 (un anticuerpo contra la subunidad no fosforilada de alto peso molecular del triplete de los neurofilamentos) ha permitido clasificar estas CGRif posnatales y asociarlas a los tipos adultos. Así, las CGRif tipo I ($m^+SMI32^+$), II y III ($m^+SMI32^-$) corresponden a las M4, M2 y M1, respectivamente[96,113]. Estas CGRif disminuyen tanto en número como en fotosensibilidad durante el desarrollo posnatal temprano hasta la edad adulta, lo que se debe principalmente a la muerte y la disminución de expresión melanopsina de las CGRif M4[114].

Las funciones de las CGRif durante el desarrollo posnatal temprano son: *1)* regular el desarrollo del patrón de ramificación vascular en la retina y la regresión de la vasculatura hialoidea embrionaria; ratones que carecen de melanopsina ($Opn4^{-/-}$) presentan desarrollo vascular y regresión hialoidea anómalos[115]; *2)* la aversión a la luz de ratones neonatales (P6)[7,98]; *3)* el acoplamiento inter-CGRif necesario para producir las ondas de actividad retiniana espontáneas[116] que regulan el refinamiento de la segregación ocular de los terminales retinianos axonales en el geniculado y CS; las CGRif M1 $Brn3b^-$ regulan las propiedades de disparo de las CGR a través de señales por sus colaterales axonales intrarretinianas[56]; *4)* la maduración del ritmo circadiano, esto es, el establecimiento de la duración de las fases del ritmo circadiano; el subgrupo de 200 CGRif M1$Brn3b^-$ que proyecta exclusivamente al NSQ, es responsable de la maduración del reloj circadiano y del establecimiento inicial de la duración de las fases[56,96,117], y *5)* la organización de la arquitectura retiniana y laminación de los conos. Ratones $Opn4^{DTA/DTA}$ carentes de CGRif presentaban una desorganización de los conos a P7 y P16, y un desplazamiento anómalo de estos a otras capas de la retina. En estos ratones se documentó que la luz durante la primera semana posnatal contribuye a restringir los somas de los conos a la nuclear externa e influencia la laminación de los conos a su capa. Se ha postulado que en estos ratones las CGRif utilizan sus dendritas externas para comunicarse con los conos y regular el número de conos desplazados fuera de la NE[72].

## Fototransducción de la melanopsina

Las opsinas son receptores acoplados a una proteína G que convierten la energía de un fotón en un cambio del potencial de membrana. Los pigmentos visuales constan de una apoproteína (la opsina) a la que se une una molécula cromófora, un derivado de la vitamina A1, el 11-cis-retinaldehído. Pequeñas modificaciones en la estructura de la proteína cambian el espectro de absorción. La melanopsina es un pigmento visual con una $\lambda_{máx}$ de 480 nm.

La eficiencia de la melanopsina es comparable con las opsinas de conos y bastones, pero hay diferencias entre la fototransducción de la melanopsina y las opsinas clásicas: *1)* la fototransducción en conos y bastones resulta en una hiperpolarización transitoria y, como consecuencia, la señal que se transmite en el pie sináptico es una reducción de la liberación de glutamato; la cascada de fototransducción de la melanopsina se asemeja más a la de los invertebrados y resulta en una despolarización de la membrana (Graham et al.[118], 2008) y consecuentemente se produce un incremento de la frecuencia de potenciales de acción dependiente de la iluminación ambiental[69,119]; *2)* la cascada de fototransducción de la melanopsina es mucho más lenta[120]; *3)* las CGRif carecen de las especializaciones celulares (discos y sáculos) que tienen bastones y conos para optimizar las probabilidades de captura de un fotón, lo que resulta en una diferencia en densidad de moléculas/unidad de área de 8.300 veces mayor en conos y bastones con respecto a las CGRif y, por tanto, menor probabilidad de absorción de un fotón por área de fotoestimulación para las CGRif[69]; sin embargo, la melanopsina puede activarse en condiciones escotópicas, lo que confiere gran sensibilidad del sistema melanopsínico[121]; *4)* la amplificación de la cascada de fototransducción de la melanopsina compensa la escasa cantidad de melanopsina y los pocos fotones que absorben; una vez alcanzado el umbral de activación de la melanopsina, la respuesta persiste durante largos períodos de iluminación constante y se ha documentado en estudios *in vitro* que la señal melanopsínica puede mantenerse activa durante 10 h seguidas de iluminación[122]; *5)* la regeneración del pigmento visual se piensa que se produce por un mecanismo dependiente de la luz; la melanopsina fotoexpuesta se convierte en metamelanopsina que retiene el cromóforo en la forma todotrans y tras la absorción de un nuevo fotón regenera la forma 11-cis, de este modo las CGRif no se decoloran independientemente de a cuanta luz se expongan; se denominan pigmentos biestables pues poseen un mecanismo intrínseco de regeneración que les hace resistentes a la decoloración, similar a los invertebrados[92,123]; se desconoce si las células de Müller actúan como reservorio del cromóforo para la melanopsina[101], y *6)* se pensaba que la fototransducción de la melanopsina empleaba mecanismos similares en todas las CGRif y que aquellas que expresaban poca melanopsina (M4-M6) deberían su función principal a sus aferencias extrínsecas, relegando a un segundo lugar la función de su escasa melanopsina. Sin embargo, se ha documentado que la cascada intracelular de

la melanopsina utiliza mecanismos diferentes en distintos tipos de CGRif[63] y que en las CGRif implicadas en funciones FI la melanopsina, aunque escasa, puede modular el procesado de las señales procedentes de bastones y conos. Por ejemplo, incrementando la sensibilidad al contraste de las M4 involucradas en la visión espacial en un rango de iluminancia que oscila desde niveles muy altos a niveles muy bajos en los que únicamente participan los bastones, utilizando canales permeables al potasio para incrementar la excitabilidad de las M4[63].

## Consideraciones finales

Las CGRif se caracterizan por su respuesta intrínseca a la melanopsina, pero también tienen respuestas extrínsecas mediadas por los fotorreceptores clásicos a través de los mismos circuitos que las CGR convencionales, de modo que las vías melanopsínicas integran todas las señales luminosas que captura la retina. Podría plantearse entonces, ¿para qué quieren las CGRif estas aferencias integradas? Una posible explicación sería para extender su rango de actuación, ya que informan al cerebro de señales muy tenues de luz (que activan los bastones), moderadas (en los que participan los conos con una señal cinética más rápida y además informan del color), hasta niveles muy elevados y mantenidos (que activan la melanopsina).

¿Sigue siendo válida la clasificación de CGRif según sus funciones NFI y FI? La clasificación de las CGRif como responsables de funciones visuales NFI ha sido útil para estudiar en detalle estas funciones, pero a medida que se ha sabido más de estas células se comprueba que la división original en CGRif responsables de funciones NFI y FI no es tan clara. Muchas CGRif M1Brn3b$^+$ proyectan a núcleos responsables de funciones visuales NFI (p. ej., el NOP) y FI (p. ej., regiones del NGLd). Incluso una misma subpoblación de CGRif M1Brn3b$^-$ que fundamentalmente se dedica en el adulto a funciones visuales NFI (sincronizar el ritmo circadiano), durante el desarrollo posnatal temprano media, sin embargo, el refinamiento de funciones visuales FI (la segregación axonal en el NGLd) y funciones visuales NFI (como el establecimiento del periodo temporal de los ritmos circadianos)[56]. Esquemáticamente, se podría resumir esta clasificación en que las M1Brn3b$^-$ tienen fundamentalmente funciones NFI relacionadas con los ritmos circadianos, mientras que las M1Brn3b$^+$ tienen mayoritariamente funciones NFI no relacionadas con los ritmos circadianos con una contribución muy pequeña a las funciones FI; las M2, también Brn3b$^+$, serían responsables de funciones visuales NFI (el reflejo fotomotor) y de funciones visuales FI, mientras que las M3-M6, todas ellas Brn3b$^+$, serían responsables mayoritariamente de funciones visuales FI[11].

¿Podríamos ignorar una población de CGRif tan pequeña como las M4-M6? El cerebro del mamífero en general tiene muy poca redundancia y poblaciones neuronales que pueden parecer insignificantes realizan, sin embargo, funciones cruciales. Por ejemplo, sabemos que tan pocas como unas 70 CGRif M1Brn3n$^+$ forman la vía retino-perihabenular y son responsables del estado de ánimo, que se modifica sustancialmente con exposiciones irregulares a la luz durante los ciclos normales día/noche[4]. Además, se ha documentado recientemente que la melanopsina de las CGRif M4 es capaz de modular su excitabilidad en un rango muy amplio de iluminaciones, incrementando su sensibilidad al contraste. Este efecto se produce en las células M4 mediante un mecanismo hasta ahora nunca asociado a la melanopsina, consistente en el cierre de canales de fuga de potasio (canales de potasio de la subfamilia TASK, de la familia de canales de potasio con doble dominio de poro, K2P), que es selectivo de las CGRif que participan en la FI (Sonoda et al.[63], 2018). Como este mecanismo no está presente en las M1, se ha sugerido que la cascada de fototransducción de la melanopsina actuaría con diferentes mecanismos en distintos tipos de CGRif. La melanopsina sería capaz de mejorar la señal visual de las CGRif M4, que codifican la FI, en un rango de luminancias que varía desde una luz tenue que activa únicamente bastones a una luz más intensa que activa preferentemente los conos, modulando así procesos visuales en rangos mucho mayores de lo que se pensaba[63].

En resumen, las CGRif presentan múltiples características que las distinguen del resto de las CGR más convencionales: *1)* las CGRif cumplen un extenso rango de funciones; a las cada vez mejor comprendidas funciones NFI hay que añadir el conocimiento de las funciones FI que desempeñan las M4, y aún queda por descifrar el rol exacto de las M5 y M6; *2)* las CGRif expresan cantidades muy diferentes de melanopsina, altas en las M1, moderadas con un orden de magnitud inferior en las M2-3, o apenas perceptibles con 2 órdenes de magnitud inferior en las M4-6; sin embargo, independientemente de la cantidad de melanopsina, su expresión les confiere una singularidad funcional muy particular; *3)* en general, las CGR responden funcionalmente a estímulos luminosos dependiendo de la sublámina de la PI en la que extienden sus dendritas, externa (a, OFF) o interna (b, ON), de modo que las CGR que arborizan en la sublámina externa o interna tienen respuestas de centro-OFF (disminución de descargas en presencia de luz) o de centro-ON (incremento de descargas a la presencia de luz), respectivamente[124]; sin embargo, las CGRif M1, M3 y M6 a pesar de extender sus dendritas en la sublámina OFF, tienen la peculiaridad de que sus respuestas son de tipo ON mantenidas, como el resto de las CGRif; estas se producen porque las M1, M3 y M6 reciben en la sublámina OFF aferencias ectópicas *en passant* de bipolares ON, lo que ha hecho pensar que esta región de la PI podría considerarse una subdivisión adicional de la sublámina OFF que informa a las CGR ON, y *4)* por último, y aunque no ha sido objeto de esta revisión, las CGRif presentan una particular resiliencia a múltiples tipos de injuria retiniana que las hace particularmente resistentes a la lesión[42,43,45,49]. En resumen, se trata, por tanto, de un tipo de CGR, uno de los 40 tipos posibles, que en realidad está compuesto de 6 subtipos, que todavía tiene múltiples cuestiones desconocidas y que seguirá contribuyendo, sin duda, a que el sistema melanopsínico siga siendo uno de los campos de investigación más activos en visión.

## Financiación

El presente trabajo ha sido financiado en parte por la Fundación Séneca, Agencia de Ciencia y Tecnología Región de Murcia (19881/GERM/15) y por el Ministerio de Economía y Competitividad, Instituto de Salud Carlos III, Fondo Euro-

peo de Desarrollo Regional «una manera de hacer Europa» (SAF2015-67643-P; PID 2019-106498GB-I00; RD16/0008/0004; RD16/0008/0016).

## Conflicto de intereses

Los autores declaran no tener conflictos de interés.

BIBLIOGRAFÍA


1. Kolb H, Nelson RF, Ahnelt PK, Ortuño-Lizarán I, Cuenca N. The Architecture of the Human Fovea. En: Kolb H, Fernandez E, Nelson R, editores. Webvision: The Organization of the Retina and Visual System [Internet]. Salt Lake City (UT): University of Utah Health Sciences Center; 2020.
2. Hattar S, Kumar M, Park A, Tong P, Tung J, Yau K-W, et al. Central projections of melanopsin-expressing retinal ganglion cells in the mouse. J Comp Neurol. 2006;497:326–49, http://dx.doi.org/10.1002/cne.20970.
3. Panda S. Circadian physiology of metabolism. Science. 2016;354:1008–15, http://dx.doi.org/10.1126/science.aah4967.
4. Fernandez DC, Fogerson PM, Lazzerini Ospri L, Thomsen MB, Layne RM, Severin D, et al. Light affects mood and learning through distinct retina-brain pathways. Cell. 2018;175:71–84, http://dx.doi.org/10.1016/j.cell.2018.08.004, e18.
5. Rupp AC, Ren M, Altimus CM, Fernandez DC, Richardson M, Turek F, et al. Distinct ipRGC subpopulations mediate light's acute and circadian effects on body temperature and sleep. Elife. 2019;8, http://dx.doi.org/10.7554/eLife.44358.
6. Altimus CM, Guler AD, Villa KL, McNeill DS, LeGates TA, Hattar S. Rods-cones and melanopsin detect light and dark to modulate sleep independent of image formation. Proc Natl Acad Sci. 2008;105:19998–20003, http://dx.doi.org/10.1073/pnas.0808312105.
7. Delwig A, Majumdar S, Ahern K, LaVail MM, Edwards R, Hnasko TS, et al. Glutamatergic neurotransmission from melanopsin retinal ganglion cells is required for neonatal photoaversion but not adult pupillary light reflex. PLoS One. 2013;8:e83974, http://dx.doi.org/10.1371/journal.pone.0083974.
8. Noseda R, Copenhagen D, Burstein R. Current understanding of photophobia, visual networks and headaches. Cephalalgia. 2019;39:1623–34, http://dx.doi.org/10.1177/0333102418784750.
9. Seabrook TA, Burbridge TJ, Crair MC, Huberman AD. Architecture function, and assembly of the mouse visual system. Annu Rev Neurosci. 2017;40:499–538, http://dx.doi.org/10.1146/annurev-neuro-071714-033842.
10. Duda M, Domagalik A, Orlowska-Feuer P, Krzysztynska-Kuleta O, Beldzik E, Smyk MK, et al. Melanops From a small molecule to brain functions. Neurosci Biobehav Rev. 2020;113:190–203, http://dx.doi.org/10.1016/j.neubiorev.2020.03.012.
11. Sondereker KB, Stabio ME, Renna JM. The diversity of melanopsin ganglion cell types has begun to challenge the canonical divide between image-forming and non-image-forming vision. J Comp Neurol. 2020;528:2044–67, http://dx.doi.org/10.1002/cne.24873.
12. Nadal-Nicolás FM, Sobrado-Calvo P, Jiménez-López M, Vidal-Sanz M, Agudo-Barriuso M. Long-term effect of optic nerve axotomy on the retinal ganglion cell layer. Investig Ophthalmol Vis Sci. 2015;56:6095–112, http://dx.doi.org/10.1167/iovs.15-17195.
13. Baden T, Berens P, Franke K, Román Rosón M, Bethge M, Euler T. The functional diversity of retinal ganglion cells in the mouse. Nature. 2016;529:50–345, http://dx.doi.org/10.1038/nature16468.
14. Wässle H. Parallel processing in the mammalian retina. Nat Rev Neurosci. 2004;5:57–747, http://dx.doi.org/10.1038/nrn1497.
15. Morin LP, Studholme KM. Retinofugal projections in the mouse. J Comp Neurol. 2014;522:3733–53, http://dx.doi.org/10.1002/cne.23635.
16. Berson DM. Phototransduction by retinal ganglion cells that set the circadian clock. Science. 2002;295:1070–3, http://dx.doi.org/10.1126/science.1067262.
17. Hattar S. Melanopsin-containing retinal ganglion cells: architecture, projections, and intrinsic photosensitivity. Science. 2002;295:1065–70, http://dx.doi.org/10.1126/science.1069609.
18. Provencio I, Jiang G, de Grip WJ, Hayes WP, Rollag MD. Melanopsin: An opsin in melanophores, brain, and eye. Proc Natl Acad Sci. 1998;95:340–5, http://dx.doi.org/10.1073/pnas.95.1.340.
19. Provencio I, Rodriguez IR, Jiang G, Hayes WP, Moreira EF, Rollag MD. A novel human opsin in the inner retina. J Neurosci. 2000;20:600–5, http://dx.doi.org/10.1523/JNEUROSCI.20-02-00600.2000.
20. Hannibal J, Hindersson P, Østergaard J, Georg B, Heegaard S, Larsen PJ, et al. Melanopsin is expressed in PACAP-containing retinal ganglion cells of the human retinohypothalamic tract. Investig Opthalmology Vis Sci. 2004;45:4202, http://dx.doi.org/10.1167/iovs.04-0313.
21. Dacey DM, Liao H-W, Peterson BB, Robinson FR, Smith VC, Pokorny J, et al. Melanopsin-expressing ganglion cells in primate retina signal colour and irradiance and project to the LGN. Nature. 2005;433:749–54, http://dx.doi.org/10.1038/nature03387.
22. Hannibal J, Møller M, Ottersen OP, Fahrenkrug J. PACAP and glutamate are co-stored in the retinohypothalamic tract. J Comp Neurol. 2000;418:147–55.
23. Lucas RJ. Diminished pupillary light reflex at high irradiances in melanopsin-knockout mice. Science. 2003;299:245–7, http://dx.doi.org/10.1126/science.1077293.
24. Hattar S, Lucas RJ, Mrosovsky N, Thompson S, Douglas RH, Hankins MW, et al. Melanopsin and rod-cone photoreceptive systems account for all major accessory visual functions in mice. Nature. 2003;424:75–81, http://dx.doi.org/10.1038/nature01761.
25. Güler AD, Ecker JL, Lall GS, Haq S, Altimus CM, Liao HW, et al. Melanopsin cells are the principal conduits for rod-cone input to non-image-forming vision. Nature. 2008;453:102–5, http://dx.doi.org/10.1038/nature06829.
26. Hatori M, Le H, Vollmers C, Keding SR, Tanaka N, Schmedt C, et al. Inducible ablation of melanopsin-expressing retinal ganglion cells reveals their central role in non-image forming visual responses. PLoS One. 2008;3:e2451, http://dx.doi.org/10.1371/journal.pone.0002451.
27. Hannibal J, Hindersson P, Knudsen SM, Georg B, Fahrenkrug J. The photopigment melanopsin is exclusively present in pituitary adenylate cyclase-activating polypeptide-containing retinal ganglion cells of the retinohypothalamic tract. J Neurosci. 2002;22, http://dx.doi.org/10.1523/JNEUROSCI.22-01-j0002.2002. RC191-RC191.
28. Brown TM, Gias C, Hatori M, Keding SR, Semo M, Coffey PJ, et al. Melanopsin contributions to irradiance coding in the thalamo-cortical visual system. PLoS Biol. 2010;8:e1000558, http://dx.doi.org/10.1371/journal.pbio.1000558.
29. Ecker JL, Dumitrescu ON, Wong KY, Alam NM, Chen S-K, LeGates T, et al. Melanopsin-expressing retinal ganglion-cell

photoreceptors: Cellular diversity and role in pattern vision. Neuron. 2010;67:49–60, http://dx.doi.org/10.1016/j.neuron.2010.05.023.
30. Estevez ME, Fogerson PM, Ilardi MC, Borghuis BG, Chan E, Weng S, et al. Form function of the M4 cell an intrinsically photosensitive retinal ganglion cell type contributing to geniculocortical. Vision J Neurosci. 2012;32:13608–20, http://dx.doi.org/10.1523/JNEUROSC.I.20121422-12.
31. Schmidt TM, Alam NM, Chen S, Kofuji P, Li W, Prusky GT, et al. A role for melanopsin in alpha retinal ganglion cells and contrast detection. Neuron. 2014;82:781–8, http://dx.doi.org/10.1016/j.neuron.2014.03.022.
32. Stabio ME, Sabbah S, Quattrochi LE, Ilardi MC, Fogerson PM, Leyrer ML, et al. The M5 cell: A color-opponent intrinsically photosensitive retinal ganglion cell. Neuron. 2018;97:150–63, http://dx.doi.org/10.1016/j.neuron.2017.11.030, e4.
33. Quattrochi LE, Stabio ME, Kim I, Ilardi MC, Michelle Fogerson P, Leyrer ML, et al. The M6 cell: A small-field bistratified photosensitive retinal ganglion cell. J Comp Neurol. 2019;527:297–311, http://dx.doi.org/10.1002/cne.24556.
34. Allen AE, Storchi R, Martial FP, Bedford RA, Lucas RJ. Melanopsin contributions to the representation of images in the early visual system. Curr Biol. 2017;27:1623–32, http://dx.doi.org/10.1016/j.cub.2017.04.046, e4.
35. Allen AE, Martial FP, Lucas RJ. Form vision from melanopsin in humans. Nat Commun. 2019;10:2274, http://dx.doi.org/10.1038/s41467-019-10113-3.
36. Berson DM, Castrucci AM, Provencio I. Morphology and mosaics of melanopsin-expressing retinal ganglion cell types in mice. J Comp Neurol. 2010;518, http://dx.doi.org/10.1002/cne.22381. NA-NA.
37. Schmidt TM, Chen S-K, Hattar S. Intrinsically photosensitive retinal ganglion cells: Many subtypes, diverse functions. Trends Neurosci. 2011;34:572–80, http://dx.doi.org/10.1016/j.tins.2011.07.001.
38. Lazzerini Ospri L, Prusky G, Hattar S. Mood, the circadian system, and melanopsin retinal ganglion cells. Annu Rev Neurosci. 2017;40:539–56, http://dx.doi.org/10.1146/annurev-neuro-072116-031324.
39. Berg DJ, Kartheiser K, Leyrer M, Saali A, Berson DM. Transcriptomic signatures of postnatal adult intrinsically photosensitive ganglion cells. eNneuro. 2019;6, http://dx.doi.org/10.1523/ENEURO.10022-19.2019. ENEURO.0022-19.2019.
40. Schmidt TM, Kofuji P. Structure and function of bistratified intrinsically photosensitive retinal ganglion cells in the mouse. J Comp Neurol. 2011;519:1492–504, http://dx.doi.org/10.1002/cne.22579.
41. Nadal-Nicolás FM, Salinas-Navarro M, Jiménez-López M, Sobrado-Calvo P, Villegas-Pérez MP, Vidal-Sanz M, et al. Displaced retinal ganglion cells in albino and pigmented rats. Front Neuroanat. 2014;8:9, http://dx.doi.org/10.3389/fnana.2014.00099.
42. Vidal-Sanz M, Valiente-Soriano FJ, Ortín-Martínez A, Nadal-Nicolás FM, Jiménez-López M, Salinas-Navarro M, et al. Retinal neurodegeneration in experimental glaucoma. Prog Brain Res. 2015;220:1–35.
43. Vidal-Sanz M, Nadal-Nicolás FM, Valiente-Soriano FJ, Agudo-Barriuso M, Villegas-Pérez MP. Identifying specific RGC types may shed light on their idiosyncratic responses to neuroprotection. Neural Regen Res. 2015;10:1228–30, http://dx.doi.org/10.4103/1673-5374.162751.
44. Vidal-Sanz M, Galindo-Romero C, Valiente-Soriano FJ, Nadal-Nicolás FM, Ortin-Martinez A, Rovere G, et al. Shared and differential retinal responses against optic nerve injury and ocular hypertension. Front Neurosci. 2017;11:235, http://dx.doi.org/10.3389/fnins.2017.00235.
45. Agudo-Barriuso M, Nadal-Nicolás F, Madeira M, Rovere G, Vidal-Villegas B, Vidal-Sanz M. Melanopsin expression is an indicator of the well-being of melanopsin-expressing retinal ganglion cells but not of their viability. Neural Regen Res. 2016;11:1243, http://dx.doi.org/10.4103/1673-5374.189182.
46. Sánchez-Migallón MC, Valiente-Soriano FJ, Salinas-Navarro M, Nadal-Nicolás FM, Jiménez-López M, Vidal-Sanz M, et al. Nerve fibre layer degeneration and retinal ganglion cell loss long term after optic nerve crush or transection in adult mice. Exp Eye Res. 2018;170:40–50, http://dx.doi.org/10.1016/j.exer.2018.02.010.
47. Valiente-Soriano FJ, Salinas-Navarro M, Jiménez-López M, Alarcón-Martínez L, Ortín-Martínez A, Bernal-Garro JM, et al. Effects of ocular hypertension in the visual system of pigmented mice. PLoS One. 2015;10:e0121134, http://dx.doi.org/10.1371/journal.pone.0121134.
48. Valiente-Soriano FJ, Nadal-Nicolás FM, Salinas-Navarro M, Jiménez-López M, Bernal-Garro JM, Villegas-Pérez MP, et al. BDNF rescues RGCs but not intrinsically photosensitive RGCs in ocular hypertensive albino rat retinas. Investig Ophthalmol Vis Sci. 2015;56:1924–36, http://dx.doi.org/10.1167/iovs.15-16454.
49. Vidal-Villegas B, di Pierdomenico J, Miralles de Imperial-Ollero JA, Ortín-Martínez A, Nadal-Nicolás FM, Bernal-Garro JM, et al. Melanopsin + RGCs are fully resistant to NMDA-induced excitotoxicity. Int J Mol Sci. 2019;20:3012, http://dx.doi.org/10.3390/ijms20123012.
50. García-Ayuso D, di Pierdomenico J, Esquiva G, Nadal-Nicolás FM, Pinilla I, Cuenca N, et al. Inherited photoreceptor degeneration causes the death of melanopsin-positive retinal ganglion cells and increases their coexpression of Brn3a. Investig Opthalmology Vis Sci. 2015;56:4592, http://dx.doi.org/10.1167/iovs.15-16808.
51. García-Ayuso D, Galindo-Romero C, di Pierdomenico J, Vidal-Sanz M, Agudo-Barriuso M, Villegas Pérez MP. Light-induced retinal degeneration causes a transient downregulation of melanopsin in the rat retina. Exp Eye Res. 2017;161:10–6, http://dx.doi.org/10.1016/j.exer.2017.05.010.
52. Rovere G, Nadal-Nicolás FM, Wang J, Bernal-Garro JM, García-Carrillo N, Villegas-Pérez MP, et al. Melanopsin-containing or non-melanopsin-containing retinal ganglion cells response to acute ocular hypertension with or without brain-derived neurotrophic factor neuroprotection. Investig Ophthalmol Vis Sci. 2016;57:6652–61, http://dx.doi.org/10.1167/iovs.16-20146.
53. Nadal-Nicolás FM, Jiménez-López M, Salinas-Navarro M, Sobrado-Calvo P, Alburquerque-Béjar JJ, Vidal-Sanz M, et al. Whole number, distribution and co-expression of Brn3 transcription factors in retinal ganglion cells of adult albino and pigmented rats. PLoS One. 2012;7:e49830, http://dx.doi.org/10.1371/journal.pone.0049830.
54. Galindo-Romero C, Jiménez-López M, García-Ayuso D, Salinas-Navarro M, Nadal-Nicolás FM, Agudo-Barriuso M, et al. Number and spatial distribution of intrinsically photosensitive retinal ganglion cells in the adult albino rat. Exp Eye Res. 2013;108:84–93, http://dx.doi.org/10.1016/j.exer.2012.12.010.
55. Chen S-K, Badea TC, Hattar S. Photoentrainment and pupillary light reflex are mediated by distinct populations of ipRGCs. Nature. 2011;476:92–5, http://dx.doi.org/10.1038/nature10206.
56. Chew KS, Renna JM, McNeill DS, Fernandez DC, Keenan WT, Thomsen MB, et al. A subset of ipRGCs regulates both maturation of the circadian clock and segregation of retinogeniculate projections in mice. Elife. 2017;6, http://dx.doi.org/10.7554/eLife.22861.
57. Valiente-Soriano FJ, Garcí-a-Ayuso D, Ortín-Martínez A, Jiménez-López M, Galindo-Romero C, Villegas-Pérez MP,

et al. Distribution of melanopsin positive neurons in pigmented and albino mice: Evidence for melanopsin interneurons in the mouse retina. Front Neuroanat. 2014;8:131, http://dx.doi.org/10.3389/fnana.2014.00131.
58. Hannibal J, Georg B, Hindersson P, Fahrenkrug J. Light and darkness regulate melanopsin in the retinal ganglion cells of the albino wistar rat. J Mol Neurosci. 2005;27:147–56, http://dx.doi.org/10.1385/JMN:27:2:147.
59. Hannibal J, Georg B, Fahrenkrug J. Melanopsin changes in neonatal albino rat independent of rods and cones. Neuroreport. 2007;18:81–5, http://dx.doi.org/10.1097/WNR.0b013e328010ff56.
60. Hannibal J, Georg B, Fahrenkrug J. Differential expression of melanopsin mRNA and protein in Brown Norwegian rats. Exp Eye Res. 2013;106:55–63, http://dx.doi.org/10.1016/j.exer.2012.11.006.
61. Pires SS, Hughes S, Turton M, Melyan Z, Peirson SN, Zheng L, et al. Differential expression of two distinct functional isoforms of melanopsin (Opn4) in the mammalian retina. J Neurosci. 2009;29:12332–42, http://dx.doi.org/10.1523/JNEUROSC.I.2009.2036-09.
62. Hannibal J, Christiansen AT, Heegaard S, Fahrenkrug J, Kiilgaard JF. Melanopsin expressing human retinal ganglion cells: Subtypes, distribution, and intraretinal connectivity. J Comp Neurol. 2017;525:1934–61, http://dx.doi.org/10.1002/cne.24181.
63. Sonoda T, Lee SK, Birnbaumer L, Schmidt TM. Melanopsin phototransduction is repurposed by ipRGC subtypes to shape the function of distinct visual circuits. Neuron. 2018;99:754–67, http://dx.doi.org/10.1016/j.neuron.2018.06.032, e4.
64. Duan X, Qiao M, Bei F, Kim I-J, He Z, Sanes JR. Subtype-specific regeneration of retinal ganglion cells following axotomy: Effects of osteopontin and mTOR signaling. Neuron. 2015;85:1244–56, http://dx.doi.org/10.1016/j.neuron.2015.02.017.
65. LeGates TA, Fernandez DC, Hattar S. Light as a central modulator of circadian rhythms, sleep and affect. Nat Rev Neurosci. 2014;15:443–54, http://dx.doi.org/10.1038/nrn3743.
66. Delwig A, Larsen DD, Yasumura D, Yang CF, Shah NM, Copenhagen DR. Retinofugal projections from melanopsin-expressing retinal ganglion cells revealed by intraocular injections of cre-dependent virus. PLoS One. 2016;11:e0149501, http://dx.doi.org/10.1371/journal.pone.0149501.
67. Gooley JJ, Lu J, Fischer D, Saper CB. A broad role for melanopsin in nonvisual photoreception. J Neurosci. 2003;23:7093–106, http://dx.doi.org/10.1523/JNEUROSCI.23-18-07093.2003.
68. Li JY, Schmidt TM. Divergent projection patterns of M1 ipRGC subtypes. J Comp Neurol. 2018;526:2010–8, http://dx.doi.org/10.1002/cne.24469.
69. Do MTH. Melanopsin and the intrinsically photosensitive retinal ganglion cells: Biophysics to behavior. Neuron. 2019;104:205–26, http://dx.doi.org/10.1016/j.neuron.2019.07.016.
70. Lucas RJ, Allen AE, Milosavljevic N, Storchi R, Woelders T. Can we see with melanopsin? Annu Rev Vis Sci. 2020;6:453–68, http://dx.doi.org/10.1146/annurev-vision-030320-041239.
71. Sondereker KB, Onyak JR, Islam SW, Ross CL, Renna JM. Melanopsin ganglion cell outer retinal dendrites: Morphologically distinct and asymmetrically distributed in the mouse retina. J Comp Neurol. 2017;525:3653–65, http://dx.doi.org/10.1002/cne.24293.
72. Tufford AR, Onyak JR, Sondereker KB, Lucas JA, Earley AM, Mattar P, et al. Melanopsin retinal ganglion cells regulate cone photoreceptor lamination in the mouse retina. Cell Rep. 2018;23:2416–28, http://dx.doi.org/10.1016/j.celrep.2018.04.086.
73. Joo HR, Peterson BB, Dacey DM, Hattar S, Chen SK. Recurrent axon collaterals of intrinsically photosensitive retinal ganglion cells. Vis Neurosci. 2013;30:82–175, http://dx.doi.org/10.1017/S0952523813000199.
74. Prigge CL, Yeh P-T, Liou N-F, Lee C-C, You S-F, Liu L-L, et al. M1 ipRGCs influence visual function through retrograde signaling in the retina. J Neurosci. 2016;36:7184–97, http://dx.doi.org/10.1523/JNEUROSC.I.2016 3500-15.
75. Fernandez DC, Chang YT, Hattar S, Chen SK. Architecture of retinal projections to the central circadian pacemaker. Proc Natl Acad Sci. 2016;113:6047–52, http://dx.doi.org/10.1073/pnas.1523629113.
76. Zhao X, Stafford BK, Godin AL, King WM, Wong KY. Photoresponse diversity among the five types of intrinsically photosensitive retinal ganglion cells. J Physiol. 2014;592:1619–36, http://dx.doi.org/10.1113/jphysiol.2013.262782.
77. Sonoda T, Okabe Y, Schmidt TM. Overlapping morphological and functional properties between M4 and M5 intrinsically photosensitive retinal ganglion cells. J Comp Neurol. 2020;528:1028–40, http://dx.doi.org/10.1002/cne.24806.
78. Schroeder MM, Harrison KR, Jaeckel ER, Berger HN, Zhao X, Flannery MP, et al. The roles of rods, cones, and melanopsin in photoresponses of M4 intrinsically photosensitive retinal ganglion cells (ipRGCs) and optokinetic visual behavior. Front Cell Neurosci. 2018;12:203, http://dx.doi.org/10.3389/fncel.2018.00203.
79. Krieger B, Qiao M, Rousso DL, Sanes JR, Meister M. Four alpha ganglion cell types in mouse retina: Function, structure, and molecular signatures. PLoS One. 2017;12:e0180091, http://dx.doi.org/10.1371/journal.pone.0180091.
80. Walmsley L, Hanna L, Mouland J, Martial F, West A, Smedley AR, et al. Colour as a signal for entraining the mammalian circadian clock. PLOS Biol. 2015;13:e1002127, http://dx.doi.org/10.1371/journal.pbio.1002127.
81. Liao H-W, Ren X, Peterson BB, Marshak DW, Yau K-W, Gamlin PD, et al. Melanopsin-expressing ganglion cells on macaque and human retinas form two morphologically distinct populations. J Comp Neurol. 2016;524:2845–72, http://dx.doi.org/10.1002/cne.23995.
82. Esquiva G, Hannibal J. Melanopsin-expressing retinal ganglion cells in aging and disease. Histol Histopathol. 2019;34:1299–311, http://dx.doi.org/10.14670/HH-18-138.
83. La Morgia C, Ross-Cisneros FN, Sadun AA, Hannibal J, Munarini A, Mantovani V, et al. Melanopsin retinal ganglion cells are resistant to neurodegeneration in mitochondrial optic neuropathies. Brain. 2010;133:2426–38, http://dx.doi.org/10.1093/brain/ awq155.
84. Lax P, Ortuño-Lizarán I, Maneu V, Vidal-Sanz M, Cuenca N. Photosensitive melanopsin-containing retinal ganglion cells in health and disease: Implications for circadian rhythms. Int J Mol Sci. 2019;20:3164, http://dx.doi.org/10.3390/ijms20133164.
85. Patterson SS, Kuchenbecker JA, Anderson JR, Neitz M, Neitz J. A color vision circuit for non-image-forming vision in the primate retina. Curr Biol. 2020;30:1269–74, http://dx.doi.org/10.1016/j.cub.2020.01.040, e2.
86. Hannibal J, Kankipati L, Strang CE, Peterson BB, Dacey D, Gamlin PD. Central projections of intrinsically photosensitive retinal ganglion cells in the macaque monkey. J Comp Neurol. 2014;522, http://dx.doi.org/10.1002/cne.23588. Spc1-Spc1.
87. Göz D, Studholme K, Lappi DA, Rollag MD, Provencio I, Morin LP. Targeted destruction of photosensitive retinal ganglion cells with a saporin conjugate alters the effects of

light on mouse circadian rhythms. PLoS One. 2008;3:e3153, http://dx.doi.org/10.1371/journal.pone.0003153.
88. Ksendzovsky A, Pomeraniec IJ, Zaghloul KA, Provencio JJ, Provencio I. Clinical implications of the melanopsin-based non-image-forming visual system. Neurology. 2017;88:1282–90, http://dx.doi.org/10.1212/WN.L.0000000000003761.
89. Del Río-Martín A, Pérez-Taboada I, Fernández-Pérez A, Moratalla R, de la Villa P, Vallejo M. Hypomorphic expression of Pitx3 disrupts circadian clocks and prevents metabolic entrainment of energy expenditure. Cell Rep. 2019;29:3678–92, http://dx.doi.org/10.1016/j.celrep.2019.11.027, e4.
90. Buhr Van Gelder RN. Local photic entrainment of the retinal circadian oscillator in the absence of rods, cones, and melanopsin. Proc Natl Acad Sci. 2014;111:8625–30, http://dx.doi.org/10.1073/pnas.1323350111.
91. Kankipati L, Girkin CA, Gamlin PD. The post-illumination pupil response is reduced in glaucoma patients. Investig Opthalmology Vis Sci. 2011;52:2287, http://dx.doi.org/10.1167/iovs.10-6023.
92. Lucas RJ, Peirson SN, Berson DM, Brown TM, Cooper HM, Czeisler CA, et al. Measuring and using light in the melanopsin age. Trends Neurosci. 2014;37:1–9, http://dx.doi.org/10.1016/j.tins.2013.10.004.
93. Zivcevska M, Blakeman A, Lei S, Goltz HC, Wong AMF. Binocular summation in postillumination pupil response driven by melanopsin-containing retinal ganglion cells. Investig Opthalmology Vis Sci. 2018;59:4968, http://dx.doi.org/10.1167/iovs.18-24639.
94. Hayter EA, Brown TM. Additive contributions of melanopsin and both cone types provide broadband sensitivity to mouse pupil control. BMC Biol. 2018;16:83, http://dx.doi.org/10.1186/s12915-018-0552-1.
95. Lupi D, Oster H, Thompson S, Foster RG. The acute light-induction of sleep is mediated by OPN4-based photoreception. Nat Neurosci. 2008;11:1068–73, http://dx.doi.org/10.1038/nn.2179.
96. Sexton TJ, Bleckert A, Turner MH, van Gelder RN. Type I Intrinsically photosensitive retinal ganglion cells of early post-natal development correspond to the M4 subtype. Neural Dev. 2015;10:17, http://dx.doi.org/10.1186/s13064-015-0042-x.
97. Semo M, Gias C, Ahmado A, Sugano E, Allen AE, Lawrence JM, et al. Dissecting a role for melanopsin in behavioural light aversion reveals a response independent of conventional photoreception. PLoS One. 2010;5:e15009, http://dx.doi.org/10.1371/journal.pone.0015009.
98. Johnson J, Wu V, Donovan M, Majumdar S, Renteria RC, Porco T, et al. Melanopsin-dependent light avoidance in neonatal mice. Proc Natl Acad Sci. 2010;107:17374–8, http://dx.doi.org/10.1073/pnas.1008533107.
99. Routtenberg A, Strop M, Jerdan J. Response of the infant rat to light prior to eyelid opening: Mediation by the superior colliculus. Dev Psychobiol. 1978;11:469–78, http://dx.doi.org/10.1002/dev.420110510.
100. McNeill DS, Sheely CJ, Ecker JL, Badea TC, Morhardt D, Guido W, et al. Development of melanopsin-based irradiance detecting circuitry. Neural Dev. 2011;6:8, http://dx.doi.org/10.1186/1749-8104-6-8.
101. Viney TJ, Balint K, Hillier D, Siegert S, Boldogkoi Z, Enquist LW, et al. Local retinal circuits of melanopsin-containing ganglion cells identified by transsynaptic viral tracing. Curr Biol. 2007;17:981–8, http://dx.doi.org/10.1016/j.cub.2007.04.058.
102. Jackson CR, Ruan G-X, Aseem F, Abey J, Gamble K, Stanwood G, et al. Retinal dopamine mediates multiple dimensions of light-adapted. Vision J Neurosci. 2012;32:9359–68, http://dx.doi.org/10.1523/JNEUROSC.I.20120711-12.
103. Prusky GT, West PW, Douglas RM. Behavioral assessment of visual acuity in mice and rats. Vision Res. 2000;40:2201–9, http://dx.doi.org/10.1016/S0042-6989(00)00081-X.
104. Storchi R, Milosavljevic N, Eleftheriou CG, Martial FP, Orlowska-Feuer P, Bedford RA, et al. Melanopsin-driven increases in maintained activity enhance thalamic visual response reliability across a simulated dawn. Proc Natl Acad Sci. 2015;112:E5734-43, http://dx.doi.org/10.1073/pnas.1505274112.
105. Van Diepen HC, Foster RG, Meijer JH. A colourful clock. PLOS Biol. 2015;13:e1002160, http://dx.doi.org/10.1371/journal.pbio.1002160.
106. Spitschan M, Lucas RJ, Brown TM. Chromatic clocks: Color opponency in non-image-forming visual function. Neurosci Biobehav Rev. 2017;78:24–33, http://dx.doi.org/10.1016/j.neubiorev.2017.04.016.
107. Ortuño-Lizarán I, Esquiva G, Beach TG, Serrano GE, Adler CH, Lax P, et al. Degeneration of human photosensitive retinal ganglion cells may explain sleep and circadian rhythms disorders in Parkinson's disease. Acta Neuropathol Commun. 2018;6:90, http://dx.doi.org/10.1186/s40478-018-0596-z.
108. Esquiva G, Lax P, Pérez-Santonja JJ, García-Fernández JM, Cuenca N. Loss of melanopsin-expressing ganglion cell subtypes and dendritic degeneration in the aging human retina. Front Aging Neurosci. 2017;9:79, http://dx.doi.org/10.3389/fnagi.2017.00079.
109. La Morgia C, Ross-Cisneros FN, Koronyo Y, Hannibal J, Gallassi R, Cantalupo G, et al. Melanopsin retinal ganglion cell loss in Alzheimer disease. Ann Neurol. 2016;79:109–90, http://dx.doi.org/10.1002/ana.24548.
110. Hull JT, Czeisler CA, Lockley SW. Suppression of melatonin secretion in totally visually blind people by ocular exposure to white light. Ophthalmology. 2018;125:1160–71, http://dx.doi.org/10.1016/j.ophtha.2018.01.036.
111. Flynn-Evans EE, Tabandeh H, Skene DJ, Lockley SW. Circadian rhythm disorders and melatonin production in 127 blind women with and without light perception. J Biol Rhythms. 2014;29:215–24, http://dx.doi.org/10.1177/0748730414536852.
112. Tu DC, Zhang D, Demas J, Slutsky EB, Provencio I, Holy TE, et al. Physiologic diversity and development of intrinsically photosensitive retinal ganglion cells. Neuron. 2005;48:987–99, http://dx.doi.org/10.1016/j.neuron.2005.09.031.
113. Lucas JA, Schmidt TM. Cellular properties of intrinsically photosensitive retinal ganglion cells during postnatal development. Neural Dev. 2019;14:8, http://dx.doi.org/10.1186/s13064-019-0132-2.
114. Sekaran S, Lupi D, Jones SL, Sheely CJ, Hattar S, Yau KW, et al. Melanopsin-dependent photoreception provides earliest light detection in the mammalian retina. Curr Biol. 2005;15:1099–107, http://dx.doi.org/10.1016/j.cub.2005.05.053.
115. Rao S, Chun C, Fan J, Kofron JM, Yang MB, Hegde RS, et al. A direct and melanopsin-dependent fetal light response regulates mouse eye development. Nature. 2013;494:243–6, http://dx.doi.org/10.1038/nature11823.
116. Kirkby LA, Feller MB. Intrinsically photosensitive ganglion cells contribute to plasticity in retinal wave circuits. Proc Natl Acad Sci. 2013;110:12090–5, http://dx.doi.org/10.1073/pnas.1222150110.
117. Renna JM, Weng S, Berson DM. Light acts through melanopsin to alter retinal waves and segregation of retinogeniculate afferents. Nat Neurosci. 2011;14:827–9, http://dx.doi.org/10.1038/nn.2845.

118. Graham DM, Wong KY, Shapiro P, Frederick C, Pattabiraman K, Berson DM. Melanopsin ganglion cells use a membrane-associated rhabdomeric phototransduction cascade. J Neurophysiol. 2008;99:2522–32, http://dx.doi.org/10.1152/jn.01066.2007.
119. Hughes S, Rodgers J, Hickey D, Foster RG, Peirson SN, Hankins MW. Characterisation of light responses in the retina of mice lacking principle components of rod, cone and melanopsin phototransduction signalling pathways. Sci Rep. 2016;6:28086, http://dx.doi.org/10.1038/srep28086.
120. Brown TM, Lucas RJ. Melanopsin phototransduction: Great excitement over a poor catch. Curr Biol. 2009;19:R256–7, http://dx.doi.org/10.1016/j.cub.2009.01.034.
121. Lee SK, Sonoda T, Schmidt TM. M1 intrinsically photosensitive retinal ganglion cells integrate rod and melanopsin inputs to signal in low light. Cell Rep. 2019;29:3349–55, http://dx.doi.org/10.1016/j.celrep.2019.11.024, e2.
122. Wong KY. Retinal ganglion cell that can signal irradiance continuously for 10 A. Hours J Neurosci. 2012;32:11478–85, http://dx.doi.org/10.1523/JNEUROSC.I.2012.1423-12.
123. Lucas RJ. Chromophore regeneration: Melanopsin does its own thing. Proc Natl Acad Sci. 2006;103:10153–4, http://dx.doi.org/10.1073/pnas.0603955103.
124. Famiglietti E, Kolb H. Structural basis for ON-and OFF-center responses in retinal ganglion cells. Science. 1976;194:193–5, http://dx.doi.org/10.1126/science.959847.

Experimental Eye Research 210 (2021) 108694

Contents lists available at ScienceDirect

Experimental Eye Research

journal homepage: www.elsevier.com/locate/yexer

# Systemic treatment with 7,8-Dihydroxiflavone activates TtkB and affords protection of two different retinal ganglion cell populations against axotomy in adult rats

Beatriz Vidal-Villegas [a,b], Johnny Di Pierdomenico [b], Alejandro Gallego-Ortega [b], Caridad Galindo-Romero [b], Jose M. Martínez-de-la-Casa [a], Julian García-Feijoo [a], María P. Villegas-Pérez [a,b], Manuel Vidal-Sanz [b,*]

[a] Servicio de Oftalmología, Hospital Clínico San Carlos, Instituto de Investigación Sanitaria del Hospital Clínico San Carlos (IdISSC), 28040 Madrid, Spain
[b] Departamento de Oftalmología, Universidad de Murcia e Instituto Murciano de Investigación Biosanitaria (IMIB) Virgen de la Arrixaca. Campus de CC de la Salud, 30120, El Palmar, Murcia, Spain

ARTICLE INFO

*Keywords:*
Optic nerve section
Axotomy
Intraorbital optic nerve transection
Intrinsically photosensitive retinal ganglion cells
BDNF neuroprotection
7,8-Dihydroxiflavone
Melanopsin
Retinal ganglion cells
Apoptosis
Adult albino rats
Brn3a
Neuroprotection
BDNF-Mimetic

ABSTRACT

*Purpose:* To analyze responses of different RGC populations to left intraorbital optic nerve transection (IONT) and intraperitoneal (i.p.) treatment with 7,8-Dihydroxyflavone (DHF), a potent selective TrkB agonist.
*Methods:* Adult albino Sprague-Dawley rats received, following IONT, daily i.p. injections of vehicle (1%DMSO in 0.9%NaCl) or DHF. Group-1 (n = 58) assessed at 7days (d) the optimal DHF amount (1–25 mg/kg). Group-2, using freshly dissected naïve or treated retinas (n = 28), investigated if DHF treatment was associated with TrkB activation using Western-blotting at 1, 3 or 7d. Group-3 (n = 98) explored persistence of protection and was analyzed at survival intervals from 7 to 60d after IONT. Groups 2–3 received daily i.p. vehicle or DHF (5 mg/kg). Retinal wholemounts were immunolabelled for Brn3a and melanopsin to identify Brn3a$^+$RGCs and m$^+$RGCs, respectively.
*Results:* Optimal neuroprotection was achieved with 5 mg/kg DHF and resulted in TrkB phosphorylation. The percentage of surviving Brn3a$^+$RGCs in vehicle treated rats was 60, 28, 18, 13, 12 or 8% of the original value at 7, 10, 14, 21, 30 or 60d, respectively, while in DHF treated retinas was 94, 70, 64, 17, 10 or 9% at the same time intervals. The percentages of m$^+$RGCs diminished by 7d–13%, and recovered by 14d–38% in vehicle-treated and to 48% in DHF-treated retinas, without further variations.
*Conclusions:* DHF neuroprotects Brn3a$^+$ RGCs and m$^+$ RGCs; its protective effects for Brn3a$^+$RGCs are maximal at 7 days but still significant at 21d, whereas for m$^+$RGCs neuroprotection was significant at 14d and permanent.

## 1. Introduction

Adult mammalian central nervous system (CNS) diseases or injuries proceed with neuronal loss, which is frequently progressive and courses with increasing functional deficits. A great interest has attracted the study of neuronal death and its possible prevention, known as neuroprotection. One part of the CNS particularly suited for neuroprotection studies is the retina, a peripheral extension of our central nervous system that senses luminous information and analyzes and conveys it to the brain through the retinal ganglion cell (RGC) axons. This allows perception of the visual stimuli which is mediated by image-forming visual functions, and a number of unconscious autonomic functions that are largely dependent on nonimage-forming visual functions (Van Gelder and Buhr, 2016; Vidal-Villegas et al., 2020).

RGCs and their axons can be lesioned and as a consequence visual information acquired in the retina is lost. The responses of RGCs to

*Abbreviations:* Intraorbital Optic Nerve Transection (IONT), Intraperitoneal (i.p.); 7,8-Dihydroxyflavone (DHF), Central Nervous System (CNS); Retinal Ganglion Cell (RGC), Tropomyosin Related Kinase B (TrkB); Neurotrophin Brain Derived Neurotrophic Factor (BDNF), Optic Nerve (ON); melanopsin expressing retinal ganglion cells (m$^+$RGCs), Brn3a expressing retinal ganglion cells (Brn3a$^+$RGCs).

* Corresponding author. Dpto Oftalmología, Facultad de Medicina, Universidad de Murcia, IMIB-Arrixaca. Campus de CC de la Salud, 30120, El Palmar, Murcia, Spain.
*E-mail address:* manuel.vidal@um.es (M. Vidal-Sanz).

https://doi.org/10.1016/j.exer.2021.108694
Received 1 April 2021; Received in revised form 26 May 2021; Accepted 1 July 2021
Available online 8 July 2021
0014-4835/

retinal injury have been studied using a wide variety of animal models including spontaneous (Pérez de Lara et al, 2014, 2019) or induced chronic (Vidal-Sanz et al, 2015b, 2017) or acute (Gallego-Ortega et al., 2020; Rovere et al., 2016; Wang et al., 2017) ocular hypertension, or NMDA mediated excitotoxicity (Vidal-Villegas et al., 2019a). A classic model involves lesion of the optic nerve (ON) which causes axotomy of the entire RGC population. This model has been used to study the responses of adult rodent RGCs (Aguayo et al., 1987; Vidal-Sanz et al., 2017; Villegas-Perez et al., 1988) following intraorbital optic nerve transection (IONT) (Agudo et al, 2008, 2009; Lindqvist et al., 2004; McKerracher et al., 1990) or crush (Agudo et al, 2008, 2009; Parrilla-Reverter et al, 2009a, 2009b), and results in selective loss of RGCs that has been characterized in detail, in terms of severity and time course (Nadal-Nicolás et al., 2015b; Parrilla-Reverter et al, 2009a, 2009b; Rovere et al., 2015; Sánchez-Migallón et al., 2018a, 2018b; Villegas-Pérez et al., 1993), molecular changes (Agudo-Barriuso et al., 2013; Agudo et al, 2008, 2009; McKerracher et al., 1990), morphology (Agostinone et al., 2018), electrophysiological responses (Alarcón--Martínez et al, 2009, 2010), retinal topography (Nadal-Nicolás et al., 2015b) and their response to neuroprotectants (Galindo-Romero et al., 2013b; Lindqvist et al., 2004; Lucas-Ruiz et al., 2019; Osborne et al., 2018; Parrilla-Reverter et al., 2009b; Vidal-Sanz et al, 2000, 2015b, 2017).

The RGC population in rodents is composed of up to 46 different cell types (Baden et al., 2016; Tran et al., 2019) and projects to over 45 different target regions in the brain (Morin and Studholme, 2014). At present, there are several molecular markers that identify large proportions or most of the RGCs (Guymer et al., 2019; Nadal-Nicolás et al., 2014; Rodriguez et al., 2014) including Brn3a (Nadal-Nicolás et al., 2014) and a few that identify specific cell types (Yang et al., 2020), including melanopsin (Galindo-Romero et al., 2013a) and others (Kim et al., 2008; Tran et al., 2019).

Two RGC markers that allow to study in parallel but independently the fate of two RGC populations against retinal injury, are Brn3a and melanopsin. In adult rats, Brn3a is expressed by the vast majority of the RGC population (≈96%) (Nadal-Nicolás et al, 2014, 2015a, 2015b) (Brn3a$^+$RGCs) responsible for image-forming visual functions, while melanopsin is expressed in a small subset of RGCs (m$^+$RGCs; ≈2.5%) named intrinsically photosensitive RGCs (Galindo-Romero et al., 2013a; Nadal-Nicolás et al., 2014) and are mainly responsible for nonimage-forming visual functions (Vidal-Villegas et al., 2020). Previous studies, have documented that these markers are expressed long term after retinal injury (Agudo-Barriuso et al., 2016; Nadal-Nicolás et al, 2015a, 2015b; Sánchez-Migallón et al, 2011, 2016), and this is important because injured RGCs undergo changes in their morphology, physiological properties and gene expression that renders their identification difficult (Agostinone and Di Polo, 2015; Agudo-Barriuso et al., 2013; Agudo et al, 2008, 2009; Chidlow et al., 2005).

The flavonoid, 7,8-Dihydroxyflavone (DHF) is a potent mimetic of the neurotrophin brain derived neurotrophic factor (BDNF) (Barde et al., 1982) and exhibits neuroprotective properties in several CNS degenerative diseases through activation of the tropomyosin related kinase B (TrkB) receptor through its phosphorylation, internalization and the consequent initiation of downstream survival pathways (Emili et al., 2020; Jang et al., 2010). DHF presents several advantages for its use as neuroprotectant (Jang et al., 2010; Liu et al., 2010) when compared to BDNF (Ochs et al., 2000; Thoenen and Sendtner, 2002; Zhang and Pardridge, 2001), namely; i) because it is lipophilic and of small size (MW 254 gr/mol) when administered systemically, DHF crosses the blood brain barrier (Jang et al., 2010; Liu et al, 2013, 2014; Zhang et al., 2014) while BDNF (27 kDa) does not; ii) the DHF-induced TrkB response is quick, longer and more robust (Liu et al, 2010, 2014) and; iii) DHF has a longer plasma half-life than BDNF (Ochs et al., 2000; Price et al., 2007; Zhang et al., 2014). In addition, DHF it is not toxic when administered acutely or chronically (He et al., 2016; Liu et al., 2010; Seppa et al., 2021).

BDNF has been shown to be the most efficacious neuroprotectant for RGCs in several retinal injury models (Mansour-Robaey et al., 1994; Ortín-Martínez et al., 2014; Valiente-Soriano et al., 2019; Wójcik-Gryciuk et al., 2020), including optic nerve lesions (Almasieh et al., 2012; Di Polo et al., 1998; Galindo-Romero et al., 2013b; Mansour-Robaey et al., 1994; Peinado-Ramón et al., 1996; Sánchez-Migallón et al., 2011, 2016; Vidal-Sanz et al., 2017). Its neuroprotective effects are likely due to the activation of its high affinity receptor TrkB wich is largely present in the adult rat retina (Di Polo et al., 2000; Lindqvist et al, 2002, 2010). However, few studies have examined the neuroprotective effects of DHF in the retina. *In vitro* studies on RGC and RGC5 line cells suggest a protective effect for DHF against excitotoxic and oxidative stress (Gupta et al., 2013). Moreover, DHF prevents *in vitro* high glucose induced apoptosis of human retinal pigment epithelial cells (Yu et al., 2018), and in a zebrafish model of inherited retinal disease, DHF prevents cone photoreceptor loss and ameliorates visual function (Daly et al., 2017). More recently, in vivo studies have shown that DHF protects immature retina against hypoxic-ischemic injury (Huang et al., 2018) and prevents optic nerve degeneration in the congenic neurodegenerative Wolfram syndrome rat model (Seppa et al., 2021). The above-mentioned studies suggest that DHF may prevent retinal injury induced by excitotoxicity, oxidative stress or apoptosis. However, there are no adult in vivo studies examining the potential of DHF to prevent injury-induced RGC death or to investigate its mechanism of action.

In this work, we investigate the response of two different populations of RGCs, the Brn3a- and the melanopsin-expressing RGCs, to IONT and systemic administration of DHF. The purpose of this study is to investigate in adult albino rats: i) if DHF administered systemically affords RGC neuroprotection; ii) What is the optimal neuroprotective dose of DHF; iii) if the DHF neuroprotective effects on the Brn3a$^+$RGC population are long-lasting; iv) if DHF is neuroprotective for m$^+$RGCs? and; v) if the DHF afforded neuroprotection is mediated by activation of the tyrosine kinase receptor B (trkB) signalling pathway. Using an in vivo adult rat model of axonal injury, we report for the first time that systemically administered DHF results in phosphorylation of the TrkB receptor, and in prevention of RGC death, a protection that affects both populations, Brn3a$^+$RGCs and m$^+$RGCs. (Short accounts of this work have been published in abstract format Vidal-Villegas et al., 2019b).

## 2. Material and methods

Because our previous studies on axotomy and neuroprotection were done in adult female SD rats (for review see Vidal-Sanz et al., 2000, 2015b, 2017) for comparison in the present studies we used adult female Sprague-Dawley rats (180–220g) from the animal house of the University of Murcia, that were housed in temperature-controlled rooms with 12 h/12h light/dark cycles and water and food ad libitum. All experiments were approved by the University of Murcia ethical animal studies committee (Codes: A13170110, A13170111), and followed the Spanish and European Union Directives for animal experiments and the ARVO Statement for the Use of Animals in Ophthalmic and Vision Research. Efforts were made to minimize the number of animals employed.

### 2.1. Intraorbital optic nerve transection

Rats were anaesthetized with i.p. ketamine (60 mg/kg bw, Ketolar; Pfizer, Alcobendas, Madrid, Spain) and xylazine (10 mg/kg Rompun; Bayer, Kiel, Germany). In the experimental rats, left intraorbital optic nerve transection (IONT) was performed as described (Vidal-Sanz et al., 1987). In brief, through a superior temporal approach the orbital contents were dissected and the left ON was exposed. The dura sheath was opened longitudinally and the ON was divided close to its origin without damaging the retinal vessels running on the inferomedial aspect of the sheath. At the end of the procedure, subcutaneous bruprenorfin (0.1 mg/kg; Buprex, Schering-Plough, Madrid, Spain) was administered as analgesic, the eye fundus was inspected to assess retinal blood flow, and

an ophthalmic ungüent was applied on both eyes to prevent corneal desiccation (Tobrex®; Alcon S.A., Barcelona, Spain).

### 2.2. Animal groups, experimental design and drug administrion

The animals were divided in three experimental groups. A first group (G1; n = 58) was examined 7d after IONT and used to determine if DHF could prevent IONT-induced RGC death and its optimal dose. A second group (G2; n = 26) was used to investigate if the DHF-afforded neuroprotection produced retinal TrkB phosphorylation, and in this group naïve (n = 2) or experimental (n = 24) rats were examined 1(n = 8), 3(n = 8) or 7(n = 8) d after IONT. A third group (G3; n = 96) investigated if DHF-afforded neuroprotection for Brn3a$^+$RGCs and m$^+$RGCs lasted for long periods of time; these rats were examined 7(n = 16), 10(n = 16), 14 (n = 16), 21(n = 16), 30(n = 16) or 60(n = 16) days after IONT. Following IONT rats received daily i.p injections of: i) vehicle (0.9% NaCl containing 1% DMSO) (n = 16) or 1(n = 6), 2(n = 6), 4(n = 6), 5(n = 12), 10(n = 6) or 25(n = 6) mg/kg DHF (7,8-Dihydroxyflavone hydrate, Sigma D5446, Merck Life Science SL, Madrid, Spain) diluted in vehicle for G1; ii) vehicle or 5 mg/kg DHF for G2 and G3. All treatments were administered between 10 and 11 (a.m.). Animals from groups with 10d or longer survival intervals were examined routinely for general appearance and weekly for weight loss.

### 2.3. Animal processing and preparation of the retinas for immunocytochemistry

Animals were sacrificed with an i.p. overdose of barbituric (Dolethal, Vetoquinol®, Especialidades Veterinarias S.A., Madrid, Spain) and perfused through the heart with saline and 4% paraformaldehyde in 0.1M PBS (phosphate buffer saline). Both eyes were enucleated, the position of the superior pole was marked with a 6/0 silk suture, and both retinas were dissected and prepared as flattened wholemounts, postfixed for an additional hour in fixative and rinsed in PBS (Vidal-Villegas et al., 2019a).

### 2.4. Immunocytochemistry for Brn3a and melanopsin

Experimental (left IONT) and contralateral (intact right) retinas from G1 were immunolabelled for Brn3a, whereas retinas from G3 were doubly immunolabelled for Brn3a and melanopsin, as described (Vidal-Villegas et al., 2019a). In brief, retinas were incubated overnight in a PBS 0.5% Triton X-100 (Tx) solution containing primary antibodies against Brn3a and melanopsin (goat anti-Brn3a, 1:500 dilution, C-20 Santa Cruz Biothechology, Heidelberg, Germany and rabbit anti melanopsin, 1:500 dilution, PAI-780, Invitrogen, Thermo Fisher Scientific, Alcobendas, Madrid, Spain), rinsed in PBS and incubated 2h with a mixture of secondary antibodies (1:500 in PBS-2% Tx, donkey anti goat Alexa 488 and donkey anti rabbit Alexa 647; Molecular Probes Thermo-Fisher, Madrid, Spain), rinsed in PBS, mounted vitreal side-up with antifading solution on subbed slides and covered with a coverslip sealed with nail polish. Slides were kept refrigerated until examination under the fluorescence microscope.

### 2.5. TrkB phosphorylation studies. Western blot analysis

In the second group (G2; n = 26), naïve (n = 4) or experimental (n = 24) retinas were freshly dissected and frozen in dry ice. Retinas were homogenized in 300 μL lysis buffer (PRO-PREPTM Protein Extraction Solution, Intron Biotechnology Inc. Cat. No. 17081) and the amount of protein was determined using a bicinchoninic acid test (BCA, B9643 Sigma-Aldrich) with cupric sulfate (CuSO4, 7758-98-7 Sigma-Aldrich). Protein pool samples, composed by four individual samples of each retina, were run on 1% SDS-PAGE, transferred to a nitrocellulose membrane and incubated with the following protein specific antibodies overnight at 4 °C: Rabbit anti-phospho TrkB 1:1000 (Abcam, ab228507), and rabbit anti-TrkB 1:1000 (Cell Signalling, 80E3). Secondary detection was carried out with donkey anti-rabbit antibody conjugated to horseradish peroxidase (1:5000; Santa Cruz Biotechnologies) and visualized by chemiluminescence (Enhanced Chemo Luminiscence [ECL]; Amersham GE Healthcare Europe GmBH). The signal was acquired with an Image LAS 500 (Amersham GE Healthcare Europe GmbH). Westerns were replicated three times and the protein concentration was calculated considering the intact retinas as 100%. As a loading control, β-actin (mouse anti- β Actin HRP conjugated 1:5000, Abcam ab49900) detection was carried out.

### 2.6. Assessment of retinal ganglion cell survival

#### 2.6.1. Microscopic analysis, image acquisition and whole-mount reconstruction

Whole-mount image reconstructions of immunolabelled retinas were obtained as described (Gallego-Ortega et al., 2020). In brief, using epifluorescence microscopy Leica DM6-B (Leica Microsytems, Wetzlar, Germany), retinas were photographed (x10) in a raster-scan manner without overlap or gap between images. Before each image acquisition, individual frames were manually focused under specific filters to allow identification of Brna3a$^+$RGCs or m$^+$RGCs, respectively.

#### 2.6.2. Image analysis of retinal wholemounts. Cell counts

Quantification of Brn3a$^+$RGCs and m$^+$RGCs was performed as described (Galindo-Romero et al., 2013a; Vidal-Villegas et al., 2019a). For Brn3a$^+$RGCs, wholemount reconstructs were processed to obtain automatic counts of the total number of Brn3a$^+$RGCs for each retina. The m$^+$RGCs were dotted manually on the photomontages and quantified with the aid of the graphic editing software Adobe Photoshop CS8.01 (Adobe Systems, Inc., San José, CA, USA).

#### 2.6.3. Topological maps

The distribution of RGCs within each retina was examined using isodensity or neighbor maps for the population of Brn3a$^+$RGCs or m$^+$RGCs, respectively (Galindo-Romero et al., 2013a; Nadal-Nicolás et al., 2014). Brn3a$^+$RGC isodensity maps were constructed using the cell densities obtained for each individual frame and presented with a color scale from 0 (purple) to ≥ 2500 (red) RGCs/mm$^2$. m$^+$RGCs neighbor maps depict their retinal distribution, and each dot represents individual cells with a color revealing the number of neighboring m$^+$RGCs within a radius of 0.276 mm from 0 to 4 (purple) to ≥ 32–35 (red) neighbors. Isodensity and neighbor maps were constructed with Sigmaplot (SigmaPlot 9.0 for Windows; Systat Software, Inc., Richmond, CA, USA).

### 2.7. Statistics

Total numbers of labelled RGCS with Brn3a or melanopsin per retina were introduced in excel worksheet to obtain histograms and to analyze differences in cell survival between different groups. RGCs numbers are expressed as mean ± standard deviation (SD) of the mean. Statistical comparisons between different groups were done use one-way analysis of variance (ANOVA- Tukey's Post hoc tests), and comparisons between two groups were done use Mann-Whitney test with the software Graph Pad Prism. A value of $p < 0.05$ was considered statistically significant.

## 3. Results

### 3.1. DHF administered systemically neuroprotects Brn3a$^+$RGCs

This group (G-1; n = 58) received daily i.p. vehicle or DHF at different doses and was analyzed at 7d to determine Brn3a$^+$RGC survival. Total numbers of Brn3a$^+$RGCs in the untouched right eye retinas (n = 58) were similar between different subgroups (One way Anova test, p > 0,05) and thus, were pooled together (Table 1). When Brn3a$^+$RGC

**Table 1**
Numbers of Brn3a$^+$RGCs following IONT and increasing doses of DHF.

| | | Left Retinas | | | | | | |
|---|---|---|---|---|---|---|---|---|
| | | DHF concentration | | | | | | |
| Brn3a$^+$ RGCs | Right retinas n = 58 | Vehicle n = 16 | 1 mg/kg n = 6 | 2 mg/kg n = 6 | 4 mg/kg n = 6 | 5 mg/kg n = 12 | 10 mg/kg n = 6 | 25 mg/kg n = 6 |
| Mean | 77,781 | 47,457[a,b,c] | 49,040[a,b,c] | 46,339[a,b,c] | 68,128[b] | 74,268[b] | 58,017[a,b,c] | 55,935[a,b,c] |
| SD | 6371 | 9088 | 1502 | 7079 | 5213 | 5942 | 3058 | 10,227 |
| % | 100% | 61% | 63% | 60% | 88% | 95% | 76% | 72% |

Mean ± standard deviation (SD) of the numbers of Brn3a$^+$RGCs in the right contralateral and experimental retinas analyzed 7 days after left IONT. Animals received daily i.p. treatment with Vehicle or DHF at 1, 2, 4, 5, 10 or 25 mg/kg.
[a] Significant when compared to retinas treated with Vehicle (Mann Whitney test, $p < 0.001$).
[b] Significant when compared to Right retinas (Mann Whitney test, $p < 0.001$).
[c] Significant when compared to retinas treated with 4 or 5 mg/kg (Mann Whitney test, $p < 0.05$).

densities were compared between DHF- and vehicle-treated retinas, treatment with DHF at a dose of 1, 2, 10 or 25 mg/kg did not show significant RGC rescue effects (one way, Anova test, $p > 0.05$) (Fig. 1, Table 1). However, significant protection of Brn3a$^+$RGCs was observed in rats treated with DHF at 4 or 5 mg/kg ($p < 0.001$) (Table 1, Fig. 1). Vehicle-treatment resulted in death of ≈39% of the original Brn3a$^+$RGC population whereas DHF-treatment (5 mg/kg) resulted at 7d in the survival of ≈95% Brn3a$^+$RGCs, documenting that systemic DHF prevents IONT-induced Brn3a$^+$RGC loss (Table 1). The protection obtained with 5 mg/kg DHF yielded best results and thus, this amount was considered optimal and used for the other groups.

### 3.2. Systemic DHF administration results in retinal TrkB activation

This second group (G-2) assessed the expression of TrkB and phosphorylated TrkB in the left retinas treated with DHF or vehicle at 1, 3 or 7 d after IONT (n = 4/group), and compared it with the expression in naïve retinas (n = 4) by Western Blotting. The amount of TrkB in experimental retinas decreases as the time post-lesion increases, paralleling the progressive loss of the RGC population. Comparing between DHF and vehicle-treated groups, there were no differences between normalized p-TrkB/TrkB protein expression at 1 and 3 d, but the phosphorylation levels of TrkB were significantly higher at 7 d in DHF-treated retinas (One way, Anova test, $p < 0.05$), a time interval when DHF afforded neuroprotection was maximal and resulted in survival of almost the entire RGC population (Fig. 2).

### 3.3. DHF blunts IONT-induced Brn3a$^+$RGC loss and affords long-lasting protection

This third group (G3, n = 96) investigated short and long term DHF-afforded protection of Brn3a$^+$RGCs. General appearance of rats surviving 10 days or longer in this group was normal without weight loss. Examined under fluorescence microscopy (Fig. 3), the control right retinas showed a normal distribution of Brn3a$^+$RGCs with greatest densities in the superior temporal quadrant, as described (Nadal-Nicolás et al., 2014) (Figs. 3 and 4A,B). The left experimental vehicle- or DHF-treated retinas showed Brn3a$^+$RGC losses which were much less apparent in the 4–5 mg/kg DHF-treated retinas (Figs. 3 and 4). In the vehicle-treated retinas, Brn3a$^+$RGCs diminished by 7d to approximately 60% of their contralateral uninjured population. This loss further progressed significantly to 12% at 21d, with no further significant losses by 30-60d after IONT (Table 2. Fig. 5). However, significantly greater total numbers of Brn3a$^+$RGCs were found in the DHF treated retinas when compared to vehicle at 7, 10, 14 or 21d, but not at 30 or 60d (Table 2. Figs. 3 and 4). Thus, DHF treatment hindered the abrupt exponential phase of Brn3a$^+$RGC cell loss that follows IONT and significant neuroprotective effects were maintained up to 21 days (Figs. 3 and 4).

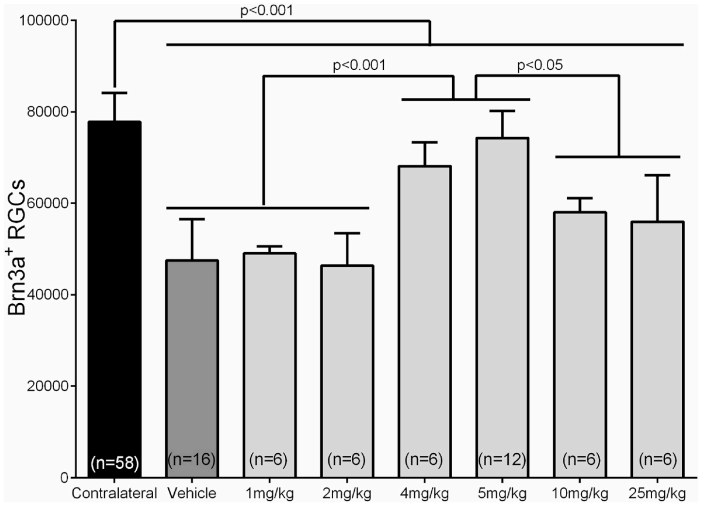


**Fig. 1.** Effects of different doses of DHF on the survival of axotomized Brn3a$^+$ RGCs. **A:** Bar graph showing mean total densities ±SD of Brn3a$^+$RGCs in contralateral intact (right) retinas, and in experimental left retinas of rats treated daily with vehicle or DHF at 1, 2, 4, 5, 10 or 25 mg/kg and analyzed 7 days after left IONT. Optimal protection was obtained with daily i.p. administration of 4 or 5 mg/kg of DHF. Groups were compared with ANOVA tests, and significant differences between groups are indicated.

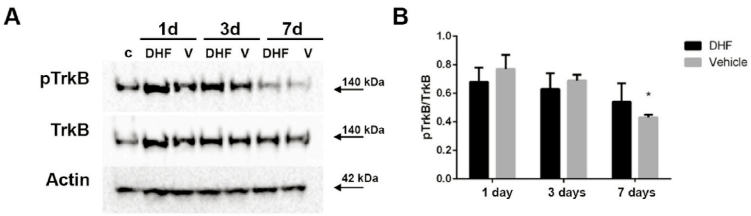


**Fig. 2.** Western Blotting. **A:** Representative Western Blot images of retinal extracts from naïve (c) and from left injured retinas daily treated i.p. with vehicle (V) or 5 mg/kg DHF (DHF) analyzed at 1, 3 or 7d after IONT. pTrkB, TrkB and Actin protein expression were analyzed. **B:** Bar graph of the quantitative analysis of the above shown values. Naïve retinas were considered 1.0 and normalized pTrkB/TrkB is shown in B. The DHF-treated group had higher levels of normalized pTrkB/TrkB at 7 days after IONT than the vehicle-treated group (mean ± SD; One way, Anova test, *$p < 0.05$, $n = 4$ retinas per group).

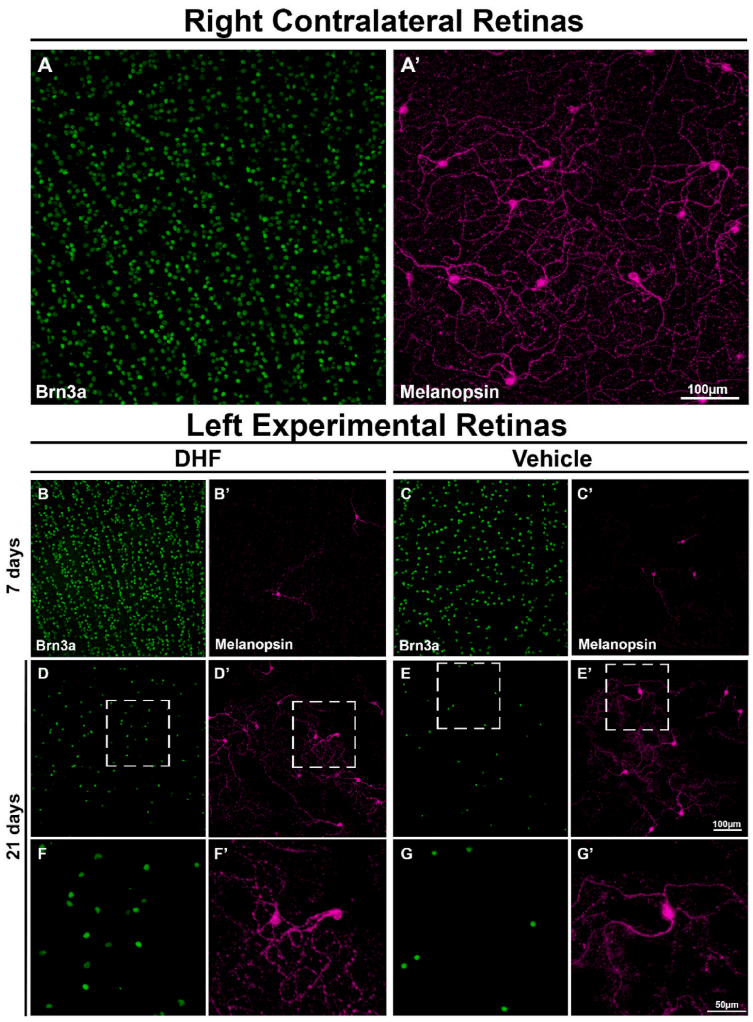


**Fig. 3.** Long-term neuroprotection of axotomized *Brn3a*$^+$RGCs and *m*$^+$*RGCs* by systemic administration of DHF. Fluorescence micrographs showing a representative intact contralateral right retina (A,A′) photographed with different filters to identify Brn3a$^+$RGCs (A) and melanopsin$^+$RGCs (A′), and the experimental left retinas (B-E′) with IONT of animals that were treated daily with i.p. 5 mg/kg DHF (B,B′, D,D′) or vehicle (C, C′, E,E′), and analyzed 7 (B–C′) or 21 (D-E′) days later. While the staining of Brn3a is nuclear, melanopsin appears within the soma and primary dendrites located in the plane of focus. Note the larger number of Brn3a$^+$RGCs surviving at 7 (B,C) or 21 (D,E) days in retinas treated with DHF as compared to those treated with vehicle. Similarly, more melanopsin$^+$RGCs survive in the DHF treated as compared to the vehicle treated retinas (D′,E′). F, F′, G and G′ are high power images of inserts in D, D′, E and E′, respectively, showing the different nuclear or cytoplasmic staining of Brn3a (D, E) or melanopsin (D′, E′) and illustrating the lack of colocalization of these RGC markers.

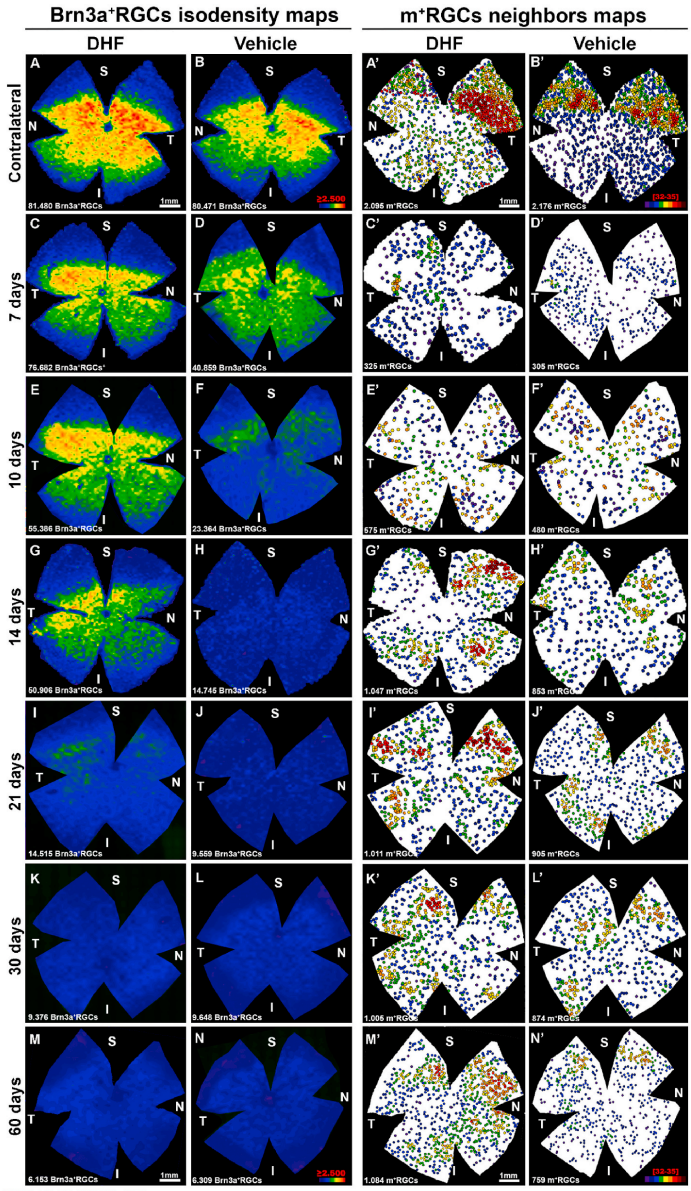


**Fig. 4.** Isodensity and Neighbor maps showing Brn3a$^+$RGCs and melanopsin$^+$RGCs topography. Representative isodensity (left columns, A,B) and neighbor (right columns, A′,B′) maps showing the topographical distribution of Brn3a$^+$RGCs and m$^+$RGCs, respectively, from two untouched Contralateral retinas of a rat treated with DHF (A,A′) or vehicle (B,B′), or from the IONT eye retinas treated with 5 mg/kg DHF or Vehicle and analyzed at 7 (C-D′), 10 (E-F′), 14 (G-H′), 21 (I-J′), 30 (K-L′) or 60 (M-N′) days. Isodensity maps illustrate the neuroprotective effects of DHF (first column) when compared to vehicle (second column) for the Brn3a$^+$RGCs. These same retinas were also examined for the distribution of m$^+$RGCs and the neighbor maps illustrate that, following a transient down-regulation of melanopsin expression, DHF afforded neuroprotection (third column) when compared to vehicle (fourth column) that is evident by 14 days and persistent. Below each map is indicated the total number of Brn3a$^+$RGCs or m$^+$RGCs counted for that retina. S: superior, N: nasal, I inferior, T, temporal. Isodensity map color scale from 0 RGCs/mm$^2$ (purple) to ≥2500 RGCs/mm$^2$ (red). Neighbor maps color scale from 0 to 4 (purple) to ≥32–35 (red) neighbors in a radius of 0.276 mm.



### 3.4. *DHF blunts IONT-induced loss of m$^+$RGCs and affords permanent protection*

Retinas from G3 group were also examined for m$^+$RGC survival and their response to DHF treatment (Fig. 3). The distribution of m$^+$RGCs was assessed with neighbor maps which illustrate the typical distribution of these cells in control right retinas (Fig. 4 A′,B′) with greater numbers in the superior retina, as described (Galindo-Romero et al., 2013a; Nadal-Nicolás et al., 2014). Shortly after IONT, the vehicle-treated retinas showed diminutions of total numbers of m$^+$RGCs that were maximal at 7-10d. By this time the numbers of m$^+$RGCs amounted to ≈13%–21% of their contralateral intact retinas. However,

**Table 2**
Long term survival of Brn3a$^+$RGCs and m$^+$RGCs after left IONT in Vehicle- or DHF-treated rats.

| | *Right retinas* | *Left retinas* | | | | | | |
|---|---|---|---|---|---|---|---|---|
| | *Time after IONT* | | | | | | | |
| *Brn3a$^+$RGCs* | | Contralateral n = 48 | *7 days n=8* | 10 days n = 8 | 14 days n = 8 | 21 days n = 8 | *30 days n=8* | 60 days n = 8 |
| **Vehicle** | Mean | 81,457 | 48,019[b] | 22,464[b,c] | 14,001[b,c] | 10,960[b,c] | 8,455[b] | 6,822[b] |
| | SD | 1158 | 8704 | 4983 | 3796 | 2241 | 2250 | 2552 |
| | % | 100 | 59 | 28 | 17 | 13 | 10 | 8 |
| **DHF** | Mean | 81,112 | 75,094[a,b] | 57,372[a,b,c] | 52,306[a,b] | 14,194[a,b,c] | 8,334[b,c] | 6,935[b,c] |
| | SD | 1298 | 4878 | 6208 | 3795 | 2274 | 1468 | 1109 |
| | % | 100 | 96 | 71 | 65 | 17 | 10 | 8 |
| **m$^+$RGCs** | | | | | | | | |
| **Vehicle** | Mean | 2094 | 299[b] | 497[b,c] | 864[b,c] | 922[b] | 896[b] | 771[b] |
| | SD | 58 | 63 | 81 | 88 | 122 | 67 | 105 |
| | % | 100 | 14 | 24 | 41 | 44 | 43 | 37 |
| **DHF** | Mean | 2101 | 306[b] | 522[b,c] | 1,102[a,b,c] | 1077[a,b] | 1,061[a,b] | 1,017[a,b] |
| | SD | 89 | 60 | 92 | 218 | 115 | 203 | 113 |
| | % | 100 | 15 | 25 | 52 | 51 | 50 | 48 |

Numbers of Brn3a$^+$RGCs and m$^+$RGCs (mean ± SD; Standard Deviation) in contralateral and experimental retinas analyzed 7, 10, 14, 21, 30 or 60 days after IONT of the left eye and daily i.p. treatment with Vehicle or DHF (5 mg/kg).
[a] Significant differences when compared with vehicle-treated retinas, at the same time intervals ($p < 0.05$).
[b] Significant differences when compared with Contralateral retinas (Mann Whitney test, $p < 0.001$).
[c] Significant differences when compared with the previous time interval ($p < 0.05$).

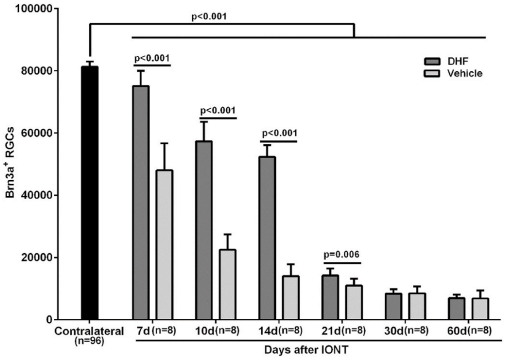


**Fig. 5.** Long-term neuroprotection of Brn3a$^+$RGCs with systemic DHF. Bar graph showing the mean total numbers ± SD of Brn3a$^+$RGCs in contralateral (right intact) retinas, and in experimental left retinas of rats treated i.p. daily with 5 mg/kg DHF or Vehicle and analyzed 7, 10, 14, 21, 30 or 60 days after intraorbital optic nerve transection (IONT) of the left eye. Statistically significant protection was obtained with DHF, when compared to vehicle, up to 21 days. Groups were compared with ANOVA tests, and significant differences between groups are indicated.

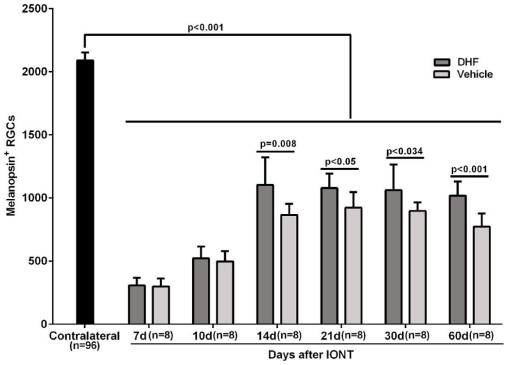


**Fig. 6.** Long-term neuroprotection of m$^+$RGCs with systemic DHF. Bar graph showing the mean total numbers ±SD of m$^+$RGCs in contralateral (right) intact retinas, and in experimental left retinas of rats treated i.p. daily with 5 mg/kg DHF or Vehicle and analyzed 7, 10, 14, 21, 30 or 60 days after left IONT. Following a transient downregulation of melanopsin expression, both in Vehicle- and DHF-treated retinas at 7 and 10d, DHF-treated retinas showed a significant rescue of m$^+$RGCs that was first evident by 14 days and persisted for the time period of the study. Groups were compared with ANOVA tests, and significant differences between groups are indicated.

these numbers increased to ≈38% by 14d and remained without further variations at longer survival intervals (Table 2, Fig. 6), indicating that the decreased numbers of m$^+$RGCs in the left retinas are due, at least in part, to melanopsin downregulation, in addition to m$^+$RGC death.

The DHF-treated retinas also showed an initial apparent loss of m$^+$RGCs that was also maximal 7-10d after IONT, and at these times there were no significant differences in m$^+$RGC numbers between the vehicle- and DHF-treated left retinas. However, in the DHF-treated retinas, by 14d the m$^+$RGCs increased to ≈48% of the original population and this was significantly greater when compared to the vehicle-treated group, indicating that DHF also protects m$^+$RGCs. Moreover, total numbers of m$^+$RGCs remained without further decreases at increasing survival intervals of up to 60d, suggesting that DHF-afforded protection was permanent (Figs. 4 and 6).

### 3.5. Responses of Brn3a$^+$ RGCs versus m$^+$ RCCs to IONT and DHF

Following IONT, the experimental vehicle-treated retinas showed important losses of Brn3a$^+$RGCs and m$^+$RGCs (Table 2, Figs. 3–6) that by 14d amounted to 82% and 64%, respectively. The loss of Brn3a$^+$RGCs progressed further to 21d whereas m$^+$RGCs did not. Moreover, the IONT-induced loss of m$^+$RGCs was considerably smaller than that of Brn3a$^+$RGCs. For example, 60 days after IONT, the proportion of surviving m$^+$RGCs (37%) was almost five times greater than Brn3a$^+$RGCs (8%), indicating a greater resilience for m$^+$RGCs against IONT (Table 2).

Retinal distribution illustrates that in vehicle-treated rats, IONT induced loss of Brn3a$^+$RGCs and m$^+$RGCs was diffuse throughout the retina and more pronounced on the superior retina but without a typical geographical pattern for both populations (Fig. 4), as has been shown in other types of retinal injuries such as ocular hypertension or transient

ischemia (Vidal-Sanz et al., 2015a, 2017).

When the retinal distribution of Brn3a$^+$RGCs or m$^+$RGCs in the vehicle- or DHF-treated retinas was compared at similar time intervals, the DHF-treated retinas showed a greater survival of both populations. The numbers of Brn3a$^+$RGCs were greater at early time intervals up to 21d, and the numbers of m$^+$RGCs were greater from 14 days onward (Fig. 4).

Overall, when comparing the responses of the m$^+$RGC with the Brn3a$^+$RGC population, the loss of m$^+$RGCs was less abrupt (38% vs 82% at 14d) and ended earlier (14d vs 21d). DHF-afforded protection for Brn3a$^+$RGCs lasted up to 21d, and was permanent for m$^+$RGCs.

## 4. Discussion

DHF has been shown to mimic many of the neuroprotective effects of BDNF in several CNS injuries or disease models through activation of the TrkB receptor (Emili et al., 2020; Jang et al., 2010), but whether DHF could rescue in vivo injured RGCs had not been investigated before. In the present studies, we used modern tools developed in our laboratory to identify, quantify and map the responses in adult rats of two different populations of RGCs, Brn3a$^+$RGCs and m$^+$RGCs, to IONT and systemic treatment with vehicle or DHF. We report for the first time that DHF administered systemically: i) may prevent IONT-induced Brn3a$^+$RGC loss; ii) induces optimal rescuing effects with daily i.p. 5 mg/kg DHF; iii) results in phosphorylation of the TrkB receptor in the retina; iv) rescues a substantial proportion of Brn3a$^+$RGCs, an effect that persists for up to 21 days after IONT, and; v) diminishes m$^+$RGC loss, an effect that appears permanent.

### 4.1. DHF afforded Brn3a $^+$ RGC survival

In adult rodents, IONT results in a predictable rapid and massive loss of RGCs that tappers off within the first weeks, followed by a slow protracted loss that proceeds during the following months (Nadal-Nicolás et al., 2015b; Rovere et al., 2015; Villegas-Pérez et al., 1993). The use of several neuroprotectants to blunt such a rapid cell loss has documented that rescue of injured RGCs is possible (Di Polo et al., 1998; Galindo-Romero et al., 2013b; Lucas-Ruiz et al., 2019; Mansour-Robaey et al., 1994; Parrilla-Reverter et al., 2009b; Peinado-Ramón et al., 1996; Sánchez-Migallón et al., 2011, 2016; Vidal-Sanz et al., 2000). Here we document that daily i.p. treatment with DHF at concentrations of 4 or 5 mg/kg resulted in maximal protection, but treatment with other amounts of 1, 2, 10 or 25 mg/kg were not significantly different from vehicle-treatment. Thus, as shown *in vitro* for RGC-5 cells (Gupta et al., 2013), it is tempting to suggests that DHF for small amounts protects in a dose-dependent manner, although higher doses resulted in decreased protection and this may be explained by an overactivation of the low affinity TrkA receptor (Ichim et al., 2012; Kowiański et al., 2018). Because the protection obtained with 5 mg/kg DHF yielded best results (i.e., the survival of ≈95% Brn3a$^+$RGCs 7d after IONT), this dose was used for the rest of the study. Comparable neuroprotection at similar time intervals up 14 days following complete optic nerve injury was documented in previous studies from this Laboratory with a single intravitreal administration of BDNF (Galindo-Romero et al., 2013b; Parrilla-Reverter et al., 2009b; Peinado-Ramón et al., 1996; Sánchez-Migallón et al, 2011, 2016). Moreover, DHF-afforded protection of Brn3a$^+$RGCs was maintained for up to 21d after IONT, an interesting effect considering previous studies suggesting that TrkB receptor downregulation following retinal injury may be responsible for the lack of a longer neuroprotection (Di Polo et al., 1998; Osborne et al., 2018).

### 4.2. m$^+$RGCs respond to DHF afforded protection

It is known that m$^+$RGCs are particularly resilient to ON injury (Cui et al., 2015; Pérez de Lara et al., 2014; Robinson and Madison, 2004). Indeed, recent studies that have compared the responses of m$^+$RGCs to those of the population of Brn3a$^+$RGCs have shown that m$^+$RGCs are more resilient to light induced phototoxicity (García-Ayuso et al., 2017), acute ocular hypertension (Rovere et al., 2016), NMDA-induced excitotoxity (Vidal-Villegas et al., 2019a) or ON injury (Nadal-Nicolás et al, 2015a, 2015b; Sánchez-Migallón et al., 2018a). Our present studies confirm previous findings (see Fig 11 of Nadal-Nicolás et al., 2015a) and add new data concerning the response of m$^+$RGCs to IONT and DHF afforded neuroprotection. For example, after IONT and vehicle treatment, our results show by 60d a proportion of surviving m$^+$RGCs (37%) approximately fivefold the proportion of surviving Brn3a$^+$RGCs (≈8%) (Table 2), confirming its greater resistance to axotomy.

We also show that following IONT there is a transient loss of m$^+$RGCs that recovers by 14 days. This agrees with previous studies from this Laboratory showing that following optic nerve injury (Nadal-Nicolás et al., 2015a), light induced retinal damage (García-Ayuso et al., 2017), acute ocular hypertension (Rovere et al., 2016) or NMDA-induced excitotoxicity (Vidal-Villegas et al., 2019a) the adult rat retina exhibits a transient downregulation of melanopsin expression.

In addition, we document that in the DHF-treated group there was a substantial rescue of m$^+$RGCs when compared to the vehicle-treated group, by 14d survived 53% vs 41% of the original population (Table 2). Such DHF afforded neuroprotection is underscored by the observation that persisted for up to 60 days, the longest time point examined in this study.

### 4.3. Systemic DHF results in TrkB activation in the retina

Although the precise mechanisms implicated in the pathogenesis of IONT-induced RGC death are not completely understood (Agudo-Barriuso et al., 2013; Agudo et al, 2008, 2009), previous studies indicate that following IONT the loss of RGCs is mainly due to apoptosis (Almasieh et al., 2012; Kerrigan, 1997; Mansour-Robaey et al., 1994; Sánchez-Migallón et al, 2011, 2016). Indeed, a detailed quantitative study of the co-expression of the nuclear vital marker Brn3a and caspase-3 documented that at least 50% of the axotomy-induced RGC death was apoptotic (Sánchez-Migallón et al., 2016), and this could be prevented, at least in part, with the intravitreal administration of BDNF or an antiapoptotic compound, a caspase 3 inhibitor (Z-DEVD-fmk) (Sánchez-Migallón et al., 2016). In the present studies we find that DHF, a BDNF-mimetic, prevents axotomy-induced RGC loss. Moreover, because the retinas treated with DHF showed at 7d both significantly increased RGC survival and phosphorylation of TrkB (pTrkB) it is tempting to suggest that DHF-afforded protection is associated with pTRkB (Patapoutian and Reichardt, 2001). Thus, because following systemic administration of DHF, TrkB becomes phosphorylated, it is likely that DHF reaches the retina and activates TrkB.

### 4.4. Limitations of present studies

We rationalized that because previous work in our Lab documented that BDNF administration prevented axotomy-induced apoptotic RGC loss (Sánchez-Migallón et al., 2016), the BDNF-mimetic, DHF, could have a similar effect, and such presumption agrees with our present findings. However, future studies are needed to determine which of the following three main signalling pathways that may be activated following TrkB activation: i) phosphatidylinositol 3-kinase/protein kinase B (PI3K/Akt); ii) mitogen activated protein kinases extracellular signal regulated kinases 1 and 2 (MAPK/ErK; ErK1/2), or; iii) phospholipase C-γ (PLC-γ), are responsible for neuroprotection of RGCs after IONT. Moreover, because of the diversity in RGC types and their idiosyncratic responses to injury and neuroprotection, it remains to be determined which of these survival promoting pathways is responsible for the rescue of Brn3a$^+$RGCs and m$^+$RGCs observed in the present studies.

At present we ignore if rescued RGCs, that still account for a very

large proportion of RGCs by 14 days, have their functional and morphological properties intact, as documented in mice for certain types of resilient mice RGCs after intraorbital optic nerve crush (Tran et al., 2019). Thus, it would be interesting to analyze responses in the axotomized DHF-treated versus axotomized vehicle-treated retinas by recording full field ERGs and focusing on the scotopic threshold response which is thought to the largely mediated by RGC activity (Alarcón-Martínez et al., 2009, 2010; Salinas-Navarro et al., 2009; Gallego-Ortega et al., 2020).

A common need to many chronic neurological disorders cursing with unknown mechanisms of neuronal death is the identification of neuroprotective agents that could slow or prevent such irreplaceable neuronal loss (Chidlow et al., 2007; Guymer et al., 2019; Vidal-Sanz et al., 2017). The rationale being that neuroprotectants could act on a number of death pathways and thus provide a putative treatment irrespective of the mechanisms of cell loss. Our present results point to DHF as a promising compound that could eventually be translated from bench- to bed-side. The main arguments in favour of this statement are: i) DHF prevents oxidative stress (Zhang et al., 2009) which is a common mechanism of cell loss in retinal diseases; ii) DHF is a potent BDNF mimetic (Jang et al., 2010) that has shown neuroprotective effects in a number of *in vitro* and in vivo animal models of central nervous system diseases or injuries, including the retina (for review see Table 1 of Emili et al., 2020), and; iii) DHF is a selective TrkB agonist with a number of pharmacokinetic properties that make it advantageous for its use as neuroprotectant (see introduction) including its capacity to cross the blood brain barrier when administered systemically, its potent and long lasting activation of the TrkB receptor and its apparent lack of toxicity (Zhang et al., 2014; Liu et al., 2014; He et al., 2016).

Neuroprotection studies in the retina are presently hampered by several limitations, including; the need to identify individual types of RGCs and further understand their responses to injury and protection, and the need to design protective strategies that impinge on various injury activated death pathways. There is the need to further understand the responses of RGCs to axotomy and protection. The rodent retina has probably over 46 different types of RGCs (Baden et al., 2016; Rheaume et al., 2018; Sanes and Masland, 2015; Tran et al., 2019; VanderWall et al., 2020), and such RGC diversity requires a detailed understanding of the responses of each type to injury and protection. This is underscored by recent studies (Agudo-Barriuso et al., 2016; Christensen et al., 2019; Ou et al., 2016; Puyang et al., 2017; Rovere et al., 2016; Tran et al., 2019; Valiente-Soriano et al., 2015a, 2015b; VanderWall et al., 2020; Vidal-Sanz et al., 2015a, 2015b; Yang et al., 2020) including the present one, indicating that specific types of RGCs have idiosyncratic responses to injury and protection. Moreover, $m^+$RGCs have attracted a great interest due to their idiosyncratic responses, including their capacity to resist retinal injuries. Indeed, the vast majority of RGCs resistant to intraorbital optic nerve crush in adult pigmented mice correspond to the $m^+$RGCs type, including all subtypes (M1-M6) (see Fig. 3H in Tran et al., 2019). One possible explanation for such resilience is the upregulation of a specific sets of genes. For instance, $m^+$RGCs upregulate Thrombospondin 1 for up to 14 days after lesion that could be implicated in $m^+$RGC resilience, in addition to the expression of Opn4 (Tran et al., 2019).

Our studies rely on immunocytochemical identification of the nuclear marker Brn3a or the cytosolic photopigment melanopsin, to identify $Brn3a^+$RGCs or $m^+$RGCs, respectively. Brn3a labels a large proportion (≈96%) of the entire RGC population that have in common their involvement in image-forming visual functions (Nadal-Nicolás et al, 2014, 2015a, 2015b), but include many different types of RGCs. Melanopsin, on the other hand, identifies a small population (≈2.5%) characterized by their intrinsic capacity to sense light, and are mainly involved in nonimage-forming visual functions (Galindo-Romero et al., 2013a; Nadal-Nicolás et al., 2014; Vidal-Villegas et al., 2020). Standard immunocytochemical techniques, as used in the present studies, detect the melanopsin subtypes M1-M3 which express more melanopsin than the M4-M6 subtypes (Duan et al., 2015; LeGates et al., 2014; Vidal-Villegas et al., 2020). Thus, even such a specific marker, is only indicative of the response of a few but not all of the $m^+$RGC subtypes. Nevertheless, because Brn3a and melanopsin are very seldomly co-expressed in the same RGC (Fig. 3 FF'GG') and are expressed long after injury, the use of both markers allows parallel but independent long-term studies of these two RGC populations and thus, to assess their response to axotomy and neuroprotection (Agudo-Barriuso et al., 2016; Galindo-Romero et al., 2013a; Nadal-Nicolás et al., 2015b; Sánchez-Migallón et al., 2016; Vidal-Sanz et al., 2015a, 2015b, 2017).

The other challenge refers to the design of protection strategies that impinge on the various death pathways activated by retinal injury (Agudo-Barriuso et al., 2013; Agudo et al, 2008, 2009; Tran et al., 2019), i.e. using a dual neuroprotection strategy to modulate the extrinsic apoptosis pathway with antagonists of the tumor necrosis factor-α and to activate survival pathways with BNDF (Lucas-Ruiz et al., 2019). Such strategies based on the combination of dual or multiple neuroprotective approaches (Harvey, 2007) need further elaboration and are also promising.

## 5. Conclusions

We report here for the first time that daily systemic administration of DHF blunts axotomy-induced RGC loss in vivo in adult albino rats. This effect is dose-dependent, long lasting for the image-forming population of $Brn3a^+$RGCs and permanent for the nonimage-forming population of $m^+$RGCs. The neuroprotective effects of DHF appear to be mediated by phosphorylation of TrkB in the retina, and thus it is conceivable that DHF-activated TrkB results in activation of intracellular signals that lead to RGC survival.

## Acknowledgements

The technical help provided by José M Bernal and Dr. Antonio Parrado (from the Genomic Platform at IMIB-Arrixaca for his help to perform Western Blotting) is greatly acknowledged.

This work was funded by the Fundación Séneca, Agencia de Ciencia y Tecnología Región de Murcia: 19881/GERM/15; Spanish Ministry of Economy and Competitiveness ISCIII-FEDER "Una manera de hacer Europa", PI19/00203, RD16/0008/0004, RD16/0008/0026; Spanish Ministry of Science, Innovation and Universities, RED2018-102499-T, and; Spanish Ministry of Science and Innovation, PID2019-106498 GB-I00.

## References

Agostinone, J., Alarcon-Martinez, L., Gamlin, C., Yu, W.-Q., Wong, R.O.L., Di Polo, A., 2018. Insulin signalling promotes dendrite and synapse regeneration and restores circuit function after axonal injury. Brain 141, 1963–1980. https://doi.org/10.1093/brain/awy142.

Agostinone, J., Di Polo, A., 2015. Retinal ganglion cell dendrite pathology and synapse loss. In: Progress in Brain Research. Elsevier B.V., pp. 199–216. https://doi.org/10.1016/bs.pbr.2015.04.012

Aguayo, A.J., Vidal-Sanz, M., Villegas-Pérez, M.P., Bray, G.M., 1987. Growth and connectivity of axotomized retinal neurons in adult rats with optic nerves substituted by PNS grafts linking the eye and the midbrain. Ann. N. Y. Acad. Sci. 495, 1–9. https://doi.org/10.1111/j.1749-6632.1987.tb23661.x.

Agudo-Barriuso, M., Lahoz, A., Nadal-Nicolás, F.M., Sobrado-Calvo, P., Piquer-Gil, M., Díaz-Llopis, M., Vidal-Sanz, M., Mullor, J.L., 2013. Metabolomic changes in the rat retina after optic nerve crush. Investig. Opthalmology Vis. Sci. 54, 4249. https://doi.org/10.1167/iovs.12-11451.

Agudo-Barriuso, M., Nadal-Nicolás, F., Madeira, M., Rovere, G., Vidal-Villegas, B., Vidal-Sanz, M., 2016. Melanopsin expression is an indicator of the well-being of melanopsin-expressing retinal ganglion cells but not of their viability. Neural Regen. Res. 11, 1243. https://doi.org/10.4103/1673-5374.189182.

Agudo, M., Pérez-Marín, M.C., Lönngren, U., Sobrado, P., Conesa, A., Cánovas, I., Salinas-Navarro, M., Miralles-Imperial, J., Hallböök, F., Vidal-Sanz, M., 2008. Time course profiling of the retinal transcriptome after optic nerve transection and optic nerve crush. Mol. Vis. 14, 1050–1063.

Agudo, M., Pérez-Marín, M.C., Sobrado-Calvo, P., Lönngren, U., Salinas-Navarro, M., Cánovas, I., Nadal-Nicolás, F.M., Miralles-Imperial, J., Hallböök, F., Vidal-Sanz, M., 2009. Immediate upregulation of proteins belonging to different branches of the

apoptotic cascade in the retina after optic nerve transection and optic nerve crush. Investig. Opthalmology Vis. Sci. 50, 424. https://doi.org/10.1167/iovs.08-2404.
Alarcón-Martínez, L., Avilés-Trigueros, M., Galindo-Romero, C., Valiente-Soriano, J., Agudo-Barriuso, M., Villa, P. de la, Villegas-Pérez, M.P., Vidal-Sanz, M., 2010. ERG changes in albino and pigmented mice after optic nerve transection. Vis. Res. 50, 2176–2187. https://doi.org/10.1016/j.visres.2010.08.014.
Alarcón-Martínez, L., de la Villa, P., Avilés-Trigueros, M., Blanco, R., Villegas-Pérez, M. P., Vidal-Sanz, M., 2009. Short and long term axotomy-induced ERG changes in albino and pigmented rats. Mol. Vis. 15, 2373–2383.
Almasieh, M., Wilson, A.M., Morquette, B., Cueva Vargas, J.L., Di Polo, A., 2012. The molecular basis of retinal ganglion cell death in glaucoma. Prog. Retin. Eye Res. 31, 152–181. https://doi.org/10.1016/j.preteyeres.2011.11.002.
Baden, T., Berens, P., Franke, K., Román Rosón, M., Bethge, M., Euler, T., 2016. The functional diversity of retinal ganglion cells in the mouse. Nature 529, 345–350. https://doi.org/10.1038/nature16468.
Barde, Y.A., Edgar, D., Thoenen, H., 1982. Purification of a new neurotrophic factor from mammalian brain. Hoppe. Seylers. Z. Physiol. Chem. 363, 1295–1296.
Chidlow, G., Casson, R.J., Sobrado-Calvo, P., Vidal-Sanz, M., Osborne, N.N., 2005. Measurement of retinal injury in the rat after optic nerve transection: an RT-PCR study. Mol. Vis. 11, 387–396.
Chidlow, G., Wood, J.P.M., Casson, R.J., 2007. Pharmacological neuroprotection for glaucoma. Drugs 67, 725–759. https://doi.org/10.2165/00003495-200767050-00006.
Christensen, I., Lu, B., Yang, N., Huang, K., Wang, P., Tian, N., 2019. The susceptibility of retinal ganglion cells to glutamatergic excitotoxicity is type-specific. Front. Neurosci. 13 https://doi.org/10.3389/fnins.2019.00219.
Cui, Q., Ren, C., Sollars, P.J., Pickard, G.E., So, K.-F., 2015. The injury resistant ability of melanopsin-expressing intrinsically photosensitive retinal ganglion cells. Neuroscience 284, 845–853. https://doi.org/10.1016/j.neuroscience.2014.11.002.
Daly, C., Shine, L., Heffernan, T., Deeti, S., Reynolds, A.L., O'Connor, J.J., Dillon, E.T., Duffy, D.J., Kolch, W., Cagney, G., Kennedy, B.N., 2017. A brain-derived neurotrophic factor mimetic is sufficient to restore cone photoreceptor visual function in an inherited blindness model. Sci. Rep. 7, 11320. https://doi.org/10.1038/s41598-017-11513-5.
Di Polo, A., Aigner, L.J., Dunn, R.J., Bray, G.M., Aguayo, A.J., 1998. Prolonged delivery of brain-derived neurotrophic factor by adenovirus-infected Muller cells temporarily rescues injured retinal ganglion cells. Proc. Natl. Acad. Sci. Unit. States Am. 95, 3978–3983. https://doi.org/10.1073/pnas.95.7.3978.
Di Polo, A., Luo, C., Bray, G.M., Aguayo, A.J., 2000. Colocalization of TrkB and brain-derived neurotrophic factor proteins in green-red-sensitive cone outer segments - PubMed. Investig. Ophthalmol. Vis. Sci. 41, 4014–4021.
Duan, X., Qiao, M., Bei, F., Kim, I.-J., He, Z., Sanes, J.R., 2015. Subtype-specific regeneration of retinal ganglion cells following axotomy: effects of osteopontin and mTOR signaling. Neuron 85, 1244–1256. https://doi.org/10.1016/j.neuron.2015.02.017.
Emili, M., Guidi, S., Uguagliati, B., Giacomini, A., Bartesaghi, R., Stagni, F., 2020. Treatment with the flavonoid 7,8-Dihydroxyflavone: a promising strategy for a constellation of body and brain disorders. Crit. Rev. Food Sci. Nutr. 1–38. https://doi.org/10.1080/10408398.2020.1810625.
Galindo-Romero, C., Jiménez-López, M., García-Ayuso, D., Salinas-Navarro, M., Nadal-Nicolás, F.M., Agudo-Barriuso, M., Villegas-Pérez, M.P., Avilés-Trigueros, M., Vidal-Sanz, M., 2013a. Number and spatial distribution of intrinsically photosensitive retinal ganglion cells in the adult albino rat. Exp. Eye Res. 108, 84–93. https://doi.org/10.1016/j.exer.2012.12.010.
Galindo-Romero, C., Valiente-Soriano, F.J., Jiménez-López, M., García-Ayuso, D., Villegas-Pérez, M.P., Vidal-Sanz, M., Agudo-Barriuso, M., 2013b. Effect of brain-derived neurotrophic factor on mouse axotomized retinal ganglion cells and phagocytic microglia. Investig. Ophthalmol. Vis. Sci. 54, 974–985. https://doi.org/10.1167/iovs.12-11207.
Gallego-Ortega, A., Norte-Muñoz, M., Miralles de Imperial-Ollero, J.A., Bernal-Garro, J. M., Valiente-Soriano, F.J., de la Villa Polo, P., Avilés-Trigueros, M., Villegas-Pérez, M.P., Vidal-Sanz, M., 2020. Functional and morphological alterations in a glaucoma model of acute ocular hypertension. In: Progress in Brain Research. https://doi.org/10.1016/bs.pbr.2020.07.003.
García-Ayuso, D., Galindo-Romero, C., Di Pierdomenico, J., Vidal-Sanz, M., Agudo-Barriuso, M., Villegas Pérez, M.P., 2017. Light-induced retinal degeneration causes a transient downregulation of melanopsin in the rat retina. Exp. Eye Res. 161, 10–16. https://doi.org/10.1016/j.exer.2017.05.010.
Gupta, V.K., You, Y., Li, J.C., Klistorner, A., Graham, S.L., 2013. Protective effects of 7,8-dihydroxyflavone on retinal ganglion and RGC-5 cells against excitotoxic and oxidative stress. J. Mol. Neurosci. 49, 96–104. https://doi.org/10.1007/s12031-012-9899-x.
Guymer, C., Wood, J.P.M., Chidlow, G., Casson, R.J., 2019. Neuroprotection in glaucoma: recent advances and clinical translation. Clin. Exp. Ophthalmol. 47, 88–105. https://doi.org/10.1111/ceo.13336.
Harvey, A.R., 2007. Combined therapies in the treatment of neurotrauma: polymers, bridges and gene therapy in visual system repair. Neurodegener. Dis. 4, 300–305. https://doi.org/10.1159/000101886.
He, J., Xiang, Z., Zhu, X., Ai, Z., Shen, J., Huang, T., Liu, L., Ji, W., Li, T., 2016. Neuroprotective effects of 7, 8-dihydroxyflavone on midbrain dopaminergic neurons in MPP+-treated monkeys. Sci. Rep. 6, 34339 https://doi.org/10.1038/srep34339.
Huang, H.-M., Huang, C.-C., Tsai, M.-H., Poon, Y.-C., Chang, Y.-C., 2018. Systemic 7,8-dihydroxyflavone treatment protects immature retinas against hypoxic-ischemic injury via müller glia regeneration and MAPK/ERK activation. Investig. Opthalmology Vis. Sci. 59, 3124. https://doi.org/10.1167/iovs.18-23792.
Ichim, G., Tauszig-Delamasure, S., Mehlen, P., 2012. Neurotrophins and cell death. Exp. Cell Res. 318, 1221–1228. https://doi.org/10.1016/j.yexcr.2012.03.006.
Jang, S.-W., Liu, X., Yepes, M., Shepherd, K.R., Miller, G.W., Liu, Y., Wilson, W.D., Xiao, G., Blanchi, B., Sun, Y.E., Ye, K., 2010. A selective TrkB agonist with potent neurotrophic activities by 7,8-dihydroxyflavone. Proc. Natl. Acad. Sci. Unit. States Am. 107, 2687–2692. https://doi.org/10.1073/pnas.0913572107.
Kerrigan, L.A., 1997. TUNEL-positive ganglion cells in human primary open-angle glaucoma. Arch. Ophthalmol. 115, 1031. https://doi.org/10.1001/archopht.1997.01100160201010.
Kim, I.-J., Zhang, Y., Yamagata, M., Meister, M., Sanes, J.R., 2008. Molecular identification of a retinal cell type that responds to upward motion. Nature 452, 478–482. https://doi.org/10.1038/nature06739.
Kowiański, P., Lietzau, G., Czuba, E., Waśkow, M., Steliga, A., Moryś, J., 2018. BDNF: a key factor with multipotent impact on brain signaling and synaptic plasticity. Cell. Mol. Neurobiol. 38, 579–593. https://doi.org/10.1007/s10571-017-0510-4.
LeGates, T.A., Fernandez, D.C., Hattar, S., 2014. Light as a central modulator of circadian rhythms, sleep and affect. Nat. Rev. Neurosci. 15, 443–454. https://doi.org/10.1038/nrn3743.
Lindqvist, N., Lönngren, U., Agudo, M., Näpänkangas, U., Vidal-Sanz, M., Hallböök, F., 2010. Multiple receptor tyrosine kinases are expressed in adult rat retinal ganglion cells as revealed by single-cell degenerate primer polymerase chain reaction. Ups. J. Med. Sci. 115, 65–80. https://doi.org/10.3109/03009731003597119.
Lindqvist, N., Peinado-Ramón, P., Vidal-Sanz, M., Hallböök, F., 2004. GDNF, Ret, GFRalpha1 and 2 in the adult rat retino-tectal system after optic nerve transection. Exp. Neurol. 187, 487–499. https://doi.org/10.1016/j.expneurol.2004.02.002.
Lindqvist, N., Vidal-Sanz, M., Hallböök, F., 2002. Single cell RT-PCR analysis of tyrosine kinase receptor expression in adult rat retinal ganglion cells isolated by retinal sandwiching. Brain Res. Protoc. 10, 75–83. https://doi.org/10.1016/S1385-299X(02)00184-8.
Liu, X., Chan, C.-B., Jang, S.-W., Pradoldej, S., Huang, J., He, K., Phun, L.H., France, S., Xiao, G., Jia, Y., Luo, H.R., Ye, K., 2010. A synthetic 7,8-dihydroxyflavone derivative promotes neurogenesis and exhibits potent antidepressant effect. J. Med. Chem. 53, 8274–8286. https://doi.org/10.1021/jm101206p.
Liu, X., Obianyo, O., Chan, C.B., Huang, J., Xue, S., Yang, J.J., Zeng, F., Goodman, M., Ye, K., 2014. Biochemical and biophysical investigation of the brain-derived neurotrophic factor mimetic 7,8-dihydroxyflavone in the binding and activation of the TrkB receptor. J. Biol. Chem. 289, 27571–27584. https://doi.org/10.1074/jbc.M114.562561.
Liu, X., Qi, Q., Xiao, G., Li, J., Luo, H.R., Ye, K., 2013. O-methylated metabolite of 7,8-dihydroxyflavone activates TrkB receptor and displays antidepressant activity. Pharmacology 91, 185–200. https://doi.org/10.1159/000346920.
Lucas-Ruiz, F., Galindo-Romero, C., Rodríguez-Ramírez, K.T., Vidal-Sanz, M., Agudo-Barriuso, M., 2019. Neuronal death in the contralateral un-injured retina after unilateral axotomy: role of microglial cells. Int. J. Mol. Sci. 20 https://doi.org/10.3390/ijms20225733.
Mansour-Robaey, S., Clarke, D.B., Wang, Y.C., Bray, G.M., Aguayo, A.J., 1994. Effects of ocular injury and administration of brain-derived neurotrophic factor on survival and regrowth of axotomized retinal ganglion cells. Proc. Natl. Acad. Sci. U.S.A. 91, 1632–1636. https://doi.org/10.1073/pnas.91.5.1632.
McKerracher, L., Vidal-Sanz, M., Essagian, C., Aguayo, A., 1990. Selective impairment of slow axonal transport after optic nerve injury in adult rats. J. Neurosci. 10, 2834–2841. https://doi.org/10.1523/JNEUROSCI.10-08-02834.1990.
Morin, L.P., Studholme, K.M., 2014. Retinofugal projections in the mouse. J. Comp. Neurol. 522, 3733–3753. https://doi.org/10.1002/cne.23635.
Nadal-Nicolás, F.M., Madeira, M.H., Salinas-Navarro, M., Jiménez-López, M., Galindo-Romero, C., Ortín-Martínez, A., Santiago, A.R., Vidal-Sanz, M., Agudo-Barriuso, M., 2015a. Transient downregulation of melanopsin expression after retrograde tracing or optic nerve injury in adult rats. Investig. Opthalmology Vis. Sci. 56, 4309. https://doi.org/10.1167/iovs.15-16963.
Nadal-Nicolás, F.M., Salinas-Navarro, M., Jiménez-López, M., Sobrado-Calvo, P., Villegas-Pérez, M.P., Vidal-Sanz, M., Agudo-Barriuso, M., 2014. Displaced retinal ganglion cells in albino and pigmented rats. Front. Neuroanat. 8 https://doi.org/10.3389/fnana.2014.00099.
Nadal-Nicolás, F.M., Sobrado-Calvo, P., Jiménez-López, M., Vidal-Sanz, M., Agudo-Barriuso, M., 2015b. Long-term effect of optic nerve axotomy on the retinal ganglion cell layer. Investig. Opthalmology Vis. Sci. 56, 6095. https://doi.org/10.1167/iovs.15-17195.
Ochs, G., Penn, R.D., York, M., Giess, R., Beck, M., Tonn, J., Haigh, J., Malta, E., Traub, M., Sendtner, M., Toyka, K.V., 2000. A phase I/II trial of recombinant methionyl human brain derived neurotrophic factor administered by intrathecal infusion to patients with amyotrophic lateral sclerosis. Amyotroph Lateral Scler. 1, 201–206. https://doi.org/10.1080/14660820050515197.
Ortín-Martínez, A., Valiente-Soriano, F.J., García-Ayuso, D., Alarcón-Martínez, L., Jiménez-López, M., Bernal-Garro, J.M., Nieto-López, L., Nadal-Nicolás, F.M., Villegas-Pérez, M.P., Wheeler, L.A., Vidal-Sanz, M., 2014. A novel in vivo model of focal light emitting diode-induced cone-photoreceptor phototoxicity: neuroprotection afforded by brimonidine, BDNF, PEDF or bFGF. PloS One 9, e113798. https://doi.org/10.1371/journal.pone.0113798.
Osborne, A., Khatib, T.Z., Songra, L., Barber, A.C., Hall, K., Kong, G.Y.X., Widdowson, P. S., Martin, K.R., 2018. Neuroprotection of retinal ganglion cells by a novel gene therapy construct that achieves sustained enhancement of brain-derived neurotrophic factor/tropomyosin-related kinase receptor-B signaling. Cell Death Dis. 9 https://doi.org/10.1038/s41419-018-1041-8.
Ou, Y., Jo, R.E., Ullian, E.M., Wong, R.O.L., Della Santina, L., 2016. Selective vulnerability of specific retinal ganglion cell types and synapses after transient

ocular hypertension. J. Neurosci. 36, 9240–9252. https://doi.org/10.1523/JNEUROSCI.0940-16.2016.
Parrilla-Reverter, G., Agudo, M., Nadal-Nicolás, F., Alarcón-Martínez, L., Jiménez-López, M., Salinas-Navarro, M., Sobrado-Calvo, P., Bernal-Garro, J.M., Villegas-Pérez, M.P., Vidal-Sanz, M., 2009a. Time-course of the retinal nerve fibre layer degeneration after complete intra-orbital optic nerve transection or crush: a comparative study. Vis. Res. 49, 2808–2825. https://doi.org/10.1016/j.visres.2009.08.020.
Parrilla-Reverter, G., Agudo, M., Sobrado-Calvo, P., Salinas-Navarro, M., Villegas-Pérez, M.P., Vidal-Sanz, M., 2009b. Effects of different neurotrophic factors on the survival of retinal ganglion cells after a complete intraorbital nerve crush injury: a quantitative in vivo study. Exp. Eye Res. 89, 32–41. https://doi.org/10.1016/j.exer.2009.02.015.
Patapoutian, A., Reichardt, L.F., 2001. Trk receptors: mediators of neurotrophin action. Curr. Opin. Neurobiol. https://doi.org/10.1016/S0959-4388(00)00208-7.
Peinado-Ramón, P., Salvador, M., Villegas-Pérez, M.P., Vidal-Sanz, M., 1996. Effects of axotomy and intraocular administration of NT-4, NT-3, and brain-derived neurotrophic factor on the survival of adult rat retinal ganglion cells: a quantitative in vivo study. Investig. Ophthalmol. Vis. Sci. 37, 489–500.
Pérez de Lara, M.J., Avilés-Trigueros, M., Guzmán-Aránguez, A., Valiente-Soriano, F.J., de la Villa, P., Vidal-Sanz, M., Pintor, J., 2019. Potential role of P2X7 receptor in neurodegenerative processes in a murine model of glaucoma. Brain Res. Bull. 150, 61–74. https://doi.org/10.1016/j.brainresbull.2019.05.006.
Pérez de Lara, M.J., Santano, C., Guzmán-Aránguez, A., Valiente-Soriano, F.J., Avilés-Trigueros, M., Vidal-Sanz, M., de la Villa, P., Pintor, J., 2014. Assessment of inner retina dysfunction and progressive ganglion cell loss in a mouse model of glaucoma. Exp. Eye Res. 122, 40–49. https://doi.org/10.1016/j.exer.2014.02.022.
Price, R.D., Milne, S.A., Sharkey, J., Matsuoka, N., 2007. Advances in small molecules promoting neurotrophic function. Pharmacol. Ther. https://doi.org/10.1016/j.pharmthera.2007.03.005.
Puyang, Z., Gong, H.-Q., He, S.-G., Troy, J.B., Liu, X., Liang, P.-J., 2017. Different functional susceptibilities of mouse retinal ganglion cell subtypes to optic nerve crush injury. Exp. Eye Res. 162, 97–103. https://doi.org/10.1016/j.exer.2017.06.014.
Rheaume, B.A., Jereen, A., Bolisetty, M., Sajid, M.S., Yang, Y., Renna, K., Sun, L., Robson, P., Trakhtenberg, E.F., 2018. Single cell transcriptome profiling of retinal ganglion cells identifies cellular subtypes. Nat. Commun. 9, 2759. https://doi.org/10.1038/s41467-018-05134-3.
Robinson, G.A., Madison, R.D., 2004. Axotomized mouse retinal ganglion cells containing melanopsin show enhanced survival, but not enhanced axon regrowth into a peripheral nerve graft. Vis. Res. 44, 2667–2674. https://doi.org/10.1016/j.visres.2004.06.010.
Rodriguez, A.R., de Sevilla Müller, L.P., Brecha, N.C., 2014. The RNA binding protein RBPMS is a selective marker of ganglion cells in the mammalian retina. J. Comp. Neurol. 522, 1411–1443. https://doi.org/10.1002/cne.23521.
Rovere, G., Nadal-Nicolás, F.M., Agudo-Barriuso, M., Sobrado-Calvo, P., Nieto-López, L., Nucci, C., Villegas-Pérez, M.P., Vidal-Sanz, M., 2015. Comparison of retinal nerve fiber layer thinning and retinal ganglion cell loss after optic nerve transection in adult albino rats. Investig. Ophthalmol. Vis. Sci. 56, 4487–4498. https://doi.org/10.1167/iovs.15-17145.
Rovere, G., Nadal-Nicolás, F.M., Wang, J., Bernal-Garro, J.M., García-Carrillo, N., Villegas-Pérez, M.P., Agudo-Barriuso, M., Vidal-Sanz, M., 2016. Melanopsin-containing or non-melanopsin–containing retinal ganglion cells response to acute ocular hypertension with or without brain-derived neurotrophic factor neuroprotection. Investig. Opthalmology Vis. Sci. 57, 6652. https://doi.org/10.1167/iovs.16-20146.
Sánchez-Migallón, M.C., Nadal-Nicolás, F.M., Jiménez-López, M., Sobrado-Calvo, P., Vidal-Sanz, M., Agudo-Barriuso, M., 2011. Brain derived neurotrophic factor maintains Brn3a expression in axotomized rat retinal ganglion cells. Exp. Eye Res. 92, 260–267. https://doi.org/10.1016/j.exer.2011.02.001.
Sánchez-Migallón, M.C., Valiente-Soriano, F.J., Nadal-Nicolás, F.M., Di Pierdomenico, J., Vidal-Sanz, M., Agudo-Barriuso, M., 2018a. Survival of melanopsin expressing retinal ganglion cells long term after optic nerve trauma in mice. Exp. Eye Res. 174, 93–97. https://doi.org/10.1016/j.exer.2018.05.029.
Sánchez-Migallón, M.C., Valiente-Soriano, F.J., Nadal-Nicolás, F.M., Vidal-Sanz, M., Agudo-Barriuso, M., 2016. Apoptotic retinal ganglion cell death after optic nerve transection or crush in mice: delayed RGC loss with BDNF or a caspase 3 inhibitor. Investig. Opthalmology Vis. Sci. 57, 81. https://doi.org/10.1167/iovs.15-17841.
Sánchez-Migallón, M.C., Valiente-Soriano, F.J., Salinas-Navarro, M., Nadal-Nicolás, F.M., Jiménez-López, M., Vidal-Sanz, M., Agudo-Barriuso, M., 2018b. Nerve fibre layer degeneration and retinal ganglion cell loss long term after optic nerve crush or transection in adult mice. Exp. Eye Res. 170, 40–50. https://doi.org/10.1016/j.exer.2018.02.010.
Sanes, J.R., Masland, R.H., 2015. The types of retinal ganglion cells: current status and implications for neuronal classification. Annu. Rev. Neurosci. 38, 221–246. https://doi.org/10.1146/annurev-neuro-071714-034120.
Seppa, K., Jagomäe, T., Kukker, K.G., Reimets, R., Pastak, M., Vasar, E., Terasmaa, A., Plaas, M., 2021. Liraglutide, 7,8-DHF and their co-treatment prevents loss of vision and cognitive decline in a Wolfram syndrome rat model. Sci. Rep. 11 https://doi.org/10.1038/s41598-021-81768-6.
Thoenen, H., Sendtner, M., 2002. Neurotrophins: from enthusiastic expectations through sobering experiences to rational therapeutic approaches. Nat. Neurosci. 5, 1046–1050. https://doi.org/10.1038/nn938.
Tran, N.M., Shekhar, K., Whitney, I.E., Jacobi, A., Benhar, I., Hong, G., Yan, W., Adiconis, X., Arnold, M.E., Lee, J.M., Levin, J.Z., Lin, D., Wang, C., Lieber, C.M., Regev, A., He, Z., Sanes, J.R., 2019. Single-cell profiles of retinal ganglion cells differing in resilience to injury reveal neuroprotective genes. Neuron 104, 1039–1055. https://doi.org/10.1016/j.neuron.2019.11.006 e12.
Valiente-Soriano, F.J., Nadal-Nicolás, F.M., Salinas-Navarro, M., Jiménez-López, M., Bernal-Garro, J.M., Villegas-Pérez, M.P., Agudo-Barriuso, M., Vidal-Sanz, M., 2015a. BDNF rescues RGCs but not intrinsically photosensitive RGCs in ocular hypertensive albino rat retinas. Investig. Opthalmology Vis. Sci. 56, 1924 https://doi.org/10.1167/iovs.15-16454.
Valiente-Soriano, F.J., Ortín-Martínez, A., Pierdomenico, J.Di, García-Ayuso, D., Gallego-Ortega, A., Miralles de Imperial-Ollero, J.A., Jiménez-López, M., Villegas-Pérez, M. P., Wheeler, L.A., Vidal-Sanz, M., 2019. Topical brimonidine or intravitreal bdnf, cntf, or bfgf protect cones against phototoxicity. Transl. Vis. Sci. Technol. 8, 36. https://doi.org/10.1167/tvst.8.6.36.
Valiente-Soriano, F.J., Salinas-Navarro, M., Jiménez-López, M., Alarcón-Martínez, L., Ortín-Martínez, A., Bernal-Garro, J.M., Avilés-Trigueros, M., Agudo-Barriuso, M., Villegas-Pérez, M.P., Vidal-Sanz, M., 2015b. Effects of ocular hypertension in the visual system of pigmented mice. PloS One 10, e0121134. https://doi.org/10.1371/journal.pone.0121134.
Van Gelder, R.N., Buhr, E.D., 2016. Ocular photoreception for circadian rhythm entrainment in mammals. Annu. Rev. Vis. Sci. 2, 153–169. https://doi.org/10.1146/annurev-vision-111815-114558.
VanderWall, K.B., Lu, B., Alfaro, J.S., Allsop, A.R., Carr, A.S., Wang, S., Meyer, J.S., 2020. Differential susceptibility of retinal ganglion cell subtypes in acute and chronic models of injury and disease. Sci. Rep. 10, 17359. https://doi.org/10.1038/s41598-020-71460-6.
Vidal-Sanz, M., Bray, G., Villegas-Perez, M., Thanos, S., Aguayo, A., 1987. Axonal regeneration and synapse formation in the superior colliculus by retinal ganglion cells in the adult rat. J. Neurosci. 7, 2894–2909. https://doi.org/10.1523/JNEUROSCI.07-09-02894.1987.
Vidal-Sanz, M., Galindo-Romero, C., Valiente-Soriano, F.J., Nadal-Nicolás, F.M., Ortin-Martinez, A., Rovere, G., Salinas-Navarro, M., Lucas-Ruiz, F., Sanchez-Migallon, M. C., Sobrado-Calvo, P., Aviles-Trigueros, M., Villegas-Pérez, M.P., Agudo-Barriuso, M., 2017. Shared and differential retinal responses against optic nerve injury and ocular hypertension. Front. Neurosci. 11 https://doi.org/10.3389/fnins.2017.00235.
Vidal-Sanz, M., Lafuente, M., Sobrado-Calvo, P., SellÉs-Navarro, I., Rodriguez, E., Mayor-Torroglosa, S., Villegas-Pérez, M.P., 2000. Death and neuroprotection of retinal ganglion cells after different types of injury. Neurotox. Res. 2, 215–227. https://doi.org/10.1007/bf03033795.
Vidal-Sanz, M., Nadal-Nicolás, F.M., Valiente-Soriano, F.J., Agudo-Barriuso, M., Villegas-Pérez, M.P., 2015a. Identifying specific RGC types may shed light on their idiosyncratic responses to neuroprotection. Neural Regen. Res. https://doi.org/10.4103/1673-5374.162751.
Vidal-Sanz, M., Valiente-Soriano, F.J., Ortín-Martínez, A., Nadal-Nicolás, F.M., Jiménez-López, M., Salinas-Navarro, M., Alarcón-Martínez, L., Garcfa-Ayuso, D., Avilés-Trigueros, M., Agudo-Barriuso, M., Villegas-Pérez, M.P., 2015b. Retinal Neurodegeneration in Experimental Glaucoma. In: Progress in Brain Research. Elsevier B.V., pp. 1–35. https://doi.org/10.1016/bs.pbr.2015.04.008
Vidal-Villegas, B., Di Pierdomenico, J., Miralles de Imperial-Ollero, J.A., Ortín-Martínez, A., Nadal-Nicolás, F.M., Bernal-Garro, J.M., Cuenca Navarro, N., Villegas-Pérez, M.P., Vidal-Sanz, M., 2019a. Melanopsin+RGCs are fully resistant to NMDA-induced excitotoxicity. Int. J. Mol. Sci. 20, 3012. https://doi.org/10.3390/ijms20123012.
Vidal-Villegas, B., Di Pierdomenico, J., Salinas-Navarro, M., Manuel Bernal-Garro, J., Agudo-Barriuso, M., Paz Villegas-Pérez, M., Martínez de la Casa, J.M., García-Feijoo, J., Vidal-Sanz, M., 2019b. 7,8-Dihydroxyflavone protects axotomy-induced retinal ganglion cell loss in adult albino rats. Acta Ophthalmol. 97, 1755–3768. https://doi.org/10.1111/j.1755-3768.2019.5413, 2019.5413.
Vidal-Villegas, B., Gallego-Ortega, A., Miralles de Imperial-Ollero, J.A., Martínez de la Casa, J.M., García Feijoo, J., Vidal-Sanz, M., 2020. Células ganglionares fotosensibles: una población diminuta pero esencial. Arch. Soc. Esp. Oftalmol. https://doi.org/10.1016/j.oftal.2020.06.032.
Villegas-Pérez, M.-P., Vidal-Sanz, M., Rasminsky, M., Bray, G.M., Aguayo, A.J., 1993. Rapid and protracted phases of retinal ganglion cell loss follow axotomy in the optic nerve of adult rats. J. Neurobiol. 24, 23–36. https://doi.org/10.1002/neu.480240103.
Villegas-Perez, M.P., Vidal-Sanz, M., Bray, G.M., Aguayo, A.J., 1988. Influences of peripheral nerve grafts on the survival and regrowth of axotomized retinal ganglion cells in adult rats. J. Neurosci. 8, 265–280. https://doi.org/10.1523/jneurosci.08-01-00265.1988.
Wang, J., Valiente-Soriano, F.J., Nadal-Nicolás, F.M., Rovere, G., Chen, S., Huang, W., Agudo-Barriuso, M., Jonas, J.B., Vidal-Sanz, M., Zhang, X., 2017. MicroRNA regulation in an animal model of acute ocular hypertension. Acta Ophthalmol. 95, e10–e21. https://doi.org/10.1111/aos.13227.
Wójcik-Gryciuk, A., Gajewska-Woźniak, O., Kordecka, K., Boguszewski, P.M., Waleszczyk, W., Skup, M., 2020. Neuroprotection of retinal ganglion cells with AAV2-BDNF pretreatment restoring normal TrkB receptor protein levels in glaucoma. Int. J. Mol. Sci. 21, 6262. https://doi.org/10.3390/ijms21176262.
Yang, N., Young, B.K., Wang, P., Tian, N., 2020. The susceptibility of retinal ganglion cells to optic nerve injury is type specific. Cells 9, 677. https://doi.org/10.3390/cells9030677.
Yu, X., Liu, Q., Wang, X., Liu, H., Wang, Y., 2018. 7,8-Dihydroxyflavone ameliorates high-glucose induced diabetic apoptosis in human retinal pigment epithelial cells by activating TrkB. Biochem. Biophys. Res. Commun. 495, 922–927. https://doi.org/10.1016/j.bbrc.2017.11.007.
Zhang, R., Kang, K.A., Piao, M.J., Ko, D.O., Wang, Z.H., Chang, W.Y., You, H.J., Lee, I.K., Kim, B.J., Kang, S.S., Hyun, J.W., 2009. Preventive effect of 7,8-dihydroxyflavone

against oxidative stress induced genotoxicity. Biol. Pharm. Bull. 32, 166–171. https://doi.org/10.1248/bpb.32.166.
Zhang, Y., Pardridge, W.M., 2001. Neuroprotection in transient focal brain ischemia after delayed intravenous administration of brain-derived neurotrophic factor conjugated to a blood-brain barrier drug targeting system. Stroke 32, 1378–1384. https://doi.org/10.1161/01.STR.32.6.1378.
Zhang, Z., Liu, X., Schroeder, J.P., Chan, C.B., Song, M., Yu, S.P., Weinshenker, D., Ye, K., 2014. 7,8-dihydroxyflavone prevents synaptic loss and memory deficits in a mouse model of Alzheimer's disease. Neuropsychopharmacology 39, 638–650. https://doi.org/10.1038/npp.2013.243.

# 4. DISCUSSION

Some human diseases such as glaucoma and optic neuropathies affect almost selectively the RGCs. These cells belong to the CNS and when lesioned in mammals they suffer a retrograde degeneration and die massively[1,5–7], causing blindness. Some studies have documented, however, that it is possible to rescue these cells after an injury, at least temporarily, with peripheral nerve grafts[12] and with neurotrophic factors such as BDNF[61,63,64,253,261,266,272,320]. Also, it has been documented that the surviving RGCs have the capacity to regenerate when the CNS environment is substituted by a peripheral nerve graft and to make appropriate, functional and persistent synaptic connections[12,16,18,19]. It is believed that if the numbers of RGCs that survive after an injury is increased using neuroprotective strategies, the numbers of regenerating RGCs would also increase and also the possibilities of restoration of the visual system[5,17,296]. But not all RGCs behave similarly after an injury. Recent studies have documented that different types of RGCs can respond differently to different types of injury and even to neuroprotection[69,267,268]**.** Particularly, the ipRGCs[32,67,75] seem to be more resistant to different injuries. The investigation of the types of RGCs that survive better after an injury or after pharmacologic neuroprotection is important because it could increase our knowledge of the cellular characteristics that mediate cell survival and allow in the future the development of neuroprotective and neuroregenerative strategies.

In the articles included in this Thesis we have used immunocytochemistry and modern imaging, state of the art, techniques for identification, mapping and quantification of two different RGC populations: Brn3a$^+$RGCs and m$^+$RGCs in the adult rat. Most RGCs express Brna3 and thus the Brn3a$^+$RGCs represent almost the whole RGC

population[81], while the m+RGC population represents only 2.5% of the RGC population[81] and most of the ipRGCs do not express Brn3a. Thus, the identification with immunhistochemical techniques of these two populations, have allowed us to investigate in parallel, but independently, the survival of these two RGC populations after two different types of injury: an excitotoxic injury caused by intravitreal injection of NMDA, and optic nerve section, to ascertain whether these cells respond differently to these two lesions. We have also explored the capability of SD-OCT to document the retinal degeneration and its progression after NMDA administration. Finally, we have investigated if injured RGCs may be neuroprotected after optic nerve section with DHF, an agonist of the TrkB receptor that mediates the action of the neurotrophic factors BDNF and NT4/5[308,334] and whether its neurotrophic action is mediated through the stimulation of this receptor.

### 4.1. Brn3a+RGCs and m+RGCs

In the studies presented in this Thesis, we have used antibodies against Brn3a to label the general population of RGCs. Using these immunocytochemical techniques, we have labelled 78,903±3573(n=10[140]) and 81,112±1,298 (n=48[212]) RGCs in the control rat retinas. These total numbers of Brn3a+RGCs were similar to those found in the right fellow retinas[140,212] and to other control retinas in previous studies[77,80,81,261]. This marker has been shown to label the whole population of RGCs except the m+RGCs (only 0.2% express Brn3a) and one half of the ipsilaterally projecting RGCs[81]. Since we use Sprague-Dawley albino rats, and in this strain only 2.5% of the total population of RGCs project ipsilaterally[81], we can say that this marker labels 98.75% of the general population of RGCs, but not the m+RGCs. This antibody also labels most RGCs after an injury: optic nerve crush or axotomy[80,261]. In addition, it has the

advantage that there is no need to lesion the RGC projections or their target territories for its application, like when using neuronal tract-tracing dyes[193]; and that it does not label neighbouring cells by diffusion[141]. Thus, the antibodies against Brn3a are a good marker to study the effects of different lesions on the general RGC population.

In the studies presented in this Thesis we have also used anti-melanopsin antibodies to label the ipRGCs. We have immunolabelled 2,358±143 (n=10[140]) and 2,101±89 (n=48[212]) $m^+$RGCs in control retinas and these numbers were similar to those reported before in control retinas[139,167]. Using neighbour maps, we have shown the distribution of the $m^+$RGCs in the albino rat retina and we document that these cells concentrate in the upper retina, in accordance with previous studies[66,139,143,266]. Since only 0.23% of the $m^+$RGCs are also $Brn3a^+$[81], using a combination of antibodies against melanopsin and Brn3a we have been able to study in parallel but independently the response of the populations of $Brn3a^+$RGCs and $m^+$RGCs to two different lesions and their neuroprotection by DHF.

To label $m^+$RGCs we have used immunocytochemistry techniques, so we believe that we are labelling the M1, M2 and M3 ipRGCs, but not the M4, M5 and M6 whose small expression levels of melanopsin are below immunocytochemical detection[94,335]. Using this technique, we and other investigators have documented that there are approximately 2,400 $m^+$RGCs (belonging to the M1, M2 and M3 subtypes) and this represents 2.5 to 2.7% of the total RGC population in adult albino or pigmented rats, respectively[77,139,140,336]. However, because no authors have been able to label all the populations of ipRGCs at once, the total numbers of ipRGCs in the rat retina are unknown at present and therefore we do not know which percentage of the total ipRGC population is labelled with this antibody. An ongoing study (Gallego-Ortega, Vidal-Villegas et al., 2021, submitted) has documented that there are around 1,000 M4

ipRGCs in the rat retina. Because most authors believe that the numbers of M5 and M6 RGCs are very low, we believe that in the studies presented in this Thesis we are labelling more than two thirds of the ipRGC population. However, we could be labelling more, as other authors have suggested that the subtypes M1 and M2 amount to 74-90% of the ipRGC population in the rat retina[67], but both these assumptions should be taken with caution because, as mentioned above, standard immunohistochemistry only labels a proportion of ipRGCs.

Indeed, there are no comprehensive quantitative studies of ipRGCs in adult rats, but a recent study in transgenic mice has suggested that all ipRGCs expressing the T-box transcription factor T-brain 2 (Tbr2, also known as Eomes) (Tbr2$^{+}$RBPMS$^{+}$RGCs), which is considered a pan-marker for ipRGCs[70,96,97,337], account for 12% of the mice RGC population, and this proportion is twice the proportion of RBPMS$^{+}$RGCs that express detectable levels of melanopsin with standard immunohistochemistry (6% of all RGCs)[337]. Thus, considering that in pigmented mice, total numbers of RGCs retrogradely labelled with fluorogold applied to the optic nerve head account for ~42,600 RGCs[338], total numbers of ipRGCs would account for 5,112, while total numbers of ipRGCs expressing detectable levels of melanopsin (M1-M3 ipRGCs) would account to 2,520. Thus, there is quite a large number of ipRGCs that do not express detectable levels of melanopsin (M4-M6) yet to be identified and characterized properly in terms of their response to injury and neuroprotection.

In ongoing studies (Gallego-Ortega, Vidal-Villegas et al., 2021, submitted) we have continued with the characterization of the rat ipRGCs using techniques that would label the populations that we cannot identify with immunocytochemistry, namely, the M4-M6 ipRGCs. In the absence of markers that readily identify rat M4, also known as M4/α ON-sustained RGCs[102], we have used double labelling of ipRGCs with

osteopontin which in mice labels all alpha RGCS[339] and Tbr2 which in mice labels all ipRGCs[70,337,339]. In control rat retinas, approximately 1,000 M4 cells were labelled with a distribution somewhat different from mice[135], whereas in mice M4 concentrate within the superior temporal quadrant, in rat these cells concentrate within the inferior temporal quadrant (Gallego-Ortega, Vidal-Villegas et al., 2021 in preparation).

### 4.2. NMDA induces RGC death

In the first article presented in this Thesis[140] we have investigated the short- and long-term effects of intravitreally administered NMDA on the two populations of RGCs: Brn3a$^+$RGCs and m$^+$RGCs. We have injected a single dose of 5 µl of 100mM NMDA. This dose was used following preliminary experiments testing different doses and concentrations of NMDA that triggered a consistent percentage of RGC death (JA Miralles de Imperial Ollero, personal communication).

Glutamate is the major excitatory neurotransmitter in the CNS and retina of mammals[340]. When administered at a high dose it may cause neuronal cell death, this is known as excitotoxicity[282]. The administration of NMDA, agonist of one of the ionotropic glutamate receptors also causes neuronal death and RGC death[341–343]. Although the exact mechanism of neuronal cell death following NMDA administration is as yet not completely understood[294,344], it is believed to be mediated through an excessive activation of the ionotropic NMDA glutamate receptor, which eventually activates cellular apoptotic pathways[345]. Likewise, excitotoxicity has been postulated as causative mechanism for some neurodegenerative diseases, including glaucoma[88,271,282,344].

Our data[140] documents that an intravitreal injection of 5 µl of 100mM NMDA causes rapid and massive death of Brn3a$^+$RGCs. Hence, only 49%, 28%, 24% and 19% of the

total Brn3a$^+$RGC population survive by 3, 7, 14 days or 15 months after the injection, respectively. However, the m$^+$RGC population is fully resilient to excitotoxicity since 62%, 92%, 102% and 90% survived at 3, 7, 14 days or 15 months, after the injection respectively; and the numbers of surviving m$^+$RGCs 15 months after the injection were similar to those found in contralateral and naïve retinas. We also show thinning of the retina, using SD-OCT, that is significant at 3 months and progresses up to 15 months[140]. We will now discuss this data.

### 4.2.1. NMDA neurotoxicity on the Brn3a$^+$RGC population

After the intravitreal injection of 5 µl of 100mM NMDA, we have observed the rapid and progressive death of Brn3a$^+$RGCs[140]. Cell loss was more marked between 0 and 3 days after the injection, when there was loss of approximately 50% of the Brn3a$^+$RGC population and continued up to day 7, when there was loss of 72% of the Brn3a$^+$RGC population. Cell loss did not seem to progress further, as 15 months after the injection there was loss of 80% of the Brn3a$^+$RGC population. However, when we compared Brn3a$^+$RGC survival between the different survival periods, we found significant differences only between 0 and 3 days and between 3 days and 15 months, indicating that NMDA caused acute cell loss and that this occurred mainly in the first 3 days after the injection. This acute cell loss is comparable to that found by others. Thus, two thirds or more of the RGCs are lost in mice [289,295] and rats[280,287,333], with interval survival follow-up ranging from 3-58 days after injury. Three days after the injection, we observed certain inter-animal variability[140], as reported also by other authors previously[287,295]. This inter-animal variability has been shown likewise in other types of RGC injury, such as optic nerve section[11,65] and optic nerve crush[267] and could be due to individual susceptibility or to the fact that cell death has not yet concluded by

that time. Another possible explanation, at least in our study, would be a slight variation in NMDA concentration due to a small and inconstant reflux of the injected volume. Though we have not studied survival intervals shorter than 3 days, one study[346] has documented RGC loss as soon as 6 hours after intraocular injection of NMDA in mice[346].

The death of RGCs that we observe after NMDA injection did not seem to progress after 7 days, since the numbers of Brn3a$^+$RGCs were similar between 7 days and 15 months after the injection, and this death pattern is different from the one that we observe after optic nerve section (see section 3). However, other authors have reported progressive RGC death between 12 hours and 58 days after excitotoxic injury[333]. It is possible that the difference between our study and the abovementioned could be due to the fact that these authors used antibodies against Neu-N to mark the RGCs but these antibodies also label the amacrine cells that could also die after injury (see section 2.3.). Another difference between their study and ours is that we count all the RGCs in the retina and they only counted small areas and extrapolated the numbers. However, long-term RGC survival was somewhat comparable in both studies, as Huang et al. reported loss of 67% of the RGC population and we report loss of 76% of the RGC population by 14 days, our closest time point analysed to theirs.

In our excitotoxic model of RGC death, the loss of RGCs appeared diffuse throughout the retina, a pattern that is quite similar to that observed after optic nerve section[11,12,65]. Other retinal injuries used to study experimental glaucoma involve chronic[83] or acute[66] elevation of the intraocular pressure, and these cause retinal degeneration with typical RGC loss in sectors[83] or in retinal patches[66]. These different patterns of RGC loss have been interpreted as a consequence of damage to axon bundles near the ON head[83] or retinal ischemia[66], respectively. However, in some animals we observed increased cell

loss within the superotemporal quadrant, the quadrant where the intraocular injection took place, and thus we interpret these results as a consequence of the increased NMDA concentration in this quadrant[140].

It is believed that NMDA causes neuronal death through the overactivation of the NMDA receptor and subsequent calcium entry into the neuron that activates apoptotic pathways[345], but the signalling pathways that mediate the excitotoxic injury are not yet completely known[294]. However, calcium entry is also observed in other types of neuronal injury, like after optic nerve injury and it is a well-recognized cause of neuronal degeneration and death[10,271]. Thus, calcium channel blockers have been shown to reduce RGC death in experimental models of excitotoxicity[347,348] and to decrease progression in human low pressure glaucoma[271,347,349]

### 4.2.2. m$^+$RGCs are resistant to NMDA-induced excitotoxicity

We could not document m$^+$RGC death after intravitreal injection of NMDA[140]. However, we show that there is a transient downregulation in melanopsin expression by m$^+$RGCs at 3 days after injury, which recovers fully by 14 days and lasts up to 15 months. Recent studies have also demonstrated in the adult rat a transient downregulation of melanopsin expression in response to diverse retinal injuries, such as: acute light-induced retinal degeneration[350], retrograde transport of neuronal tracers[65], temporary elevation of intraocular pressure[66] and optic nerve crush or section[65]. However, this transient downregulation in melanopsin expression has not been found in adult mice following optic nerve section[255,256], which might suggest that mice do not show melanopsin downregulation in RGCs after an injury[139,168,213,256,350]. In our study[140], after the transient downregulation, the numbers of m$^+$RGC recovered and were comparable to those found in untreated retinas 14 days and 15 months after

the injection. Consequently, we find a remarkable endurance of $m^+$RGCs to NMDA-mediated excitotoxicity. The survival of the entire population of $m^+$RGCs 15 months after the insult is impressive, particularly if one takes into account that at this survival interval there is loss of approximately 81% of the $Brn3a^+$RGC population together with an important thinning of the inner retina (see below).

Two previous studies have analysed in mice $m^+$RGC survival following intravitreal injection of NMDA and have shown large differences in $m^+$RGC survival. In one study the authors document no melanopsin downregulation and survival of the whole RGC population by 6 days after the injection[295]. In the second, loss of approximately half the population of $m^+$RGCs is observed at 21 days after the injection[289]. The differences between these studies could be explained when taken into account the different concentrations and amounts of NMDA that were injected intravitreally (3µl of 10 mM NMDA and 1µl of 40 mM NMDA respectively) or because mice do not show melanopsin expression downregulation after retinal injury, as discussed above.

From all the different RGC injury models examined thus far, it is apparent that $m^+$RGCs seem to be particularly resilient to NMDA induced excitotoxicity. The reasons why they have different survival rates to different retinal injuries remain unclear, further studies are still needed. However, several hypotheses have been put forward. One particular hypothesis proposes that their large dendrites within the inner plexiform layer may be enough to provide them of trophic support, even in the absence of brain target-derived trophic support[351–354]. Another theory has hypothesized that their resistance to NMDA induced excitotoxicity may be due to absence of NMDA receptors in the ipRGC, but this has been disproven, as studies have shown that all RGCs express NMDA receptors[355], including ipRGCs[293,356]. Other factors which might have been causing this ipRGC resistance to excitotoxicity have also been

disproven, such as pigmentation, presence of photoreceptors, genetic background or the activation of the JAK/STAT survival pathway[295].

As we will see in section 2.4. of the discussion, other intrinsic characteristics of ipRGCs like their subtype, their melanopsin content, their neurotransmitter PACAP (Pituitary adenylate cyclase-activating peptide) or their thrombospondin 1 expression could also act as endogenous neuroprotectants (see below, section 2.4.).

### 4.2.3. Intravitreal injection of NMDA results in a progressive retinal thinning

In our study[140] we document that intravitreal NMDA injection causes total retinal thinning, and in particular, thinning of the inner retinal layers that is already significant by 3 months and progresses up to 15 months after the injection[140]. Other studies have also shown thinning of the inner retina as measured by SD-OCT after intravitreal injection of NMDA in rabbits[357] and mice[358]. In our work, the inner retina comprised all layers from the INL to the ILM. These layers contain RGCs but also amacrine, bipolar, horizontal and Müller cells and thus inner retinal thinning could be due to loss of RGCs or all of these cells.

Thinning of the inner retina could be due to the loss of RGCs, as these cells have been documented to die preferentially after intravitreal injection of NMDA in various animals[359–361]. This would be in agreement with the massive death of Brn3a$^+$RGCs that we found after NMDA injection, as only 21% survived 15 months after the injection[140] and these cells and their dendrites and axons are located in the inner retinal layers. In fact, in rat and mice one of the thicker layers of the retina is the IPL, a layer that is formed mainly by RGC dendrites that establish contacts with processes of amacrine cells and axon terminals of bipolar cells.

Inner retina thinning after NMDA injection could be the result of death of RGCs and also of other retinal cells. One study in rabbits documented histopathologically necrosis of cells in the GCL and INL 4 hours after NMDA injection[357]. Furthermore, a study in adult rats comparing three typical animal models of glaucoma (microbead injection in the anterior chamber, episcleral veins cauterization and NMDA intravitreal injection) found in hematoxylin and eosin stained sections similar thinning of the inner retina in all cases[361].

The NMDA models of excitotoxicity have documented in addition to the loss of RGCs, death of other retinal neurons. Loss of amacrine cells has been shown to occur in albino rats [333,362,363], pigmented mice[364,365], and rabbits[357]. Furthermore, in a morphofunctional study conducted on mice which combined injection of two glutamate receptor agonists (1 µL of PBS containing NMDA 30 mM and Kainic Acid 10 mM) reports thinning on the GCL, IPL and INL and damage to bipolar, amacrine and ganglion cells[341]. In mice around 72% of the RGCs synapse with amacrine cells via gap junctions[366], and thus it has been hypothesized that RGC could cause secondary amacrine cell loss[364].

In our study[140] we also document a thinning of the contralateral untreated retinas, that is small but significant between 3 months and 15 months after the NMDA injection. We have argued that the thinning observed in the contralateral retinas is possibly due to the physiological thinning of the aging retina, as shown in other studies[336]. However, in the treated retinas the retinal thinning observed between 3 and 15 months was greater than the physiological thinning, indicating a continuing progressive degeneration of the retinal architecture prolonged beyond the period of Brn3a$^{+}$RGC loss, which we have shown concludes between 3 and 7 days after the insult[140]. Thus, the observed SD-OCT thinning in the NMDA-treated retinas between 3 and 15 months

indicates that although Brn3a$^+$RGC death occurs in the first days after the injection, retinal degeneration continued long term, probably through degeneration of other retinal cells[140]. At present we have no convincing explanations for such a protracted but important inner retinal degeneration, and it is certainly an issue that requires further studies to unravel the underlying mechanisms.

### 4.2.4. ipRGCs are more resistant to retinal disease and injury

We have documented that m$^+$RGCs are completely resilient to NMDA excitotoxicity, at least at the concentration used[140]. This is not surprising as different laboratories have demonstrated that ipRGCs show a much better survival rate than the general population of RGCs after different insults, such as: optic nerve crush both in mice[152,256,267,367,368] and rats[167], transient retinal ischemia[66], and ocular hypertension both in rats[167,369] and mice[370].

The ipRGCs have been reported to be more resistant to degeneration in human mitochondrial optic neuropathies, such as Leber hereditary optic neuropathy and autosomal dominant optic atrophy[32,67,75,99]. On the other hand, ipRGCs have not been shown to be more resilient in other diseases such as: i) glaucoma[32,67,75]; ii) neural degenerative diseases like Huntinton's[371], Parkinson[372] and Alzheimer´s[32,67,75,373]; iii) inherited retinal degenerations[374–376]; and iv) aging[75,336].

Why ipRGCs are more resilient to some types of injury is a question still under debate. Melanopsin itself has been thought to promote cell survival, but since we document in our study using NMDA induced excitotoxicity in adult rats[140] and in other studies[139,168,213,256,350] that many ipRGCs survive with a lower expression of melanopsin only to recover fully, this seems unlikely. However, the recovery of melanopsin expression could be an indication of its neuroprotective properties.

The m+RGC's contain glutamate, but they also selectively express a second neurotransmitter: Pituitary Adenylate Cyclase-Activating Polypeptide[57] (PACAP). This expression may promote ipRGCs survival, since the exogenous administration of PACAP has been documented to increase RGC survival after different injuries: i) intravitreal injection of kainic acid[377] or of NMDA[346] in mice, ii) ocular hypertension in mice[378] and iii) optic nerve transection in rats[379]. For this reason, it has been suggested that their resilience might be due to their PACAP neurotransmitter that would confer these neurons a special endurance.

The m+RGCs have been shown to upregulate thrombospondin 1 expression after optic nerve crush in mice[70] and this molecule is an extracellular matrix protein that promotes RGC regeneration[380] and regeneration may associate long term survival of RGCs.

Finally, it could also be argued that rat m+RGC resilience to different lesions could be a cell subtype-specific characteristic. Thus, in an animal model for Huntington disease it has been documented that the M1 ipRGCs were affected by the disease but the non-M1 ipRGCs were resilient[381]. This has been shown previously also for other subtypes of RGCs that respond differently to different lesions such as NMDA administration[268] or optic nerve crush[267] (see next section). For example, the alfa-RGC subtype[152,369], and the BD-RGC subtype[267] (a type of RGCs that becomes marked with reporter genes in genetically engineered mice) are more resistant to optic nerve crush and NMDA-induced excitotoxicity[267,268] whereas the J-RGCs (Junction adhesion molecules B expressing RGCs, also a type of RGC that is labelled in transgenic mice) have a particularly low survival rate[267,268]. Furthermore, even different subtypes of alfa-RGC in mice have been found to have different susceptibilities in ocular hypertension models[382,383], and after optic nerve crush[267]. Thus, the alpha OFF-transient were more susceptible to death than the alpha ON-sustained or OFF-sustained RGCs[382,383]

### 4.3. Optic nerve section causes loss of Brn3a$^+$RGCs and m$^+$RGCs

In one study presented in this Thesis we sectioned the optic nerve at its exit from the eye in rats and we observed that the lesion caused death of 41% and 92% of the Brn3a$^+$RGC population and of 86% and 63% of the m$^+$RGC population between 7 and 60 days after the lesion, respectively[212]. Thus, although all axons of Brn3a$^+$RGCs and m$^+$RGCs are lesioned, optic nerve section caused long term more death of Brn3a$^+$RGCs than of m$^+$RGCs. Other authors have also documented similar percentages of death of the general population of RGC after similar optic nerve section in rats, amounting to around 80% by 14 days after the lesion[11,12,61,65,242]. Also, other authors have found similar percentages of m$^+$RGC death after similar optic nerve section in rats, amounting to 55-65% of this population at long term periods[65]. The percentages of m$^+$RGC survival that we observed were lower at 7 and 10 days (14% and 24% respectively) than 14 and 60 days after the lesion (41% and 37%) and this indicates also a transient downregulation of melanopsin synthesis in the first 10 days after the injury. This has been documented also after other RGC lesions in rats[65,66,140,350]. Thus, the m$^+$RGC population is more resistant than the Brn3a$^+$RGC population after ON section and shows downregulation of melanopsin expression short term after injury. As reviewed in the previous sections, there are many subtypes of RGCs and differential survival and/or regenerative capacities of the various subtypes has been observed in human glaucoma and also in experimental models[70,267,268,381,384]. Also, differential m$^+$RGC survival and even of the different m$^+$RGC subtypes has been observed in various human diseases and experimental models[57,67,75,99,142,384]. Using a mouse model of Huntington's disease (HD), it has been documented that the M1 ipRGCs were more susceptible to death than the non-M1 ipRGCs[381]. In fact, in an ongoing study in which the M4 RGCs have been labelled with osteopontin and Trb2, we have observed higher proportions of M4 RGC death than of Brn3$^+$RGC or M1-M3

RGC death after optic nerve section (Gallego-Ortega, Vidal-Villegas et al. in preparation) and thus the M4 appear to be more vulnerable to this type of lesion. Various hypotheses have tried to explain the increased resistance or vulnerability of different RGC or ipRGC subtypes to different lesions (see section 2.4.). Further studies are warranted to ascertain the molecular correlates of these built-in cell characteristics as they could be used for the implementation of neuroprotective strategies against different insults.

### 4.3.1. DHF Neuroprotection

Although previous studies have documented a neuroprotective effect of DHF in several models[323,324], whether this molecule has also neuroprotective properties for RGCs had not been investigated before. In the third article presented in this Thesis[212] we document for the first time in the literature that systemically administered DHF has neuroprotective effects *in vivo* for both the Brn3a$^+$RGC and m$^+$RGC populations after optic nerve section in adult rats (see next sections). In our study, first we determined the daily i.p. dose with optimal rescuing effects on Brn3a$^+$RGCs that we found was 5mg/kg, because it rescued 95% of the Brn3a$^+$RGC population from cell death 7 days after optic nerve transection. Doses of 4 mg/mg had slightly lower but significant effects. However, doses of 1, 2, 10 or 25mg/kg did not show significant RGC rescue effects. We have postulated that, as documented in RGC-5 cells in vitro[308], small doses of DHF may protect RGCs in a dose-dependent manner, but higher doses may result in decreased protection due to the overactivation of the low affinity TrkA receptor[385,386].

#### 4.3.1.1. Neuroprotection of Brn3a$^+$RGCs

In our study[212], we find that the percentages of Brn3a$^+$RGCs that survived optic nerve section were 59%, 28%, 17%, 13%, 10% and 8% by 7, 10, 14, 21, 30 and 60 days,

respectively, after vehicle administration. However, the percentages of Brn3a$^+$RGCs that survived in the DHF treated group were 96%, 71%, 65%, 17%, 10% and 8% at the same survival periods. The numbers of surviving Brn3a+RGCs were significantly greater in the DHF treated group up to 21 days after the injury and thus we document a strong neuroprotective effect of a daily dose of DHF that lasts up to 21 days.

A recent ongoing study further examines RGC survival and retinal function after optic nerve section and vehicle or DHF administration. This study shows similar percentages of Brn3a$^+$RGC survival, and thus confirms the results documented in this Thesis. Moreover, it also documents using full field electroretinogram recordings a better preservation of the retinal function in the DHF-treated when compared to vehicle-treated retinas (Gallego-Ortega, Vidal-Villegas et al., 2021 in preparation).

The effects of optic nerve section on the population of RGCs has been characterized previously, resulting in a predictable fast and massive loss of Brn3a$^+$RGCs within the first few weeks, which then slows down but continues on for months[11,12,213,242]. The exact mechanism by which RGC death occurs after optic nerve section is not completely characterised[215–217], though previous studies suggest apoptosis as a principal component[63,64,253,272,387], and apoptosis is the type of cell death preeminent after loss of trophic support[251]. On the other hand, other studies have documented that is possible to rescue RGC from death after optic nerve section by administration of various neurotrophic factors: BDNF[63,64,253,254,261,265,320,388], NT-3[388], NT-4[254,388] and CNTF[254].

The strong neuroprotective effect of DHF that we find in our study after optic nerve section[212] is similar to that achieved in previous studies for up to 14 days after injury with a single intravitreal administration of BDNF. The neurotrophin BDNF is the neurotrophic factor that has shown greater rescue effect on RGCs after optic nerve

section[61,64,167,320]. BDNF is an endogenous neurotrophin produced by neurons (such as RGCs, amacrine cells and photoreceptors) and glial cells[389] in the retina and also in the target territories of RGCs[390,391]. Amongst its primary functions we can find neural development control, synaptogenesis modulation, and neuroprotection[385]. BDNF exerts its effects through its high affinity receptor TrkB, which is a member of the tyrosine kinase family of receptors and that is expressed by RGCs[392]. Its activation and phosphorylation stimulate the major downstream pro-survival signalling pathways, involving phosphatidylinositol 3-kinases (PI3K), phospholipase C-γ1 and mitogen-activated protein kinase (MAPK)[392,393].

DHF is a naturally occurring flavonoid found in some tree leaves[322] that has been shown to be a potent and selective agonist of the TrkB receptor, which is the main high affinity receptor of the neurotrophin BDNF. Thus, the neuroprotective effects of DHF could be due to the stimulation the BDNF TrkB receptor (see section 3.1.2.1). When compared to BDNF as a neuroprotective agent, DHF may have various advantages over BDNF, namely: it can cross the blood-brain barrier[323,325–327] due to its small size (MW 254gr/mol) and lipophilic qualities. Furthermore, DHF has a longer half-life than BDNF[327–329] and, when coupled to the TrkB receptors, elicits a stronger, faster and longer lasting response than BDNF[326,330]. Also, it has been shown that DHF displays the same neuroprotective effects as BDNF through TrkB receptor activation and autophosphorylation and initiation of survival pathways *in vivo*[323,324,394]. Furthermore, DHF has been shown to mimic the neuroprotective effects of BDNF in several CNS disease models or injuries[323,324] like Alzheimer's[395], Parkinson's[323], Huntington's[396]. DHF has also been shown to alleviate chronic intermittent hypoxia-induced oxidative stress damage of the retinal ganglion cells[397]. Finally, other TrkB agonists, for example the monoclonal antibody 29D7, have also been shown to enhance RGC survival *in*

*vitro* in adult rats[398] and *in vivo* in mice[399]. However, the potential of DHF to neuroprotect RGCs *in vivo* after optic nerve injury had not been investigated before.

In our study[212] we document neuroprotection of Brn3a$^+$RGCs for up to 21 days after optic nerve section, while the studies using BDNF documented increased RGC survival only during the first 14 days[63,64,253,254,261,265,320,388]. Previous studies have suggested that administration of BDNF has a time-limited effect due to the downregulation of TrkB that follows after chronic exposure *in vitro*[400–402]. In fact, Cheng et al.,[403] found that in rats after optic nerve section, TrkB mRNA expression rapidly decreased in RGCs to approximately 50% of the level found in intact retinas. Other studies have also documented downregulation of the RGCs TrkB receptor in animal models of glaucoma[404–406]. This suggests that injury-induced downregulation of neurotrophin receptors may limit the response of neurons to trophic factors, compromising their ability to survive [264,320,403,407].

#### 4.3.1.2. Neuroprotection of ipRGC with DHF

In our study presented in this Thesis[212], we find that the percentages of m$^+$RGCs that survived optic nerve section were 14%, 24%, 41%, 44%, 43% and 37% by 7, 10, 14, 21, 30 and 60 days, respectively, after vehicle administration. However, the percentages of Brn3a$^+$RGCs that survived in the DHF treated group were 15%, 25%, 52%, 51%, 50% and 48% at the same survival periods. We thus show that DHF protects a percentage of m$^+$RGCs after optic nerve section and that this neuroprotective effect lasts up to 60 days, the longest survival interval analysed in this study. The numbers of surviving m$^+$RGCs were significantly greater in the DHF treated group from 14 days and until the end of the study. Therefore, we show that DHF also has a very strong neuroprotective effect on the population of m$^+$RGCs, diminishing cell loss in an effect that appears permanent. It is possible that this neuroprotective effect was

present from the first survival period after after optic nerve section but was not detected due to the melanopsin expression downregulation observed in the first 10 days after the injury (see section 3.1.). As reviewed before, melanopsin expression downregulation has been observed in rats after different types of retinal lesions[66,140,213,350].

Based in the results of our study[212], we can conclude that approximately 50% of the $m^+$RGCs survive permanently in the DHF treated retinas, while 40% survive in the vehicle treated eyes. These percentages of survival were very consistent in the different survival periods analysed. The observed $m^+$RGC survival is high both in the vehicle-treated and the DHF-treated groups if we compare it with Brn3a$^+$RGC survival that was only 8% in the same groups 60 days after the injury. Thus, $m^+$RGCs show an idiosyncratic resilience to optic nerve section. Previous studies have documented that rat and mice $m^+$RGC are more resilient than of Brn3a$^+$RGC to optic nerve injury[65,213,256,352,367] but also to other injuries such as NMDA-induced excitotoxicity[140], light induced phototoxicity[350] and acute ocular hypertension[66]. Why $m^+$RGCs or even different subtypes of ipRGCs are more resistant to injury is not known at present (see section 2.4.), so future studies are still needed to unravel the mechanism of action by which they achieve this particular resilience. Furthermore, these cells may be useful to study the molecular changes after injury that confer them better or worse, as in the case of M4 (Gallego-Ortega, Vidal-Villegas et al., in preparation), survival rates and to design neuroprotective strategies.

#### 4.3.1.3. TrkB receptor activation

We document in our study presented in this Thesis[212] that DHF increases survival of Brn3a$^+$RGCs and $m^+$RGCs after optic nerve section. As DHF is a selective agonist of

the TrkB receptor, which is the high affinity receptor for BDNF[408] and BDNF has been shown to have a strong neuroprotective effect on RGCs (see Introduction, section 5.1.), it is possible that the neuroprotective effects of DHF could be due to TrkB receptor activation.

The neurotrophins are a family of structurally related factors that comprise BDNF, NGF, NT3 and NT4/5 that exert their effects by binding to the neuronal p75 and Trk receptors. The responses to the TrkB receptors are neuroprotective, while the responses to the p75NTR are both neuroprotective and neurotoxic[298]. There are three types of Trk receptor: A, B and C and the TrkB receptor is the receptor used by BDNF, NT4/5, and, less importantly, by NT3[308,409]. In the CNS, TrkB expression can be found in the brain cortex, thalamus, hippocampus, parts of the cerebellum, brain stem, spinal cord and the retina, which interests us the most[309,310,397,409–411].

In our study[212] we have used western blotting to analyse TrkB receptor phosphorylation after optic nerve section both in the vehicle and DHF treated groups. Our results document that 7 days after optic nerve section, there is significantly more TrkB phosphorylation in the group with systemic administration of DHF than in the group treated with systemic vehicle, and therefore it is likely that DHF neuroprotection is mediated in this manner. At 7 days after injury is also the time point when we observed maximal survival of Brn3a$^+$RGCs in the DHF-treated group. In fact, no significant cell death can be documented at this survival period while in the vehicle treated group 40% of the Brn3a$^+$RGC population is already lost. Other studies have also used western blot to document that the neurotrophic effect of DHF is mediated through the TrkB receptor[324,333,397,412] and various survival signalling pathways have been documented to be activated by the stimulation of the TrkB receptor that could

have neuroprotective effects in different experimental models such as optic nerve section and experimental glaucoma[397,412,413].

Several studies have pursued a number of questions raised in our studies, which tried to investigate for example, the pathways activated after DHF induced TrkB phosphorylation. Indeed, in a recent study[412], we have further examined the signalling pathways responsible for the *in vivo* afforded protection of DHF after optic nerve section, which were unknown. Moreover, whether different neuronal and nonneuronal retinal cells are involved in the DHF neuroprotection process is also unknown. This recent study documents that following optic nerve section and DHF-treatment there is TrkB activation of two signalling pathways: PI3K/AKT, and MAPK/ERK as well as the involvement of Müller cells and RGCs[412].

## 5. CONCLUSIONS

In the articles presented in this Thesis we have reached the following original conclusions:

1 The intravitreal injection of 5 µl of 100mM NMDA in adult albino rats produces:

1.1 The rapid and massive loss of between 15 and 80% of the Brn3a$^+$RGC population in the first 3 to 7 days after injury, but does not progress further (up to 15 months).

1.2 Reduction of the total retinal thickness and of the inner retinal thickness that can be measured with SD-OCT in the first 3 months after the injury, and progresses up to 15 months.

1.3 A transient downregulation of melanopsin expression by m$^+$RGCs, that is evident at 3 days after injury but recovers fully by 14 days.

1.4 No noticeable m$^+$RGC loss. Thus, intrinsically photosensitive RGCs are resistant to NMDA-induced toxicity.

2.Intraorbital optic nerve section in adult albino rats produces:

2.1. The rapid and massive loss of 80% of the Brn3a$^+$RGC population, and 60% of the m$^+$RGC population in the first 14 days after injury.

2.2. Temporary downregulation of melanopsin expression in m$^+$RGCs in the first 14 days after the injury.

3. Systemic administration of DHF (at an optimal dose of 5 mg/kg) after intraorbital nerve section produces:

3.1. Neuroprotection of the Brn3a$^+$RGC population for up to 21 days.

3.2. Neuroprotection of the m$^+$RGC population for up to 60 days.

3.3. TrkB phosphorylation in the retina.

## 6. REFERENCE LIST


1. Purves D, Augustine GJ, Fitzpatrick D, et al., eds. *Neuroscience*. Second edi. Sunderland (MA): Sinauer Associates; 2001.
2. Kuhn S, Gritti L, Crooks D, Dombrowski Y. Oligodendrocytes in Development, Myelin Generation and Beyond. *Cells*. 2019;8(11). doi:10.3390/cells8111424
3. Jessen KR, Mirsky R. The repair Schwann cell and its function in regenerating nerves. *J Physiol*. 2016;594(13):3521-3531. doi:10.1113/JP270874
4. Gradišnik L, Bošnjak R, Maver T, Velnar T. Advanced Bio-Based Polymers for Astrocyte Cell Models. *Materials (Basel)*. 2021;14(13):3664. doi:10.3390/ma14133664
5. Aguayo AJ, Rasminsky M, Bray GM, et al. Degenerative and regenerative responses of injured neurons in the central nervous system of adult mammals. *Philos Trans R Soc Lond B Biol Sci*. 1991;331(1261):337-343. doi:10.1098/rstb.1991.0025
6. FRISEN J. Determinants of axonal regeneration. *Histol Histopathol*. 1997;12(12):857-868.
7. Rotshenker S. Wallerian degeneration: the innate-immune response to traumatic nerve injury. *J Neuroinflammation*. 2011;8(1):109. doi:10.1186/1742-2094-8-109
8. Carroll SL, Worley SH. Wallerian Degeneration. *Curated Ref Collect Neurosci Biobehav Psychol*. January 2017:485-491. doi:10.1016/B978-0-12-809324-5.02077-0
9. SPERRY RW. The problem of central nervous reorganization after nerve regeneration and muscle transposition. *Q Rev Biol*. 1945;20:311-369. doi:10.1086/394990
10. Fague L, Liu YA, Marsh-Armstrong N. The basic science of optic nerve regeneration. *Ann Transl Med*. 2021;9(15):1276-1276. doi:10.21037/atm-20-5351
11. Villegas-Pérez M-PP, Vidal-Sanz M, Rasminsky M, Bray GM, Aguayo AJ. Rapid and protracted phases of retinal ganglion cell loss follow axotomy in the optic nerve of adult rats. *J Neurobiol*. 1993;24(1):23-36. doi:10.1002/neu.480240103
12. Villegas-Pérez MP, Vidal-Sanz M, Bray GM, Aguayo AJ. Influences of peripheral nerve grafts on the survival and regrowth of axotomized retinal ganglion cells in adult rats. *J Neurosci*. 1988;8(1):265-280. http://www.ncbi.nlm.nih.gov/pubmed/2448429.
13. Tello F. La influencia del neurotropismo en la regeneración de los centros nerviosos. *Trab Lab Inv BIol*. 1911;(9):123-160.
14. Leoz Ortin, G, Arcaute L. Procesos regenerativos del nervio óptico y retina con ocasión de injertos nerviosos. *Trab Lab Inv BIol*. 1913;(11):239.
15. Ramon y Cajal S. El neurotropismo y la trasplantación de los nervios. *Trab Lab Inv BIol*. 1913;(11):102.
16. Vidal-Sanz M, Bray GM, Villegas-Pérez MP, Thanos S, Aguayo AJ. Axonal regeneration and synapse formation in the superior colliculus by retinal ganglion cells in the adult rat. *J Neurosci*. 1987;7(9):2894-2909. http://www.ncbi.nlm.nih.gov/pubmed/3625278.
17. Bray GM, Villegas-Pérez MP, Vidal-Sanz M, Carter DA, Aguayo AJ. Neuronal and nonneuronal influences on retinal ganglion cell survival, axonal

regrowth, and connectivity after axotomy. *Ann N Y Acad Sci*. 1991;633:214-228. doi:10.1111/j.1749-6632.1991.tb15613.x
18. Carter DA, Bray GM, Aguayo AJ. Long-term growth and remodeling of regenerated retino-collicular connections in adult hamsters. *J Neurosci*. 1994;14(2):590-598. http://www.ncbi.nlm.nih.gov/pubmed/7507980.
19. Vidal-Sanz M, Bray GM, Aguayo AJ. Regenerated synapses persist in the superior colliculus after the regrowth of retinal ganglion cell axons. *J Neurocytol*. 1991;20(11):940-952. doi:10.1007/BF01190471
20. Dowling J. *The Retina: An Approachable Part of the Brain.* The Belknap Press; 2012.
21. Grossniklaus HE, Geisert EE, Nickerson JM. Introduction to the Retina. *Prog Mol Biol Transl Sci*. 2015;134:383-396. doi:10.1016/bs.pmbts.2015.06.001
22. Villegas-Pérez MP, Vidal-Sanz M. Fisiología de la Retina. In: García-Feijoó, Julián ; Pablo-Julvez L, ed. *Manual de Oftalmología*. 1st ed. Barcelona: Elsevier; 2012:31-38.
23. SeftonlAJ, Dreher, B and Harvey A. No Title. In: G P, ed. *The Rat Nervous System*. third. Elsevier; 2004:1083-1164.
24. Ksendzovsky A, Pomeraniec IJ, Zaghloul KA, Provencio JJ, Provencio I. Clinical implications of the melanopsin-based non-image-forming visual system. *Neurology*. 2017;88(13):1282-1290. doi:10.1212/WNL.0000000000003761
25. Esquiva G, Hannibal J. Melanopsin-expressing retinal ganglion cells in aging and disease. *Histol Histopathol*. 2019;34(12):1299-1311. doi:10.14670/HH-18-138
26. Murcia-Belmonte V, Erskine L. Wiring the Binocular Visual Pathways. *Int J Mol Sci*. 2019;20(13). doi:10.3390/ijms20133282
27. Grill-Spector K, Malach R. The human visual cortex. *Annu Rev Neurosci*. 2004;27:649-677. doi:10.1146/annurev.neuro.27.070203.144220
28. Hubel D. *Ojo, Cerebro y Visión.* Segunda. Murcia: Servicio de Publicaciones Universidad de Murcia; 2000.
29. Dacey D. Origins of perception: retinal ganglion cell diversity and the creation of parallel visual pathways. In: Gazzaniga M, ed. *The Cognitive Neurosciences*. 4th ed. Cambridge, MA: MIT press; 2009:281-301.
30. Farrow K, Isa T, Luksch H, Yonehara K. Editorial: The Superior Colliculus/Tectum: Cell Types, Circuits, Computations, Behaviors. *Front Neural Circuits*. 2019;13:39. doi:10.3389/fncir.2019.00039
31. Wu J, Yan T, Zhang Z, Jin F, Guo Q. Retinotopic mapping of the peripheral visual field to human visual cortex by functional magnetic resonance imaging. *Hum Brain Mapp*. 2012;33(7):1727-1740. doi:10.1002/hbm.21324
32. Mure LS. Intrinsically Photosensitive Retinal Ganglion Cells of the Human Retina. *Front Neurol*. 2021;12. doi:10.3389/fneur.2021.636330
33. Sondereker KB, Stabio ME, Renna JM. Crosstalk: The diversity of melanopsin ganglion cell types has begun to challenge the canonical divide between image-forming and non-image-forming vision. *J Comp Neurol*. 2020;528(12):2044-2067. doi:10.1002/cne.24873
34. Aranda ML, Schmidt TM. Diversity of intrinsically photosensitive retinal ganglion cells: circuits and functions. *Cell Mol Life Sci*. 2021;78(3):889-907. doi:10.1007/s00018-020-03641-5
35. Hattar S, Lucas RJ, Mrosovsky N, et al. Melanopsin and rod–cone photoreceptive systems account for all major accessory visual functions in

mice. *Nature*. 2003;424(6944):75-81. doi:10.1038/nature01761
36. Rosenwasser AM, Turek FW. Neurobiology of Circadian Rhythm Regulation. *Sleep Med Clin*. 2015;10(4):403-412. doi:10.1016/j.jsmc.2015.08.003
37. Fernandez DC, Fogerson PM, Lazzerini Ospri L, et al. Light Affects Mood and Learning through Distinct Retina-Brain Pathways. *Cell*. 2018;175(1):71-84.e18. doi:10.1016/j.cell.2018.08.004
38. Rupp AC, Ren M, Altimus CM, et al. Distinct ipRGC subpopulations mediate light's acute and circadian effects on body temperature and sleep. *Elife*. 2019;8. doi:10.7554/eLife.44358
39. Altimus CM, Güler AD, Villa KL, et al. Rods-cones and melanopsin detect light and dark to modulate sleep independent of image formation. *Proc Natl Acad Sci*. 2008;105(50):19998-20003. doi:10.1073/pnas.0808312105
40. Delwig A, Majumdar S, Ahern K, et al. Glutamatergic Neurotransmission from Melanopsin Retinal Ganglion Cells Is Required for Neonatal Photoaversion but Not Adult Pupillary Light Reflex. Tosini G, ed. *PLoS One*. 2013;8(12):e83974. doi:10.1371/journal.pone.0083974
41. Noseda R, Copenhagen D, Burstein R. Current understanding of photophobia, visual networks and headaches. *Cephalalgia*. 2019;39(13):1623-1634. doi:10.1177/0333102418784750
42. Ramon y Cajal S. La Rétine des Vertébrés. In: *La Cellule*. ; 1893:236-237.
43. Ramon y Cajal S. *The Structure of the Retina*. Charles C. Thomas Publisher; 1972.
44. Hoon M, Okawa H, Della Santina L, Wong ROL. Functional architecture of the retina: development and disease. *Prog Retin Eye Res*. 2014;42:44-84. doi:10.1016/j.preteyeres.2014.06.003
45. Gariano RF. Special features of human retinal angiogenesis. *Eye (Lond)*. 2010;24(3):401-407. doi:10.1038/eye.2009.324
46. Sobrado-Calvo P, Vidal-Sanz M, Villegas-Pérez MP. Rat retinal microglial cells under normal conditions, after optic nerve section, and after optic nerve section and intravitreal injection of trophic factors or macrophage inhibitory factor. *J Comp Neurol*. 2007;501(6):866-878. doi:10.1002/cne.21279
47. Silverman SM, Wong WT. Microglia in the Retina: Roles in Development, Maturity, and Disease. *Annu Rev Vis Sci*. 2018;4:45-77. doi:10.1146/annurev-vision-091517-034425
48. Reichenbach A, Bringmann A. Glia of the human retina. *Glia*. 2020;68(4):768-796. doi:10.1002/glia.23727
49. Sun Y, Smith LEH. Retinal Vasculature in Development and Diseases. *Annu Rev Vis Sci*. 2018;4:101-122. doi:10.1146/annurev-vision-091517-034018
50. Selvam S, Kumar T, Fruttiger M. Retinal vasculature development in health and disease. *Prog Retin Eye Res*. 2018;63:1-19. doi:10.1016/j.preteyeres.2017.11.001
51. Jonas, Jost B., Guggenmoos-Holzmann, I., Naumann GOH, Jonas JB, Guggenmoos-Holzmann I, Naumann GO. Cilioretinal arteries in large optic disks. *Ophthalmic Res*. 1988;20(5):269-274. doi:10.1159/000266723
52. Runkle EA, Antonetti DA. The Blood-Retinal Barrier: Structure and Functional Significance. *Methods Mol Biol*. 2011;686:133-148. doi:10.1007/978-1-60761-938-3_5
53. Blume C, Garbazza C, Spitschan M. Effects of light on human circadian rhythms, sleep and mood. *Somnologie*. 2019;23(3):147-156. doi:10.1007/s11818-019-00215-x

54. Joselevitch C. Human retinal circuitry and physiology. *Psychol Neurosci*. 2008;1(2):141-165. doi:10.3922/j.psns.2008.2.008
55. Davies WL, Foster RG, Hankins MW. Focus on molecules: melanopsin. *Exp Eye Res*. 2012;97(1):161-162. doi:10.1016/j.exer.2010.07.020
56. Hughes S, Hankins MW, Foster RG, Peirson SN. Melanopsin phototransduction: slowly emerging from the dark. *Prog Brain Res*. 2012;199(June 2016):19-40. doi:10.1016/B978-0-444-59427-3.00002-2
57. Vidal-Villegas B, Gallego-Ortega A, Miralles de Imperial-Ollero JA, Martínez de la Casa JM, García Feijoo J, Vidal-Sanz M. Células ganglionares fotosensibles: una población diminuta pero esencial. *Arch Soc Esp Oftalmol*. 2021;96(6):299-315. doi:10.1016/j.oftal.2020.06.032
58. Salazar J j, Ramírez AI, De Hoz R, et al. Anatomy of the Human Optic Nerve: Structure and Function. In: *Optic Nerve*. IntechOpen; 2019. doi:10.5772/intechopen.79827
59. Jonas JB, Schmidt AM, Müller-Bergh JA, Schlötzer-Schrehardt UM, Naumann GO. Human optic nerve fiber count and optic disc size. *Invest Ophthalmol Vis Sci*. 1992;33(6):2012-2018. http://www.ncbi.nlm.nih.gov/pubmed/1582806.
60. Kanamori A, Catrinescu M-M, Belisle JM, Costantino S, Levin LA. Retrograde and Wallerian axonal degeneration occur synchronously after retinal ganglion cell axotomy. *Am J Pathol*. 2012;181(1):62-73. doi:10.1016/j.ajpath.2012.03.030
61. Peinado-Ramón P, Salvador M, Villegas-Pérez MP, Vidal-Sanz M. Effects of axotomy and intraocular administration of NT-4, NT-3, and brain-derived neurotrophic factor on the survival of adult rat retinal ganglion cells. A quantitative in vivo study. *Invest Ophthalmol Vis Sci*. 1996;37(4):489-500. http://www.ncbi.nlm.nih.gov/pubmed/8595949.
62. Parrilla-Reverter G, Agudo M, Nadal-Nicolás F, et al. Time-course of the retinal nerve fibre layer degeneration after complete intra-orbital optic nerve transection or crush: a comparative study. *Vision Res*. 2009;49(23):2808-2825. doi:10.1016/j.visres.2009.08.020
63. Sánchez-Migallón MC, Nadal-Nicolás FM, Jiménez-López M, Sobrado-Calvo P, Vidal-Sanz M, Agudo-Barriuso M. Brain derived neurotrophic factor maintains Brn3a expression in axotomized rat retinal ganglion cells. *Exp Eye Res*. 2011;92(4):260-267. doi:10.1016/j.exer.2011.02.001
64. Sánchez-Migallón MC, Valiente-Soriano FJ, Nadal-Nicolás FM, Vidal-Sanz M, Agudo-Barriuso M. Apoptotic Retinal Ganglion Cell Death After Optic Nerve Transection or Crush in Mice: Delayed RGC Loss With BDNF or a Caspase 3 Inhibitor. *Investig Opthalmology Vis Sci*. 2016;57(1):81. doi:10.1167/iovs.15-17841
65. Nadal-Nicolás FM, Sobrado-Calvo P, Jiménez-López M, Vidal-Sanz M, Agudo-Barriuso M. Long-Term Effect of Optic Nerve Axotomy on the Retinal Ganglion Cell Layer. *Invest Ophthalmol Vis Sci*. 2015;56(10):6095-6112. doi:10.1167/iovs.15-17195
66. Rovere G, Nadal-Nicolás FM, Wang J, et al. Melanopsin-Containing or Non-Melanopsin–Containing Retinal Ganglion Cells Response to Acute Ocular Hypertension With or Without Brain-Derived Neurotrophic Factor Neuroprotection. *Investig Opthalmology Vis Sci*. 2016;57(15):6652-6661. doi:10.1167/iovs.16-20146
67. Kim US, Mahroo OA, Mollon JD, Yu-Wai-Man P. Retinal Ganglion Cells-

Diversity of Cell Types and Clinical Relevance. *Front Neurol*. 2021;12(May):661938. doi:10.3389/fneur.2021.661938
68. Vrabec F. "Displaced nerve cells" in the human retina. *Graefes Arch Clin Exp Ophthalmol*. 1986;224(2):143-146. doi:10.1007/BF02141487
69. Baden T, Berens P, Franke K, Román Rosón M, Bethge M, Euler T. The functional diversity of retinal ganglion cells in the mouse. *Nature*. 2016;529(7586):345-350. doi:10.1038/nature16468
70. Tran NM, Shekhar K, Whitney IE, et al. Single-Cell Profiles of Retinal Ganglion Cells Differing in Resilience to Injury Reveal Neuroprotective Genes. *Neuron*. 2019;104(6):1039-1055.e12. doi:10.1016/j.neuron.2019.11.006
71. Wässle H. Parallel processing in the mammalian retina. *Nat Rev Neurosci*. 2004;5(10):747-757. doi:10.1038/nrn1497
72. Sanes JR, Masland RH. The types of retinal ganglion cells: current status and implications for neuronal classification. *Annu Rev Neurosci*. 2015;38:221-246. doi:10.1146/annurev-neuro-071714-034120
73. Kolb H, Fernandez E, Nelson R. Webvision. *Webvision*. 1995:1-31. https://www.ncbi.nlm.nih.gov/books/NBK11530/. Accessed August 12, 2021.
74. Hannibal J, Christiansen AT, Heegaard S, Fahrenkrug J, Kiilgaard JF. Melanopsin expressing human retinal ganglion cells: Subtypes, distribution, and intraretinal connectivity. *J Comp Neurol*. 2017;525(8):1934-1961. doi:10.1002/cne.24181
75. Lax P, Ortuño-Lizarán I, Maneu V, Vidal-Sanz M, Cuenca N. Photosensitive Melanopsin-Containing Retinal Ganglion Cells in Health and Disease: Implications for Circadian Rhythms. *Int J Mol Sci*. 2019;20(13):3164. doi:10.3390/ijms20133164
76. Dräger UC, Olsen JF. Ganglion cell distribution in the retina of the mouse. *Invest Ophthalmol Vis Sci*. 1981;20(3):285-293. http://www.ncbi.nlm.nih.gov/pubmed/6162818.
77. Nadal-Nicolás FM, Salinas-Navarro M, Jiménez-López M, et al. Displaced retinal ganglion cells in albino and pigmented rats. *Front Neuroanat*. 2014;8(99):99. doi:10.3389/fnana.2014.00099
78. Salinas-Navarro M, Alarcón-Martínez L, Valiente-Soriano FJ, et al. Functional and morphological effects of laser-induced ocular hypertension in retinas of adult albino Swiss mice. *Mol Vis*. 2009;15:2578-2598. http://www.ncbi.nlm.nih.gov/pubmed/20011633.
79. Ortín-Martínez A, Valiente-Soriano FJ, García-Ayuso D, et al. A novel in vivo model of focal light emitting diode-induced cone-photoreceptor phototoxicity: neuroprotection afforded by brimonidine, BDNF, PEDF or bFGF. *PLoS One*. 2014;9(12):e113798. doi:10.1371/journal.pone.0113798
80. Nadal-Nicolás FM, Jiménez-López M, Sobrado-Calvo P, et al. Brn3a as a marker of retinal ganglion cells: qualitative and quantitative time course studies in naive and optic nerve-injured retinas. *Invest Ophthalmol Vis Sci*. 2009;50(8):3860-3868. doi:10.1167/iovs.08-3267
81. Nadal-Nicolás FM, Jiménez-López M, Salinas-Navarro M, et al. Whole number, distribution and co-expression of brn3 transcription factors in retinal ganglion cells of adult albino and pigmented rats. Harvey AR, ed. *PLoS One*. 2012;7(11):e49830. doi:10.1371/journal.pone.0049830
82. Ortín-Martínez A, Jiménez-López M, Nadal-Nicolás FM, et al. Automated quantification and topographical distribution of the whole population of S- and

L-cones in adult albino and pigmented rats. *Invest Ophthalmol Vis Sci*. 2010;51(6):3171-3183. doi:10.1167/iovs.09-4861
83. Salinas-Navarro M, Alarcón-Martínez L, Valiente-Soriano FJ, et al. Ocular hypertension impairs optic nerve axonal transport leading to progressive retinal ganglion cell degeneration. *Exp Eye Res*. 2010;90(1):168-183. doi:10.1016/j.exer.2009.10.003
84. Wong KY. A Retinal Ganglion Cell That Can Signal Irradiance Continuously for 10 Hours. *J Neurosci*. 2012;32(33):11478-11485. doi:10.1523/JNEUROSCI.1423-12.2012
85. Boycott BB, Wässle H. The morphological types of ganglion cells of the domestic cat's retina. *J Physiol*. 1974;240(2):397-419. doi:10.1113/jphysiol.1974.sp010616
86. Kuffler SW. DISCHARGE PATTERNS AND FUNCTIONAL ORGANIZATION OF MAMMALIAN RETINA. *J Neurophysiol*. 1953;16(1):37-68. doi:10.1152/jn.1953.16.1.37
87. Nelson R, Famiglietti E V., Kolb H. Intracellular staining reveals different levels of stratification for on- and off-center ganglion cells in cat retina. *J Neurophysiol*. 1978;41(2):472-483. doi:10.1152/jn.1978.41.2.472
88. Boia R, Ruzafa N, Aires ID, et al. Neuroprotective Strategies for Retinal Ganglion Cell Degeneration: Current Status and Challenges Ahead. *Int J Mol Sci*. 2020;21(7). doi:10.3390/ijms21072262
89. Provencio I, Jiang G, De Grip WJ, Hayes WP, Rollag MD. Melanopsin: An opsin in melanophores, brain, and eye. *Proc Natl Acad Sci U S A*. 1998;95(1):340-345. doi:10.1073/pnas.95.1.340
90. Provencio I, Rodriguez IR, Jiang G, Hayes WP, Moreira EF, Rollag MD. A novel human opsin in the inner retina. *J Neurosci*. 2000;20(2):600-605. doi:10632589
91. Berson DM. Phototransduction by Retinal Ganglion Cells That Set the Circadian Clock. *Science (80- )*. 2002;295(5557):1070-1073. doi:10.1126/science.1067262
92. Hannibal J, Hindersson P, Østergaard J, et al. Melanopsin Is Expressed in PACAP-Containing Retinal Ganglion Cells of the Human Retinohypothalamic Tract. *Investig Opthalmology Vis Sci*. 2004;45(11):4202. doi:10.1167/iovs.04-0313
93. Dacey DM, Liao H-W, Peterson BB, et al. Melanopsin-expressing ganglion cells in primate retina signal colour and irradiance and project to the LGN. *Nature*. 2005;433(7027):749-754. doi:10.1038/nature03387
94. Hattar S, Liao HW, Takao M, Berson DM, Yau KW. Melanopsin-Containing Retinal Ganglion Cells: Architecture, Projections, and Intrinsic Photosensitivity. *Science (80- )*. 2002;295(5557):1065-1070. doi:10.1126/science.1069609
95. Münch M, Kawasaki A. Intrinsically photosensitive retinal ganglion cells: classification, function and clinical implications. *Curr Opin Neurol*. 2013;26(1):45-51. doi:10.1097/WCO.0b013e32835c5e78
96. Sweeney NT, Tierney H, Feldheim DA. Tbr2 is required to generate a neural circuit mediating the pupillary light reflex. *J Neurosci*. 2014;34(16):5447-5453. doi:10.1523/JNEUROSCI.0035-14.2014
97. Mao CAC-A, Li H, Zhang Z, et al. T-box Transcription Regulator Tbr2 Is Essential for the Formation and Maintenance of Opn4/Melanopsin-Expressing Intrinsically Photosensitive Retinal Ganglion Cells. *J Neurosci*.

2014;34(39):13083-13095. doi:10.1523/JNEUROSCI.1027-14.2014
98. Do MTH. Melanopsin and the Intrinsically Photosensitive Retinal Ganglion Cells: Biophysics to Behavior. *Neuron*. 2019;104(2):205-226. doi:10.1016/j.neuron.2019.07.016
99. La Morgia C, Carelli V, Sadun AA. Retina and melanopsin neurons. *Handb Clin Neurol*. 2021;179:315-329. doi:10.1016/B978-0-12-819975-6.00020-0
100. Matsuyama T, Yamashita T, Imamoto Y, Shichida Y. Photochemical properties of mammalian melanopsin. *Biochemistry*. 2012;51(27):5454-5462. doi:10.1021/bi3004999
101. Do MTH, Kang SH, Xue T, et al. Photon capture and signalling by melanopsin retinal ganglion cells. *Nature*. 2009;457(7227):281-287. doi:10.1038/nature07682
102. Reifler AN, Chervenak AP, Dolikian ME, et al. The rat retina has five types of ganglion-cell photoreceptors. *Exp Eye Res*. 2015;130:17-28. doi:10.1016/j.exer.2014.11.010
103. Hattar S, Kumar M, Park A, et al. Central projections of melanopsin-expressing retinal ganglion cells in the mouse. *J Comp Neurol*. 2006;497(3):326-349. doi:10.1002/cne.20970
104. Brown TM, Gias C, Hatori M, et al. Melanopsin Contributions to Irradiance Coding in the Thalamo-Cortical Visual System. Rieke F, ed. *PLoS Biol*. 2010;8(12):e1000558. doi:10.1371/journal.pbio.1000558
105. Ecker JL, Dumitrescu ON, Wong KY, et al. Melanopsin-Expressing Retinal Ganglion-Cell Photoreceptors: Cellular Diversity and Role in Pattern Vision. *Neuron*. 2010;67(1):49-60. doi:10.1016/j.neuron.2010.05.023
106. Allen AE, Storchi R, Martial FP, Bedford RA, Lucas RJ. Melanopsin Contributions to the Representation of Images in the Early Visual System. *Curr Biol*. 2017;27(11):1623-1632.e4. doi:10.1016/j.cub.2017.04.046
107. Allen AE, Martial FP, Lucas RJ. Form vision from melanopsin in humans. *Nat Commun*. 2019;10(1):2274. doi:10.1038/s41467-019-10113-3
108. Schmidt TM, Chen S-K, Hattar S. Intrinsically photosensitive retinal ganglion cells: many subtypes, diverse functions. *Trends Neurosci*. 2011;34(11):572-580. doi:10.1016/j.tins.2011.07.001
109. Seabrook TA, Burbridge TJ, Crair MC, Huberman AD. Architecture, Function, and Assembly of the Mouse Visual System. *Annu Rev Neurosci*. 2017;40(1):499-538. doi:10.1146/annurev-neuro-071714-033842
110. Duda M, Domagalik A, Orlowska-Feuer P, et al. Melanopsin: From a small molecule to brain functions. *Neurosci Biobehav Rev*. 2020;113(March):190-203. doi:10.1016/j.neubiorev.2020.03.012
111. Walch OJ, Zhang LS, Reifler AN, Dolikian ME, Forger DB, Wong KY. Characterizing and modeling the intrinsic light response of rat ganglion-cell photoreceptors. *J Neurophysiol*. 2015;114(5):2955-2966. doi:10.1152/jn.00544.2015
112. Brown TM, Tsujimura S-I, Allen AE, et al. Melanopsin-based brightness discrimination in mice and humans. *Curr Biol*. 2012;22(12):1134-1141. doi:10.1016/j.cub.2012.04.039
113. Hicks D. Second sight? Ecker JL, Dumitrescu ON, Wong KY, Alam NM, Chen SK, LeGates T, Renna JM, Prusky GT, Berson DM, Hattar S (2010) Melanopsin-expressing retinal ganglion-cell photoreceptors: cellular diversity and role in pattern vision. Neuron 67:49-60. *Graefes Arch Clin Exp Ophthalmol*. 2011;249(3):313-314. doi:10.1007/s00417-011-1631-y

114. Freedman MS, Lucas RJ, Soni B, et al. Regulation of mammalian circadian behavior by non-rod, non-cone, ocular photoreceptors. *Science*. 1999;284(5413):502-504. doi:10.1126/science.284.5413.502
115. Lucas RJ, Douglas RH, Foster RG. Characterization of an ocular photopigment capable of driving pupillary constriction in mice. *Nat Neurosci*. 2001;4(6):621-626. doi:10.1038/88443
116. Lucas RJ, Foster RG. Neither functional rod photoreceptors nor rod or cone outer segments are required for the photic inhibition of pineal melatonin. *Endocrinology*. 1999;140(4):1520-1524. doi:10.1210/endo.140.4.6672
117. Schmidt TM, Alam NM, Chen S, et al. A role for melanopsin in alpha retinal ganglion cells and contrast detection. *Neuron*. 2014;82(4):781-788. doi:10.1016/j.neuron.2014.03.022
118. Zaidi FH, Hull JT, Peirson SN, et al. Short-wavelength light sensitivity of circadian, pupillary, and visual awareness in humans lacking an outer retina. *Curr Biol*. 2007;17(24):2122-2128. doi:10.1016/j.cub.2007.11.034
119. Lucas RJ, Hattar S, Takao M, Berson DM, Foster RG, Yau KW. Diminished Pupillary Light Reflex at High Irradiances in Melanopsin-Knockout Mice. *Science (80- )*. 2003;299(5604):245-247. doi:10.1126/science.1077293
120. Güler AD, Ecker JL, Lall GS, et al. Melanopsin cells are the principal conduits for rod–cone input to non-image-forming vision. *Nature*. 2008;453(7191):102-105. doi:10.1038/nature06829
121. Hatori M, Le H, Vollmers C, et al. Inducible Ablation of Melanopsin-Expressing Retinal Ganglion Cells Reveals Their Central Role in Non-Image Forming Visual Responses. Hendricks M, ed. *PLoS One*. 2008;3(6):e2451. doi:10.1371/journal.pone.0002451
122. Zhao X, Stafford BK, Godin AL, King WM, Wong KY. Photoresponse diversity among the five types of intrinsically photosensitive retinal ganglion cells. *J Physiol*. 2014;592(7):1619-1636. doi:10.1113/jphysiol.2013.262782
123. Chen S-KS-K, Badea TC, Hattar S. Photoentrainment and pupillary light reflex are mediated by distinct populations of ipRGCs. *Nature*. 2011;476(7358):92-95. doi:10.1038/nature10206
124. Hannibal J, Hindersson P, Knudsen SM, Georg B, Fahrenkrug J. The Photopigment Melanopsin Is Exclusively Present in Pituitary Adenylate Cyclase-Activating Polypeptide-Containing Retinal Ganglion Cells of the Retinohypothalamic Tract. *J Neurosci*. 2002;22(1):RC191-RC191. doi:10.1523/JNEUROSCI.22-01-j0002.2002
125. Berson DM, Castrucci AM, Provencio I. Morphology and mosaics of melanopsin-expressing retinal ganglion cell types in mice. *J Comp Neurol*. 2010;518:NA-NA. doi:10.1002/cne.22381
126. Lazzerini Ospri L, Prusky G, Hattar S. Mood, the Circadian System, and Melanopsin Retinal Ganglion Cells. *Annu Rev Neurosci*. 2017;40(1):539-556. doi:10.1146/annurev-neuro-072116-031324
127. Estevez ME, Fogerson PM, Ilardi MC, et al. Form and Function of the M4 Cell, an Intrinsically Photosensitive Retinal Ganglion Cell Type Contributing to Geniculocortical Vision. *J Neurosci*. 2012;32(39):13608-13620. doi:10.1523/JNEUROSCI.1422-12.2012
128. Stabio ME, Sabbah S, Quattrochi LE, et al. The M5 Cell: A Color-Opponent Intrinsically Photosensitive Retinal Ganglion Cell. *Neuron*. 2018;97(1):150-163.e4. doi:10.1016/j.neuron.2017.11.030
129. Quattrochi LE, Stabio ME, Kim I, et al. The M6 cell: A small-field bistratified

photosensitive retinal ganglion cell. *J Comp Neurol*. 2019;527(1):297-311. doi:10.1002/cne.24556

130. Berg DJ, Kartheiser K, Leyrer M, Saali A, Berson DM. Transcriptomic Signatures of Postnatal and Adult Intrinsically Photosensitive Ganglion Cells. *eneuro*. 2019;6(4):ENEURO.0022-19.2019. doi:10.1523/ENEURO.0022-19.2019
131. Baver SB, Pickard GEGEGE, Sollars PJ, Pickard GEGEGE. Two types of melanopsin retinal ganglion cell differentially innervate the hypothalamic suprachiasmatic nucleus and the olivary pretectal nucleus. *Eur J Neurosci*. 2008;27(7):1763-1770. doi:10.1111/j.1460-9568.2008.06149.x
132. Fernandez DC, Chang Y-T, Hattar S, Chen S-K. Architecture of retinal projections to the central circadian pacemaker. *Proc Natl Acad Sci U S A*. 2016;113(21):6047-6052. doi:10.1073/pnas.1523629113
133. Li JY, Schmidt TM. Divergent projection patterns of M1 ipRGC subtypes. *J Comp Neurol*. 2018;526(13):2010-2018. doi:10.1002/cne.24469
134. Schmidt TM, Do MTH, Dacey D, Lucas R, Hattar S, Matynia A. Melanopsin-Positive Intrinsically Photosensitive Retinal Ganglion Cells: From Form to Function. *J Neurosci*. 2011;31(45):16094-16101. doi:10.1523/JNEUROSCI.4132-11.2011
135. Sonoda T, Okabe Y, Schmidt TM. Overlapping morphological and functional properties between M4 and M5 intrinsically photosensitive retinal ganglion cells. *J Comp Neurol*. 2020;528(6):1028-1040. doi:10.1002/cne.24806
136. Schroeder MM, Harrison KR, Jaeckel ER, et al. The Roles of Rods, Cones, and Melanopsin in Photoresponses of M4 Intrinsically Photosensitive Retinal Ganglion Cells (ipRGCs) and Optokinetic Visual Behavior. *Front Cell Neurosci*. 2018;12:203. doi:10.3389/fncel.2018.00203
137. Walmsley L, Hanna L, Mouland J, et al. Colour As a Signal for Entraining the Mammalian Circadian Clock. Kramer A, ed. *PLOS Biol*. 2015;13(4):e1002127. doi:10.1371/journal.pbio.1002127
138. Quattrochi LE, Stabio ME, Kim I, et al. The M6 cell: A small-field bistratified photosensitive retinal ganglion cell. *J Comp Neurol*. 2019;527(1):297-311. doi:10.1002/cne.24556
139. Galindo-Romero C, Jiménez-López M, García-Ayuso D, et al. Number and spatial distribution of intrinsically photosensitive retinal ganglion cells in the adult albino rat. *Exp Eye Res*. 2013;108:84-93. doi:10.1016/j.exer.2012.12.010
140. Vidal-Villegas B, Di Pierdomenico J, Miralles de Imperial-Ollero JA, et al. Melanopsin+RGCs Are fully Resistant to NMDA-Induced Excitotoxicity. *Int J Mol Sci*. 2019;20(12):3012. doi:10.3390/ijms20123012
141. Vidal-Sanz M, Valiente-Soriano FJ, Ortín-Martínez A, et al. Retinal neurodegeneration in experimental glaucoma. *Prog Brain Res*. 2015;220:1-35. doi:10.1016/bs.pbr.2015.04.008
142. Vidal-Sanz M, Nadal-Nicolás FM, Valiente-Soriano FJ, Agudo-Barriuso M, Villegas-Pérez MP. Identifying specific RGC types may shed light on their idiosyncratic responses to neuroprotection. *Neural Regen Res*. 2015;10(8):1228-1230. doi:10.4103/1673-5374.162751
143. Valiente-Soriano FJ, GarcÃ-a-Ayuso D, OrtÃ-n-MartÃ-nez A, et al. Distribution of melanopsin positive neurons in pigmented and albino mice: evidence for melanopsin interneurons in the mouse retina. *Front Neuroanat*. 2014;8(20):131. doi:10.3389/fnana.2014.00131
144. LeGates TA, Fernandez DC, Hattar S. Light as a central modulator of

circadian rhythms, sleep and affect. *Nat Rev Neurosci*. 2014;15(7):443-454. doi:10.1038/nrn3743
145. Hannibal J, Georg B, Hindersson P, Fahrenkrug J. Light and Darkness Regulate Melanopsin in the Retinal Ganglion Cells of the Albino Wistar Rat. *J Mol Neurosci*. 2005;27(2):147-156. doi:10.1385/JMN:27:2:147
146. Hannibal J, Georg B, Fahrenkrug J. Melanopsin changes in neonatal albino rat independent of rods and cones. *Neuroreport*. 2007;18(1):81-85. doi:10.1097/WNR.0b013e328010ff56
147. Hannibal J, Georg B, Fahrenkrug J. Differential expression of melanopsin mRNA and protein in Brown Norwegian rats. *Exp Eye Res*. 2013;106:55-63. doi:10.1016/j.exer.2012.11.006
148. Pires SS, Hughes S, Turton M, et al. Differential Expression of Two Distinct Functional Isoforms of Melanopsin (Opn4) in the Mammalian Retina. *J Neurosci*. 2009;29(39):12332-12342. doi:10.1523/JNEUROSCI.2036-09.2009
149. Jagannath A, Hughes S, Abdelgany A, et al. Isoforms of Melanopsin Mediate Different Behavioral Responses to Light. *Curr Biol*. 2015;25(18):2430-2434. doi:10.1016/j.cub.2015.07.071
150. Hughes S, Jagannath A, Rodgers J, Hankins MW, Peirson SN, Foster RG. Signalling by melanopsin (OPN4) expressing photosensitive retinal ganglion cells. *Eye (Lond)*. 2016;30(2):247-254. doi:10.1038/eye.2015.264
151. Sonoda T, Lee SK, Birnbaumer L, Schmidt TM. Melanopsin Phototransduction Is Repurposed by ipRGC Subtypes to Shape the Function of Distinct Visual Circuits. *Neuron*. 2018;99(4):754-767.e4. doi:10.1016/j.neuron.2018.06.032
152. Duan X, Qiao M, Bei F, Kim I-J, He Z, Sanes JR. Subtype-Specific Regeneration of Retinal Ganglion Cells following Axotomy: Effects of Osteopontin and mTOR Signaling. *Neuron*. 2015;85(6):1244-1256. doi:10.1016/j.neuron.2015.02.017
153. Delwig A, Larsen DD, Yasumura D, Yang CF, Shah NM, Copenhagen DR. Retinofugal Projections from Melanopsin-Expressing Retinal Ganglion Cells Revealed by Intraocular Injections of Cre-Dependent Virus. Badea TC, ed. *PLoS One*. 2016;11(2):e0149501. doi:10.1371/journal.pone.0149501
154. Sondereker KB, Onyak JR, Islam SW, Ross CL, Renna JM. Melanopsin ganglion cell outer retinal dendrites: Morphologically distinct and asymmetrically distributed in the mouse retina. *J Comp Neurol*. 2017;525(17):3653-3665. doi:10.1002/cne.24293
155. Bleckert A, Schwartz GW, Turner MH, Rieke F, Wong ROL. Visual space is represented by nonmatching topographies of distinct mouse retinal ganglion cell types. *Curr Biol*. 2014;24(3):310-315. doi:10.1016/j.cub.2013.12.020
156. Dreher B, Sefton AJ, Ni SY, Nisbett G. The morphology, number, distribution and central projections of Class I retinal ganglion cells in albino and hooded rats. *Brain Behav Evol*. 1985;26(1):10-48. doi:10.1159/000118764
157. Gooley JJ, Lu J, Fischer D, Saper CB. A Broad Role for Melanopsin in Nonvisual Photoreception. *J Neurosci*. 2003;23(18):7093-7106. doi:10.1523/JNEUROSCI.23-18-07093.2003
158. Lewandowski MH, Usarek A. Effects of intergeniculate leaflet lesions on circadian rhythms in the mouse. *Behav Brain Res*. 2002;128(1):13-17. doi:10.1016/S0166-4328(01)00264-9
159. Liao H, Ren X, Peterson BB, et al. Melanopsin-expressing ganglion cells on macaque and human retinas form two morphologically distinct populations. *J*

*Comp Neurol*. 2016;524(14):2845-2872. doi:10.1002/cne.23995
160. Sefton A, Dreher B, Harvey A. The Rat Visual System. In: Paxinos G, ed. *The Rat Nervous System*. third. London: Elsevier; 2004:1083-1164.
161. LeVere TE. The primary visual system of the rat: A primer of its anatomy. *Physiol Psychol*. 1978;6(2):142-169. doi:10.3758/BF03326707
162. Szél A, Röhlich P. Two cone types of rat retina detected by anti-visual pigment antibodies. *Exp Eye Res*. 1992;55(1):47-52. doi:10.1016/0014-4835(92)90090-f
163. Carter-Dawson LD, LaVail MM. Rods and cones in the mouse retina. I. Structural analysis using light and electron microscopy. *J Comp Neurol*. 1979;188(2):245-262. doi:10.1002/cne.901880204
164. Jeon C-JJ, Strettoi E, Masland RH. The Major Cell Populations of the Mouse Retina. *J Neurosci*. 1998;18(21):8936-8946. doi:10.1523/JNEUROSCI.18-21-08936.1998
165. Masland RH. The fundamental plan of the retina. *Nat Neurosci*. 2001;4(9):877-886. doi:10.1038/nn0901-877
166. Williams RW, Strom RC, Rice DS, Goldowitz D. Genetic and environmental control of variation in retinal ganglion cell number in mice. *J Neurosci*. 1996;16(22):7193-7205. http://www.ncbi.nlm.nih.gov/pubmed/8929428.
167. Valiente-Soriano FJ, Nadal-Nicolás FM, Salinas-Navarro M, et al. BDNF Rescues RGCs But Not Intrinsically Photosensitive RGCs in Ocular Hypertensive Albino Rat Retinas. *Invest Ophthalmol Vis Sci*. 2015;56(3):1924-1936. doi:10.1167/iovs.15-16454
168. Agudo-Barriuso M, Nadal-Nicolás F, Madeira M, Rovere G, Vidal-Villegas B, Vidal-Sanz M. Melanopsin expression is an indicator of the well-being of melanopsin-expressing retinal ganglion cells but not of their viability. *Neural Regen Res*. 2016;11(8):1243. doi:10.4103/1673-5374.189182
169. Perry VH. The ganglion cell layer of the retina of the rat: a Golgi study. *Proc R Soc London Ser B, Biol Sci*. 1979;204(1156):363-375. doi:10.1098/rspb.1979.0033
170. Fitzgibbon T, Reese BE. Organization of retinal ganglion cell axons in the optic fiber layer and nerve of fetal ferrets. *Vis Neurosci*. 13(5):847-861. doi:10.1017/s095252380000910x
171. Guillery RW, Mason CA, Taylor JS. Developmental determinants at the mammalian optic chiasm. *J Neurosci*. 1995;15(7 Pt 1):4727-4737. http://www.ncbi.nlm.nih.gov/pubmed/7623106.
172. Jeffery G. Architecture of the Optic Chiasm and the Mechanisms That Sculpt Its Development. *Physiol Rev*. 2001;81(4):1393-1414. doi:10.1152/physrev.2001.81.4.1393
173. Howell GR, Libby RT, Jakobs TC, et al. Axons of retinal ganglion cells are insulted in the optic nerve early in DBA/2J glaucoma. *J Cell Biol*. 2007;179(7):1523-1537. doi:10.1083/jcb.200706181
174. Jeffery G. Distribution and trajectory of uncrossed axons in the optic nerves of pigmented and albino rats. *J Comp Neurol*. 1989;289(3):462-466. doi:10.1002/cne.902890310
175. May CA, Lütjen-Drecoll E. Morphology of the murine optic nerve. *Invest Ophthalmol Vis Sci*. 2002;43(7):2206-2212. http://www.ncbi.nlm.nih.gov/pubmed/12091418.
176. Schlamp CL, Li Y, Dietz JA, Janssen KT, Nickells RW. Progressive ganglion cell loss and optic nerve degeneration in DBA/2J mice is variable and

asymmetric. *BMC Neurosci*. 2006;7:66. doi:10.1186/1471-2202-7-66
177. Lund RD, Land PW, Boles J. Normal and abnormal uncrossed retinotectal pathways in rats: an HRP study in adults. *J Comp Neurol*. 1980;189(4):711-720. doi:10.1002/cne.901890407
178. Colello SJ, Guillery RW. The changing pattern of fibre bundles that pass through the optic chiasm of mice. *Eur J Neurosci*. 1998;10(12):3653-3663. doi:10.1046/j.1460-9568.1998.00416.x
179. Lund RD. Uncrossed Visual Pathways of Hooded and Albino Rats. *Science*. 1965;149(3691):1506-1507. doi:10.1126/science.149.3691.1506
180. Linden R, Perry VH. Massive retinotectal projection in rats. *Brain Res*. 1983;272(1):145-149. doi:10.1016/0006-8993(83)90371-2
181. Rice DS, Williams RW, Goldowitz D. Genetic control of retinal projections in inbred strains of albino mice. *J Comp Neurol*. 1995;354(3):459-469. doi:10.1002/cne.903540312
182. Mason C, Slavi N. Retinal Ganglion Cell Axon Wiring Establishing the Binocular Circuit. *Annu Rev Vis Sci*. 2020;6:215-236. doi:10.1146/annurev-vision-091517-034306
183. Hofbauer A, Dräger UC. Depth segregation of retinal ganglion cells projecting to mouse superior colliculus. *J Comp Neurol*. 1985;234(4):465-474. doi:10.1002/cne.902340405
184. Martin PR. The projection of different retinal ganglion cell classes to the dorsal lateral geniculate nucleus in the hooded rat. *Exp brain Res*. 1986;62(1):77-88. doi:10.1007/BF00237404
185. Kondo Y, Takada M, Honda Y, Mizuno N. Bilateral projections of single retinal ganglion cells to the lateral geniculate nuclei and superior colliculi in the albino rat. *Brain Res*. 1993;608(2):204-215. doi:10.1016/0006-8993(93)91460-a
186. Anderson KJ, Borja MA, Cotman CW, Moffett JR, Namboodiri MA, Neale JH. N-acetylaspartylglutamate identified in the rat retinal ganglion cells and their projections in the brain. *Brain Res*. 1987;411(1):172-177. doi:10.1016/0006-8993(87)90696-2
187. Fleming MD, Benca RM, Behan M. Retinal projections to the subcortical visual system in congenic albino and pigmented rats. *Neuroscience*. 2006;143(3):895-904. doi:10.1016/j.neuroscience.2006.08.016
188. Badea TC, Williams J, Smallwood P, Shi M, Motajo O, Nathans J. Combinatorial expression of Brn3 transcription factors in somatosensory neurons: genetic and morphologic analysis. *J Neurosci*. 2012;32(3):995-1007. doi:10.1523/JNEUROSCI.4755-11.2012
189. Morin LP, Studholme KM. Retinofugal projections in the mouse. *J Comp Neurol*. 2014;522(16):3733-3753. doi:10.1002/cne.23635
190. Martersteck EM, Hirokawa KE, Evarts M, et al. Diverse Central Projection Patterns of Retinal Ganglion Cells. *Cell Rep*. 2017;18(8):2058-2072. doi:10.1016/j.celrep.2017.01.075
191. Parmhans N, Fuller AD, Nguyen E, et al. Identification of retinal ganglion cell types and brain nuclei expressing the transcription factor Brn3c/Pou4f3 using a Cre recombinase knock-in allele. *J Comp Neurol*. 2021;529(8):1926-1953. doi:10.1002/cne.25065
192. Perry VH. Evidence for an amacrine cell system in the ganglion cell layer of the rat retina. *Neuroscience*. 1981;6(5):931-944. doi:10.1016/0306-4522(81)90174-3

193. Saleeba C, Dempsey B, Le S, Goodchild A, McMullan S. A Student's Guide to Neural Circuit Tracing. *Front Neurosci*. 2019;13. doi:10.3389/fnins.2019.00897
194. Hendelman WJ, Marshall KC. Axonal projection patterns visualized with horseradish peroxidase in organized cultures of cerebellum. *Neuroscience*. 1980;5(11):1833-1846. doi:10.1016/0306-4522(80)90033-0
195. LaVail JH, LaVail MM. Retrograde axonal transport in the central nervous system. *Science*. 1972;176(4042):1416-1417. doi:10.1126/science.176.4042.1416
196. Hansson HA. Uptake and intracellular bidirectional transport of horseradish peroxidase in retinal ganglion cells. *Exp Eye Res*. 1973;16(5):377-388. doi:10.1016/0014-4835(73)90132-2
197. Bunt AH, Lund RD, Lund JS. Retrograde axonal transport of horseradish peroxidase by ganglion cells of the albino rat retina. *Brain Res*. 1974;73(2):215-228. doi:10.1016/0006-8993(74)91045-2
198. So KF, Aguayo AJ. Lengthy regrowth of cut axons from ganglion cells after peripheral nerve transplantation into the retina of adult rats. *Brain Res*. 1985;328(2):349-354. doi:10.1016/0006-8993(85)91047-9
199. Picanço-Diniz CW, Silveira LC, Yamada ES, Martin KA. Biocytin as a retrograde tracer in the mammalian visual system. *Brazilian J Med Biol Res = Rev Bras Pesqui medicas e Biol*. 1992;25(1):57-62. http://www.ncbi.nlm.nih.gov/pubmed/1304945.
200. Gerfen CR, O'Leary DD, Cowan WM. A note on the transneuronal transport of wheat germ agglutinin-conjugated horseradish peroxidase in the avian and rodent visual systems. *Exp brain Res*. 1982;48(3):443-448. doi:10.1007/BF00238621
201. Galli L, Rao K, Lund RD. Transplanted rat retinae do not project in a topographic fashion on the host tectum. *Exp brain Res*. 1989;74(2):427-430. doi:10.1007/BF00248878
202. Vidal-Sanz M, Villegas-Pérez MP, Bray GM, Aguayo AJ. Persistent retrograde labeling of adult rat retinal ganglion cells with the carbocyanine dye diI. *Exp Neurol*. 1988;102(1):92-101. doi:10.1016/0014-4886(88)90081-7
203. Dann JF, Buhl EH. Retinal ganglion cells projecting to the accessory optic system in the rat. *J Comp Neurol*. 1987;262(1):141-158. doi:10.1002/cne.902620111
204. Huxlin KR, Goodchild AK. Retinal ganglion cells in the albino rat: revised morphological classification. *J Comp Neurol*. 1997;385(2):309-323. http://www.ncbi.nlm.nih.gov/pubmed/9268130.
205. Thanos S. Specific transcellular carbocyanine-labelling of rat retinal microglia during injury-induced neuronal degeneration. *Neurosci Lett*. 1991;127(1):108-112. doi:10.1016/0304-3940(91)90906-a
206. Beale R, Osborne NN. Localization of the Thy-1 antigen to the surfaces of rat retinal ganglion cells. *Neurochem Int*. 1982;4(6):587-595. doi:10.1016/0197-0186(82)90049-3
207. Bernstein SL, Koo JH, Slater BJ, Guo Y, Margolis FL. Analysis of optic nerve stroke by retinal Bex expression. *Mol Vis*. 2006;12:147-155. http://www.ncbi.nlm.nih.gov/pubmed/16541015.
208. Díaz F, Villena A, Moreno M, et al. Effects of a non-selective beta-blocker on adult rat anterograde axonal transport and retinal ganglion layer after increased intraocular pressure. *Histol Histopathol*. 2005;20(4):1077-1084.

doi:10.14670/HH-20.1077
209. Kwong JMK, Caprioli J, Piri N. RNA binding protein with multiple splicing: a new marker for retinal ganglion cells. *Invest Ophthalmol Vis Sci*. 2010;51(2):1052-1058. doi:10.1167/iovs.09-4098
210. Rodriguez AR, de Sevilla Müller LP, Brecha NC. The RNA binding protein RBPMS is a selective marker of ganglion cells in the mammalian retina. *J Comp Neurol*. 2014;522(6):1411-1443. doi:10.1002/cne.23521
211. Siddiqui AM, Sabljic TF, Koeberle PD, Ball AK. Downregulation of BM88 after optic nerve injury. *Invest Ophthalmol Vis Sci*. 2014;55(3):1919-1929. doi:10.1167/iovs.13-12986
212. Vidal-Villegas B, Di Pierdomenico J, Gallego-Ortega A, et al. Systemic treatment with 7,8-Dihydroxiflavone activates TtkB and affords protection of two different retinal ganglion cell populations against axotomy in adult rats. *Exp Eye Res*. 2021;210:108694. doi:10.1016/j.exer.2021.108694
213. Nadal-Nicolás FM, Madeira MH, Salinas-Navarro M, et al. Transient Downregulation of Melanopsin Expression After Retrograde Tracing or Optic Nerve Injury in Adult Rats. *Investig Opthalmology Vis Sci*. 2015;56(8):4309. doi:10.1167/iovs.15-16963
214. Chidlow G, Casson RJ, Sobrado-Calvo P, Vidal-Sanz M, Osborne NN. Measurement of retinal injury in the rat after optic nerve transection: An RT-PCR study. *Mol Vis*. 2005;11:387-396.
215. Agudo M, Pérez-Marín MC, Lönngren U, et al. Time course profiling of the retinal transcriptome after optic nerve transection and optic nerve crush. *Mol Vis*. 2008;14:1050-1063.
216. Agudo M, Pérez-Marín MC, Sobrado-Calvo P, et al. Immediate Upregulation of Proteins Belonging to Different Branches of the Apoptotic Cascade in the Retina after Optic Nerve Transection and Optic Nerve Crush. *Investig Opthalmology Vis Sci*. 2009;50(1):424. doi:10.1167/iovs.08-2404
217. Agudo-Barriuso M, Lahoz A, Nadal-Nicolás FM, et al. Metabolomic Changes in the Rat Retina After Optic Nerve Crush. *Investig Opthalmology Vis Sci*. 2013;54(6):4249. doi:10.1167/iovs.12-11451
218. Agostinone J, Di Polo A. Retinal ganglion cell dendrite pathology and synapse loss. In: *Progress in Brain Research*. Vol 220. Elsevier B.V.; 2015:199-216. doi:10.1016/bs.pbr.2015.04.012
219. Surgucheva I, Weisman AD, Goldberg JL, Shnyra A, Surguchov A. Gamma-synuclein as a marker of retinal ganglion cells. *Mol Vis*. 2008;14:1540-1548. http://www.ncbi.nlm.nih.gov/pubmed/18728752.
220. Feng G, Mellor RH, Bernstein M, et al. Imaging neuronal subsets in transgenic mice expressing multiple spectral variants of GFP. *Neuron*. 2000;28(1):41-51. doi:10.1016/s0896-6273(00)00084-2
221. Leung CK, Weinreb RN, Li ZW, et al. Long-term in vivo imaging and measurement of dendritic shrinkage of retinal ganglion cells. *Invest Ophthalmol Vis Sci*. 2011;52(3):1539-1547. doi:10.1167/iovs.10-6012
222. Thanos S, Indorf L, Naskar R. In vivo FM: using conventional fluorescence microscopy to monitor retinal neuronal death in vivo. *Trends Neurosci*. 2002;25(9):441-444. doi:10.1016/s0166-2236(02)02246-4
223. Smith CA, Chauhan BC. Imaging retinal ganglion cells: enabling experimental technology for clinical application. *Prog Retin Eye Res*. 2015;44:1-14. doi:10.1016/j.preteyeres.2014.10.003
224. Smith CA, Chauhan BC. In vivo imaging of adeno-associated viral vector

labelled retinal ganglion cells. *Sci Rep*. 2018;8(1):1490. doi:10.1038/s41598-018-19969-9
225. Cordeiro MF, Migdal C, Bloom P, Fitzke FW, Moss SE. Imaging apoptosis in the eye. *Eye (Lond)*. 2011;25(5):545-553. doi:10.1038/eye.2011.64
226. Qiu X, Johnson JR, Wilson BS, Gammon ST, Piwnica-Worms D, Barnett EM. Single-cell resolution imaging of retinal ganglion cell apoptosis in vivo using a cell-penetrating caspase-activatable peptide probe. *PLoS One*. 2014;9(2):e88855. doi:10.1371/journal.pone.0088855
227. Badea TC, Cahill H, Ecker J, Hattar S, Nathans J. Distinct roles of transcription factors brn3a and brn3b in controlling the development, morphology, and function of retinal ganglion cells. *Neuron*. 2009;61(6):852-864. doi:10.1016/j.neuron.2009.01.020
228. Badea TC, Nathans J. Quantitative analysis of neuronal morphologies in the mouse retina visualized by using a genetically directed reporter. *J Comp Neurol*. 2004;480(4):331-351. doi:10.1002/cne.20304
229. Nadal-Nicolás FM, Valiente-Soriano FJ, Salinas-Navarro M, Jiménez-López M, Vidal-Sanz M, Agudo-Barriuso M. Retino-retinal projection in juvenile and young adult rats and mice. *Exp Eye Res*. 2015;134:47-52. doi:10.1016/j.exer.2015.03.015
230. Galindo-Romero C, Avilés-Trigueros M, Jiménez-López M, et al. Axotomy-induced retinal ganglion cell death in adult mice: quantitative and topographic time course analyses. *Exp Eye Res*. 2011;92(5):377-387. doi:10.1016/j.exer.2011.02.008
231. Quina LA, Pak W, Lanier J, et al. Brn3a-expressing retinal ganglion cells project specifically to thalamocortical and collicular visual pathways. *J Neurosci*. 2005;25(50):11595-11604. doi:10.1523/JNEUROSCI.2837-05.2005
232. García-Ayuso D, Salinas-Navarro M, Agudo M, et al. Retinal ganglion cell numbers and delayed retinal ganglion cell death in the P23H rat retina. *Exp Eye Res*. 2010;91(6):800-810. doi:10.1016/j.exer.2010.10.003
233. García-Ayuso D, Salinas-Navarro M, Agudo-Barriuso M, Alarcón-Martínez L, Vidal-Sanz M, Villegas-Pérez MP. Retinal ganglion cell axonal compression by retinal vessels in light-induced retinal degeneration. *Mol Vis*. 2011;17:1716-1733. http://www.ncbi.nlm.nih.gov/pubmed/21738401.
234. Huang D, Swanson EA, Lin CP, et al. Optical coherence tomography. *Science*. 1991;254(5035):1178-1181. doi:10.1126/science.1957169
235. Fujimoto J, Swanson E. The Development, Commercialization, and Impact of Optical Coherence Tomography. *Invest Ophthalmol Vis Sci*. 2016;57(9):OCT1-OCT13. doi:10.1167/iovs.16-19963
236. Adhi M, Duker JS. Optical coherence tomography--current and future applications. *Curr Opin Ophthalmol*. 2013;24(3):213-221. doi:10.1097/ICU.0b013e32835f8bf8
237. Spaide RF, Fujimoto JG, Waheed NK, Sadda SR, Staurenghi G. Optical coherence tomography angiography. *Prog Retin Eye Res*. 2018;64:1-55. doi:10.1016/j.preteyeres.2017.11.003
238. Schuman JS, Pedut-Kloizman T, Pakter H, et al. Optical coherence tomography and histologic measurements of nerve fiber layer thickness in normal and glaucomatous monkey eyes. *Invest Ophthalmol Vis Sci*. 2007;48(8):3645. doi:10.1167/iovs.06-0876
239. Nagata A, Higashide T, Ohkubo S, Takeda H, Sugiyama K. In vivo quantitative evaluation of the rat retinal nerve fiber layer with optical

coherence tomography. *Invest Ophthalmol Vis Sci*. 2009;50(6):2809-2815. doi:10.1167/iovs.08-2764
240. Gabriele ML, Ishikawa H, Schuman JS, et al. Reproducibility of Spectral-Domain Optical Coherence Tomography Total Retinal Thickness Measurements in Mice. *Investig Opthalmology Vis Sci*. 2010;51(12):6519. doi:10.1167/iovs.10-5662
241. McLellan GJ, Rasmussen CA. Optical coherence tomography for the evaluation of retinal and optic nerve morphology in animal subjects: practical considerations. *Vet Ophthalmol*. 2012;15 Suppl 2:13-28. doi:10.1111/j.1463-5224.2012.01045.x
242. Rovere G, Nadal-Nicolás FM, Agudo-Barriuso M, et al. Comparison of Retinal Nerve Fiber Layer Thinning and Retinal Ganglion Cell Loss After Optic Nerve Transection in Adult Albino Rats. *Invest Ophthalmol Vis Sci*. 2015;56(8):4487-4498. doi:10.1167/iovs.15-17145
243. Choe TE, Abbott CJ, Piper C, Wang L, Fortune B. Comparison of Longitudinal In Vivo Measurements of Retinal Nerve Fiber Layer Thickness and Retinal Ganglion Cell Density after Optic Nerve Transection in Rat. Chidlow G, ed. *PLoS One*. 2014;9(11):e113011. doi:10.1371/journal.pone.0113011
244. Hein K, Gadjanski I, Kretzschmar B, et al. An optical coherence tomography study on degeneration of retinal nerve fiber layer in rats with autoimmune optic neuritis. *Invest Ophthalmol Vis Sci*. 2012;53(1):157-163. doi:10.1167/iovs.11-8092
245. Guo L, Normando EM, Nizari S, Lara D, Cordeiro MF. Tracking longitudinal retinal changes in experimental ocular hypertension using the cSLO and spectral domain-OCT. *Invest Ophthalmol Vis Sci*. 2010;51(12):6504-6513. doi:10.1167/iovs.10-5551
246. Gallego-Ortega A, Norte-Muñoz M, Miralles de Imperial-Ollero JA, et al. Functional and morphological alterations in a glaucoma model of acute ocular hypertension. *Prog Brain Res*. 2020;256(1):1-29. doi:10.1016/bs.pbr.2020.07.003
247. Berkelaar M, Clarke DB, Wang YC, Bray GM, Aguayo AJ. Axotomy results in delayed death and apoptosis of retinal ganglion cells in adult rats. *J Neurosci*. 1994;14(7):4368-4374. http://www.ncbi.nlm.nih.gov/pubmed/8027784.
248. Levin LA. Apoptosis of Retinal Ganglion Cells in Anterior Ischemic Optic Neuropathy. *Arch Ophthalmol*. 1996;114(4):488. doi:10.1001/archopht.1996.01100130484027
249. Quigley HA. Neuronal death in glaucoma. *Prog Retin Eye Res*. 1999;18(1):39-57. doi:10.1016/s1350-9462(98)00014-7
250. Thomas CN, Berry M, Logan A, Blanch RJ, Ahmed Z. Caspases in retinal ganglion cell death and axon regeneration. *Cell death Discov*. 2017;3:17032. doi:10.1038/cddiscovery.2017.32
251. Bähr M. Live or let die – retinal ganglion cell death and survival during development and in the lesioned adult CNS. *Trends Neurosci*. 2000;23(10):483-490. doi:10.1016/S0166-2236(00)01637-4
252. Yoles E, Schwartz M. Elevation of intraocular glutamate levels in rats with partial lesion of the optic nerve. *Arch Ophthalmol (Chicago, Ill 1960)*. 1998;116(7):906-910. doi:10.1001/archopht.116.7.906
253. Mansour-Robaey S, Clarke DB, Wang YC, Bray GM, Aguayo AJ. Effects of

ocular injury and administration of brain-derived neurotrophic factor on survival and regrowth of axotomized retinal ganglion cells. *Proc Natl Acad Sci U S A*. 1994;91(5):1632-1636. doi:10.1073/pnas.91.5.1632

254. Parrilla-Reverter G, Agudo M, Sobrado-Calvo P, Salinas-Navarro M, Villegas-Pérez MP, Vidal-Sanz M. Effects of different neurotrophic factors on the survival of retinal ganglion cells after a complete intraorbital nerve crush injury: a quantitative in vivo study. *Exp Eye Res*. 2009;89(1):32-41. doi:10.1016/j.exer.2009.02.015
255. Sánchez-Migallón MCC, Valiente-Soriano FJJ, Salinas-Navarro M, et al. Nerve fibre layer degeneration and retinal ganglion cell loss long term after optic nerve crush or transection in adult mice. *Exp Eye Res*. 2018;170:40-50. doi:10.1016/j.exer.2018.02.010
256. Sánchez-Migallón MCC, Valiente-Soriano FJJ, Nadal-Nicolás FMM, Di Pierdomenico J, Vidal-Sanz M, Agudo-Barriuso M. Survival of melanopsin expressing retinal ganglion cells long term after optic nerve trauma in mice. *Exp Eye Res*. 2018;174:93-97. doi:10.1016/j.exer.2018.05.029
257. McKerracher L, Vidal-Sanz M, Essagian C, Aguayo A. Selective impairment of slow axonal transport after optic nerve injury in adult rats. *J Neurosci*. 1990;10(8):2834-2841. doi:10.1523/JNEUROSCI.10-08-02834.1990
258. Agostinone J, Alarcon-Martinez L, Gamlin C, Yu W-Q, Wong ROL, Di Polo A. Insulin signalling promotes dendrite and synapse regeneration and restores circuit function after axonal injury. *Brain*. 2018;141(7):1963-1980. doi:10.1093/brain/awy142
259. Alarcón-Martínez L, de la Villa P, Avilés-Trigueros M, Blanco R, Villegas-Pérez MP, Vidal-Sanz M. Short and long term axotomy-induced ERG changes in albino and pigmented rats. *Mol Vis*. 2009;15:2373-2383.
260. Alarcón-Martínez L, Avilés-Trigueros M, Galindo-Romero C, et al. ERG changes in albino and pigmented mice after optic nerve transection. *Vision Res*. 2010;50(21):2176-2187. doi:10.1016/j.visres.2010.08.014
261. Galindo-Romero C, Valiente-Soriano FJ, Jiménez-López, M, et al. Effect of brain-derived neurotrophic factor on mouse axotomized retinal ganglion cells and phagocytic microglia. *Investig Ophthalmol Vis Sci*. 2013;54(2):974-985. doi:10.1167/iovs.12-11207
262. Lindqvist N. GDNF, Ret, GFRalpha1 and 2 in the adult rat retino-tectal system after optic nerve transection. *Exp Neurol*. 2004;187(2):487-499. doi:10.1016/j.expneurol.2004.02.002
263. Lucas-Ruiz F, Galindo-Romero C, Rodríguez-Ramírez KT, Vidal-Sanz M, Agudo-Barriuso M. Neuronal death in the contralateral un-injured retina after unilateral axotomy: Role of microglial cells. *Int J Mol Sci*. 2019;20(22). doi:10.3390/ijms20225733
264. Osborne A, Khatib TZ, Songra L, et al. Neuroprotection of retinal ganglion cells by a novel gene therapy construct that achieves sustained enhancement of brain-derived neurotrophic factor/tropomyosin-related kinase receptor-B signaling. *Cell Death Dis*. 2018;9(10). doi:10.1038/s41419-018-1041-8
265. Vidal-Sanz M, Lafuente M, Sobrado-Calvo P, et al. Death and neuroprotection of retinal ganglion cells after different types of injury. *Neurotox Res*. 2000;2(2-3):215-227. doi:10.1007/BF03033795
266. Vidal-Sanz M, Galindo-Romero C, Valiente-Soriano FJ, et al. Shared and Differential Retinal Responses against Optic Nerve Injury and Ocular Hypertension. *Front Neurosci*. 2017;11:235. doi:10.3389/fnins.2017.00235

267. Yang N, Young BK, Wang P, Tian N. The Susceptibility of Retinal Ganglion Cells to Optic Nerve Injury is Type Specific. *Cells*. 2020;9(3). doi:10.3390/cells9030677
268. Christensen I, Lu B, Yang N, Huang K, Wang P, Tian N. The Susceptibility of Retinal Ganglion Cells to Glutamatergic Excitotoxicity Is Type-Specific. *Front Neurosci*. 2019;13:219. doi:10.3389/fnins.2019.00219
269. Massey SC, Miller RF. N-methyl-D-aspartate receptors of ganglion cells in rabbit retina. *J Neurophysiol*. 1990;63(1):16-30. doi:10.1152/jn.1990.63.1.16
270. LUCAS DR, NEWHOUSE JP. The toxic effect of sodium L-glutamate on the inner layers of the retina. *AMA Arch Ophthalmol*. 1957;58(2):193-201. doi:10.1001/archopht.1957.00940010205006
271. Vidal-Sanz M, Vidal-Villegas B, Miralles de Imperial-Ollero, Juan Antonio Villegas-Pérez. MP. Neuroprotección. In: Garcia-Feijoo J, Julvez L, eds. *Glaucoma*. 1st ed. Buenos Aires, Argentina: Lerner, SF; 2021:338-344.
272. Almasieh M, Wilson AM, Morquette B, Cueva Vargas JL, Di Polo A. The molecular basis of retinal ganglion cell death in glaucoma. *Prog Retin Eye Res*. 2012;31(2):152-181. doi:10.1016/j.preteyeres.2011.11.002
273. Choi DW. Glutamate neurotoxicity and diseases of the nervous system. *Neuron*. 1988;1(8):623-634. doi:10.1016/0896-6273(88)90162-6
274. Dreyer EB. Elevated Glutamate Levels in the Vitreous Body of Humans and Monkeys With Glaucoma. *Arch Ophthalmol*. 1996;114(3):299. doi:10.1001/archopht.1996.01100130295012
275. Tezel G. Immune regulation toward immunomodulation for neuroprotection in glaucoma. *Curr Opin Pharmacol*. 2013;13(1):23-31. doi:10.1016/j.coph.2012.09.013
276. Izzotti A, Bagnis A, Saccà SC. The role of oxidative stress in glaucoma. *Mutat Res*. 2006;612(2):105-114. doi:10.1016/j.mrrev.2005.11.001
277. Vorwerk CK, Kreutz MR, Böckers TM, Brosz M, Dreyer EB, Sabel BA. Susceptibility of retinal ganglion cells to excitotoxicity depends on soma size and retinal eccentricity. *Curr Eye Res*. 1999;19(1):59-65. doi:10.1076/ceyr.19.1.59.5336
278. Vorwerk CK, Zurakowski D, McDermott LM, Mawrin C, Dreyer EB. Effects of axonal injury on ganglion cell survival and glutamate homeostasis. *Brain Res Bull*. 2004;62(6):485-490. doi:10.1016/S0361-9230(03)00075-3
279. Lam TT, Siew E, Chu R, Tso MO. Ameliorative effect of MK-801 on retinal ischemia. *J Ocul Pharmacol Ther*. 1997;13(2):129-137. doi:10.1089/jop.1997.13.129
280. Kermer P, Klöcker N, Bähr M. Modulation of metabotropic glutamate receptors fails to prevent the loss of adult rat retinal ganglion cells following axotomy or N-methyl-D-aspartate lesion in vivo. *Neurosci Lett*. 2001;315(3):117-120. doi:10.1016/s0304-3940(01)02318-7
281. Schuettauf F, Naskar R, Vorwerk CK, Zurakowski D, Dreyer EB. Ganglion cell loss after optic nerve crush mediated through AMPA-kainate and NMDA receptors. *Invest Ophthalmol Vis Sci*. 2000;41(13):4313-4316. http://www.ncbi.nlm.nih.gov/pubmed/11095632.
282. Dong X, Wang Y, Qin Z. Molecular mechanisms of excitotoxicity and their relevance to pathogenesis of neurodegenerative diseases. *Acta Pharmacol Sin*. 2009;30(4):379-387. doi:10.1038/aps.2009.24
283. Manev H, Favaron M, Guidotti A, Costa E. Delayed increase of Ca2+ influx elicited by glutamate: role in neuronal death. *Mol Pharmacol*. 1989;36(1):106-

112. http://www.ncbi.nlm.nih.gov/pubmed/2568579.
284. Hardingham GE, Fukunaga Y, Bading H. Extrasynaptic NMDARs oppose synaptic NMDARs by triggering CREB shut-off and cell death pathways. *Nat Neurosci*. 2002;5(5):405-414. doi:10.1038/nn835
285. Stavrovskaya IG, Kristal BS. The powerhouse takes control of the cell: is the mitochondrial permeability transition a viable therapeutic target against neuronal dysfunction and death? *Free Radic Biol Med*. 2005;38(6):687-697. doi:10.1016/j.freeradbiomed.2004.11.032
286. Manabe S-I, Gu Z, Lipton SA. Activation of matrix metalloproteinase-9 via neuronal nitric oxide synthase contributes to NMDA-induced retinal ganglion cell death. *Invest Ophthalmol Vis Sci*. 2005;46(12):4747-4753. doi:10.1167/iovs.05-0128
287. Gómez-Vicente V, Lax P, Fernández-Sánchez L, et al. Neuroprotective Effect of Tauroursodeoxycholic Acid on N-Methyl-D-Aspartate-Induced Retinal Ganglion Cell Degeneration. *PLoS One*. 2015;10(9):e0137826. doi:10.1371/journal.pone.0137826
288. Kobayashi M, Hirooka K, Ono A, Nakano Y, Nishiyama A, Tsujikawa A. The Relationship Between the Renin-Angiotensin-Aldosterone System and NMDA Receptor-Mediated Signal and the Prevention of Retinal Ganglion Cell Death. *Invest Ophthalmol Vis Sci*. 2017;58(3):1397-1403. doi:10.1167/iovs.16-21001
289. Wang S, Gu D, Zhang P, et al. Melanopsin-expressing retinal ganglion cells are relatively resistant to excitotoxicity induced by N-methyl-d-aspartate. *Neurosci Lett*. 2018;662:368-373. doi:10.1016/j.neulet.2017.10.055
290. Pichavaram P, Palani CD, Patel C, et al. Targeting Polyamine Oxidase to Prevent Excitotoxicity-Induced Retinal Neurodegeneration. *Front Neurosci*. 2018;12:956. doi:10.3389/fnins.2018.00956
291. Lambuk L, Iezhitsa I, Agarwal R, Bakar NS, Agarwal P, Ismail NM. Antiapoptotic effect of taurine against NMDA-induced retinal excitotoxicity in rats. *Neurotoxicology*. 2019;70:62-71. doi:10.1016/j.neuro.2018.10.009
292. Tsoka P, Barbisan PR, Kataoka K, et al. NLRP3 inflammasome in NMDA-induced retinal excitotoxicity. *Exp Eye Res*. 2019;181:136-144. doi:10.1016/j.exer.2019.01.018
293. Ito A, Tsuda S, Kunikata H, Toshifumi A, Sato K, Nakazawa T. Assessing retinal ganglion cell death and neuroprotective agents using real time imaging. *Brain Res*. 2019;1714:65-72. doi:10.1016/j.brainres.2019.02.008
294. Fahrenthold BK, Fernandes KA, Libby RT. Assessment of intrinsic and extrinsic signaling pathway in excitotoxic retinal ganglion cell death. *Sci Rep*. 2018;8(1):4641. doi:10.1038/s41598-018-22848-y
295. DeParis S, Caprara C, Grimm C. Intrinsically photosensitive retinal ganglion cells are resistant to N-methyl-D-aspartic acid excitotoxicity. *Mol Vis*. 2012;18:2814-2827. http://www.ncbi.nlm.nih.gov/pubmed/23233784.
296. Aguayo AJ, David S, Bray GM. Influences of the glial environment on the elongation of axons after injury: transplantation studies in adult rodents. *J Exp Biol*. 1981;95:231-240. http://www.ncbi.nlm.nih.gov/pubmed/7334319.
297. Huang EJ, Reichardt LF. Trk receptors: roles in neuronal signal transduction. *Annu Rev Biochem*. 2003;72:609-642. doi:10.1146/annurev.biochem.72.121801.161629
298. Claes M, De Groef L, Moons L. Target-Derived Neurotrophic Factor Deprivation Puts Retinal Ganglion Cells on Death Row: Cold Hard Evidence and Caveats. *Int J Mol Sci*. 2019;20(17). doi:10.3390/ijms20174314

299. Allen SJ, Dawbarn D. Clinical relevance of the neurotrophins and their receptors. *Clin Sci (Lond)*. 2006;110(2):175-191. doi:10.1042/CS20050161
300. Di Polo A, Luo C, Bray GM, Aguayo AJ. Colocalization of TrkB and brain-derived neurotrophic factor proteins in green-red-sensitive cone outer segments - PubMed. *Investig Ophthalmol Vis Sci*. 2000;41(12):4014-4021.
301. Lindqvist N, Vidal-Sanz M, Hallböök F. Single cell RT-PCR analysis of tyrosine kinase receptor expression in adult rat retinal ganglion cells isolated by retinal sandwiching. *Brain Res Protoc*. 2002;10(2):75-83. doi:10.1016/S1385-299X(02)00184-8
302. Lindqvist N, Lönngren U, Agudo M, Näpänkangas U, Vidal-Sanz M, Hallböök F. Multiple receptor tyrosine kinases are expressed in adult rat retinal ganglion cells as revealed by single-cell degenerate primer polymerase chain reaction. *Ups J Med Sci*. 2010;115(1):65-80. doi:10.3109/03009731003597119
303. Cowley S, Paterson H, Kemp P, Marshall CJ. Activation of MAP kinase kinase is necessary and sufficient for PC12 differentiation and for transformation of NIH 3T3 cells. *Cell*. 1994;77(6):841-852. doi:10.1016/0092-8674(94)90133-3
304. Meakin SO, MacDonald JI, Gryz EA, Kubu CJ, Verdi JM. The signaling adapter FRS-2 competes with Shc for binding to the nerve growth factor receptor TrkA. A model for discriminating proliferation and differentiation. *J Biol Chem*. 1999;274(14):9861-9870. doi:10.1074/jbc.274.14.9861
305. Geetha T, Wooten MW. Association of the atypical protein kinase C-interacting protein p62/ZIP with nerve growth factor receptor TrkA regulates receptor trafficking and Erk5 signaling. *J Biol Chem*. 2003;278(7):4730-4739. doi:10.1074/jbc.M208468200
306. Klein R, Smeyne RJ, Wurst W, et al. Targeted disruption of the trkB neurotrophin receptor gene results in nervous system lesions and neonatal death. *Cell*. 1993;75(1):113-122. http://www.ncbi.nlm.nih.gov/pubmed/8402890.
307. Schimmang T, Minichiello L, Vazquez E, et al. Developing inner ear sensory neurons require TrkB and TrkC receptors for innervation of their peripheral targets. *Development*. 1995;121(10):3381-3391. http://www.ncbi.nlm.nih.gov/pubmed/7588071.
308. Gupta VBVK, You Y, Gupta VBVK, Klistorner A, Graham SL. TrkB receptor signalling: implications in neurodegenerative, psychiatric and proliferative disorders. *Int J Mol Sci*. 2013;14(5):10122-10142. doi:10.3390/ijms140510122
309. Perez MT, Caminos E. Expression of brain-derived neurotrophic factor and of its functional receptor in neonatal and adult rat retina. *Neurosci Lett*. 1995;183(1-2):96-99. doi:10.1016/0304-3940(94)11123-z
310. Vecino E, García-Crespo D, García-Grespo D, et al. Rat retinal ganglion cells co-express brain derived neurotrophic factor (BDNF) and its receptor TrkB. *Vision Res*. 2002;42(2):151-157. doi:10.1016/s0042-6989(01)00251-6
311. Grishanin RN, Yang H, Liu X, et al. Retinal TrkB receptors regulate neural development in the inner, but not outer, retina. *Mol Cell Neurosci*. 2008;38(3):431-443. doi:10.1016/j.mcn.2008.04.004
312. Hu B, Nikolakopoulou AM, Cohen-Cory S. BDNF stabilizes synapses and maintains the structural complexity of optic axons in vivo. *Development*. 2005;132(19):4285-4298. doi:10.1242/dev.02017

313. Lom B, Cohen-Cory S. Brain-derived neurotrophic factor differentially regulates retinal ganglion cell dendritic and axonal arborization in vivo. *J Neurosci*. 1999;19(22):9928-9938. http://www.ncbi.nlm.nih.gov/pubmed/10559401.
314. Alsina B, Vu T, Cohen-Cory S. Visualizing synapse formation in arborizing optic axons in vivo: dynamics and modulation by BDNF. *Nat Neurosci*. 2001;4(11):1093-1101. doi:10.1038/nn735
315. Lom B, Cogen J, Sanchez AL, Vu T, Cohen-Cory S. Local and target-derived brain-derived neurotrophic factor exert opposing effects on the dendritic arborization of retinal ganglion cells in vivo. *J Neurosci*. 2002;22(17):7639-7649. http://www.ncbi.nlm.nih.gov/pubmed/12196587.
316. Liu X, Grishanin RN, Tolwani RJ, et al. Brain-derived neurotrophic factor and TrkB modulate visual experience-dependent refinement of neuronal pathways in retina. *J Neurosci*. 2007;27(27):7256-7267. doi:10.1523/JNEUROSCI.0779-07.2007
317. Vecino E, Ugarte M, Nash MS, Osborne NN. NMDA induces BDNF expression in the albino rat retina in vivo. *Neuroreport*. 1999;10(5):1103-1106. doi:10.1097/00001756-199904060-00036
318. Valiente-Soriano FJ, Ortín-Martínez A, Pierdomenico J Di, et al. Topical brimonidine or intravitreal bdnf, cntf, or bfgf protect cones against phototoxicity. *Transl Vis Sci Technol*. 2019;8(6):36. doi:10.1167/tvst.8.6.36
319. Wójcik-Gryciuk A, Gajewska-Woźniak O, Kordecka K, Boguszewski PM, Waleszczyk W, Skup M. Neuroprotection of Retinal Ganglion Cells with AAV2-BDNF Pretreatment Restoring Normal TrkB Receptor Protein Levels in Glaucoma. *Int J Mol Sci*. 2020;21(17):6262. doi:10.3390/ijms21176262
320. Di Polo A, Aigner LJ, Dunn RJ, Bray GM, Aguayo AJ. Prolonged delivery of brain-derived neurotrophic factor by adenovirus-infected Müller cells temporarily rescues injured retinal ganglion cells. *Proc Natl Acad Sci U S A*. 1998;95(7):3978-3983. doi:10.1073/pnas.95.7.3978
321. Jiang H, Jin W-L, Jin D-D, Chen J-T. [Neuroprotection of a neotype transactivating-brain-derived neurotrophic factor fusion protein with penetrating activity of blood-brain barrier]. *Zhonghua Yi Xue Za Zhi*. 2011;91(25):1786-1790. http://www.ncbi.nlm.nih.gov/pubmed/22093740.
322. Barde YA, Edgar D, Thoenen H. Purification of a new neurotrophic factor from mammalian brain. *Hoppe Seylers Z Physiol Chem*. 1982;363(11):1295-1296.
323. Jang S-W, Liu X, Yepes M, et al. A selective TrkB agonist with potent neurotrophic activities by 7,8-dihydroxyflavone. *Proc Natl Acad Sci*. 2010;107(6):2687-2692. doi:10.1073/pnas.0913572107
324. Emili M, Guidi S, Uguagliati B, Giacomini A, Bartesaghi R, Stagni F. Treatment with the flavonoid 7,8-Dihydroxyflavone: a promising strategy for a constellation of body and brain disorders. *Crit Rev Food Sci Nutr*. September 2020:1-38. doi:10.1080/10408398.2020.1810625
325. Liu X, Qi Q, Xiao G, Li J, Luo HR, Ye K. O-Methylated Metabolite of 7,8-Dihydroxyflavone Activates TrkB Receptor and Displays Antidepressant Activity. *Pharmacology*. 2013;91(3-4):185-200. doi:10.1159/000346920
326. Liu X, Obianyo O, Chan CB, et al. Biochemical and Biophysical Investigation of the Brain-derived Neurotrophic Factor Mimetic 7,8-Dihydroxyflavone in the Binding and Activation of the TrkB Receptor. *J Biol Chem*. 2014;289(40):27571-27584. doi:10.1074/jbc.M114.562561

327. Zhang Z, Liu X, Schroeder JP, et al. 7,8-dihydroxyflavone prevents synaptic loss and memory deficits in a mouse model of Alzheimer's disease. *Neuropsychopharmacology*. 2014;39(3):638-650. doi:10.1038/npp.2013.243
328. Ochs G, Penn RD, York M, et al. A phase I/II trial of recombinant methionyl human brain derived neurotrophic factor administered by intrathecal infusion to patients with amyotrophic lateral sclerosis. *Amyotroph Lateral Scler Other Mot Neuron Disord*. 2000;1(3):201-206. doi:10.1080/14660820050515197
329. Price RD, Milne SA, Sharkey J, Matsuoka N. Advances in small molecules promoting neurotrophic function. *Pharmacol Ther*. 2007;115(2):292-306. doi:10.1016/j.pharmthera.2007.03.005
330. Liu X, Chan C-B, Jang S-W, et al. A Synthetic 7,8-Dihydroxyflavone Derivative Promotes Neurogenesis and Exhibits Potent Antidepressant Effect. *J Med Chem*. 2010;53(23):8274-8286. doi:10.1021/jm101206p
331. Seppa K, Jagomäe T, Kukker KG, et al. Liraglutide, 7,8-DHF and their co-treatment prevents loss of vision and cognitive decline in a Wolfram syndrome rat model. *Sci Rep*. 2021;11(1). doi:10.1038/s41598-021-81768-6
332. He J, Xiang Z, Zhu X, et al. Neuroprotective Effects of 7, 8-dihydroxyflavone on Midbrain Dopaminergic Neurons in MPP+-treated Monkeys. *Sci Rep*. 2016;6(1):34339. doi:10.1038/srep34339
333. Huang H-M, Huang C-C, Tsai M-H, Poon Y-C, Chang Y-C. Systemic 7,8-Dihydroxyflavone Treatment Protects Immature Retinas Against Hypoxic-Ischemic Injury via Müller Glia Regeneration and MAPK/ERK Activation. *Investig Opthalmology Vis Sci*. 2018;59(7):3124. doi:10.1167/iovs.18-23792
334. Proenca CC, Song M, Lee FS. Differential effects of BDNF and neurotrophin 4 (NT4) on endocytic sorting of TrkB receptors. *J Neurochem*. 2016;138(3):397-406. doi:10.1111/jnc.13676
335. Jain V, Ravindran E, Dhingra NK. Differential expression of Brn3 transcription factors in intrinsically photosensitive retinal ganglion cells in mouse. *J Comp Neurol*. 2012;520(4):742-755. doi:10.1002/cne.22765
336. Nadal-Nicolás FM, Vidal-Sanz M, Agudo-Barriuso M. The aging rat retina: from function to anatomy. *Neurobiol Aging*. 2018;61:146-168. doi:10.1016/j.neurobiolaging.2017.09.021
337. Chen CK, Kiyama T, Weber N, et al. Characterization of Tbr2-expressing retinal ganglion cells. *J Comp Neurol*. 2021;529(15):3513-3532. doi:10.1002/cne.25208
338. Salinas-Navarro M, Jiménez-López M, Valiente-Soriano FJ, et al. Retinal ganglion cell population in adult albino and pigmented mice: a computerized analysis of the entire population and its spatial distribution. *Vision Res*. 2009;49(6):637-647. doi:10.1016/j.visres.2009.01.010
339. Krieger B, Qiao M, Rousso DL, Sanes JR, Meister M. Four alpha ganglion cell types in mouse retina: Function, structure, and molecular signatures. Barnes S, ed. *PLoS One*. 2017;12(7):e0180091. doi:10.1371/journal.pone.0180091
340. Petroff OAC. GABA and glutamate in the human brain. *Neuroscientist*. 2002;8(6):562-573. doi:10.1177/1073858402238515
341. Calvo E, Milla-Navarro S, Ortuño-Lizarán I, et al. Deleterious Effect of NMDA Plus Kainate on the Inner Retinal Cells and Ganglion Cell Projection of the Mouse. *Int J Mol Sci*. 2020;21(5). doi:10.3390/ijms21051570
342. Thaler S, Choragiewicz TJ, Rejdak R, et al. Neuroprotection by acetoacetate and β-hydroxybutyrate against NMDA-induced RGC damage in rat--possible

involvement of kynurenic acid. *Graefes Arch Clin Exp Ophthalmol*. 2010;248(12):1729-1735. doi:10.1007/s00417-010-1425-7
343. Singhal S, Lawrence JM, Salt TE, Khaw PT, Limb GA. Triamcinolone attenuates macrophage/microglia accumulation associated with NMDA-induced RGC death and facilitates survival of Müller stem cell grafts. *Exp Eye Res*. 2010;90(2):308-315. doi:10.1016/j.exer.2009.11.008
344. Nakazawa T. [Mechanism of N-methyl-D-aspartate-induced retinal ganglion cell death]. *Nihon Ganka Gakkai Zasshi*. 2009;113(11):1060-1070. http://www.ncbi.nlm.nih.gov/pubmed/19994584.
345. Lebrun-Julien F, Duplan L, Pernet V, et al. Excitotoxic death of retinal neurons in vivo occurs via a non-cell-autonomous mechanism. *J Neurosci*. 2009;29(17):5536-5545. doi:10.1523/JNEUROSCI.0831-09.2009
346. Endo K, Nakamachi T, Seki T, et al. Neuroprotective Effect of PACAP Against NMDA-Induced Retinal Damage in the Mouse. *J Mol Neurosci*. 2011;43(1):22-29. doi:10.1007/s12031-010-9434-x
347. Osborne NN, Wood JPM, Cupido A, Melena J, Chidlow G. Topical flunarizine reduces IOP and protects the retina against ischemia-excitotoxicity. *Invest Ophthalmol Vis Sci*. 2002;43(5):1456-1464. http://www.ncbi.nlm.nih.gov/pubmed/11980861.
348. Yamada H, Chen Y-N, Aihara M, Araie M. Neuroprotective effect of calcium channel blocker against retinal ganglion cell damage under hypoxia. *Brain Res*. 2006;1071(1):75-80. doi:10.1016/j.brainres.2005.11.072
349. Koseki N, Araie M, Tomidokoro A, et al. A placebo-controlled 3-year study of a calcium blocker on visual field and ocular circulation in glaucoma with low-normal pressure. *Ophthalmology*. 2008;115(11):2049-2057. doi:10.1016/j.ophtha.2008.05.015
350. García-Ayuso D, Galindo-Romero C, Di Pierdomenico J, Vidal-Sanz M, Agudo-Barriuso M, Villegas Pérez MP. Light-induced retinal degeneration causes a transient downregulation of melanopsin in the rat retina. *Exp Eye Res*. 2017;161:10-16. doi:10.1016/j.exer.2017.05.010
351. Vugler A, Semo M, Ortín-Martínez A, et al. A role for the outer retina in development of the intrinsic pupillary light reflex in mice. *Neuroscience*. 2015;286:60-78. doi:10.1016/j.neuroscience.2014.11.044
352. Cui Q, Ren C, Sollars PJ, Pickard GE, So K-F. The injury resistant ability of melanopsin-expressing intrinsically photosensitive retinal ganglion cells. *Neuroscience*. 2015;284:845-853. doi:10.1016/j.neuroscience.2014.11.002
353. Semo M, Gias C, Ahmado A, Vugler A. A role for the ciliary marginal zone in the melanopsin-dependent intrinsic pupillary light reflex. *Exp Eye Res*. 2014;119:8-18. doi:10.1016/j.exer.2013.11.013
354. Pérez de Sevilla Müller L, Sargoy A, Rodriguez AR, Brecha NC. Melanopsin Ganglion Cells Are the Most Resistant Retinal Ganglion Cell Type to Axonal Injury in the Rat Retina. Tosini G, ed. *PLoS One*. 2014;9(3):e93274. doi:10.1371/journal.pone.0093274
355. Zhang X-J, Liu L-L, Jiang S-X, Zhong Y-M, Yang X-L. Activation of the ζ receptor 1 suppresses NMDA responses in rat retinal ganglion cells. *Neuroscience*. 2011;177:12-22. doi:10.1016/j.neuroscience.2010.12.064
356. Jakobs TC, Libby RT, Ben Y, John SWM, Masland RH. Retinal ganglion cell degeneration is topological but not cell type specific in DBA/2J mice. *J Cell Biol*. 2005;171(2):313-325. doi:10.1083/jcb.200506099
357. Kinoshita J, Fujita K, Yasuno K, et al. Outer retinal involvement in N-methyl-

D-aspartate-induced inner retinal injury in rabbits assessed by optical coherence tomography. *J Toxicol Sci*. 2020;45(5):261-269. doi:10.2131/jts.45.261

358. Ohno Y, Makita S, Shimazawa M, Tsuruma K, Yasuno Y, Hara H. Thickness mapping of the inner retina by spectral-domain optical coherence tomography in an N-methyl-D-aspartate-induced retinal damage model. *Exp Eye Res*. 2013;113:19-25. doi:10.1016/j.exer.2013.05.009
359. Wang Z-F, Yang X-L. [Glutamate receptor-mediated retinal neuronal injury in experimental glaucoma]. *Sheng Li Xue Bao*. 2016;68(4):483-491. http://www.ncbi.nlm.nih.gov/pubmed/27546508.
360. Nakazawa T, Takahashi H, Nishijima K, et al. Pitavastatin prevents NMDA-induced retinal ganglion cell death by suppressing leukocyte recruitment. *J Neurochem*. 2007;100(4):1018-1031. doi:10.1111/j.1471-4159.2006.04274.x
361. Huang W, Hu F, Wang M, et al. Comparative analysis of retinal ganglion cell damage in three glaucomatous rat models. *Exp Eye Res*. 2018;172:112-122. doi:10.1016/j.exer.2018.03.019
362. Siliprandi R, Canella R, Carmignoto G, et al. N-methyl-D-aspartate-induced neurotoxicity in the adult rat retina. *Vis Neurosci*. 1992;8(6):567-573. doi:10.1017/s0952523800005666
363. Lam TT, Abler AS, Kwong JM, Tso MO. N-methyl-D-aspartate (NMDA)--induced apoptosis in rat retina. *Invest Ophthalmol Vis Sci*. 1999;40(10):2391-2397. http://www.ncbi.nlm.nih.gov/pubmed/10476807.
364. Akopian A, Atlasz T, Pan F, et al. Gap junction-mediated death of retinal neurons is connexin and insult specific: a potential target for neuroprotection. *J Neurosci*. 2014;34(32):10582-10591. doi:10.1523/JNEUROSCI.1912-14.2014
365. Li Y, Schlamp CL, Nickells RW. Experimental induction of retinal ganglion cell death in adult mice. *Invest Ophthalmol Vis Sci*. 1999;40(5):1004-1008. http://www.ncbi.nlm.nih.gov/pubmed/10102300.
366. Völgyi B, Chheda S, Bloomfield SA. Tracer coupling patterns of the ganglion cell subtypes in the mouse retina. *J Comp Neurol*. 2009;512(5):664-687. doi:10.1002/cne.21912
367. Robinson GA, Madison RD. Axotomized mouse retinal ganglion cells containing melanopsin show enhanced survival, but not enhanced axon regrowth into a peripheral nerve graft. *Vision Res*. 2004;44(23):2667-2674. doi:10.1016/j.visres.2004.06.010
368. Daniel S, Clark A, McDowell C. Subtype-specific response of retinal ganglion cells to optic nerve crush. *Cell Death Discov*. 2018;4(1):67. doi:10.1038/s41420-018-0069-y
369. Li S, Yang C, Zhang L, et al. Promoting axon regeneration in the adult CNS by modulation of the melanopsin/GPCR signaling. *Proc Natl Acad Sci*. 2016;113(7):1937-1942. doi:10.1073/pnas.1523645113
370. Jakobs TC, Ben Y, Masland RH. Expression of mRNA for glutamate receptor subunits distinguishes the major classes of retinal neurons, but is less specific for individual cell types. *Mol Vis*. 2007;13:933-948. http://www.ncbi.nlm.nih.gov/pubmed/17653033.
371. Wulff K, Gatti S, Wettstein JG, Foster RG. Sleep and circadian rhythm disruption in psychiatric and neurodegenerative disease. *Nat Rev Neurosci*. 2010;11(8):589-599. doi:10.1038/nrn2868
372. Lax P, Esquiva G, Esteve-Rudd J, Otalora BB, Madrid JA, Cuenca N.

Circadian dysfunction in a rotenone-induced parkinsonian rodent model. *Chronobiol Int*. 2012;29(2):147-156. doi:10.3109/07420528.2011.649870
373. Georg B, Ghelli A, Giordano C, et al. Melanopsin-expressing retinal ganglion cells are resistant to cell injury, but not always. *Mitochondrion*. 2017;36:77-84. doi:10.1016/j.mito.2017.04.003
374. Esquiva G, Lax P, Cuenca N. Impairment of intrinsically photosensitive retinal ganglion cells associated with late stages of retinal degeneration. *Invest Ophthalmol Vis Sci*. 2013;54(7):4605-4618. doi:10.1167/iovs.13-12120
375. VUGLER AA, SEMO M, JOSEPH A, JEFFERY G. Survival and remodeling of melanopsin cells during retinal dystrophy. *Vis Neurosci*. 2008;25(2):125-138. doi:10.1017/S0952523808080309
376. García-Ayuso D, Di Pierdomenico J, Esquiva G, et al. Inherited Photoreceptor Degeneration Causes the Death of Melanopsin-Positive Retinal Ganglion Cells and Increases Their Coexpression of Brn3a. *Investig Opthalmology Vis Sci*. 2015;56(8):4592. doi:10.1167/iovs.15-16808
377. SEKI T. Neuroprotective Effect of PACAP against Kainic Acid-Induced Neurotoxicity in Rat Retina. *Ann N Y Acad Sci*. 2006;1070(1):531-534. doi:10.1196/annals.1317.074
378. Seki T, Itoh H, Nakamachi T, et al. Suppression of Rat Retinal Ganglion Cell Death by PACAP Following Transient Ischemia Induced by High Intraocular Pressure. *J Mol Neurosci*. 2011;43(1):30-34. doi:10.1007/s12031-010-9410-5
379. Seki T, Itoh H, Nakamachi T, Shioda S. Suppression of ganglion cell death by PACAP following optic nerve transection in the rat. *J Mol Neurosci*. 2008;36(1-3):57-60. doi:10.1007/s12031-008-9091-5
380. Bray ER, Yungher BJ, Levay K, et al. Thrombospondin-1 Mediates Axon Regeneration in Retinal Ganglion Cells. *Neuron*. 2019;103(4):642-657.e7. doi:10.1016/j.neuron.2019.05.044
381. Lin M-S, Liao P-Y, Chen H-M, Chang C-P, Chen S-K, Chern Y. Degeneration of ipRGCs in Mouse Models of Huntington's Disease Disrupts Non-Image-Forming Behaviors Before Motor Impairment. *J Neurosci*. 2019;39(8):1505-1524. doi:10.1523/JNEUROSCI.0571-18.2018
382. Della Santina L, Ou Y. Who's lost first? Susceptibility of retinal ganglion cell types in experimental glaucoma. *Exp Eye Res*. 2017;158:43-50. doi:10.1016/j.exer.2016.06.006
383. Ou Y, Jo RE, Ullian EM, Wong ROL, Della Santina L. Selective Vulnerability of Specific Retinal Ganglion Cell Types and Synapses after Transient Ocular Hypertension. *J Neurosci*. 2016;36(35):9240-9252. doi:10.1523/JNEUROSCI.0940-16.2016
384. Fu L, Kwok SS, Chan YK, et al. Therapeutic Strategies for Attenuation of Retinal Ganglion Cell Injury in Optic Neuropathies: Concepts in Translational Research and Therapeutic Implications. *Biomed Res Int*. 2019;2019:8397521. doi:10.1155/2019/8397521
385. Kowiański P, Lietzau G, Czuba E, Waśkow M, Steliga A, Moryś J. BDNF: A Key Factor with Multipotent Impact on Brain Signaling and Synaptic Plasticity. *Cell Mol Neurobiol*. 2018;38(3):579-593. doi:10.1007/s10571-017-0510-4
386. Ichim G, Tauszig-Delamasure S, Mehlen P. Neurotrophins and cell death. *Exp Cell Res*. 2012;318(11):1221-1228. doi:10.1016/j.yexcr.2012.03.006
387. Kerrigan LA, Zack DJ, Quigley HA, Smith SD, Pease ME. TUNEL-positive ganglion cells in human primary open-angle glaucoma. *Arch Ophthalmol*

*(Chicago, Ill 1960)*. 1997;115(8):1031-1035. doi:10.1001/archopht.1997.01100160201010
388. Peinado-Ramón P, Salvador M, Villegas-Pérez MP, Vidal-Sanz M. Effects of axotomy and intraocular administration of NT-4, NT-3, and brain-derived neurotrophic factor on the survival of adult rat retinal ganglion cells: A quantitative in vivo study. *Investig Ophthalmol Vis Sci*. 1996;37(4):489-500.
389. Fudalej E, Justyniarska M, Kasarełło K, Dziedziak J, Szaflik JP, Cudnoch-Jędrzejewska A. Neuroprotective Factors of the Retina and Their Role in Promoting Survival of Retinal Ganglion Cells: A Review. *Ophthalmic Res*. 2021;64(3):345-355. doi:10.1159/000514441
390. Bathina S, Das UN. Brain-derived neurotrophic factor and its clinical implications. *Arch Med Sci*. 2015;11(6):1164-1178. doi:10.5114/aoms.2015.56342
391. Miranda M, Morici JF, Zanoni MB, Bekinschtein P. Brain-Derived Neurotrophic Factor: A Key Molecule for Memory in the Healthy and the Pathological Brain. *Front Cell Neurosci*. 2019;13. doi:10.3389/fncel.2019.00363
392. Gupta VK, You Y, Klistorner A, Graham SL. Shp-2 regulates the TrkB receptor activity in the retinal ganglion cells under glaucomatous stress. *Biochim Biophys Acta*. 2012;1822(11):1643-1649. doi:10.1016/j.bbadis.2012.07.016
393. Numakawa T, Suzuki S, Kumamaru E, Adachi N, Richards M, Kunugi H. BDNF function and intracellular signaling in neurons. *Histol Histopathol*. 2010;25(2):237-258. doi:10.14670/HH-25.237
394. Chitranshi N, Gupta V, Kumar S, Graham SL. Exploring the Molecular Interactions of 7,8-Dihydroxyflavone and Its Derivatives with TrkB and VEGFR2 Proteins. *Int J Mol Sci*. 2015;16(9):21087-21108. doi:10.3390/ijms160921087
395. Castello NA, Nguyen MH, Tran JD, Cheng D, Green KN, LaFerla FM. 7,8-Dihydroxyflavone, a small molecule TrkB agonist, improves spatial memory and increases thin spine density in a mouse model of Alzheimer disease-like neuronal loss. *PLoS One*. 2014;9(3):e91453. doi:10.1371/journal.pone.0091453
396. Jiang M, Peng Q, Liu X, et al. Small-molecule TrkB receptor agonists improve motor function and extend survival in a mouse model of Huntington's disease. *Hum Mol Genet*. 2013;22(12):2462-2470. doi:10.1093/hmg/ddt098
397. Fang Y-Y, Luo M, Yue S, et al. 7,8-Dihydroxyflavone protects retinal ganglion cells against chronic intermittent hypoxia-induced oxidative stress damage via activation of the BDNF/TrkB signaling pathway. *Sleep Breath*. May 2021. doi:10.1007/s11325-021-02400-5
398. Hu Y, Cho S, Goldberg JL. Neurotrophic effect of a novel TrkB agonist on retinal ganglion cells. *Invest Ophthalmol Vis Sci*. 2010;51(3):1747-1754. doi:10.1167/iovs.09-4450
399. Bai Y, Xu J, Brahimi F, Zhuo Y, Sarunic M V, Saragovi HU. An agonistic TrkB mAb causes sustained TrkB activation, delays RGC death, and protects the retinal structure in optic nerve axotomy and in glaucoma. *Invest Ophthalmol Vis Sci*. 2010;51(9):4722-4731. doi:10.1167/iovs.09-5032
400. Frank L, Ventimiglia R, Anderson K, Lindsay RM, Rudge JS. BDNF down-regulates neurotrophin responsiveness, TrkB protein and TrkB mRNA levels

in cultured rat hippocampal neurons. *Eur J Neurosci*. 1996;8(6):1220-1230. doi:10.1111/j.1460-9568.1996.tb01290.x
401. Knusel B, Gao H, Okazaki T, et al. Ligand-induced down-regulation of Trk messenger RNA, protein and tyrosine phosphorylation in rat cortical neurons. *Neuroscience*. 1997;78(3):851-862. doi:10.1016/s0306-4522(96)00616-1
402. Sommerfeld MT, Schweigreiter R, Barde YA, Hoppe E. Down-regulation of the neurotrophin receptor TrkB following ligand binding. Evidence for an involvement of the proteasome and differential regulation of TrkA and TrkB. *J Biol Chem*. 2000;275(12):8982-8990. doi:10.1074/jbc.275.12.8982
403. Cheng L, Sapieha P, Kittlerova P, Hauswirth WW, Di Polo A. TrkB gene transfer protects retinal ganglion cells from axotomy-induced death in vivo. *J Neurosci*. 2002;22(10):3977-3986. doi:20026382
404. Kimura A, Namekata K, Guo X, Harada C, Harada T. Neuroprotection, Growth Factors and BDNF-TrkB Signalling in Retinal Degeneration. *Int J Mol Sci*. 2016;17(9). doi:10.3390/ijms17091584
405. Iwabe S, Moreno-Mendoza NA, Trigo-Tavera F, Crowder C, García-Sánchez GA. Retrograde axonal transport obstruction of brain-derived neurotrophic factor (BDNF) and its TrkB receptor in the retina and optic nerve of American Cocker Spaniel dogs with spontaneous glaucoma. *Vet Ophthalmol*. 10 Suppl 1:12-19. doi:10.1111/j.1463-5224.2007.00504.x
406. Pease ME, McKinnon SJ, Quigley HA, Kerrigan-Baumrind LA, Zack DJ. Obstructed axonal transport of BDNF and its receptor TrkB in experimental glaucoma. *Invest Ophthalmol Vis Sci*. 2000;41(3):764-774. http://www.ncbi.nlm.nih.gov/pubmed/10711692.
407. Cui Q, Tang LS, Hu B, So K-F, Yip HK. Expression of trkA, trkB, and trkC in injured and regenerating retinal ganglion cells of adult rats. *Invest Ophthalmol Vis Sci*. 2002;43(6):1954-1964. http://www.ncbi.nlm.nih.gov/pubmed/12037005.
408. Patapoutian A, Reichardt LF. Trk receptors: mediators of neurotrophin action. *Curr Opin Neurobiol*. 2001;11(3):272-280. doi:10.1016/s0959-4388(00)00208-7
409. Barbacid M. The Trk family of neurotrophin receptors. *J Neurobiol*. 1994;25(11):1386-1403. doi:10.1002/neu.480251107
410. Jelsma TN, Friedman HH, Berkelaar M, Bray GM, Aguayo AJ. Different forms of the neurotrophin receptor trkB mRNA predominate in rat retina and optic nerve. *J Neurobiol*. 1993;24(9):1207-1214. doi:10.1002/neu.480240907
411. Webster MJ, Herman MM, Kleinman JE, Shannon Weickert C. BDNF and trkB mRNA expression in the hippocampus and temporal cortex during the human lifespan. *Gene Expr Patterns*. 2006;6(8):941-951. doi:10.1016/j.modgep.2006.03.009
412. Galindo-Romero C, Vidal-Villegas B, Asís-Martínez J, Lucas-Ruiz F, Gallego-Ortega A, Vidal-Sanz M. 7,8-Dihydroxiflavone protects adult rat axotomized retinal ganglion cells through MAPK/ERK and PI3K/AKT activation. *Int J Mol Sci*. 2021;SUBMITTED.
413. Chitranshi N, Dheer Y, Mirzaei M, et al. Loss of Shp2 Rescues BDNF/TrkB Signaling and Contributes to Improved Retinal Ganglion Cell Neuroprotection. *Mol Ther*. 2019;27(2):424-441. doi:10.1016/j.ymthe.2018.09.019